

Predicting the Static Bending Behavior
of Pallets with Panel Decks

by

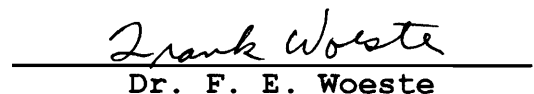
Kurt H. Mackes

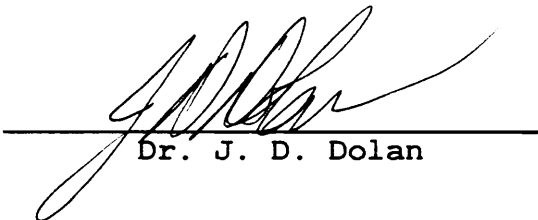
Dissertation submitted to the Faculty of the
Virginia Polytechnic Institute and State University
in partial fulfillment of the requirements for the degree of
Doctor of Philosophy
in
Wood Science and Forest Products

APPROVED:


Dr. J. R. Loferski Chairman


Dr. M. S. White


Dr. F. E. Woeste


Dr. J. D. Dolan


Dr. S. M. Holzer

March 17, 1998

Blacksburg, Virginia

Predicting the Static Bending Behavior of Pallets with Panel Decks

by

Kurt H. Mackes

Abstract

With increased use of pallets constructed utilizing structural panel decks, there is a need for a standardized, reliability-based design system, PDS-PANEL, to assist in the design and manufacture of panel-deck pallets. The primary objective of this research was to develop finite element models which predict the static bending behavior of pallets with at least one panel deck. Stringer and block pallets were modeled using plate elements to simulate deck behavior and were validated by comparing predicted deflections to experimentally measured deflections. Differences were considerably less than the allowable 15 percent for both stringer and block models. Sensitivity studies conducted with these models provided a rational basis to simplify models for use in the existing PDS-PANEL program developed at Virginia Polytechnic Institute & State University. Simplified models were required to have solution times of less than 2 minutes on a 286 type or more powerful personal computer (PC).

Simplified PC compatible models were developed for both stringer and block pallets in three principal support conditions: 1) warehouse stacking, 2) warehouse racking racked-across-deck (RAD) or racked-across-width (RAW), and 3) racked-across-stringer (RAS) or racked-across-length (RAL). Models were developed that can be used to evaluate pallets under partial-uniform, full-uniform, one, two, and three line loads. Stringer pallets with two, three, four, or five stringers, notched or unnotched, and block pallets with four, five, six, or nine blocks can be analyzed. Models were also developed to simulate pallets with features such as lead edge board reinforcement and cut-outs.

For stringer pallets, different simplified PC compatible models were used to predict panel-deck pallet behavior for each support condition. In the stack support condition, a two-dimensional beam model was used for full uniformly and line loaded pallets. A grid model was used for partial uniformly loaded pallets. Two-dimensional beam models were also used to simulate pallets in the RAD support condition and line loaded pallets in the RAS support condition. For uniformly loaded pallets in the RAS support condition, a three-dimensional grid model was used. In the stack and RAD support conditions, differences between plate and simplified model predictions were less than 15 percent. However, in the RAS support condition simplified model

predictions differed conservatively from plate model predictions by more than 15 percent. This was due to simplifying assumptions implemented to meet solution time requirements.

For block pallets, different simplified PC compatible models were used to predict panel-deck pallet behavior in the stack and rack support conditions. The same models can be used to predict block pallet behavior in the RAW and RAL support conditions. However, separate models were used to analyze block pallets with various base configurations, including unidirectional-base, perimeter-base, and panel bottom decks, with or without wheel openings.

In the stack support condition, a 19 by 19 grid of beam elements was used to simulate panel deck behavior. Simplifying assumptions resulted in significant differences between plate and simplified model stress predictions. For several test cases errors exceeded 15 percent, with mean differences as great as 26.8 percent. Deflection differences were less than 15 percent.

In the RAW and RAL support conditions, grids were again used to model panel decks. A 19 by 19 grid of beam elements was used to model the top deck and much coarser grids (either 2 by 2 or 3 by 3) to model panel bottom decks. For unidirectional- and perimeter-base pallets, assemblages of beam elements were used to simulate bottom deck behavior.

The differences between plate and simplified model predictions were less than 15 percent.

Generally, the simplified PC compatible models developed in this research adequately predicted behavior for stringer and block pallets. These models are prototypes of those used to predict the behavior of panel-deck pallets designed using PDS-PANEL.

Acknowledgments

The author wishes to express gratitude and appreciation to his major professor, Dr. Joseph R. Loferski, for his encouragement, guidance, and patience throughout this research project. Appreciation is also expressed to the advisory committee members, Dr. Marshall S. White, Dr. J. Daniel Dolan, Dr. Frank E. Woeste, and Dr. Sigfried M. Holzer. Further acknowledgment is expressed to Dr. White for his support and guidance during this project.

The author thanks VPI & SU, the NWPCA, and the APA for project funding. The author would like to thank Dr. Marvin E. Criswell at Colorado State University for his help in completing this research. Special acknowledgment is given to John A. McLeod at VPI & SU for his assistance in model development and incorporation of the models into the PDS-PANEL program. Special acknowledgment is also given to J. W. Akers who assisted with testing of pallets and pallet components.

Finally, for enduring these difficult times, the author wishes to thank his wife, Carol, by expressing his love and gratitude for her never-ending support. The author also thanks his parents and family for their encouragement and financial support.

Table of Contents

1.0	Introduction.....	1
1.1	Need for Research.....	2
1.2	Objectives.....	3
1.3	Scope of PDS-PANEL.....	3
1.4	Scope of Research & Dissertation.....	8
2.0	Literature Review.....	11
2.1	Pallet Terminology.....	11
2.2	Panel-Deck Pallet Geometries and Configurations..	20
2.2.1	Stringer Pallets with Panel Decks.....	22
2.2.2	Block Pallets with Panel Decks.....	26
2.3	Pallet Load and Support Conditions.....	28
2.4	Physical Pallet Testing.....	30
2.4.1	Air-Bag Test Machine.....	31
2.4.2	Panel-Deck Pallet Testing.....	34
2.5	Modeling Pallet Components.....	36
2.5.1	Panel Decks (Structural Panels).....	36
2.5.2	Strip-Type Decking.....	41
2.5.3	Stringers.....	46
2.5.3.1	Unnotched Stringers.....	47
2.5.3.2	Notched Stringers.....	50
2.5.4	Blocks.....	50

2.5.5	Pallet Joints.....	51
2.6	General Pallet Design.....	55
2.6.1	The Pallet Design System (PDS).....	57
2.6.2	Existing Panel-Deck Pallet Design Procedures.....	59
2.7	Finite Element Analysis.....	60
2.7.1	ABAQUS.....	61
2.7.1.1	Plate Elements in ABAQUS.....	62
2.7.1.2	Beam Elements in ABAQUS.....	65
2.7.1.2.1	Grids.....	69
2.7.1.3	Spring Elements in ABAQUS.....	71
2.7.2	Matrix Displacement Method.....	73
3.0	Modeling Pallet Components.....	76
3.1	Panel Decks.....	76
3.1.1	Modeling Panel Decks as Plates.....	78
3.1.2	Modeling Panels using a Grid.....	84
3.2	Strip-Type Decking.....	90
3.3	Stringers.....	91
3.3.1	Unnotched Stringers.....	98
3.3.2	Notched Stringers.....	105
3.4	Blocks.....	110
3.5	Joints and Contact Zones.....	115
3.5.1	Withdrawal/Head Embedment.....	116

3.5.1.1	Withdrawal Stiffness.....	120
3.5.1.2	Head Embedment Stiffness.....	123
3.5.1.3	Rotation Modulus.....	129
3.5.2	Lateral Stiffness.....	134
3.5.3	Spacer/Deck Contact.....	135
3.5.3.1	Stringer/Deck Contact.....	136
3.5.3.1.1	Stringer/Deck Contact in the Stack Support Condition.....	137
3.5.3.1.2	Stringer/Deck Contact in the RAD Support Condition.....	145
3.5.3.1.3	Stringer/Deck Contact in the RAS Support Condition.....	151
3.5.3.2	Block/Deck Contact.....	153
3.5.4	Pallet Section Models.....	157
3.6	Cut-outs.....	162
3.6.1	Top Deck Hand-Holds.....	167
3.6.2	Bottom Deck Wheel Openings.....	177
3.7	Summary.....	181
4.0	Modeling Stringer Pallets.....	185
4.1	Development of Plate Models for Stringer Pallets.	185
4.1.1	Stringer Pallets with Panel Decks Top and Bottom.....	186
4.1.2	Stringer Pallets with Panel Deck Top and Lumber Deck Bottom.....	193

4.2	Verification of Stringer Pallet Plate Models.....	193
4.2.1	Determining Pallet Member Properties.....	195
4.2.1.1	Panel Moduli of Elasticity (E_{PS} and E_{PW}).....	196
4.2.1.2	Stringer Modulus of Elasticity (E_S).....	201
4.2.1.3	Bottom Deckboard Modulus of Elasticity...	202
4.2.2	Preparation of Pallets.....	204
4.2.3	Pallet Testing.....	208
4.2.3.1	Stack Support Condition.....	210
4.2.3.2	Rack-Across-Deck (RAD) Support Condition.	214
4.2.3.3	Rack-Across-Stringer (RAS) Support Condition.....	216
4.2.4	Data Analysis and Results.....	218
4.3	Stringer Pallet Sensitivity Studies.....	222
4.3.1	Stack Support Condition.....	225
4.3.2	RAD Support Condition.....	232
4.3.3	RAS Support Condition.....	234
4.4	Development of PC Compatible Stringer Pallet Models.....	239
4.4.1	Stack Support Condition.....	239
4.4.1.1	Full Uniform and Line Load Model.....	240
4.4.1.2	Partial Uniform Load Model.....	250
4.4.2	RAD Support Condition.....	255
4.4.3	RAS Support Condition.....	269

4.4.3.1	Line Load Model.....	269
4.4.3.2	Full and Partial Uniform Load Model.....	282
5.0	Modeling Block Pallets.....	299
5.1	Development of Plate Models for Block Pallets....	299
5.1.1	Block Pallets with Panel Decks Top and Bottom.....	300
5.1.2	Block Pallet with Panel Deck Top and Panel Deck Bottom with Wheel Openings.....	305
5.1.3	Block Pallets with Panel Deck Tops and Strip-type Bottom Decks.....	307
5.1.3.1	Unidirectional-Base Pallets.....	307
5.1.3.2	Perimeter-Base Block Pallets.....	308
5.2	Validation Block Pallet Plate Models.....	311
5.2.1	Determining Pallet Member Properties.....	312
5.2.2	Preparation of Pallets.....	313
5.2.3	Block Pallet Testing.....	316
5.2.3.1	Stack Support Condition.....	316
5.2.3.2	Rack (RAW and RAL) Support Conditions....	320
5.2.4	Data Analysis and Results.....	326
5.2.4.1	Stack Support Condition.....	327
5.2.4.2	Rack (RAW and RAL) Support Conditions....	334
5.3	Block Pallet Sensitivity Studies.....	342
5.3.1	Stack Condition.....	342
5.3.2	Rack (RAW and RAL) Support Conditions.....	344

5.4	Development of PC Compatible Block Pallet Models.	348
5.4.1	Stack Support Condition.....	351
5.4.1.1	Bottom Strip-Type Deck Model.....	352
5.4.1.2	Panel Deck Model.....	354
5.4.2	Rack (RAW and RAL) Support Conditions.....	364
5.4.2.1	Unidirectional Base Model.....	368
5.4.2.2	Perimeter-Base Model.....	375
5.4.2.3	Panel Deck Top and Bottom Model.....	378
5.4.3	Models for Block Pallets with Cut-Outs.....	388
5.4.3.1	Hand-Holds.....	388
5.4.3.2	Bottom Deck Wheel Openings.....	391
5.4.3.2.1	Stack Support Condition.....	391
5.4.3.2.2	Rack (RAW and RAL) Support Conditions.....	392
6.0	Summary and Conclusions.....	399
6.1	Recommendations for Further Research.....	404
	Literature Review.....	407
	Vita.....	413

List of Figures

Figure 1.1.	PDS-PANEL Load Types.....	5
Figure 1.2.	Stringer Pallet Support Conditions.....	6
Figure 1.3.	Flow Chart of Research Plan.....	9
Figure 2.1.	Pallet exhibiting both a Top and Bottom Deck.....	12
Figure 2.2	Full Four-Way, Partial Four-Way, and Two-Way Entry Pallet Geometries.....	14
Figure 2.3	An Example of a Stringer and a Block Pallet.....	15
Figure 2.4	A Block Pallet Section Exhibiting a Stringer Board.....	17
Figure 2.5	Strip-Type Deck Configurations.....	18
Figure 2.6	Components used to Simulate a Pallet Joint.....	19
Figure 2.7	Reversible Stringer Pallet with Panel Decks Top and Bottom.....	24
Figure 2.8	Bottom Deck Configurations for Non-Reversible Stringer Pallets.....	25
Figure 2.9	Reversible Nine-Block Pallet with Panel Decks Top and Bottom.....	27
Figure 2.10	Bottom Deck Configurations for Non-Reversible Block Pallets.....	29
Figure 2.11	The Air-Bag Test Machine at VPI & SU.....	32
Figure 2.12	Schematic Diagram of the Air-Bag Test Machine at VPI & SU.....	33
Figure 2.13	Transformed Section of 5-Ply Plywood.....	39

Figure 2.14	Model Developed by Loferski (1985) which Simulates Stringer Pallets Supported in the RAD Condition.....	42
Figure 2.15	Stringer Notch used in Testing Conducted by Bastendorff and Polensek (1984).....	48
Figure 2.16	Model Developed by Loferski (1985) which Simulates Stringer Pallets Supported in the RAS Condition.....	49
Figure 2.17	Element Assemblage used in PDS (NWPCA, 1988) to Simulate Blocks.....	52
Figure 2.18	Modes of Action for a Pallet Joint.....	53
Figure 2.19	S8R and S9R5 Shell Elements in ABAQUS.....	63
Figure 2.20	B32 and B33 Beam Elements in ABAQUS.....	66
Figure 2.21	Default Integration Points for B32 and B33 Beam Elements in ABAQUS.....	68
Figure 2.22	Grid Framework Constructed with Beam Elements in ABAQUS.....	70
Figure 2.23	SPRING1 and SPRING2 Elements in ABAQUS....	72
Figure 3.1	Sign Convention used to Model pallets and Pallet Components.....	77
Figure 3.2	Test Cases used to Determine Mesh Fineness Required to Model Panel Decks....	80
Figure 3.3	Plywood Panel Used to Analyze Mesh Fineness Required to Model Panel Decks....	82
Figure 3.4	Examples of Finite Element Meshes used to Analyze Plywood Panel.....	83
Figure 3.5	Grid of Beam Elements Simulating a Panel Deck.....	86

Figure 3.6	Comparison of Finite Element Plate Model to Grid Model: Maximum Deflection.....	88
Figure 3.7	Comparison of Finite Element Plate Model to Grid Model: Maximum Normal Stresses....	89
Figure 3.8	Lumber Bottom Deck Example.....	92
Figure 3.9	Deformed States and Maximum Predicted Stress for Test Cases of Lumber Bottom Deck Example.....	93
Figure 3.10	Stringer Analyzed to Determine the Number of Concentrated Loads Required to Simulate a Uniform Load.....	95
Figure 3.11	Finite Element Mesh Simulating Stringer Bending Behavior Loaded with up to Nine Concentrated Loads.....	96
Figure 3.12	Assembly of Beam Elements used to Predict Stringer Bending Behavior.....	99
Figure 3.13	Assembly of Beam Elements used to Model Stringer Cross-Sectional Properties.....	100
Figure 3.14	Assembly of Beam Elements used to Simulate Stringers in Three-Dimensional Plate Model.....	101
Figure 3.15	Assembly of Beam Elements used to Model Stringers in PC-Based Pallet Models.....	104
Figure 3.16	Notched Stringer used in Conjugate Beam Example.....	106
Figure 3.17	Assembly of Elements used to Simulate Blocks in Plate Models.....	112
Figure 3.18	Assembly of Elements used to Model Blocks in PC-Based Pallet Models.....	114
Figure 3.19	Setup used to Determine a Stiffness Value for Withdrawal/Head Embedment Combined....	117

Figure 3.20	Plot of Load versus Withdrawal/Head Embedment Deformation.....	119
Figure 3.21	Schematic Diagram of Test Setup used to determine Withdrawal Stiffness.....	121
Figure 3.22	Plot of Load versus Withdrawal Deformation.....	122
Figure 3.23	Schematic Diagram of Test Setup used to determine Head Embedment Stiffness.....	125
Figure 3.24	Plot of Load versus Head Embedment Deformation.....	126
Figure 3.25	Replacement of the Combined Withdrawal/Head Embedment Spring with a Rotation Spring in Stringer Pallet Nail Joints.....	130
Figure 3.26	Finite Element Model used to determine Rotation Modulus for Top Deck Attachment to Edge Stringer.....	131
Figure 3.27	Finite Element Model used to determine Rotation Modulus for Bottom Deck Attachment to Edge Stringer.....	133
Figure 3.28	Finite Element Models used to Predict Stringer Contact (k_{CS}) Stiffness.....	138
Figure 3.29	Deformation Pattern Predicted by Finite Element Model used to Predict Edge Stringer Contact (k_{CS}) Stiffness.....	141
Figure 3.30	Finite Element Model used to Determine k_{LDC} Value.....	142
Figure 3.31	Contact Points of Stringers and Decks for the RAD Support Condition.....	146
Figure 3.32	Potential Contact Configurations between Edge Stringer and Bottom Deck.....	148

Figure 3.33	Profiles of Contact between the Edge Stringer and Bottom Deck.....	149
Figure 3.34	Deformation Pattern at Mid-Span for Stringer pallets in the RAS Support Condition.....	152
Figure 3.35	Potential Contact Configurations between the Edge Blocks and Bottom Deck in both the RAL and RAW Support Conditions.....	156
Figure 3.36	Pallet Section Models.....	158
Figure 3.37	Nail Joint Configurations for Pallet Section Models.....	160
Figure 3.38	Applications of Load to Pallet sections in the Stack Support Condition.....	161
Figure 3.39	Applications of Load to Pallet sections in the RAD Support Condition.....	161
Figure 3.40	Finite Element Mesh used to Simulate Hand-Holds in a Block Pallet Plate Model..	170
Figure 3.41	Setup for Testing Panels in Bending on the Air-Bag Testing Machine at VPI & SU.....	171
Figure 3.42	Allowable Locations for Hand-Hold Placement.....	175
Figure 3.43	The Simplified Finite Element Mesh Adapted to Model Hand-Holds in Block Pallets.....	176
Figure 3.44	Mesh of Shell Elements which Simulate the Bottom Deck of a Pallet with Wheel Openings.....	179
Figure 3.45	Mesh of Beam Elements which can be used to Simulate the Bottom Deck of a Pallet with Wheel Openings.....	182
Figure 4.1	Mesh Configuration used to Simulate the Panel Decks of Three-Stringer Pallets.....	187

Figure 4.2	Element Configuration used to Simulate Nail Joints and Contact Regions of Three-Stringer Pallets.....	188
Figure 4.3	Finite Element Model used to Predict the Behavior of Three-Stringer Pallets.....	190
Figure 4.4	Finite Element Mesh used to Simulate the Deck Behavior of Four- and Five-Stringer Pallets.....	191
Figure 4.5	Finite Element Mesh used to Simulate Panel Decks with Lead Edge Boards.....	192
Figure 4.6	Finite Element Mesh used to Simulate the Bottom Deck Behavior of Stringer Pallets with Bottom Decks Comprised of Five Lumber Deckboards.....	194
Figure 4.7	The Pattern used for Removal of Test Specimens from Panel Decks for the Determination of Material Properties.....	197
Figure 4.8	Typical Plot of Load versus Deflection for 2 inch Strips of OSB Tested in Bending in the Elastic Range.....	200
Figure 4.9	Typical Plot of Load versus Deflection for a Spruce-Pine-Fir Stringer in Bending in the Elastic Range.....	203
Figure 4.10	Typical Plot of Load versus Deflection for a Southern Yellow Pine Deckboard in Bending in the Elastic Range.....	205
Figure 4.11	Location of Pallet Components Comprising Test Pallet SPP3-1.....	206
Figure 4.12	Nailing Pattern used to attach Panel Decks Stringers in Pallet Assembly.....	209
Figure 4.13	Stringer Pallet being Tested in Flexure (RAS Support Condition) using the Pneumatic Pressure-Bag Test Machine at VPI & SU.....	211

Figure 4.14	Schematic of Test Setup contained within the Metal Support Frame of the Air-Bag Test Machine used to Evaluate the Panel Deck Behavior of Stringer Pallets in the Stack Support Condition.....	213
Figure 4.15	Schematic of Test Setup used to evaluate Lumber and Composite (Plywood and OSB) Strip-Type Bottom Deck Behavior of Stringer Pallets in the Stack Support Condition.....	215
Figure 4.16	Gap Formation in the Joints of Stringer Pallets tested in the RAD Support Condition.....	217
Figure 4.17	Plots of Load versus Deflection for Test Pallet SPP3-1 loaded in the Stack, RAD, and RAS Support Conditions.....	220
Figure 4.18	Pallet Section Model used to Evaluate the Effects of Lateral Stiffness in the Stack Support Condition.....	229
Figure 4.19	Two-Dimensional Cross-Section of a Three-Stringer Pallet, Cross-Section of the Stringer Pallet Plate Model, and the corresponding Simplified Model.....	241
Figure 4.20	Simplified Model Simulating the Behavior of Full Uniformly or Line Loaded Pallets in the Stack Support Condition.....	243
Figure 4.21	Schematic of Methodology used to ensure that Contact Elements are properly Activated or Dummied.....	245
Figure 4.22	Deflection Pattern predicted for the Top Deck of Test Pallet SPP3-1 by the Simplified Stringer Model for Full-Uniformly Loaded Pallets in the Stack Support Condition.....	247

Figure 4.23	Stress (S11) Profile predicted for the Top Deck of Test Pallet SPP3-1 by the Simplified Stringer Model for Full-Uniformly Loaded Pallets in the Stack Support Condition.....	248
Figure 4.24	Grid Model Simulating the Behavior of Partial Uniformly Loaded Stringer Pallets in the Stack Support Condition.....	251
Figure 4.25	Tributary Area Technique used to assign Width to the Grid Members of the Partial Uniform Load Stack Model for Stringer Pallets oriented in the 3-Direction.....	252
Figure 4.26	Deflection Pattern predicted for the Top Deck of Test Pallet SPP3-1 by the Simplified Partial Uniform Load Model for Stringer Pallets in the Stack Support Condition.....	256
Figure 4.27	S11 Stress Profile predicted for the Top Deck of Test Pallet SPP3-1 by the Simplified Partial Uniform Load Model for Stringer Pallets in the Stack Support Condition.....	257
Figure 4.28	Two-Dimensional Cross-Section of a Three-Stringer Pallet, Cross-Section of the Stringer Pallet Plate Model, and the Corresponding Simplified RAD Model.....	259
Figure 4.29	Simplified RAD Model for Stringer Pallets.	261
Figure 4.30	Partial Uniformly Loaded Stringer Pallet and the Simplified RAD Model Simulating its Behavior.....	263
Figure 4.31	Deflection Pattern predicted for Test Pallet SPP3-1 by the Simplified Model for Stringer Pallets loaded in the RAD Support Condition.....	265

Figure 4.32	Stress (S11) Profile predicted for Test Pallet SPP3-1 by the Simplified Model for Stringer Pallets loaded in the RAD Support Condition.....	266
Figure 4.33	Proposed Line Load Model for Predicting the Behavior of Stringer Pallets in the RAS Support Condition.....	272
Figure 4.34	Simplified Model for Line Loaded Pallets in the RAS Support Condition.....	274
Figure 4.35	Deflection Pattern and S11 Stress Profile predicted for Test Pallet SPP3-1 by the Simplified Line Load Model for Stringer Pallets.....	276
Figure 4.36	Enhanced Simplified Model for Simulating the Behavior of Line Loaded Stringer Pallet SPP3-1 in the RAS Support Condition.....	279
Figure 4.37	Simplified Grid Model used to Predict the Behavior of Stringer Pallets in the RAS Support Condition.....	283
Figure 4.38	Potential Locations for Attachments of Stringer Elements to Deck Elements in the RAS Grid Model.....	286
Figure 4.39	Deflection Pattern predicted for Test Pallet SPP3-1 by the Simplified RAS Grid Model.....	291
Figure 4.40	S11 Stress Profile predicted for the Bottom Deck of Test Pallet SPP3-1 by the Simplified RAS Grid Model.....	292
Figure 4.41	S11 Stress Profile predicted for the Stringers of Test Pallet SPP3-1 by the Simplified RAS Grid Model.....	293
Figure 4.42	S11 Stress Profile predicted for the Top Deck of Test Pallet SPP3-1 by the Simplified RAS Grid Model.....	294

Figure 4.43	Proposed Grid Model for Predicting the Behavior of Stringer Pallets in the RAS Support Condition.....	297
Figure 5.1	Finite Element Mesh Configuration used to Simulate the Panel Decks of Block Pallets..	301
Figure 5.2	Finite Element Mesh Configuration for Block Pallets with Panel Decks Top and Bottom.....	303
Figure 5.3	Block Activation Scheme for Modeling 4-, 5-, 6-, and 9-Block Pallets.....	304
Figure 5.4	Finite Element Mesh Configuration for Block Pallets with Bottom Deck Wheel Openings.....	306
Figure 5.5	Finite Element Mesh Configuration for Block Pallets with Panel Top Deck and Unidirectional Lumber Bottom Deck.....	309
Figure 5.6	Finite Element Mesh Configuration for Block Pallets with Panel Top Deck and Perimeter-Base of Lumber.....	310
Figure 5.7	Block Pallet Configurations Evaluated.....	315
Figure 5.8	Nailing Patterns used to Assemble Block Pallets.....	317
Figure 5.9	Diagram of Block Pallet in the Air-Bag Test Machine with I-Beams positioned to Simulate the Stack Support Condition.....	319
Figure 5.10	Block Pallet being Tested in Flexure (RAL Support Condition) using the Air-Bag Test Machine at VPI & SU.....	323
Figure 5.11	Schematic of Observed Gap Formation for BPP Type Block Pallets during Testing in the Rack Support Condition.....	324

Figure 5.12	Schematic of Observed Gap Formation for BPP Type at the Butted Joint of Perimeter-Base Block Pallets in the Rack Support Condition.....	325
Figure 5.13	Block/Top Deck Contact Profile for Test Pallet BPP-1 Loaded in the Stack Support Condition.....	328
Figure 5.14	Predicted Deflection Profile for the Top Deck of Pallet BPP-1 evaluated in the Stack Support Condition using the Block Pallet Plate Model.....	330
Figure 5.15	Stress Profile for the Top Deck of Test Pallet BPP-1 loaded in the Stack Support Condition.....	332
Figure 5.16	Block/Top Deck Contact Profile for Test Pallet BPP-1 Loaded in the RAW Support Condition.....	337
Figure 5.17	Predicted Deflection Profiles for the Decks of Pallet BPP-1 evaluated in the Racked-Across-Width Support Condition using the Block Pallet Plate Model.....	338
Figure 5.18	Stress Profile for the Top Deck of Test Pallet BPP-1 loaded in the Rack Support Condition.....	340
Figure 5.19	The Effect of Poisson's Ratio on the Maximum Predicted Top Deck Deflection of Test Pallet BPP1 Uniformly Loaded in the Stack Support Condition.....	345
Figure 5.20	The Effect of Poisson's Ratio on the Maximum Predicted Top Deck Stresses of Test Pallet BPP1 Uniformly Loaded in the Stack Support Condition.....	346
Figure 5.21	Simplified Model for the Bottom Decks of Perimeter- and Unidirectional-Base Block Pallets in the Stack Support Condition....	353

Figure 5.22	Stress (S11) and Deflection Profiles predicted for the Bottom Deck of Test Pallet BPU7 in the Stack Support Condition.....	356
Figure 5.23	Finite Element Mesh Configuration of Simplified Model for Panel Decks of Block Pallets loaded in the Stack Support Condition.....	357
Figure 5.24	Grid Member Locations used in the Simplified Stack Model for Block Pallets..	359
Figure 5.25	Block/Deck Contact Pattern used in the Simplified Stack Model for Block Pallets..	360
Figure 5.26	Predicted Deflection Profile for the Top Deck of Pallet BPP-1 evaluated in the Stack Support Condition using the Simplified Block Pallet Model.....	366
Figure 5.27	Stress Profile for the Top Deck of Test Pallet BPP-1 loaded in the Stack Support Condition.....	367
Figure 5.28	Finite Element Mesh Configuration of Simplified Model for Unidirectional-Base Block Pallets in the Rack Support Condition.....	369
Figure 5.29	Block/Upper Deck Contact Pattern used in the Simplified Model for Block Pallets supported Racked Across the Bottom Deckboards (Strips).....	371
Figure 5.30	Block/Upper Deck Contact Pattern used in the Simplified Model for Block Pallets supported Racked Along the Bottom Deckboards (Strips).....	372
Figure 5.31	Predicted Deflection Profiles for the Decks of Pallet BPU-4 evaluated in the Racked-Across-Width Support Condition using the Simplified Unidirectional-Base Block Pallet Model.....	377

Figure 5.32	Proposed Finite Element Mesh Configuration of Simplified Model for Perimeter-Base Pallets Racked Across the Butted Deck-boards.....	379
Figure 5.33	Proposed Finite Element Mesh Configuration of Simplified Model for Block Pallets with Panel Decks Top and Bottom loaded in the Rack Support Conditions.....	381
Figure 5.34	Proposed Bottom Deck Configuration of the Simplified Model for Block Pallets with Panel Decks Top and Bottom supported in a Rack Condition.....	384
Figure 5.35	Predicted Deflection Profiles for the Decks of Pallet BPP-1 evaluated in the Racked-Across-Width Support Condition using the Simplified Block Pallet Model...	386
Figure 5.36	Stress Profile predicted by the Simplified Block Model for the Top Deck of Test Pallet BPP-1 loaded in the RAW Support Condition.....	387
Figure 5.37	Configuration of Simplified Model for the Bottom Decks of Block Pallets with Wheel Openings in the Stack Support Condition...	393
Figure 5.38	Predicted Deflection and Stress Profiles for the Bottom Deck of Pallet BPPC-7 evaluated in the Stack Support Condition using the Simplified Block Pallet Model...	395
Figure 3.39	Predicted Deflection Profiles for the Decks of Pallet BPPC-4 evaluated in the Racked-Across-Width Support Condition using the Simplified Block Pallet Model...	398

List of Tables

Table 2.1	Structural Panels Recommended by the APA for Inclusion in PDS-PANEL.....	21
Table 2.2	PDS Species Classes.....	44
Table 2.3	PDS Grade Identification Guide.....	45
Table 3.1	Summary of Results for Finite Element Meshes of various Fineness used to Predict the Behavior of Panel Decks.....	85
Table 3.2	Comparison of Finite Element Results for Uniform Load Simulation Test Cases to Classical Solution.....	97
Table 3.3	Comparison of Finite Element Solution to Classical Solution for Element Assemblage used to Simulate Stringers-Test Case S-13..	103
Table 3.4	Comparison of Finite Element Results to those obtained using the Conjugate Beam Method.....	107
Table 3.5	Predicted versus Measured Deflections for Notched Stringers.....	109
Table 3.6	Withdrawal Stiffness for Selected Wood Species.....	124
Table 3.7	Head Embedment Stiffness for Selected Pallet Deck Materials.....	128
Table 3.8	Mean Modulus of Elasticity (E_{\perp}) Values for Blocks in Compression Perpendicular-to- Grain.....	154
Table 3.9	Comparison of Predicted Deflections to Experimental Results for Type A Pallet Sections.....	163

Table 3.10	Comparison of Predicted Deflections to Experimental Results for Type B Pallet Sections.....	164
Table 3.11	Comparison of Predicted Deflections to Experimental Results for Type C Pallet Sections.....	165
Table 3.12	Adjustment of EI Values determined using 40 x 48 inch Panels for Membrane (Plate Action).....	168
Table 3.13	Predicted (Finite Element) versus Measured Deflections for Panels with Hand-Holds.....	172
Table 3.14	Comparison of Finite Element Solutions for 25 and 100 Element Plate Models Checking Solution Convergence.....	174
Table 3.15	Comparison of Finite Element Solutions for Grid Model to Plate (Shell) Model for Panels with Hand-Holds.....	178
Table 3.16	Predicted (Finite Element) versus Measured Deflections for Panels with Wheel Openings.	180
Table 3.17	Comparison of Finite Element Solutions for Grid Model to Plate (Shell) Model for Panels with Wheel Openings.....	183
Table 4.1	Maximum Specimen (Strip) Lengths used to Determine Modulus of Elasticity Values for Plywood and Oriented Strand Board (OSB) Panels.....	199
Table 4.2	Comparison of Stringer Pallet Plate Model Predictions to Experimentally Measured (ABTM) Deflections in the Stack Support Condition.....	221
Table 4.3	Comparison of Stringer Pallet Plate Model Predictions to Experimentally Measured (ABTM) Deflections in the RAD Support Condition.....	223

Table 4.4	Comparison of Stringer Pallet Plate Model Predictions to Experimentally Measured (ABTM) Deflections in the RAS Support Condition.....	224
Table 4.5	Sensitivity of the Stringer Pallet Plate Model to Changes in Geometric and Material Properties in the Stack Support Condition..	226
Table 4.6	Sensitivity of the Stringer Pallet Plate Model to Changes in Stringer/Deck Contact and Nail Joint Properties in the Stack Support Condition.....	228
Table 4.7	Summary of an Evaluation conducted to determine the Effects of Lateral Stiffness on the Behavior of Stringer Pallets in the Stack Support Condition.....	230
Table 4.8	Sensitivity of the Stringer Pallet Plate Model to Changes in Stringer/Bottom Deck Contact Stiffness Properties in the Stack Support Condition.....	231
Table 4.9	Sensitivity of the Stringer Pallet Plate Model to Changes in Geometric and Material Properties in the RAD Support Condition....	233
Table 4.10	Sensitivity of the Stringer Pallet Plate Model to Changes in Stringer/Deck Contact and Nail Joint Properties in the RAD Support Condition.....	235
Table 4.11	Sensitivity of the Stringer Pallet Plate Model to Changes in Geometric and Material Properties in the RAS Support Condition....	237
Table 4.12	Sensitivity of the Stringer Pallet Plate Model to Changes in Stringer/Deck Contact and Nail Joint Properties in the RAS Support Condition.....	238

Table 4.13	Comparison of Plate (P) and Simplified (S) Maximum Stress (S11) and Deflection Predictions for Full Uniformly and Line Loaded Stringer Pallets in the Stack Support Condition.....	249
Table 4.14	Comparison of Finite Element Solutions for Partial Uniformly Stringer Pallets in the Stack Support Condition.....	254
Table 4.15	Summary of Sensitivity Study Results for the Partial Uniform Load Grid Model used to analyze Stringer Pallets in the Stack Support Condition.....	258
Table 4.16	Comparison of Maximum Stresses (S11) and Deflections predicted using Plate Models to Values obtained using the Simplified Model for Stringer Pallets in the RAD Support Condition.....	267
Table 4.17	Summary of Results for 4-Stringer Pallets Tested in the RAD Support Condition.....	270
Table 4.18	Comparison of Simplified and Plate Model Solutions for a Line Loaded Stringer Pallet in the RAS Support Condition.....	275
Table 4.19	Sensitivity of the Simplified and Plate Models to Changes in Stringer, Deck, and Nail Joint Properties for a Line Loaded Stringer Pallet in the RAS Support Condition.....	277
Table 4.20	Comparison of Enhanced Simplified and Plate Model Solutions for a Line Loaded Stringer Pallet in the RAS Support Condition.....	280
Table 4.21	Sensitivity of the Enhanced Simplified and Plate Models to Changes in Stringer, Deck, and Nail Joint Properties for a Line Loaded Stringer Pallet in the RAS Support Condition.....	281

Table 4.22	Comparison of Load Distribution predicted by the Plate Model to Predictions for Various Configurations of the Simplified Model in the RAS Support Condition.....	287
Table 4.23	Summary of the Degrees of Freedom which can be Restrained in the RAS Grid Model for Stringer Pallets without significantly impacting Stress and Deflection Predictions.....	289
Table 4.24	Comparison of selected Simplified RAS Grid Model (S-RS) Results to Plate Model (P-RS) Predictions.....	290
Table 4.25	Selected of selected Enhanced Simplified RAS Grid Model (S-RS) Results to Plate Model (P-RS) Predictions.....	296
Table 5.1	Load Applied to Block Pallets.....	321
Table 5.2	Comparison of Predicted to Experimental (ABTM) Deflections for the Top Panel Decks of Block Pallets evaluated in the Stack Support Condition.....	331
Table 5.3	Maximum Stress Predicted for the Top Panel Deck of Block Pallets evaluated in the Stack Support Condition.....	333
Table 5.4	Maximum Stresses, including Transverse (Rolling) Shear Stresses, Predicted for the Top Panel Decks of Block Pallets evaluated in the Stack Support Condition.....	335
Table 5.5	Comparison of Predicted to Experimental (ABTM) Deflections for the Bottom Decks of Block Pallets evaluated in the Rack Support Conditions.....	339
Table 5.6	Maximum Stress Predictions for Block Pallets evaluated in the Rack Support Conditions using Block Pallet Plate Models.....	341

Table 5.7	Sensitivity of the Block Pallet Plate Model to Changes in Geometric and Material Properties in the Stack Support Condition..	343
Table 5.8	Sensitivity of the Block Pallet Plate Model to Changes in Block/Deck Contact and Nail Joint Properties in the Stack Support Condition.....	347
Table 5.9	Sensitivity of the Block Pallet Plate Model to Changes in Geometric and Material Properties in the Rack (RAW) Support Condition.....	349
Table 5.10	Sensitivity of the Block Pallet Plate Model to Changes in Block/Deck Contact and Nail Joint Properties in the Rack (RAW) Support Condition.....	350
Table 5.11	Maximum Stress and Deflection Predictions generated using the Simplified Model for the Bottom Deck of Perimeter-Base Block Pallets in the Stack Support Condition.....	355
Table 5.12	Comparison of Predicted Deflections for the Top Panel Decks of Block Pallets evaluated in the Stack Support Conditions.....	362
Table 5.13	Prediction Comparisons for Various Versions of Plate and Simplified Block Models simulating Test Pallet BPP-16 Behavior in the Stack Support Condition.....	363
Table 5.14	Comparison of Maximum Stress and Deflection Predictions for Test Pallet BPP-16 in the Stack Support Condition.....	365
Table 5.15	Summary of the Degrees of Freedom which can be restrained in the Simplified Model for Unidirectional-Base Block Pallets in the Rack Support Conditions without significantly impacting Stress and Deflection Predictions.....	374

Table 5.16	Comparison of Model Predictions for Unidirectional-Base Pallets in the Racked-Across-Width Support Condition.....	376
Table 5.17	Comparison of Model Predictions for Perimeter-Base Block Pallets in the Racked-Across-Length Support Condition.....	380
Table 5.18	Comparison of Model Predictions for Block Pallets with Panel Decks Top and Bottom in the Racked-Across-Width Support Condition..	382
Table 5.19	Comparison of Model Predictions for Block Pallets with Panel Decks Top and Bottom in the Racked-Across-Width Support Condition..	385
Table 5.20	The Effect of Top Deck Hand-Holds on Simplified Model Predictions.....	390
Table 5.21	Stress and Deflection Values predicted using the Simplified Model Simulating the Bottom Deck Behavior of Block Pallets with Wheel Openings in the Stack Support Condition.....	394
Table 5.22	Comparison of Model Predictions for Block Pallets with Bottom Deck Wheel Openings in the Racked-Across-Width Support Condition..	397

1.0 Introduction

The use of pallets to store and handle goods has increased dramatically over the past four decades. In 1995, the production of new pallets exceeded 410 million units (Reddy et al., 1997). Rough estimations place the current annual production of pallets with panel decks at 10 to 15 million units. Manufacturing these units consumes significant amounts of structural panels. Reddy et al. (1997) estimated that 187 million square feet (3/8 inch thickness basis) of softwood plywood was consumed by the pallet industry in 1995 and oriented strand board (OSB) usage was estimated at 21 million square feet (3/8 inch thickness basis).

Although many types of structural panels are suitable for pallet decks (Kurtenacker, 1974), plywood and OSB are the dominant types used. Plywood-decked pallets have been found to provide excellent service in food manufacturing and distribution (Lyons, 1970). Results from the Pallet-Exchange Program (Wallin, Stern, and Strobel, 1975) indicate that plywood pallets are more durable than pallets constructed with lumber decks. Plywood pallets sustain less damage and require fewer repairs. The smooth deck of plywood pallets can reduce damage to goods. Although plywood pallets have a higher initial cost, in many

instances they are a better long-term investment than pallets with lumber decks because of longer service life.

1.1 Need for Research

The Pallet Design System (PDS) for stringer pallets constructed with lumber decks was developed through a cooperative research effort of the National Wood Pallet and Container Association (NWPCA), the USDA Forest Service, and Virginia Polytechnic Institute and State University (VPI & SU). The first generation of this reliability-based structural design procedure, PDS-STRINGER, was completed in 1984 and was copywritten by the NWPCA (NWPCA, 1984). In 1988, PDS-BLOCK was released (NWPCA, 1988). PDS-BLOCK can be used to model block pallets. These versions of PDS are currently the only reliability-based design programs for wood pallets.

Stringer and block versions of PDS are restricted to estimating static strength, stiffness and durability of pallets constructed with lumber decks. Lack of a standardized reliability-based design system for panel-deck pallets leads to over- and under-designed pallets. Over-design results in an inefficient utilization of our timber resources, while under-design can cause product damage and potentially unsafe conditions. Development of a reliability-based methodology for predicting the strength

and stiffness of panel-deck pallets (PDS-PANEL) provides a rational basis for designing efficient and safe pallets. Models developed in this research are prototypes of those used to predict pallet behavior in PDS-PANEL.

1.2 Objectives

The objective of this research was to develop a methodology for predicting the static bending behavior of pallets with panel decks, including development of three-dimensional finite element plate models to determine which properties significantly influence pallet behavior and simplified models for use in the existing PDS-PANEL program developed at VPI & SU. Simplified models had to run on a 286 type or more powerful personal computer (PC) with solution times of less than two minutes. Additionally, the simplified and plate model solutions were not to differ by more than 15 percent.

1.3 Scope of PDS-PANEL

Finite element models developed in this research were used to predict behavior of block and stringer pallets constructed with plywood or OSB decks. Analysis of full four-way, partial four-way, and two-way geometries which are shown in Chapter 2 (Figure 2.2) were completed for common pallet sizes. Models were developed to analyze stringer pallets constructed with two, three, four, or five

stringers, and block pallets constructed with four, five, six, or nine block. Behavior predictions were based on pallet condition at the time of manufacture. The models can be used to analyze pallets subjected to partial-uniform, full-uniform, one-line, two-line, and three-line loads. These load conditions are illustrated in Figure 1.1.

For stringer pallets, three support conditions were analyzed:

1. Pallet with fully supported bottom deck (stack support condition).
2. Pallet supported across the deckboards in a rack (RAD support condition).
3. Pallet supported across the stringers in a rack (RAS support condition).

Stringer pallet support conditions are shown in Figure 1.2.

Three support conditions were also analyzed for block pallets:

1. Pallet with fully supported bottom deck (stack support condition).
2. Pallet supported across the width in a rack (RAW support condition).
3. Pallet supported across the length in a rack (RAL support condition).

Specific pallet characteristics modeled in this research included:

Top Deck Characteristics:

1. Single panel

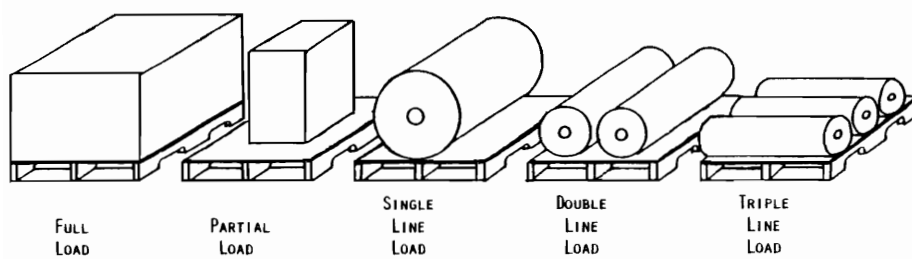
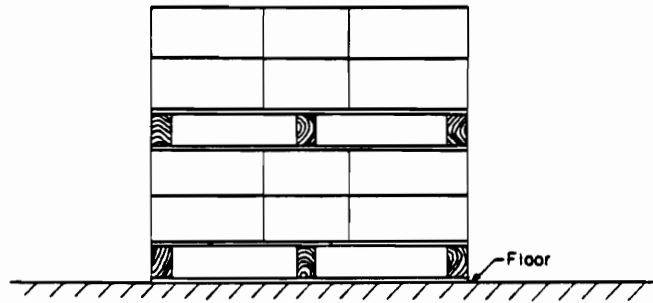
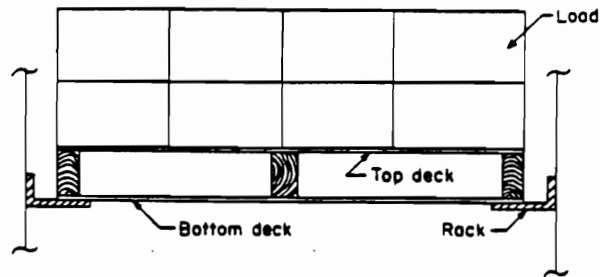


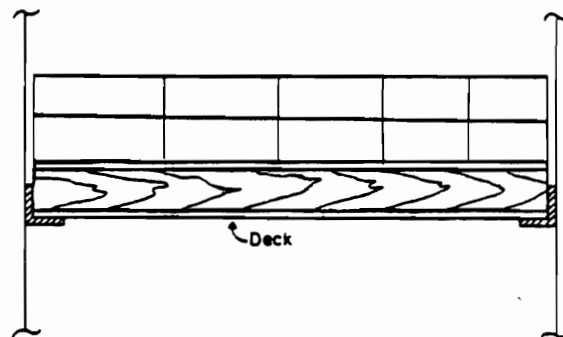
Figure 1.1. PDS-PANEL Load Types.



1. Stacked (end view)



2. Racked-across-deck (RAD)
(end view)



3. Racked-across-stringers (RAS)
(side view)

Figure 1.2. Stringer Pallet Support Conditions (Courtesy of Loferski, 1985).

2. Leading edge reinforcement (lumber or plywood strips)
3. Cut-outs (hand-holds)
4. Winged and flush designs as defined in Chapter 2 (page 13)

Bottom Deck Characteristics:

1. Lumber and plywood strips
2. Solid panel or panel with cut-outs (wheel openings)
3. Winged and flush design as defined in Chapter 2 (page 13)

Deck Spacers:

1. Composite blocks (plywood and particleboard)
2. Solid wood blocks and stringers

Leading edge boards were allowed only for stringer pallets. Cut-outs were restricted to rectangular hand-holds and wheel openings. Circular or customized cut-outs were not considered. Wing designs were not allowed for block pallets. Although not considered in this research, models were designed to permit the future inclusion of stringer boards in block pallets.

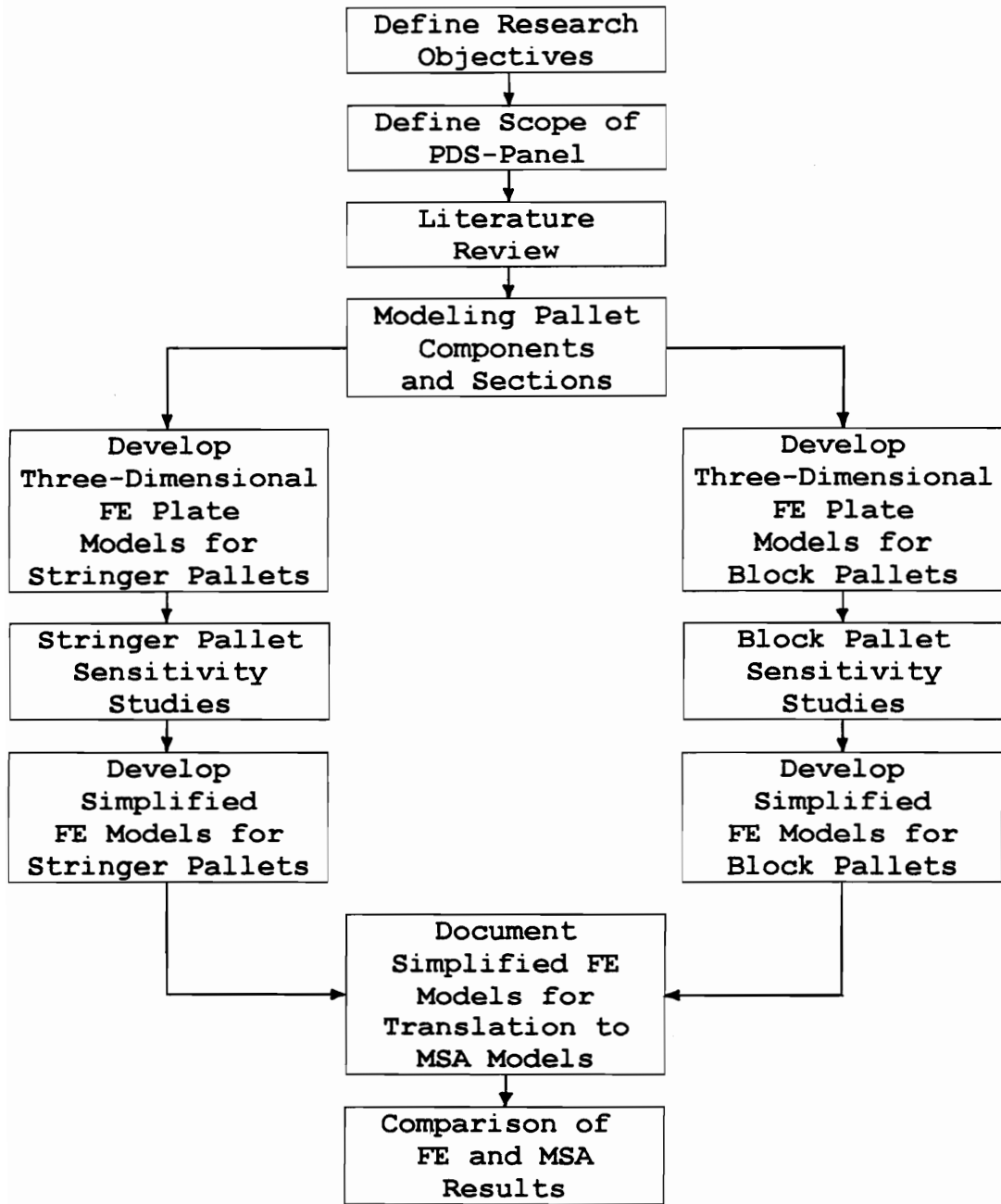
Stringer and block pallet models that considered all factors within the scope of PDS-panel were developed in this research. These models are thoroughly discussed in future chapters.

1.4 Scope of Research & Dissertation

A research plan was developed prior to beginning work which outlined the steps necessary to achieve the stated objectives. This plan is illustrated in Figure 1.3. The research conducted during this project followed this plan closely and is documented in this dissertation. Additional documentation is contained in a three volume research report (Mackes - Volumes 1, 2, and 3, 1998). The three volumes of this research report are referenced extensively in this dissertation.

Included in Chapter 2 of this dissertation is a thorough review of literature pertaining to pallets with panel decks, along with a brief discussion of the finite element method. Techniques used to model all components and nail joints commonly found in panel-deck pallets are presented in Chapter 3. Chapter 4 is devoted to modeling stringer pallets. Included in this Chapter is a discussion of finite element plate models developed for stringer pallets, sensitivity studies and subsequently, simplified model formulation. A similar presentation for block pallets can be found in Chapter 5.

A research summary and conclusions are presented in Chapter 6. Additional research needs are also discussed. In arriving at conclusions, this research spanned a time period from November, 1990 to September, 1997. This



FE Models - Finite Element Models that were developed using ABAQUS.
MSA Models - Matrix Structural Analysis Models that are compatible with existing PDS Programs.

Figure 1.3. Flow Chart of Research Plan.

dissertation is intended to provide an accurate account of the panel-deck pallet research conducted during this time period.

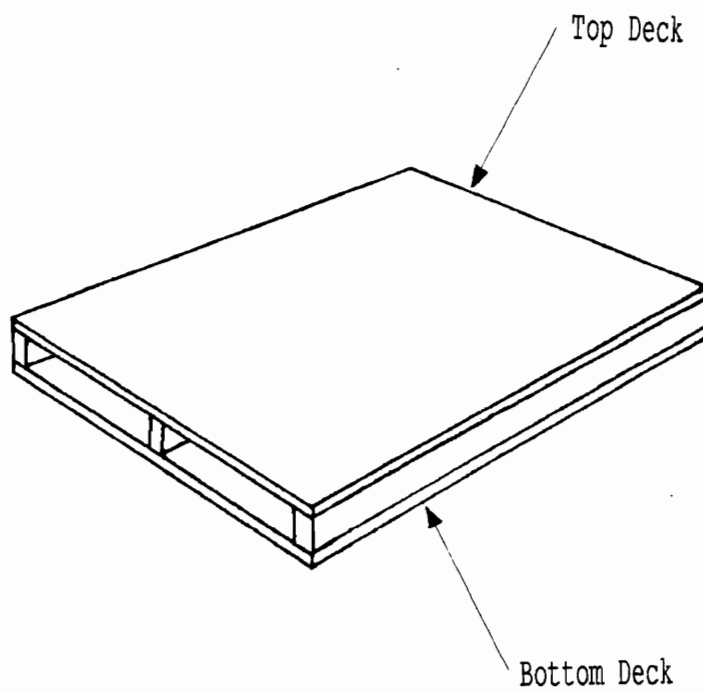
2.0 Literature Review

In this chapter, a review of pallet terminology is presented in the first section. The next section focuses on common panel-deck pallet geometries and configurations. Important pallet load and support conditions are then identified. Methodologies used to physically test pallets are critiqued, including a description of the air-bag test machine at Virginia Polytechnic Institute & State University (VPI & SU). This is followed by a review of methodologies in literature for modeling pallet components. A discussion of pallet design procedures emphasizing the Pallet Design System (PDS) and panel-deck pallets is presented. The final section is devoted to the finite element method, with emphasis on the ABAQUS finite element program and matrix structural analysis.

2.1 Pallet Terminology

Pallet definitions and terminology are contained in the standard ASME (ANSI) MH1.1.2 published by The American Society of Mechanical Engineers (1989). A discussion of pallet design terminology can also be found in the Pallet Design Short Course Manual (McLain et al., 1985).

A pallet is defined as a horizontal platform structure which acts as a base for assembling, storing, handling, and transporting materials and products in a unit load (ASME, 1989). As shown in Figure 2.1, a pallet has both a top and



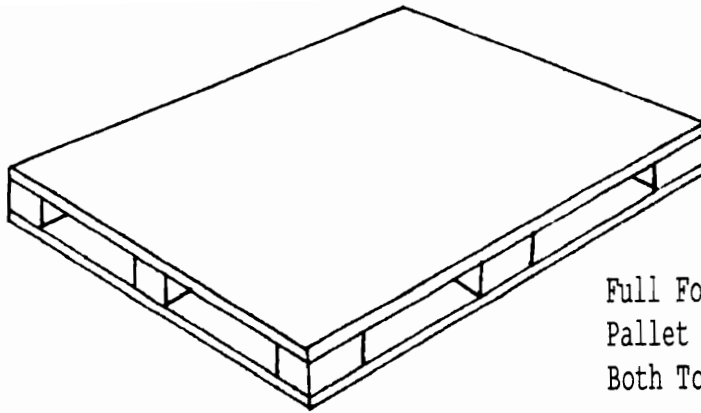
**Figure 2.1. Pallet exhibiting both
a Top and Bottom Deck.**

bottom deck, with the top deck considered to be the load-carrying surface and the bottom deck the load-bearing surface. Decks comprised of lumber strips are the most prevalent; however, panel decking such as plywood and OSB is also used.

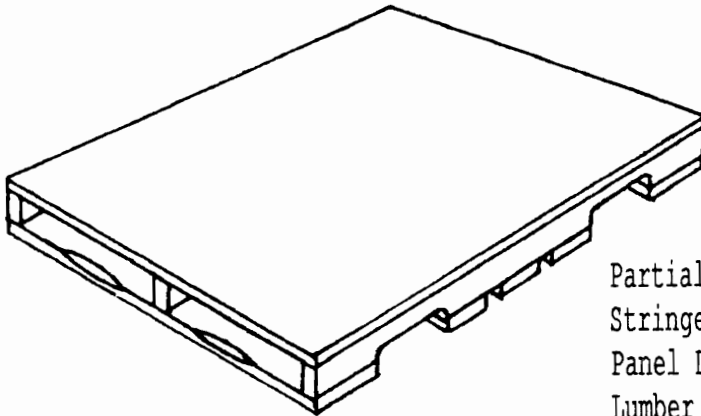
A pallet is considered to be reversible if the top and bottom deck are similar and both capable of carrying load. Non-reversible pallets have dissimilar top and bottom decks. As shown in Figure 2.2, pallets can be constructed to allow for full four-way, partial four-way, and two-way entry. Pallet decks can be flush if neither deck protrudes beyond the spacers, single winged if the top deck protrudes beyond the spacers, or double winged if both top and bottom deck protrude beyond the spacers. Pallets without a bottom deck are called skids or single faced pallets.

Pallet decks are separated by spacers, which also act to support the top deck if the bottom deck is fully supported. Pallets are manufactured with two distinct types of spacers, stringers and blocks. An example of both a stringer pallet and a block pallet is shown in Figure 2.3.

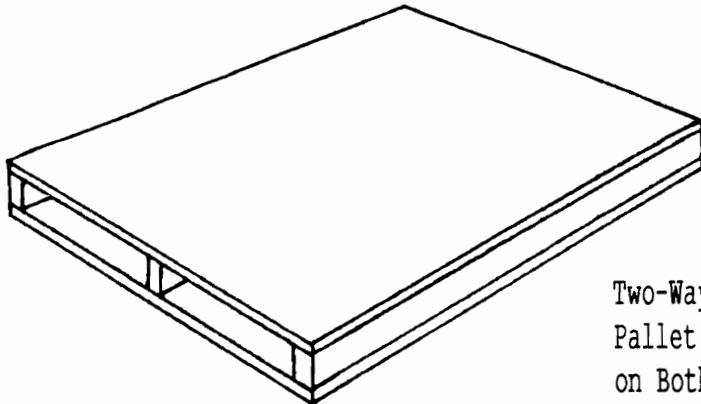
Stringers are a continuous longitudinal deck spacer normally of solid wood. Stringer pallets are typically constructed with 2 to 5 stringers. Stringers can be either unnotched or notched. Unnotched stringers only permit two-way entry, while notched stringers permit partial four-way



Full Four-Way-Entry Block
Pallet with Panel Decks on
Both Top and Bottom



Partial Four-Way-Entry
Stringer Pallet with a
Panel Deck on Top and a
Lumber Deck on Bottom

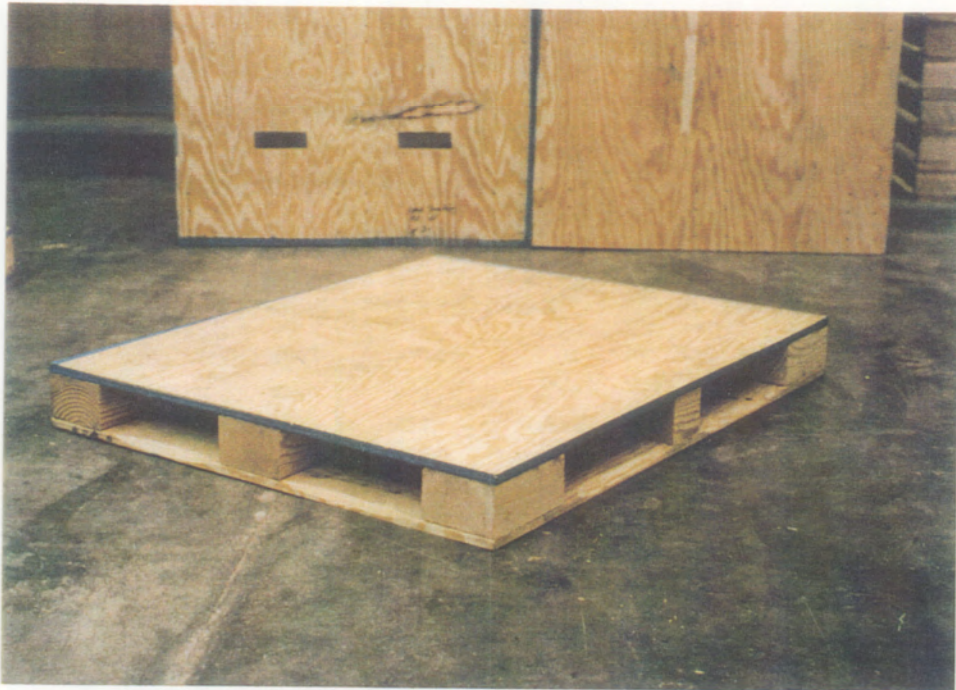


Two-Way-Entry Stringer
Pallet with Panel Decks
on Both Top and Bottom

**Figure 2.2. Full Four-Way, Partial Four-Way,
and Two-Way Entry Pallet Geometries.**



Stringer Pallet



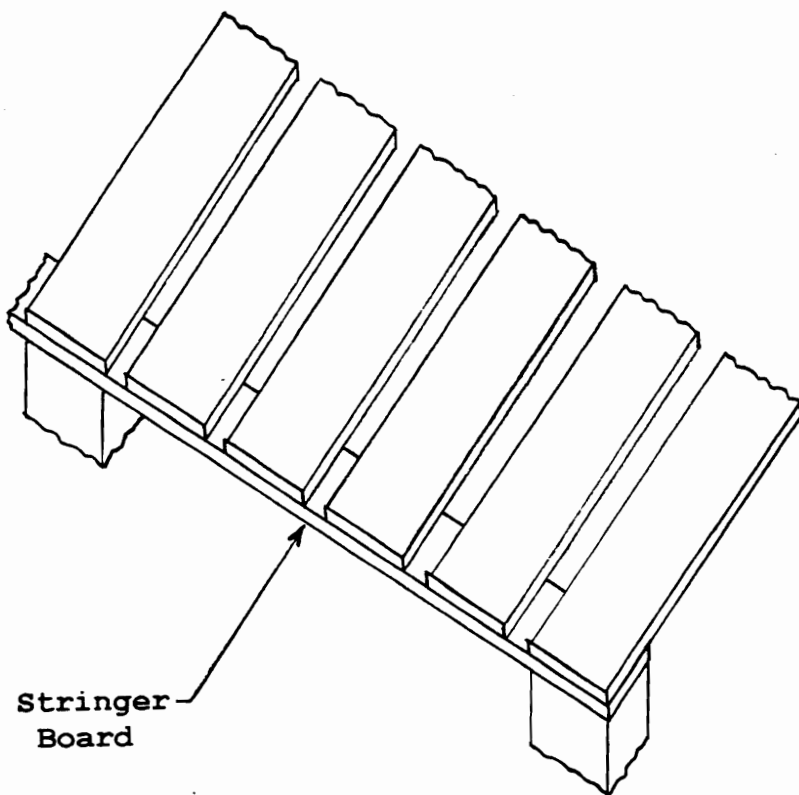
Block Pallet

Figure 2.3. An Example of a Stringer and a Block Pallet.

entry. Partial four-way pallet configurations permit full four-way entry by the forks of a lift truck, but restrict the load wheels of hand pallet jacks to two-way entry.

Blocks, legs, posts, or columns can be constructed of solid wood, composite wood-based materials, metal, plastic, corrugated paper, and other suitable materials. Block (leg, posts, or column) style pallets are typically constructed with 4 to 12 block configurations and normally allow either partial four-way or full four-way entry. Block pallets can be constructed with stringer boards as shown in Figure 2.4. Stringer boards can be cantilevered, extending beyond the block. As shown in Figure 2.5, pallet decks can have either a unidirectional or bidirectional configuration. A pallet deck is unidirectional if the deckboards (strips) are oriented in one direction. Bidirectional decks have boards (strips) which overlap or are butted in both directions, such as the perimeter-base pallet illustrated in Figure 2.5.

Pallets are assembled using nails, staples, screws, bolts, or any other suitable fastener. Helically threaded hardened or stiff-stock pallet nails are most common fasteners used. The performance of pallet joints can be described in terms of six possible modes of deformation shown in Figure 2.6 (Loferski, 1985). Generally, withdrawal/head embedment resistance, lateral resistance, and out-of-plane rotation are most important. Withdrawal



**Figure 2.4. A Block Pallet Section
Exhibiting a Stringer Board.**

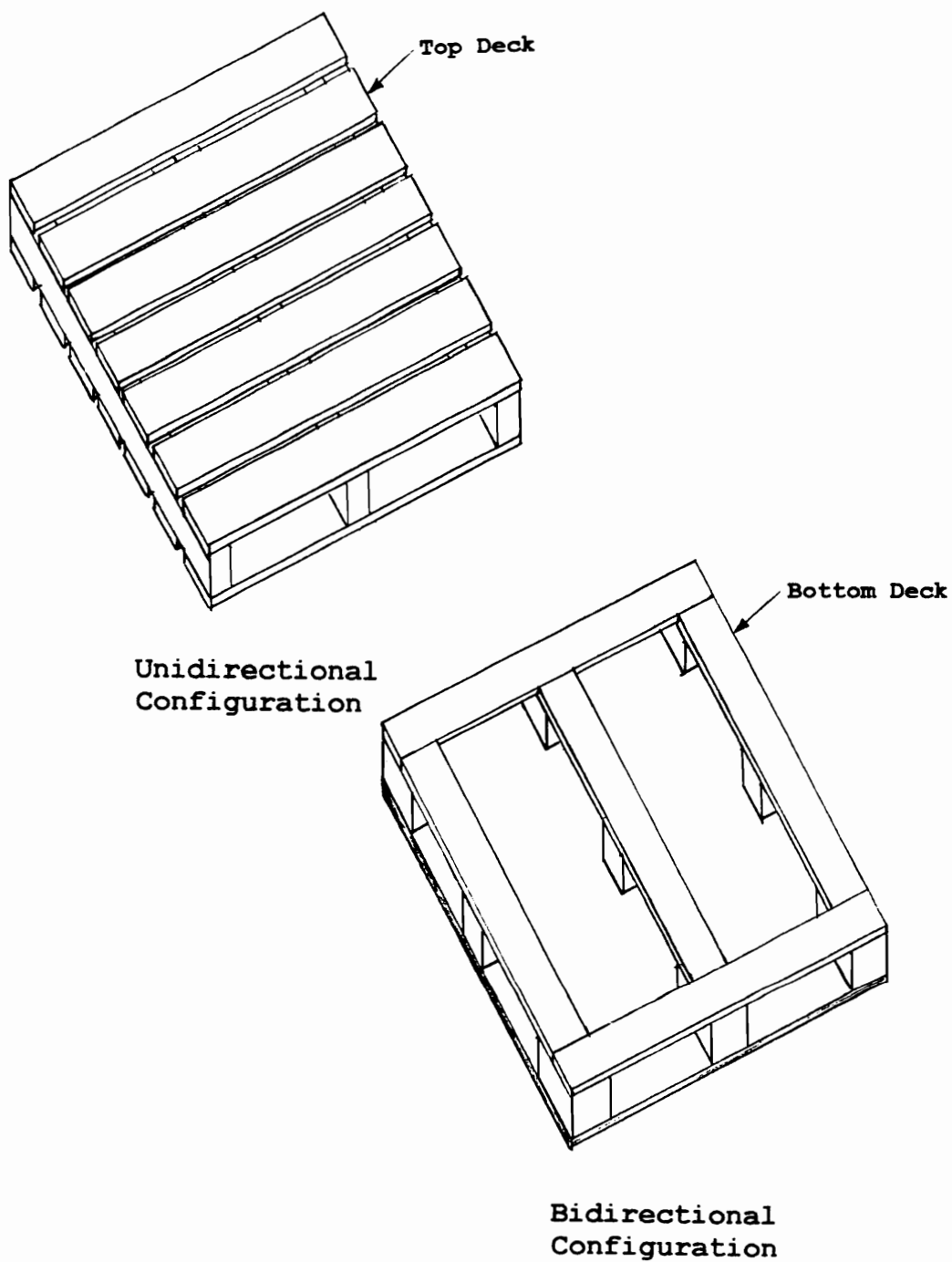


Figure 2.5. Strip-Type Deck Configurations.

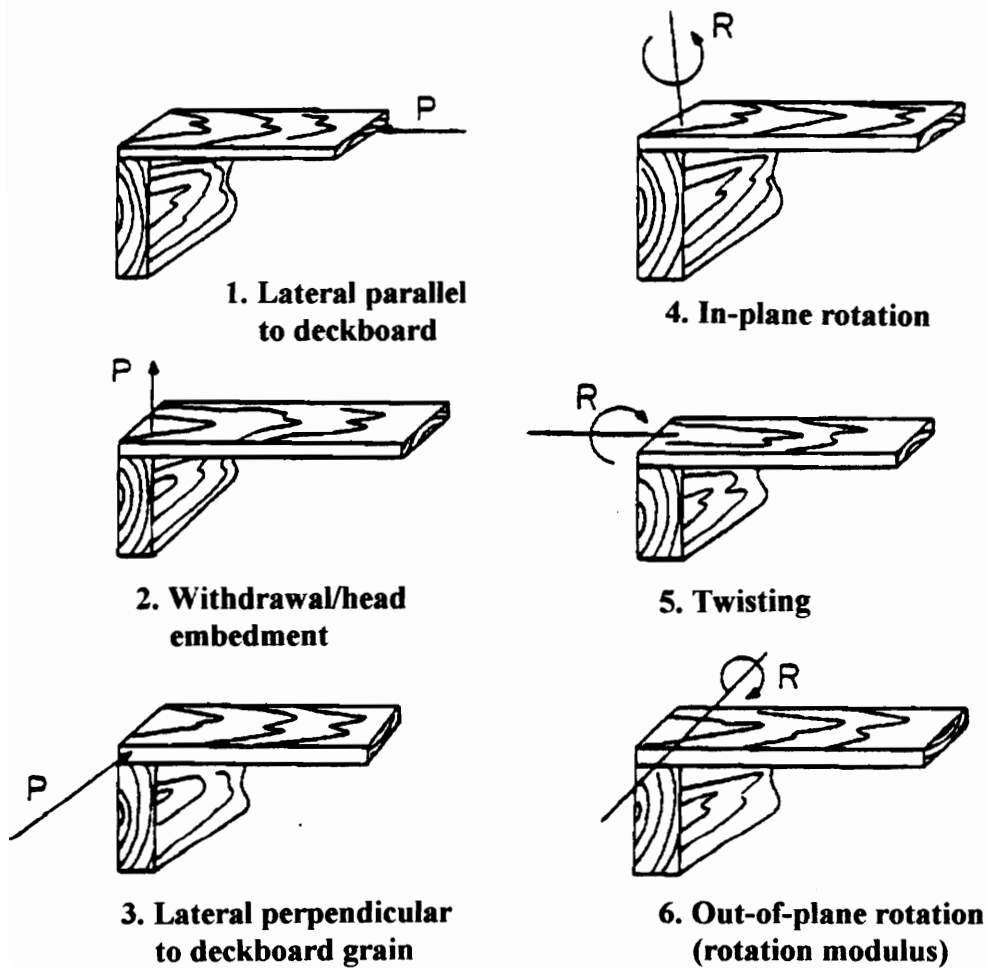


Figure 2.6. Components used to Simulate a Pallet Joint.

resistance is the ability of the spacer to impede the extraction of the fastener in withdrawal. Head embedment is the amount that the fastener head embeds into the deck as a function of load. Lateral resistance is the ability of the joint to restrain lateral movement of pallet components with respect to each other under load. Out-of-plane rotation resistance is the ability of the joint to resist deck rotation out-of-plane with the spacers (stringers or blocks).

2.2 Panel-Deck Pallet Geometries and Configurations

Panel-deck pallets have at least one deck comprised of one or more structural panels. A wide range of geometries and configurations are manufactured. Recommendations regarding geometries and configurations were published by the NWPCA and APA (1980) and the APA (1986). Because plywood and oriented strand board (OSB) are the most dominant panel types used in pallet manufacture (Krutnacker, 1974), only these panel types were considered in this study. Although potentially every grade of plywood and OSB, and even ungraded panels, can be used in pallet manufacture, the grades recommended by the APA for inclusion in PDS-PANEL are presented in Table 2.1. Grades are performance based. Design capacities of performance rated structural use panels were published by the APA (1991).

Table 2.1. Structural Panels Recommended
by the APA for Inclusion in PDS-PANEL.

SPAN RATING	PANEL THICKNESS (in.)	PANEL TYPE	NUMBER OF PLIES
24/16	7/16	OSB	-
32/16	15/32	OSB	-
		Plywood	3,4,& 5 Ply
40/20 or 20 oc	19/32	OSB	-
		Plywood	3,4,& 5 Ply
48/24 or 24 oc	23/32	OSB	-
		Plywood	4 & 5 Ply

The length of stringer pallets is defined as parallel to stringer orientation, while pallet width is perpendicular. For full four-way block pallets with panel decks, length is parallel to the strong (stiff) panel axis. Panel-deck pallets are variable in size typically ranging in both length and width from 24 to 96 inches. The most common size is 48 by 40 inches. A general discussion of pallet sizes can be found in ASME/ANSI Standard MH1.2.2 (ASME, 1997).

As with lumber deck pallets, panel-deck pallets can be manufactured with practically any fastener, including nails, staples, and bolts. However, helically-treaded hardened or stiff stock pallet nails are generally recommended for use. A wide range of fastener spacing patterns are also used. Basic recommendations for fastener selection and spacings were published for panel-deck pallets by the NWPCA and APA (NWPCA and APA, 1980).

Two general types of pallets are manufactured, stringer and block pallets. Both stringer and block (or post) pallets are manufactured with panel decks. These two pallet types are discussed in subsequent sections.

2.2.1 Stringer Pallets with Panel Decks

Panel-deck stringer pallets are generally manufactured with two to five stringers. However, three-stringer pallets

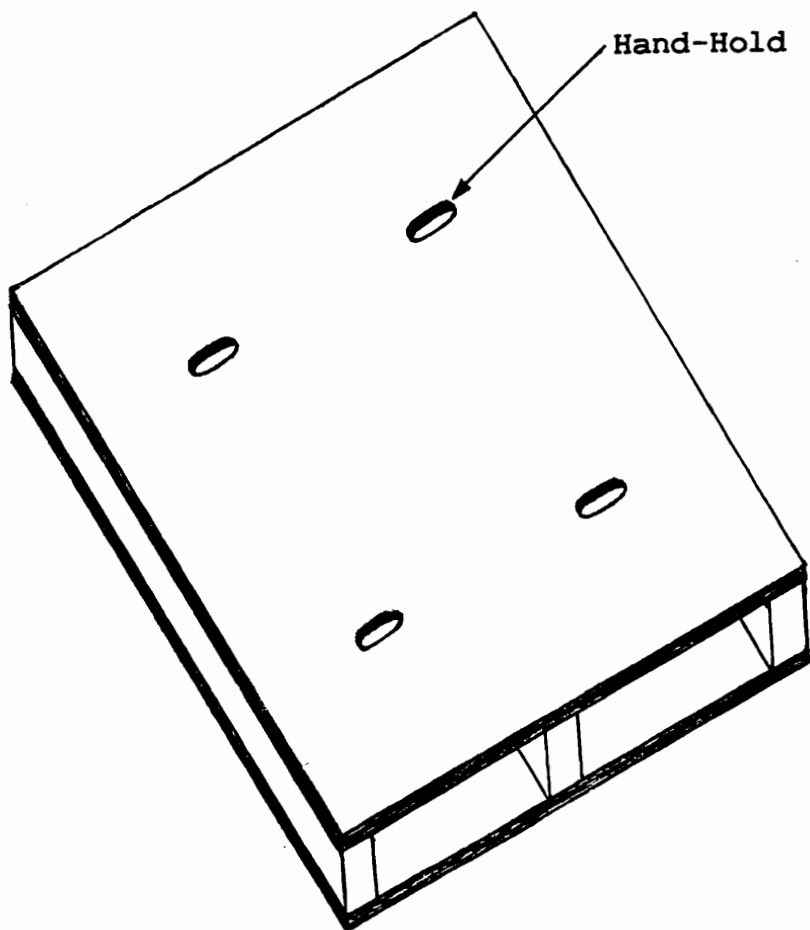
are most common. Stringers are normally solid wood of potentially any species and grade. Species commonly used for pallet stringers include oak, yellow-poplar, cottonwood, southern yellow pine, and spruce-pine-fir. Lower grades are generally used for economy. The most common cross-sectional size selected for use is 2x4, either actual or nominal, although many other sizes are used. Pallet stringers can be placed in service in the green condition or seasoned prior to use.

Stringer pallets with panel decks can be manufactured so they are reversible as shown in Figure 2.7. These pallets have full panel decks top and bottom, comprised with panels of the same grade such that either surface can potentially support a similar load. They are normally two-way entry. Reversible stringer pallets can have leading edge board reinforcement and cut-outs such as hand-holds also shown in Figure 2.7. They can be flush or winged.

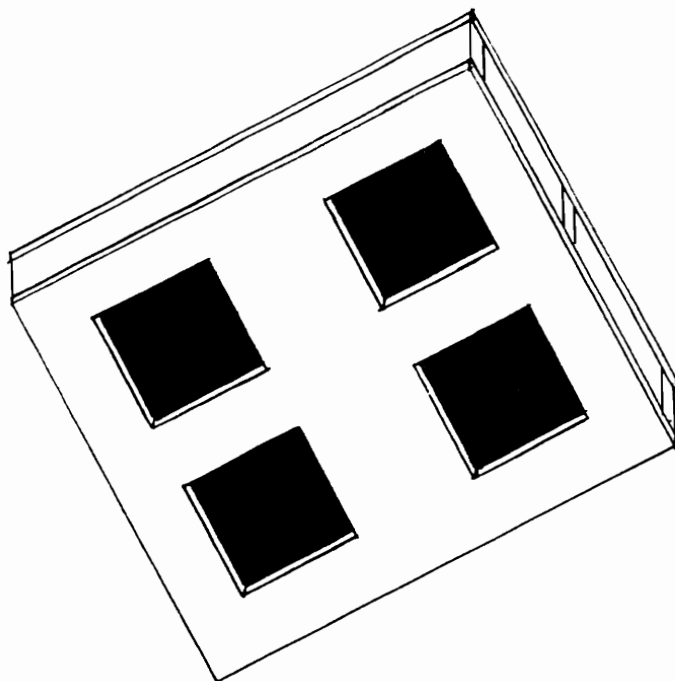
Non-reversible stringer pallets are also manufactured. Common non-reversible panel-deck pallet configurations include the following:

1. Stringer pallets having a panel deck top and a panel deck bottom with wheel openings (cut-outs).
2. Stringer pallets with a panel deck top and strip-type decking on the bottom.

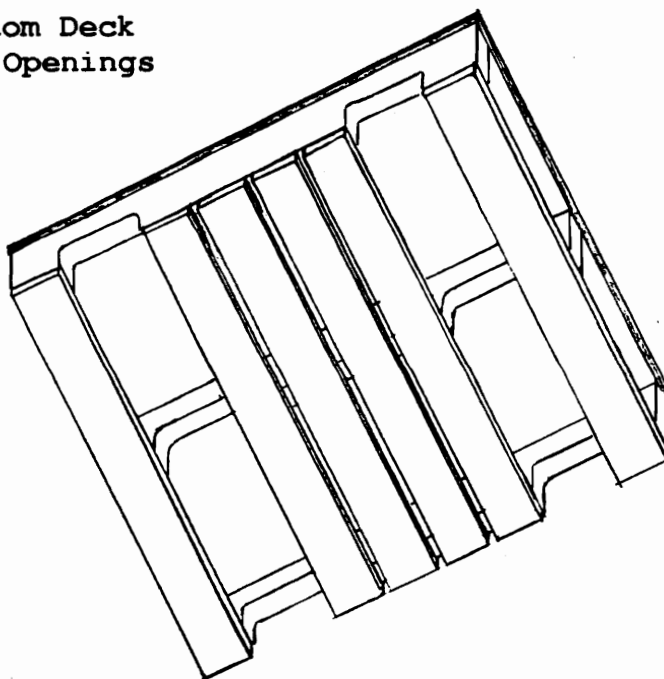
Examples of bottom deck configurations for non-reversible stringer pallets are shown in Figure 2.8. The first design



**Figure 2.7. Reversible Stringer Pallet
with Panel Decks Top and Bottom.**



Panel Bottom Deck
with Wheel Openings



Lumber Bottom Deck

**Figure 2.8. Bottom Deck Configurations
for Non-Reversible Stringer Pallets.**

is typically two-way entry; however, the latter can be either two-way entry if the stringers are unnotched or partial four-way entry if they are notched. Strip type-decking can be either lumber or structural panels cut into strips. Non-reversible stringer pallets can also be flush or winged.

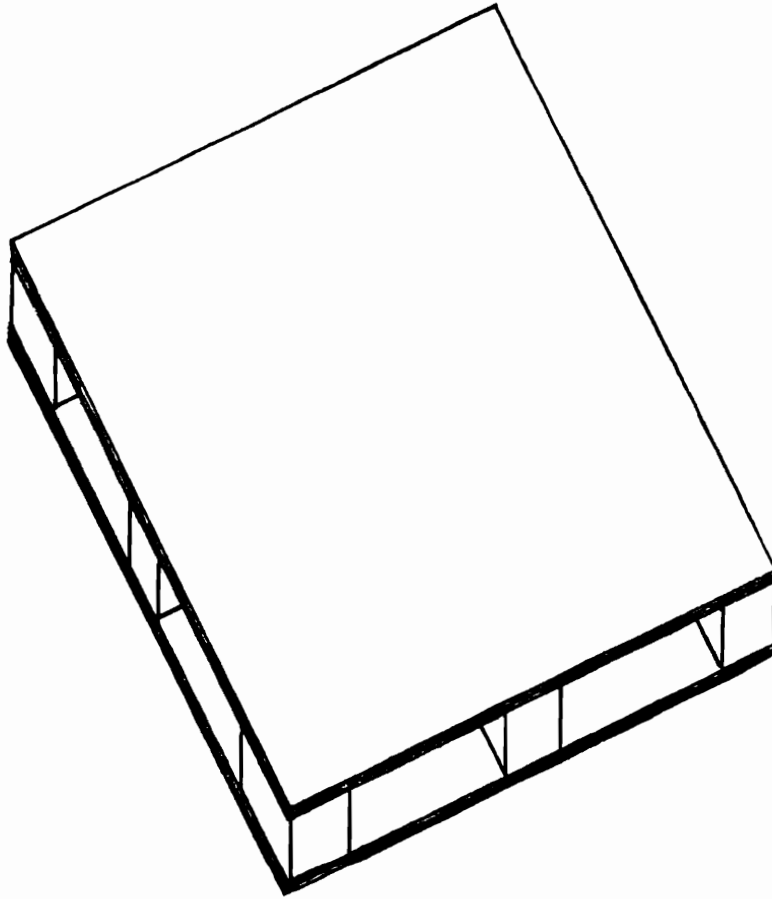
2.2.2 Block Pallets with Panel Decks

Panel-deck block (post) pallets can be manufactured with four, five, six, nine, twelve, or any other number of blocks. Nine-block pallets are most common. Blocks can be made of solid wood, composites such as plywood and OSB, metal, plastic, corrugated paper, or any other suitable material. Generally solid wood and composite blocks are the most common and are generally recommended for inclusion into PDS-PANEL.

Reversible block pallets as shown in Figure 2.9 are manufactured such that a similar load can be supported by either surface. Reversible panel-deck block pallet designs are normally full four-way entry. They can be flush or winged and have cut-outs such as hand-holds.

Several configurations of non-reversible block pallets are common, including the following:

1. Block pallets having a panel deck top and a panel deck bottom with wheel openings (cruciform).



**Figure 2.9. Reversible Nine-Block Pallet
with Panel Decks Top and Bottom.**

2. Block pallets with a panel deck top and unidirectional-base strip-type bottom deck.
3. Block pallets with a panel deck top and perimeter-base strip-type bottom deck.

Bottom deck configurations of non-reversible block pallets are shown in Figure 2.10. These designs are all normally full four-way entry. Non-reversible block pallets can also be flush or winged. Strip type-decking can be either lumber or structural panels cut into strips. Block pallets can also be manufactured with bottom deck configurations similar to those of stringer pallets with strip-type bottom decks if stringer boards are used.

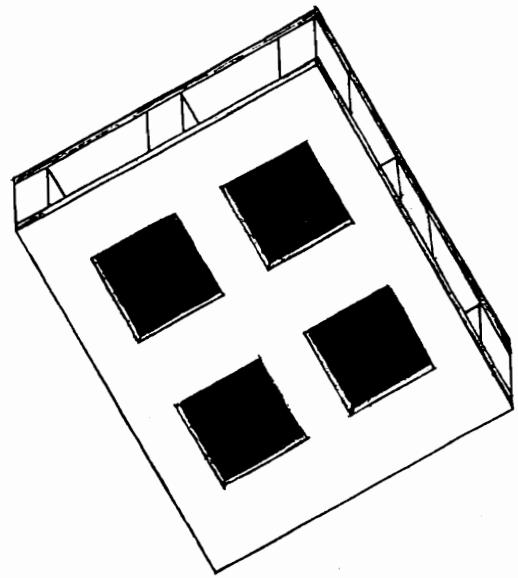
2.3 Pallet Load and Support Conditions

An on-site survey of 88 material handling environments was conducted by Goehring and Wallin (1981). Based on this survey, three classes were found to characterize the static loading of pallets:

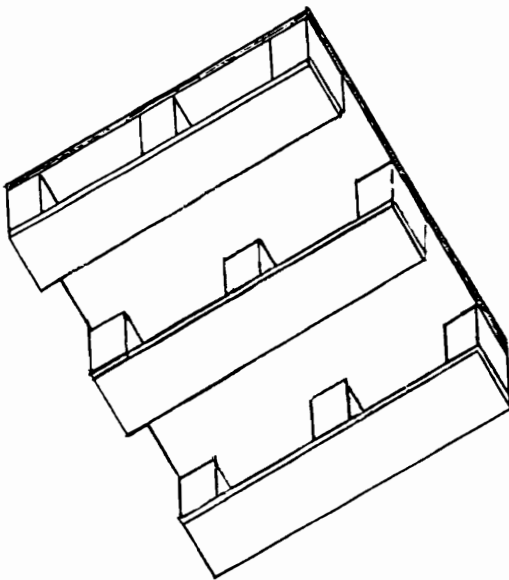
- 1) uniformly distributed loads which completely cover the deck
- 2) partially concentrated or uniform loads which cover only a portion of the deck
- 3) concentrated line or point loads

Support conditions were also classified into three classes:

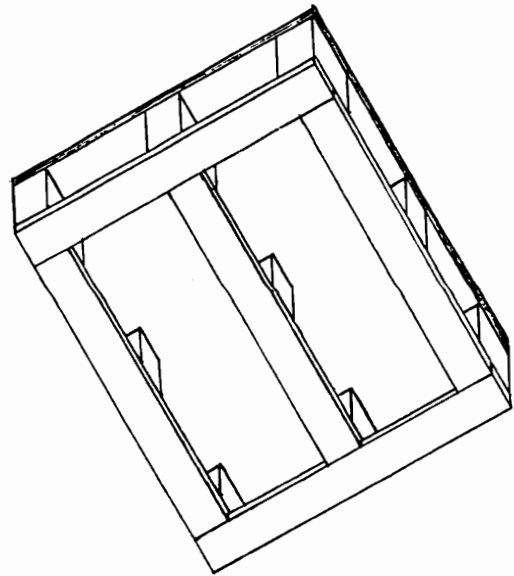
- 1) pallets loaded and dead piled in stacks (69%)
- 2) loaded pallets racked across deck (10%)
- 3) loaded pallets racked across stringers (21%)



Cruciform Base
Pallet



Unidirectional Base
Pallet



Perimeter Base
Pallet

**Figure 2.10. Bottom Deck Configurations
for Non-Reversible Block Pallets.**

Three principal PDS-PANEL load conditions are illustrated previously in Figure 1.1 and three principal PDS-PANEL support conditions in Figure 1.2. Although it was observed that there was some shift away from these theoretical load conditions in service, no attempt was made to quantify differences between theoretical and actual load conditions.

Subsequent studies by Fagan (1982) and Collie (1984) did consider the effects of load bridging on the theoretical load conditions. Load bridging was found to be dependent on load rigidity and pallet stiffness. This effect is relatively insignificant for very stiff pallets, becoming more severe with decreasing stiffness. Fagan (1982) concluded that for flexible pallets, assuming a uniformly distributed load can lead to the over-prediction of deflection by factors exceeding 50 percent.

2.4 Physical Pallet Testing

Standard test methods for evaluating pallets and related structures were published by the American Society for Testing and Materials (ASTM D 1185-94, reapproved 1994) and the American Society of Mechanical Engineers (ASME MH1.4.1M-1989). Test Methods were also published by the International Organization for Standardization (ISO 8611, 1988; ISO TR 10233, 1989). Published test standards for pallets are general in scope, although more applicable to

pallets with strip-type lumber decks. No standard test methods specifically dedicated to evaluating panel-deck pallets are currently published.

In this research, flexural stiffness tests were of particular importance. Flexural testing is usually conducted by applying line or uniform loads to the surface of the pallet. Line loads can be applied using testing machines with large platens or special racks designed for testing pallets. Uniform loads can be applied using vacuum chamber diaphragm mechanisms, pneumatic pressure bag (air bag) test machines, or traditional means such as hand loading bricks, sand bags, gravel, or some other unit load on the pallet. In this research an air-bag test machine built by researchers at VPI & SU was used to test pallets. This machine is discussed in Section 2.4.1. A review of literature pertaining to flexure testing conducted on panel-deck pallets is presented in Section 2.4.2.

2.4.1 Air-Bag Test Machine

An air-bag test machine built by researchers at VPI & SU is shown in Figure 2.11. A complete description and evaluation of this air-bag test machine is presented by Mackes et al. (1995). The machine, shown schematically in Figure 2.12, is a steel frame comprised of four legs and a top which acts as a reaction surface for the air-bag. The

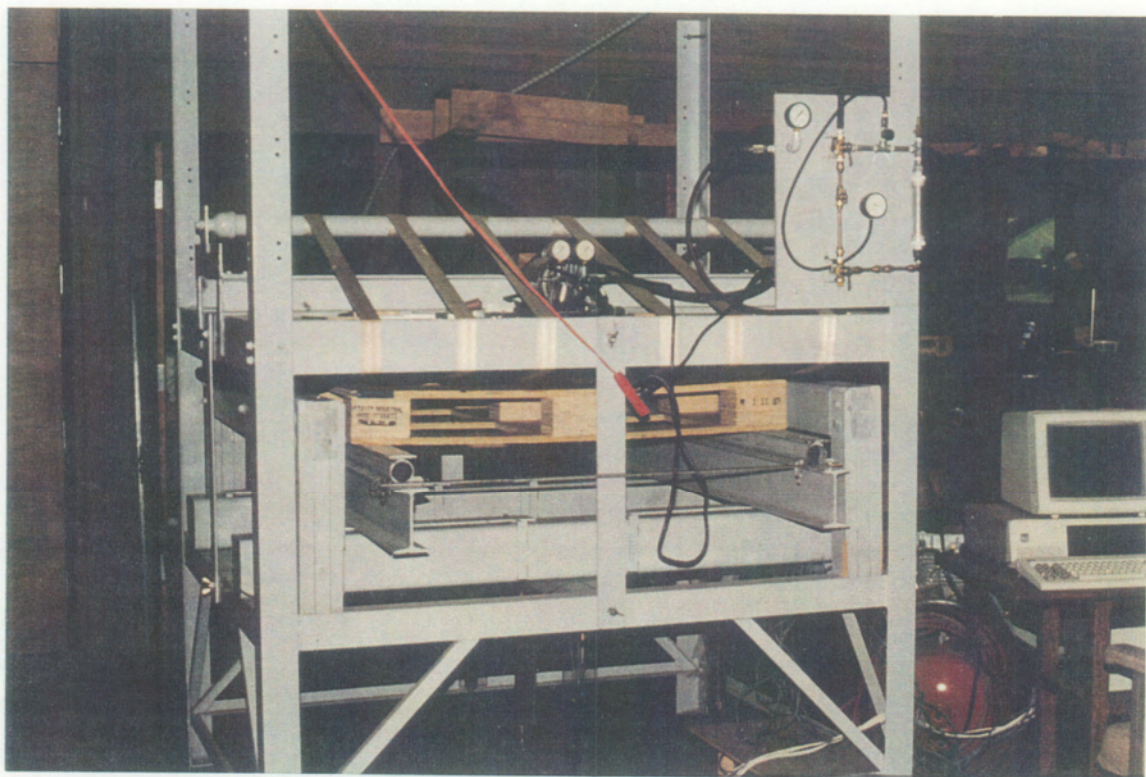
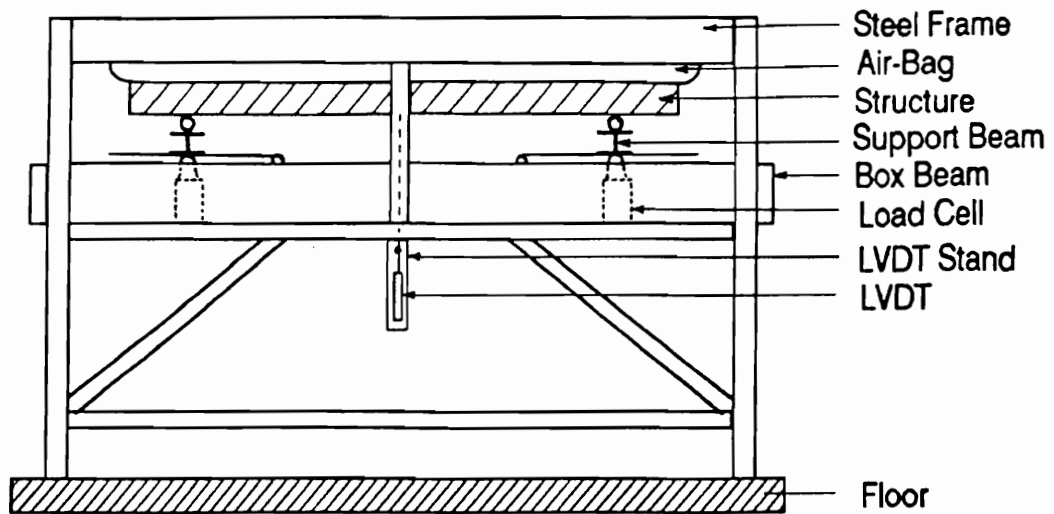
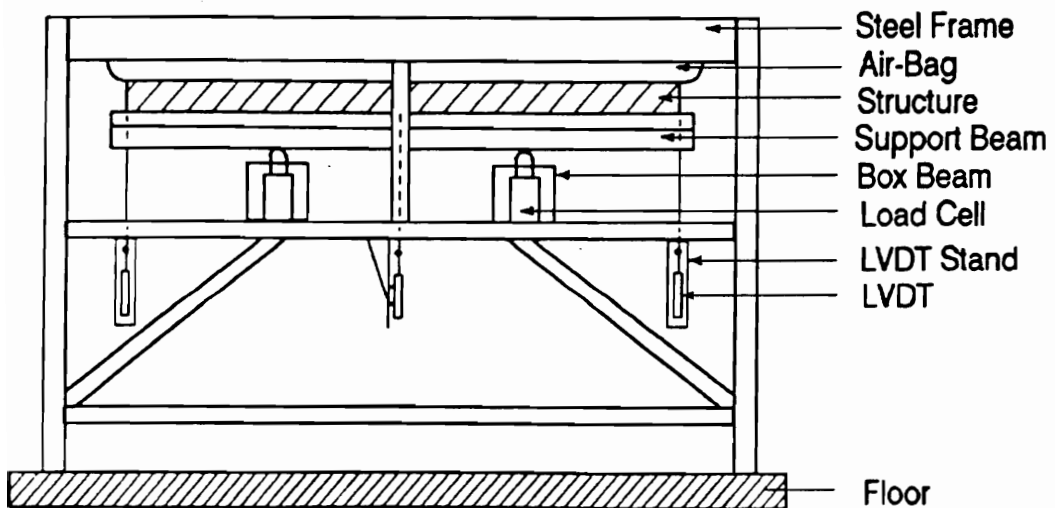


Figure 2.11. The Air-Bag Test Machine at VPI & SU.



Front View



Side View

Figure 2.12. Schematic Drawings of the Air-Bag Test Machine at VPI & SU.

air-bag is a Uniroyal PE-D-251 inflatable dunnage bag. The load rate is controlled by regulating air-flow into the dunnage bag. Four BLH Model USGI load cells are used to measure the applied load and pallet displacements are measured by Five Schaevitz Linear Variable Displacements Transformers (LVDT's). Load and deflection readings are collected using a data acquisition computer.

The air-bag test machine was built to deliver a uniform load to the decks of pallets in rack support conditions. However, the machine can be adapted to simulate all important load and support conditions for pallets. It can be used to test pallets 26 to 50 inches wide and 38 to 62 inches long. A discussion of the procedure used to operate the air-bag test machine is presented by Mackes (1998, Volume II, Section 7). Stringer pallet testing conducted in this research with the air-bag test machine is discussed in Section 4.2.3. Block pallet testing is addressed in Section 5.2.3. Panel-deck pallet testing unrelated to this research is reviewed in the next section.

2.4.2 Panel-Deck Pallet Testing

The majority of panel-deck testing to date has been conducted at VPI & SU. At VPI & SU, pallets are tested in flexure (bending) using the air-bag testing machine described in Section 2.4.1. Although much of this work is

proprietary, two reports issued by VPI & SU on panel-deck pallets are available in the public domain.

Lauer III and White (1992) evaluated the performance of perimeter base block pallets. Two versions of a 48 by 40 inch nine-block perimeter base pallet were tested. One type had a full 48 by 40 inch panel top deck and the other had a panel top with lead edge board reinforcement of nominal 1 by 4 southern yellow pine strips. Both versions exceeded ISO 8611 criteria for a working load of 2,800 pounds.

White (1993) conducted testing on 48 by 40 inch nine-block (post), non-reversible panel-deck pallets with OSB decks top and bottom. This work was part of a comparative study to determine the relative strength, stiffness, and durability of pallets constructed with wood, wood-based composites, plastics, corrugated fiberboard, and honeycomb.

Two hour static load tests were conducted on OSB pallets in accordance with ISO TR 10233 (1989). Deflection across the pallet length, which spanned 42 inches, was 0.739 inches. Deflection was 0.545 inches across the width which spanned 34 inches. Both of these deflections are within limits specified in ISO TR 10233 for a 2,800 pound load rating. Average initial pallet stiffness was 5,111 pounds per inch of pallet deflection racked across the length (RAL) and 6,851 pounds per inch of pallet deflection racked across the width (RAW).

For both the RAL and RAW support conditions, three replications of the OSB pallet were tested to failure under a uniformly distributed load. The span in the RAL support condition was again 42 inches and failure occurred at an average load of 8,507 ponds. A 34 inch span was again used in the RAW support condition, with failure occurring at an average load of 8,572 pounds. All failures were brittle, occurring almost instantaneously with the top and bottom decks both failing catastrophically at once.

2.5 Modeling Pallet Components

In this section, methodologies for modeling pallet components are reviewed. This includes panel decks, strip-type decking, stringers, blocks, and pallet joints. Methodologies used to model contact between the decks and spacers are also discussed briefly along with those used to model pallet joints.

2.5.1 Panel Decks (Structural Panels)

Structural panels are typically modeled as plates. Anisotropic (orthotropic) plate theory was summarized thoroughly by Lekhnitskii (1968). Plate bending theory is based on the assumption that the thickness of a plate is thin with respect to its length and width dimensions. Kirchhoff plate theory and the Mindlin plate theory can be used to model plates in bending (Bathe, 1982). Kirchhoff

theory ignores shear deflections, and material particles that form lines which are originally perpendicular to the mid-surface are assumed to remain straight and perpendicular during deformation. Mindlin theory considers shear, and lines normal to the mid-surface remain straight during deformation, but do not necessarily remain perpendicular.

For a homogenous orthotropic plane material, the generalized form of Hooke's law is:

$$\begin{bmatrix} \gamma_{11} \\ \gamma_{11} \\ \gamma_{12} \end{bmatrix} = \begin{bmatrix} 1/E_1 & -v_{21}/E_2 & 0 \\ -v_{12}/E_1 & 1/E_2 & 0 \\ 0 & 0 & 1/G_{12} \end{bmatrix} \begin{bmatrix} \sigma_{11} \\ \sigma_{22} \\ \sigma_{12} \end{bmatrix} \quad [2.1]$$

Where: γ = strain

σ = stress

E_1 = MOE in 1-direction

E_2 = MOE in 2-direction

v_{12} = Poisson's ratio of strain in the 2 direction to strain in the 1-direction for a normal stress in the 1-direction

v_{21} = Poisson's ratio of strain in the 1 direction to strain in the 2-direction for a normal stress in the 2-direction

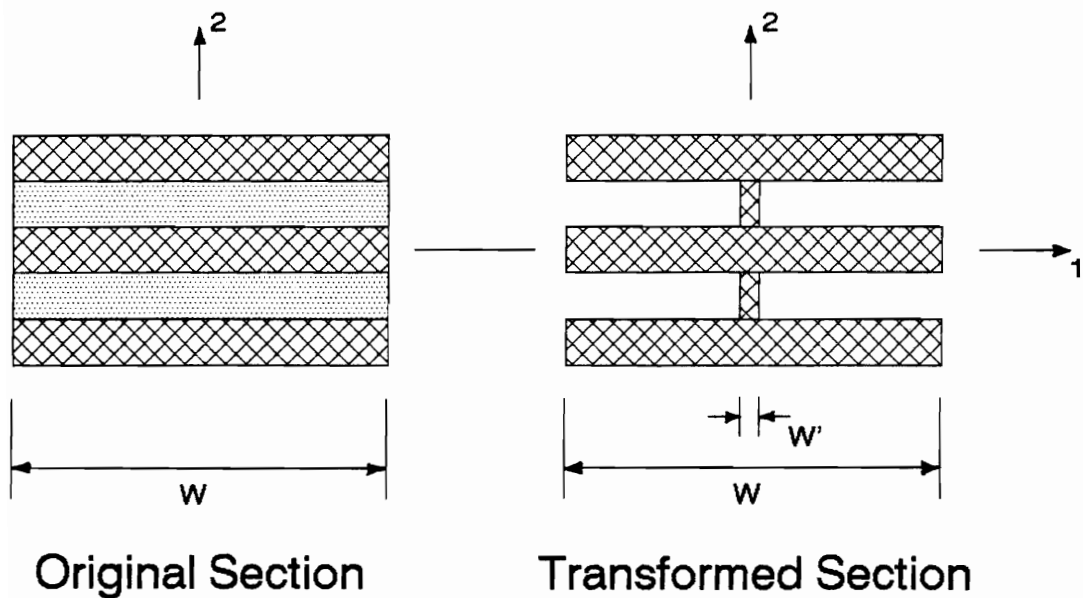
G_{12} = modulus of rigidity in the 12 plane

In this research, composite wood-based panels were assumed to have homogeneous cross-sections because MOE and MOR values provided for use in PDS-Panel were based on this assumption. However, composite wood-based panels such as

plywood and OSB are constructed with alternating plies or layers of material. Because the properties of wood are generally orthotropic, these alternating plies or layers have different stiffness properties. For rotary-cut softwood plywood, veneer plies oriented parallel-to-grain are often assumed to be 35 times stiffer than plies oriented perpendicular-to-grain (Bodig and Jayne, 1982). For five ply plywood, this is illustrated using a transformed section in Figure 2.13.

A discussion of test procedures for evaluating structural panels can be found in ASTM D 3043-87 (ASTM, 1994). Significant differences can occur depending on which test method is used to determine MOE and MOR. The relationship between MOE and MOR values determined using small-specimens (strips) and large panel bending tests was discussed by McNatt, Wellwood, and Bach (1990). MOE values are generally 10 to 20 percent lower for small specimens, while MOR values are significantly greater (up to 30 percent). The magnitude of difference is dependent on panel orientation and load and support conditions. Differences are due to plate (membrane) action present in larger panels which can be attributed to a Poisson's effect.

Measuring Poisson's ratio in structural plywood and OSB is extremely difficult. This property can be extremely variable for composite panels, varying as a function of



W - Original Width

W' - Transformed Width

▣ - Strong Axis of Panel Oriented
in the 1-Direction

▤ - Weak Axis of Panel Oriented
in the 1-Direction

Figure 2.13. Transformed
Section of 5-Ply Plywood.

material, panel thickness, number of plies or layers, adhesive quality, and so on. In this research, Poisson's ratios are taken from literature. The following relationship used for plywood is based on work by Freas (1964) and Leichti (1986):

$$\nu_{12} * \nu_{21} = 0.01 \quad [2.2]$$

Based on work by Bulleit (1985) and Leichti (1986), the relationship used for OSB is:

$$\nu_{12} * \nu_{21} = 0.04 \quad [2.3]$$

G_{12} values are also taken from literature (Bodig and Jayne, 1982).

Grid-Framework methods can also be used to model plates in flexure (Hrennikoff, 1941; Yettram and Husain, 1965). Iyer (1989) used an equivalent grid technique suitable for matrix-displacement analysis to model idealized thin, orthotropic plates. The matrix-displacement approach used is discussed further in section 2.7.2. This grid model was unique because it was extended to plates exhibiting material orthotropy and it also had fewer members than previous grid formulations. The maximum error between predicted and theoretical deflections for plywood and OSB plates was 20 percent. The use of grids to model structural panels is discussed further in Section 2.7.1.3.

2.5.2 Strip-Type Decking

Strip-type decking is generally modeled using beams or assemblages of beam elements. Loferski (1985) used beams to model stringer pallets with lumber decks in the stack support condition and a matrix structural analysis approach utilizing beam elements to simulate the lumber decks of stringer pallets supported in the RAD and RAS conditions. Figure 2.14 shows the RAD model developed by Loferski (1985) which uses beam elements to simulate lumber decks. In PDS-BLOCK (NWPCA, 1988) beam elements are utilized to model the lumber decks of block pallets. Literature on modeling plywood and OSB strip decking is scant, although the APA recommends a minimum strip width of 6 inches.

Other than coordinates which account for the length of the deck, the principal geometric requirements for modeling strip-type decks are cross-sectional dimensions (width and thickness) of the strip. When a two-dimensional model is used, the width of the strips comprising the pallet deck are usually summed and average property values for the summed strips are used. In three-dimensional models, each strip is represented by an assemblage of beam elements.

The principal property values required for modeling strip-type decking are the MOE along the length of the strip and MOR. The standard deviation of these property values is also required for reliability-based design. Methodologies

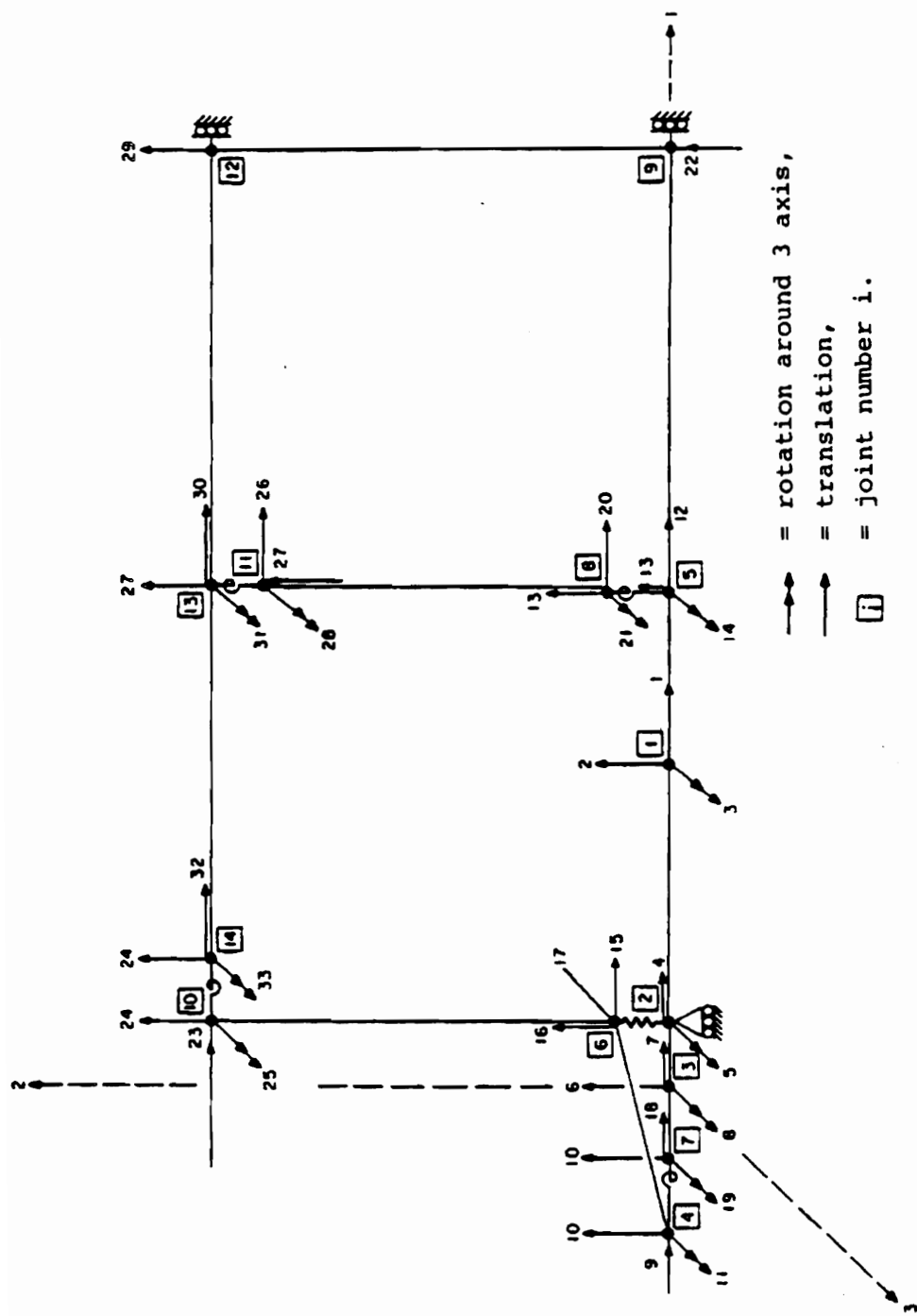


Figure 2.14. Model Developed by Loferski (1985) which Simulates Stringer Pallets Supported in the RAD Condition.

have been developed for determining the design values of lumber deckboards, which are often called pallet shook. These methodologies are generally based on modifying clear wood strength properties for defects. Methods for adjusting clear wood strength properties to allowable design values are contained in ASTM D 245-93 (ASTM, 1994). Because pallet shook is often of low quality with many defects, ASTM D 245-93 may not provide adequate adjustment.

Wallin et al. (1976) developed design values for pallet shook, recommending five visually graded classes. Strength and stiffness values were determined by testing random samples for each grade to evaluate the percentage of strength reduction. Strength reduction was expressed as a ratio and was defined by Wallin et al. as the strength of a member with defects divided by the clear wood strength. Grade-mix factors were recommended for pallet shook of mixed grade.

Hardwoods and softwoods are subdivided into classes in PDS. PDS species classes are shown in Table 2.2 for North American and European species. Classes are further segmented into grades as outlined in Table 2.3. MOR and MOE values are assigned to each class and grade based on either in-grade testing or modification of clear wood values as specified in ASTM D 245-93 (ASTM, 1994). In-grade test data are available for all commercially important domestic

Table 2.2. PDS Species Classes.

North American Species			
<u>Class 1</u> Hickory Birch: Yellow Sweet Maple: Sugar Black Red Ash: Green White Elm: Rock Slippery American Beech Black Locust Black Cherry Tanoak Dogwood Persimmon Eucalyptus <u>Class 2</u> Bigleaf Maple Oregon Ash <u>Class 3</u> Sweetgum Tupelo Paper Birch Ash: Black Pumpkin Hackberry Sycamore Maple: Silver Striped Magnolia	<u>Class 4</u> Oregon White Oak California Black Oak Cascara Chinquapin Myrtle Madrone <u>Class 6</u> Red Alder <u>Class 7</u> Aspen: Bigtooth Quaking Catalpa Buckeye Butternut American Basswood Cottonwood: Black Balsam Poplar Eastern <u>Class 11</u> Douglas-fir: Coast Interior West Interior North Interior South Western Larch Southern Pine: Loblolly Longleaf Shortleaf Slash	<u>Class 12</u> Hemlock: Western Mountain Fir: California Red Grand Noble Pacific Silver White <u>Class 13</u> Spruce: White Black Red Engelmann Sitka Pine: Sugar Western White Lodgepole Ponderosa Monterey Jack Norway Eastern White Southern Pine: Pitch Pond Spruce Virginia Fir: Subalpine Balsam Baldcypress Eastern Hemlock Western Red Cedar Redwood	<u>Class 14</u> Cedar: Alaska Incense Port Orford Atlantic White Northern White Eastern Red <u>Class 21</u> Eastern Red Oaks Eastern White Oaks <u>Class 22</u> Southern Pine: Loblolly Longleaf Shortleaf Slash <u>Class 29</u> Yellow-Poplar
European Species			
<u>Class 31</u> Mengkuiang Kapur Keruing <u>Class 32</u> Ash: European Beech: European Oak: European Pine: European	<u>Class 33</u> Douglas-fir Larch: European Japanese Pine: Maritime Scots Jack <u>Class 34</u> Poplar: Grey Black Italian Elm: Dutch Redwood	<u>Class 34 - Cont.</u> Fir: Silver Larch: Hybrid Pine: Lodgepole Corsican Fir: Silver <u>Class 35</u> Elm: English Spruce: Sitka (Canada) Whitewood	<u>Class 36</u> Pine: Radiata Spruce: Black Norway Willow: White Spruce: White Sitka (U.K., Eire) <u>Class 37</u> Poplar: Hybrid

Table 2.3. PDS Grade Identification Guide.

PDS GRADE ID	NWPCA HARDWOOD PALLET STANDARDS	NWPCA SOUTHERN PINE PALLET SPECIFICATIONS	GRADES FROM PEP STUDY REPORT
1	PRECISION	SP-1	2 & BETTER
2	PREMIUM/AA & BETTER	SP-2 & BETTER	3 & BETTER
3	A & BETTER	SP-3 & BETTER	4 & BETTER
4	ALL LUMBER	ALL LUMBER	ALL LUMBER
5	ONLY PREMIUM/AA	ONLY SP-2	ONLY 3
6	ONLY A	ONLY SP-3	ONLY 4
7	CULL	CULL	CULL
PDS GRADE ID	NWPCA WEST COAST AND WHITE WOODS PALLET STANDARDS		
11	PREMIUM		
12	STANDARD & BETTER		
13	SHIPPING & BETTER		
14	ONLY STANDARD		
15	ONLY SHIPPING		

hardwood and softwood species. Adjusted clear wood properties are used where in-grade test data is lacking, primarily for some imported species. For these species, clear wood properties are obtained from testing conducted in accordance with ASTM D 2555-88 (ASTM, 1994). Mean values and standard deviations are required for reliability based design. Therefore, strength ratios are based on mean values rather than minimums specified in the standard. Weighted averages (design values) are assigned to pallet shook of mixed grades; whereas, traditional methods use design values for the lowest grade in the mix.

2.5.3 Stringers

Stringers function differently dependent on the pallet support conditions. Stringers act as reaction supports in the stack support condition. They function as spacers in the RAD support condition, with minimal impact on pallet strength and stiffness. In the RAS support condition, stringers are stressed as multiple parallel beams. With regards to modeling stringers, the majority of research has focused on pallets supported in the RAS support condition.

Both notched and unnotched stringers are used in pallet manufacture. Notching a stringer has a dramatic impact on strength and stiffness properties in the RAS support condition. Bastendorff and Polensek (1984) tested notched

and unnotched red alder pallet stringers. They reported a 44 percent MOR reduction for double-notched stringers. The notches were 9 inches wide, 1.25 inches deep, and had corner fillet radii of 0.75 inch as shown in Figure 2.15. Methodologies used to model both unnotched and notched stringers are discussed in subsequent sections.

2.5.3.1 Unnotched Stringers

In the RAS support condition, unnotched stringers are usually modeled as beams or assemblages of beam elements. An assemblage of beam elements used by Loferski (1985) to model stringer pallets supported in the RAS condition is shown in Figure 2.16. This is a matrix grid model. With regards to stringers, other than nodal coordinates, the only geometric inputs to the model are cross-sectional dimensions (stringer height and width). The principal material property required is the MOE along the length of the stringer. Because stringers are generally of solid wood, this normally will correspond to the longitudinal direction of the wood comprising the member. Predicted stiffness values generated by this grid model were compared to experimental values collected by Collie (1984), with differences averaging 15.9 percent.

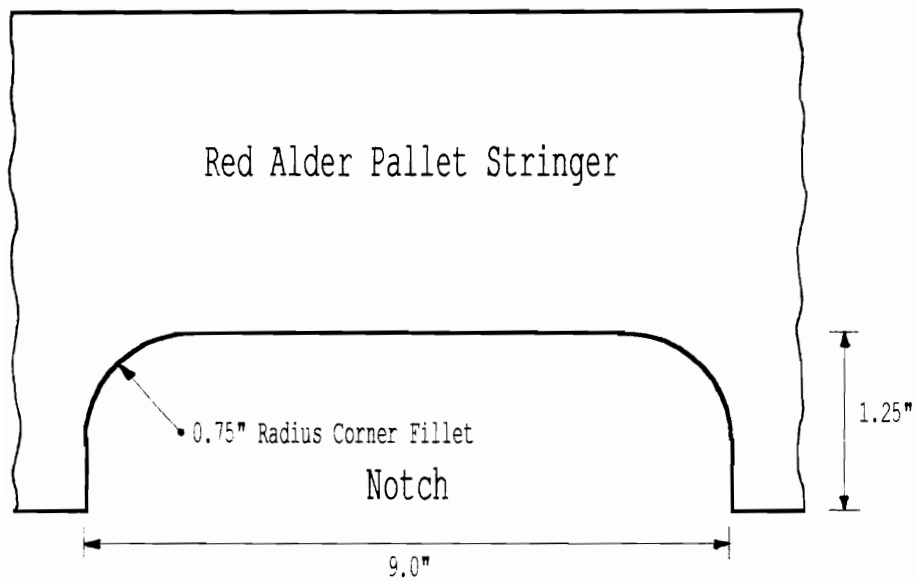


Figure 2.15. Stringer Notch used in Testing Conducted by Bastendorff and Polensek (1984).

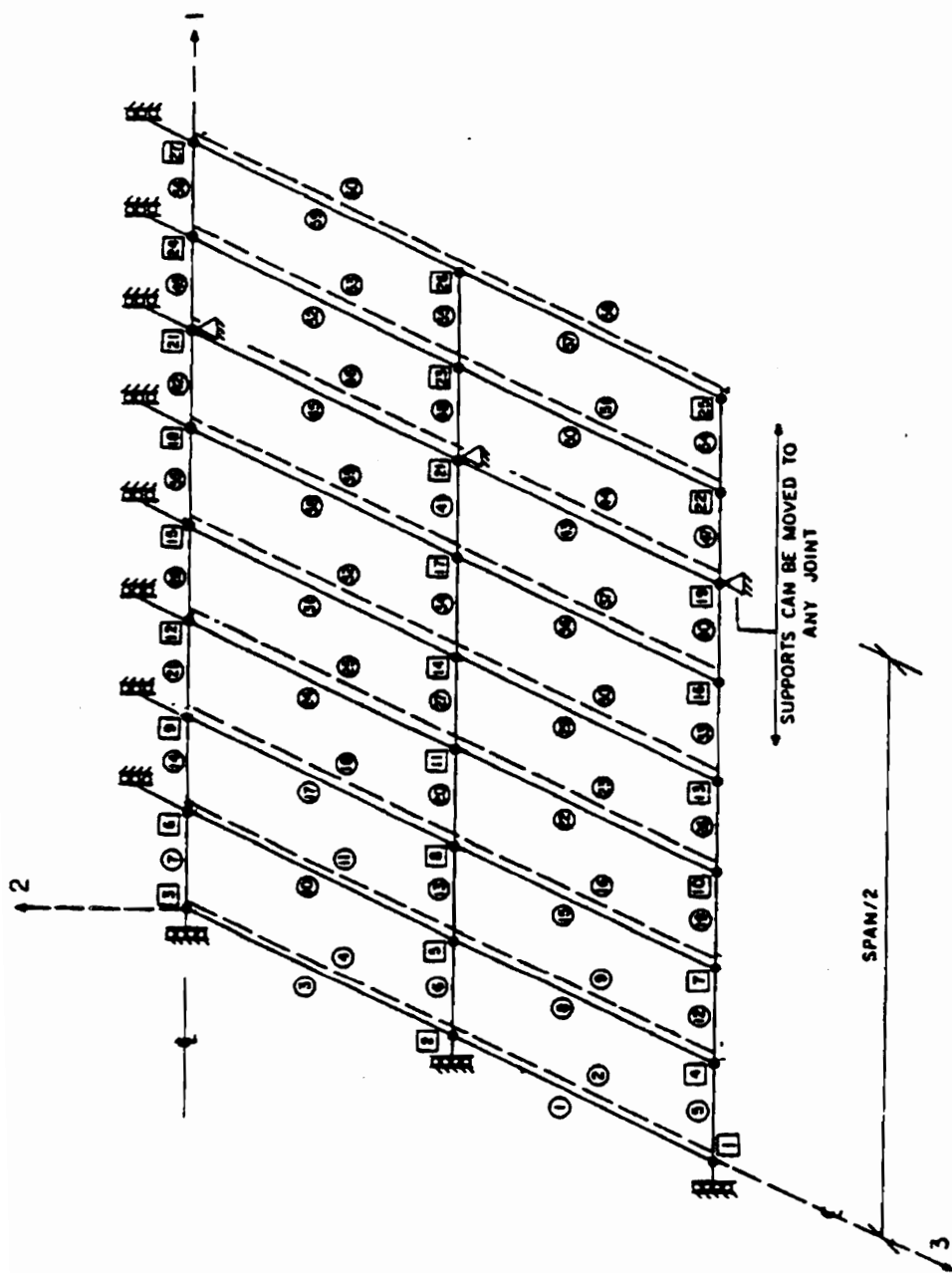


Figure 2.16. Model Developed by Loferski (1985) which Simulates Stringer Pallets Supported in the RAS Condition.

2.5.3.2 Notched Stringers

Gerhardt (1985) used the finite element method to model the behavior of notched pallet stringers in the RAS support condition. Twelve-node isoparametric plane elements were used to model single- and double-notched green oak stringers. Fillet regions of the notches were modeled using a hybrid finite element. Results from the finite element analysis showed excellent agreement with experimental values. Gerhardt used these models to develop equations for computing the stress and deflection of notched stringers. Loferski (1985) used these equations to model pallets constructed with notched stringers. The methodology currently used in PDS to predict the behavior of notched stringers is based on work by Zalph (1989).

2.5.4 Blocks

As with stringers, blocks function differently depending on the pallet support condition. Blocks act primarily as reaction supports in the stack support condition. They function principally as spacers in the rack (both RAW and RAL) support conditions.

Methodologies for modeling blocks in literature are scant. Samarasinghe (1987) used zero-length springs to simulate the localized crushing of blocks in the stack support condition. This so called *edge crushing effect*

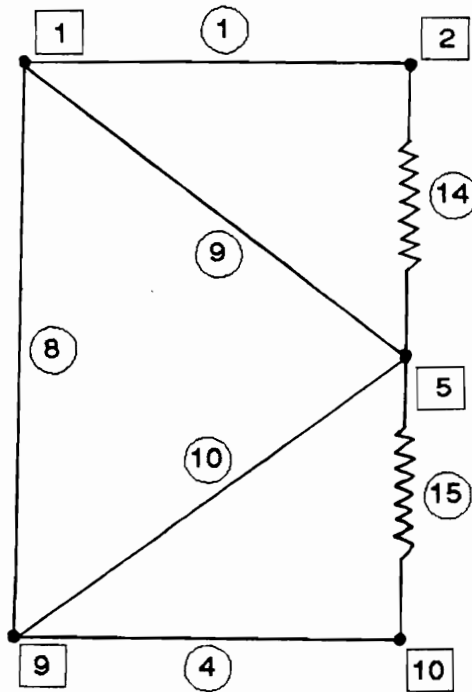
occurs at locations where the block comes in contact with the pallet deck.

In rack support conditions, blocks can be modeled using assemblages of beam elements attached to elements simulating the pallet decks using springs (Colclough, 1987 and NWPCA, 1988). An element assemblage used in PDS-BLOCK to simulate blocks is shown in Figure 2.17. Springs represent the edge crushing effect on the block caused by contact with the pallet deck.

2.5.5 Pallet Joints

Pallet joints in three dimensional space have six possible degrees of freedom or modes of action shown in Figure 2.18. Sensitivity studies conducted by Colclough (1987) showed that only out-of-plane rotation (rotation modulus) significantly influences the structural behavior of block pallets. The other stiffness components can be held constant with little loss of accuracy. Essential joint parameters for effectively modeling stringer-type pallets are the load carrying capacity, the translational stiffness (slip modulus), the separation or withdrawal modulus, and the rotational stiffness (rotation modulus) of the joint (Loferski, 1985).

Load carrying capacity of pallet joints has been extensively researched. Maximum joint capacity is

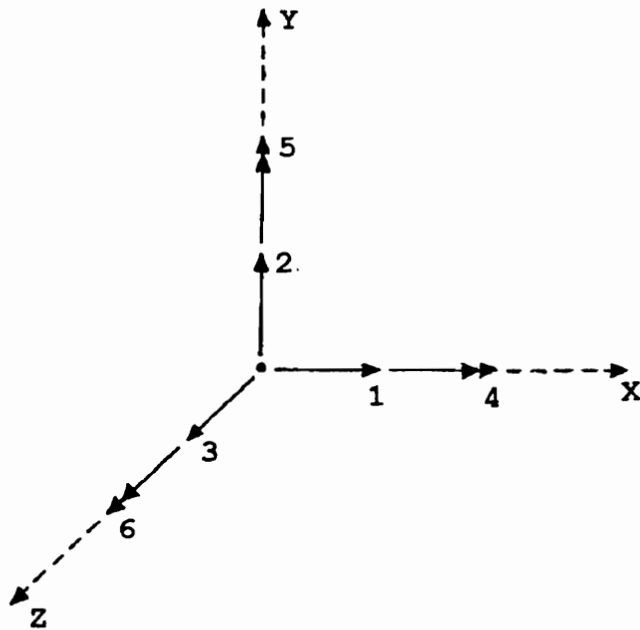


⑩ - Element

□ - Node

Edge Block - Rack Condition

Figure 2.17. Element Assemblage used in PDS (NWPCA, 1988) to Simulate Blocks.



- 1 = lateral translation parallel
- 2 = withdrawal
- 3 = lateral translation perpendicular
- 4 = twisting
- 5 = in-plane twisting
- 6 = out-of-plane rotation

Figure 2.18. Modes of Action
for a Pallet Joint.

determined experimentally by loading test joints to failure, with maximum load defining the load carrying capacity of the joint. Based on empirical data, Wallin and Stern (1974) formulated equations for calculating allowable lateral load and allowable withdrawal load for pallets joints constructed with stiff-stock and hardened steel nails.

Translational stiffness is a measure of joint stiffness in lateral loading. Translational stiffness can be obtained empirically from load-slip curves or theoretically (Wilkinson, 1971, McLain, 1976).

The separation modulus and rotational modulus are used to describe the stiffness of a nailed joint under load. Separation modulus was defined by Kyokong (1979) as the ratio of the applied withdrawal force to separation, while the rotational modulus is the ratio of the applied moment to the angular rotation (Kyokong, 1979). Because Kyokong formulated an equation relating the separation modulus to the rotation modulus, only one modulus of the two is necessary to model the stiffness of a pallet joint.

Loferski and McLain (1987) used spring elements to model the behavior of flexible nail joints found in stringer pallets. Joints were represented as beams supported by fictitious springs. Stiffness values derived from nail testing were assigned to the corresponding degree of freedom of each spring element.

Theoretical and empirical models for predicting rotation modulus of block pallets were developed by Samarasinghe (1987). Using the matrix structural analysis approach, joint actions including head embedment, shank withdrawal and block edge crushing were idealized using a spring analogy. This analogy was applied to single and multiple fastener joints with excellent agreement between empirical and theoretical predictions.

2.6 General Pallet Design

In this section, fundamental concepts used to design pallets are introduced. Criswell (1979) identified four principal sources of uncertainty and variability in the design process. Four sources identified are material resistance, applied loads, analysis methodology, and service life.

Material resistance was defined by Criswell (1979) as the ability of the structure and individual components of the structure to withstand applied loads. Resistance was generally defined in terms of geometric and material properties. For example, important material properties used to define the resistance of pallet decks comprised of plywood or OSB panels are MOE and MOR in both principal axes (strong and weak directions) of the panels. The most important geometric property is thickness. Resistance

variability is linked directly to variations in geometric and material properties.

In the design process, the applied loads a structure will experience must be anticipated. Applied loads occur in many forms. Uniformly distributed, line, and concentrated loads are examples. For many structures, the applied loads are the effects of random events caused by nature. Although the static loads applied to a pallet are generally controlled by human beings and are often precisely known, load variation can be extreme, with coefficients of variation exceeding 50 percent in many warehouses (Loferski, 1985). Variability is related to the different types and magnitudes of load a pallet will experience over its service life. Increased load variability increases the probability of pallet failure.

The analysis methodology provides a means for predicting load effects in terms of stresses and deflection. Finite element modeling is an example of an analysis methodology. The analysis methodology also provides a means for evaluating the resistance of the structure in terms of important geometric and material properties. Differences (variability) between the actual state and the analysis model arise due to simplifying assumptions, the use of idealized load and support conditions, and mathematical approximations.

When a structure is designed, the actual service life of the structure is unknown. Service life is dependent on how the structure is used over time. The interaction of load versus resistance also dictates service life. With regards to pallets, resistance to loads generally decreases over time as pallet damage caused by handling accumulates. Over time, the probability of the pallet experiencing an extreme load also increases. At some point the pallet accumulates sufficient damage and is no longer functional or fails catastrophically. The amount of time a pallet remains in service can be extremely variable, depending on the rate at which damage occurs in handling and the load variability the pallet experiences.

In this research, emphasis was placed on developing the foundation for the analysis methodology. The finite element method was used to develop models which can be incorporated into the Pallet Design System (PDS), a reliability-based design system for pallets. PDS is discussed in the next section. Existing design procedures for panel-deck pallets are then reviewed.

2.6.1 The Pallet Design System (PDS)

The Pallet Design System (PDS) allows pallet manufacturers to design pallets which meet specified performance and serviceability criteria. Important criteria

includes strength and stiffness for important load and support conditions, durability (life expectancy), and cost (minimum cost per use). The stringer version of PDS was introduced in 1985 and the scope of this version was outlined by Loferski (1985). The reliability-based design procedure used in this version of PDS was presented by Loferski and McLain (1987). Operating instructions for PDS can be found in a manual written by McLain et al. (1990). The block version of PDS (NWPCA, 1988) was introduced in 1988.

PDS is menu driven and minimal knowledge of computers and engineering concepts is required by users. The program requests the input parameters required to design a pallet. Inputs include pallet geometry, the geometry and material characteristics of components, number of fasteners, fastener characteristics, load conditions, support conditions, and so on. The program assesses input parameters for unrealistic or erroneous values, allowing the user to correct these entries.

Based on input parameters, PDS provides the user with a print out of:

1. A specification sheet summarizing input parameters.
2. Schematic diagrams of the pallet.
3. A strength and stiffness analysis of the pallet for important support conditions.

4. An analysis of lateral collapse potential.

5. A durability analysis.

6. An economic analysis based on projected durability.

It is also possible for the user to store a description of the pallet (input parameters) in a file or on diskette for future evaluation.

2.6.2 Existing Panel-Deck Pallet Design Procedures

Plywood and OSB are considered acceptable materials for pallet decks. Because available literature on OSB use is scanty, most of this discussion focuses on plywood.

Minimum product specifications for two-way, partial four-way, and full four-way entry panel-deck pallets have been published by the NWPCA and the American Plywood Association (NWPCA and APA, 1980). These specifications are for pallets constructed with one or two panel decks and fabricated with mechanical fasteners. These specifications are not intended to provide procedures for the design of pallets. They were published primarily to assist pallet manufacturers and users in producing and specifying plywood pallets.

The "APA Industrial Use Guide - Pallets" gives guidelines for selecting and specifying plywood for pallet decks (APA, 1986). This publication contains tables which list maximum uniform load schedules for certain pallet geometries over a range of sizes. Maximum uniform load is

based on plywood thickness and span rating. Pallet geometries considered are two-way entry stringer-type designs and four-way entry nine-block designs. Although these span tables can be used to design pallets, they are extremely limited in scope. This publication does not consider the racked across stringer support condition or partial four-way pallet geometry.

Elias (1986) studied the performance of plywood pallets for the racked across deck support condition. Design procedures were developed for certain stringer and block pallet geometries. These design procedures were based on standard beam formulas, employing empirical correction factors, based on interior support type and plywood grain direction.

2.7 Finite Element Analysis

A discussion of the finite element method can be found in works by Bathe (1982) and Cook (1981). In formulating a finite element model, the continuum (structure) is discretized or subdivided into finite elements. These elements are finite both in size and degrees of freedom. A model describing the behavior of the individual elements must then be formulated. In achieving this, a parent element is generated for each element type that appears in

the model. The elements are then assembled into a structural model.

The solution for a discrete model subjected to a given load condition is obtained by solving for displacements which correspond to the degrees of freedom of the structure. Solutions are typically obtained using numerical methods such as Newton-Cotes or Gaussian Quadratures (Bathe, 1982). Once solved, post-processing can begin. Post-processing involves steps such as stress and strain computations, and calculation of reaction, nodal, and elements forces. Other parameters such as strain energy can also be calculated during post-processing.

In this research, the ABAQUS finite element program was used (Hibbitt, Karlsson, and Sorenson, Inc., 1989). This versatile program is discussed further in section 2.3.1. Matrix structural analysis which is a specialized method of finite element modeling is discussed further in Section 2.3.2.

2.7.1 ABAQUS

ABAQUS (Hibbitt, Karlsson, and Sorenson, Inc., 1989) is a versatile general purpose finite element program which can be used to model a range of structures. In addition, this program can be used to model a wide range of other engineering problems such as thermal or vibrational

phenomena. ABAQUS functions as a batch program, with the main input file specifying options required by the user. The user has a large element library from which to select. This program proved extremely useful in achieving the objectives of this research.

2.7.1.1 Plate Elements in ABAQUS

In ABAQUS plates can be modeled using shell elements. Two shell elements in ABAQUS, the S9R5 and the S8R, shown in Figure 2.19, were generally selected for use in this research. These elements are good general purpose shell elements. They are isoparametric and have minimal continuity requirements for conformity. They can be joined with other element types, including beam and spring elements. They can be used to model shear deformation. Although the models constructed in this research are linear, these elements can potentially be used to model non-linear behavior.

The S9R5 is a thin shell element, having 5 degrees of freedom (three displacement and two in-surface rotations) at most nodes. This element has six degrees of freedom at the following nodes:

1. Nodes which have kinematic boundary conditions applied to rotational degrees of freedom.
2. Nodes which are used in a multi-point constraint involving a rotational degree of freedom.

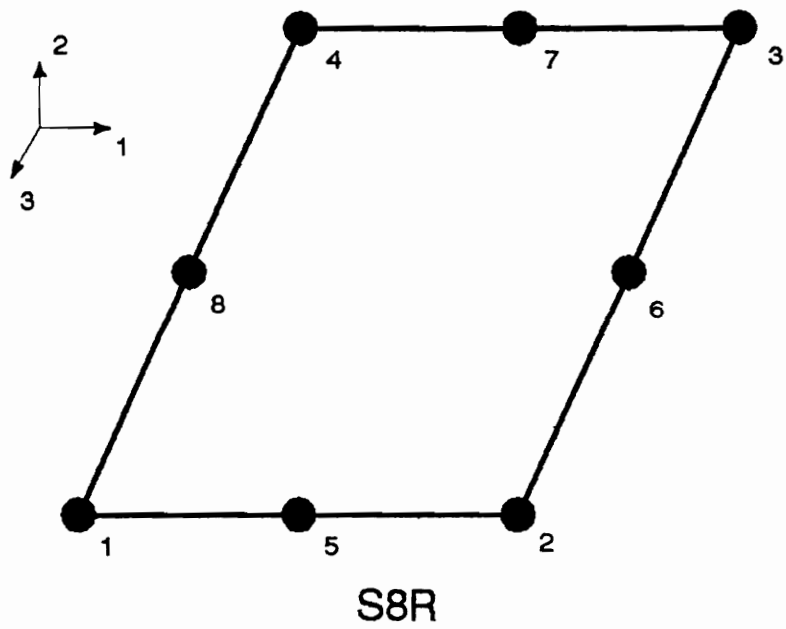
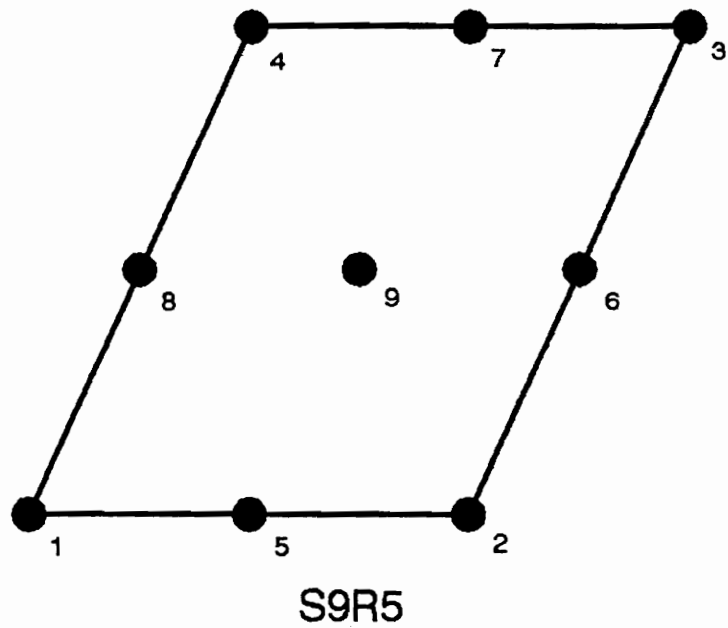


Figure 2.19. S8R and S9R5 Shell Elements in ABAQUS.

3. Nodes shared with beam or shell elements having 3 rotational degrees of freedom at all nodes.
4. Nodes which are on the fold line of a shell. (A fold line occurs where shells having different surface normals come together.)
5. Nodes which are loaded with moments.

The S9R5 element was used when shear stresses were not a factor.

The S8R is a *thick* shell element, having six degrees of freedom (three displacements and three rotations) at all nodes. This element is used when shear is considered a factor. ABAQUS can be used to provide an estimate of interlaminar shear stresses in composite shells.

The *SHELL SECTION* option in ABAQUS can be used to assign properties to these elements. Cross-sectional behavior is calculated using numerical integration. It is possible to model layers of different materials, with different orientations, through the cross-section. However, in this research uniformity through the cross-section was assumed for both plywood and OSB panels. Results obtained using this assumption are thought to more closely correspond to values reported by the APA, where the assumption of uniformity through the cross-section is also made. It is also possible to assign thickness and vary the number of integration points through the thickness. Although three integration points are sufficient for linear analysis, five points were generally used in this research.

Geometric inputs for these elements include the coordinates of the nodes and thickness. The number of integration points is also an input. For orthotropic shell elements, material properties required as input include E_1 , E_2 , ν_{12} , G_{12} , G_{13} , and G_{23} .

Output for both the S9R5 and S8R elements include normal stresses in the local 1 and 2 direction (S11 and S22) and shear through the thickness (S12). Additionally, transverse and rolling shear estimates can be reported as output for the S8R element.

2.7.1.2 Beam Elements in ABAQUS

The B32 and B33 beam elements were selected from the ABAQUS element library for use in this research. These elements are shown in Figure 2.20. Both the B32 and B33 beam elements are three-dimensional beams in space. Each node comprising these elements has six degrees of freedom (DOF), three displacement DOF's (u_x , u_y , and u_z) and three rotational DOF's (ϕ_x , ϕ_y , and ϕ_z). Global X, Y, and Z coordinates are required for each node.

The B32 has three nodes and is a quadratic beam element, utilizing quadratic interpolation for determination of displacements and rotations. Quadratic beams are based on Timoshenko beam theory and include transverse shear

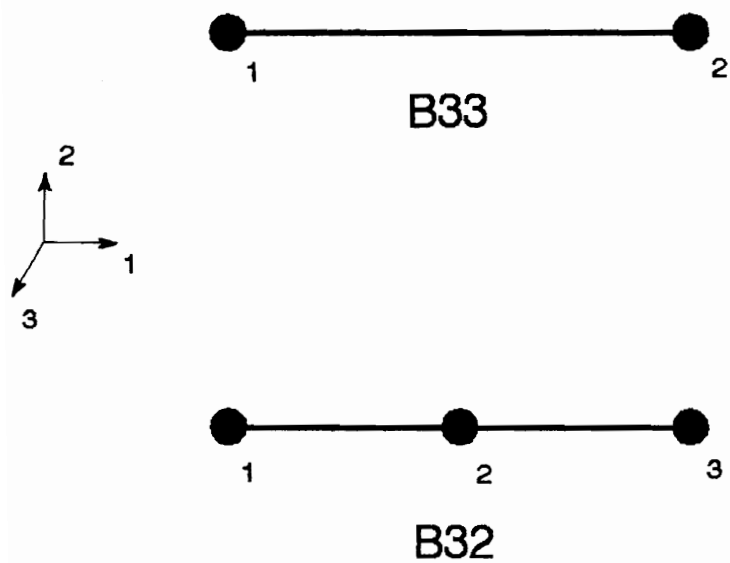


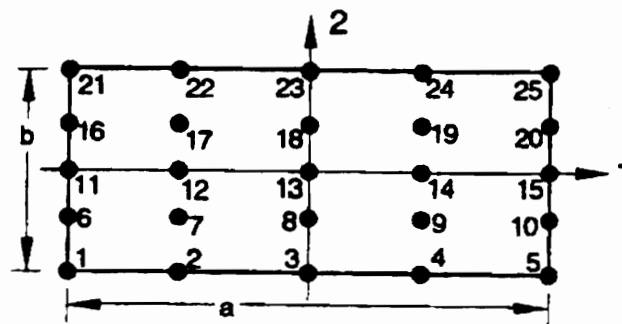
Figure 2.20. B32 and B33 Beam Elements in ABAQUS.

deformation. The B32 beam element was used in this research when transverse shear deformation is a consideration.

The B33 which has only two nodes is a cubic beam element, using cubic interpolation. Cubic beam elements in ABAQUS are based on classical Euler-Bernoulli beam theory. They are best used for small strain, large rotation analysis where changes in beam length are small. The cross section of the cubic beam element is assumed to remain unchanged. The B33 element models both bending and axial deformation. However, the axial displacement due to bending is neglected. The B33 element is only recommended for linear analysis.

The *BEAM SECTION* option is used to define element properties. Input properties for beams in space include cross-sectional dimensions and modulus of elasticity. The integration points across the cross-section can also be specified, with the default being 5 x 5 as shown in Figure 2.21.

Both uniform and concentrated loads can be applied to beams in space using ABAQUS. Concentrated loads can be applied to the beam in either the local 1- or 2-direction. Uniform loads applied to pallets are normally oriented in the local 2-direction. Concentrated loads can be applied in the global X, Y, or Z directions. Concentrated loads which simulate line-loads applied to pallets are usually oriented



Default integration,
beam in space

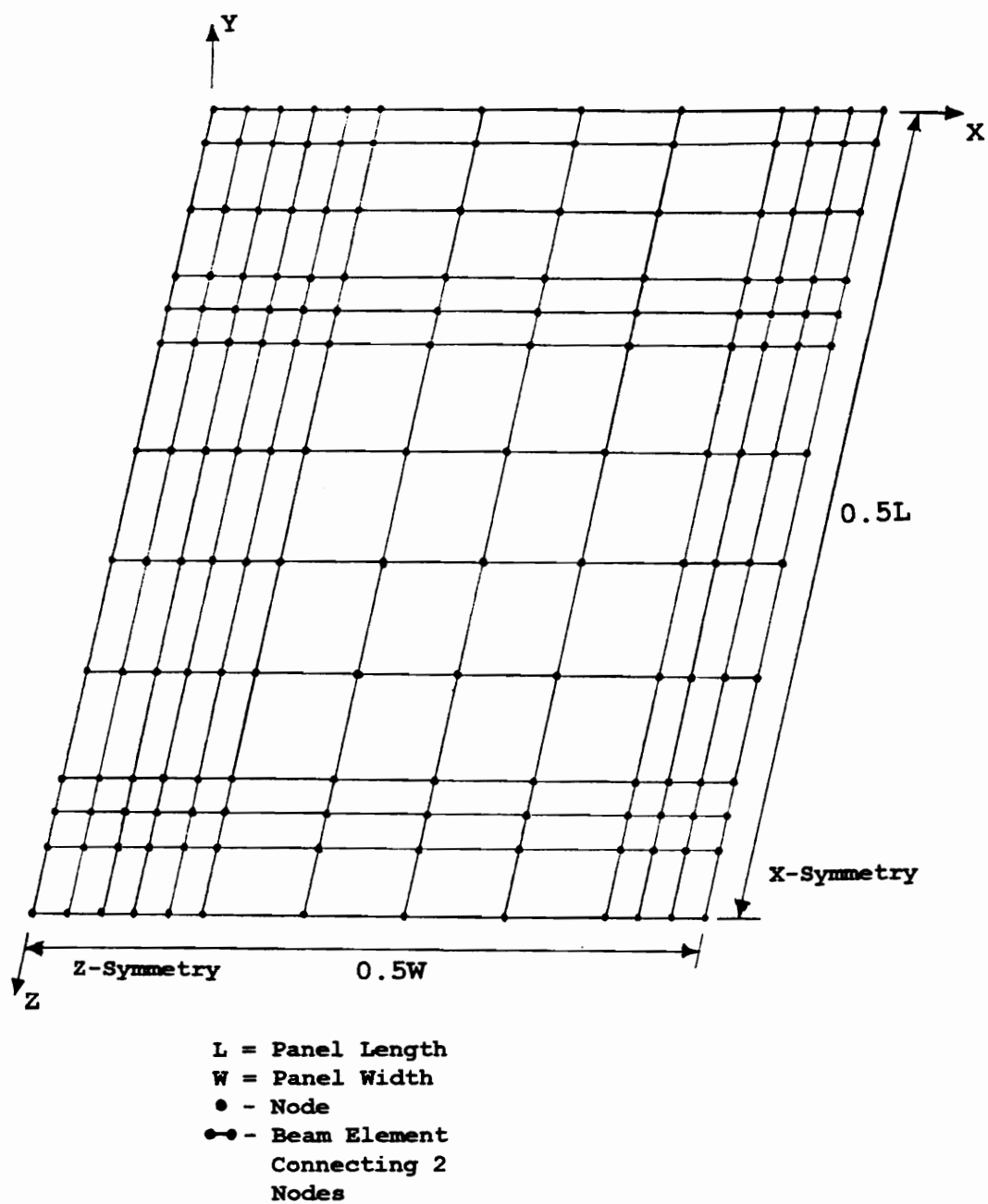
Figure 2.21. Default Integration Points for
B32 and B33 Beam Elements in ABAQUS.

in the global Y direction which normally corresponds to the local 2-direction of the beam element.

Displacement output provided by ABAQUS for beams in space includes global displacements in the X, Y, and Z directions. Stresses output by the model are axial stress (S11) and shear stress (S12) caused by torsion. Axial strain (E11) and shear strain (G12) caused by torsion can be output. Axial section force (SF1) and section moments (SM1, SM2, and SM3) can be output for beams in space, along with axial section strains (SE1) and section curvatures (SK1, SK2, and SK3). Transverse shear section forces (SF2 and SF3) and transverse shear section strains (SE2 and SE3) are only available as output for the B32 element.

2.7.1.2.1 Grids

There is not a "grid" element in the ABAQUS element library, but grids can be modeled using assemblages of beam elements as shown in Figure 2.22. The B33 element was generally selected for grid construction in this research, although the B32 element was used when transverse shear was a consideration. Each node of the grid has six degrees of freedom (DOF), three displacement DOF's and three rotational DOF's. Grids are often constructed with only three DOF's (Holzer, 1985), two displacement (local 1- and 2-direction of grid element) and one rotational (rotation about the



13 by 13 Grid Emulating a Panel

Figure 2.22. Grid Framework Constructed with Beam Elements in ABAQUS.

local 3-axis). This can be simulated in ABAQUS by fixing the local 3, 4, and 5 DOF's for each node comprising beam elements in the grid when boundary conditions are assigned to the structure.

2.7.1.3 Spring Elements in ABAQUS

Two springs elements in ABAQUS were used in this research, SPRING1 and SPRING2. An example of each spring type is shown in Figure 2.23. The element type SPRING1 acts between a node and ground in a fixed direction (degree of freedom), while SPRING2 acts between 2 nodes. Both SPRING1 and SPRING2 elements can be either displacement or rotational springs.

Displacement springs can be assigned to the global 1, 2, and 3 directions (degrees of freedom) at a given node, with displacements occurring in the u_x , u_y , or u_z direction respectively. Other than defining the node(s) to which the spring is attached, no additional geometric inputs are required. The linear behavior of displacement springs is defined in terms of spring constant (k). The spring constant (k) has units of force per unit displacement (i.e. pounds per inch). The element output from ABAQUS for displacement springs is force in the spring and change in length (displacement).



SPRING1 Elements
(Node to Ground)



SPRING2 Elements
(Node to Node)

Note: Springs are actually zero-length

Figure 2.23. SPRING1 and SPRING2
Elements in ABAQUS.

Rotational springs can be assigned to the global 4, 5, and 6 directions (degrees of freedom), with rotations occurring in the ϕ_x , ϕ_y , or ϕ_z direction respectively. As with displacement springs, other than defining the node(s) to which the spring is attached, no additional geometric inputs are required. Spring stiffness is defined in terms of a spring constant (k) that has units of moment per unit rotation (i.e. inch-pounds per radian). Element output from ABAQUS for rotational springs is the moment applied to the spring and relative rotation.

2.7.2 Matrix Displacement Method

Contained within the finite element method are matrix structural analysis methods (Livesley, 1975; McGuire and Gallagher, 1979). Matrix structural analysis involves discretizing a continuum (structure) into element models, assembling element stiffness matrices into a stiffness model, and solving the system model to determine responses. Matrix structural analysis methods are classified based on the choice of unknowns, displacements, forces, or mixed methods.

The Matrix Displacement Method is a matrix structural analysis technique. This method was addressed thoroughly by Holzer (1985). The structure is represented as an assemblage of elements interconnected by joints (or nodes in

finite element terminology). Joint displacements are unknowns. The elements are then assembled into a stiffness matrix by relating element-end displacements to element-end forces. Element stiffness matrices are then assembled into a system model by imposing conditions of compatibility and equilibrium. Compatibility refers to the conditions of continuity between element and joint displacements. Equilibrium is the balancing of applied joint forces with element forces.

The system model relates joint displacements to applied joint forces through the system stiffness matrix and is solved for joint displacements. After solving for joint displacements, any measure of response can be determined for the structure as a continuum. This is a fundamental difference between the matrix displacement method and the finite element method where the structure remains discretized in determining responses.

Matrix structural analysis can be used to model plane structures, such as trusses, beams, and frames, or space structures, such as space trusses, space frames, or grids. With regards to modeling pallets, the matrix displacement method forms the basis for predicting behavior of lumber deck stringer and block pallets in the Pallet design System (PDS). A discussion of the modeling techniques used for

stringer pallets in PDS can be found in work by Loferski (1985).

3.0 Modeling Pallet Components

Before complex pallet models could be assembled using the finite element method, it was necessary to select finite elements which adequately model the components and joints comprising the pallets. Included in this chapter is the approach used to select elements and mesh fineness in ABAQUS for modeling pallet components, including panel decks, lumber decks, stringers, and blocks. Methodologies and elements used to model joints and contact zones between the pallet decks and spacers are discussed. Techniques developed to model such pallet features as leading edge boards and cut-outs are also presented.

The sign convention used for model development throughout this research is shown in Figure 3.1. The global 1-direction was oriented along the width of the pallet, the global 2-direction through the thickness (height), and the global 3-direction along the length. This sign convention was chosen because it facilitated adaptation of two-dimensional models used to simulate pallet sections and components into 3-dimensional models. It also facilitated development of simplified PC models, such as the model used to analyze stringer pallets in the RAD support condition.

3.1 Panel Decks

In this research, pallets had panel decks constructed of plywood or OSB. In three-dimensional plate models,

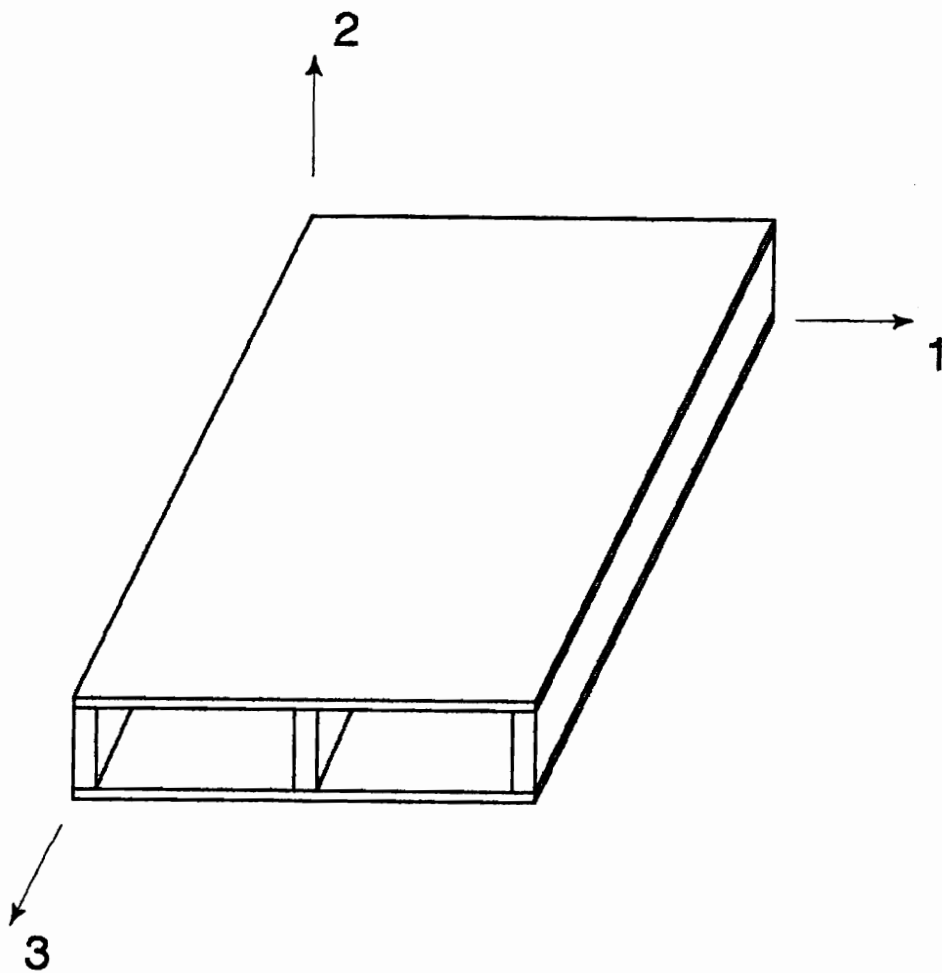


Figure 3.1. Sign Convention used to Model Pallets and Pallet Components.

panels are modeled using shell (plate) elements as in ABAQUS shown in Figure 2.19. Panels are modeled using a grid of beam elements in simplified PC models. These plate and grid methodologies for modeling a panel are discussed further in subsequent sections.

3.1.1 Modeling Panel Decks as Plates

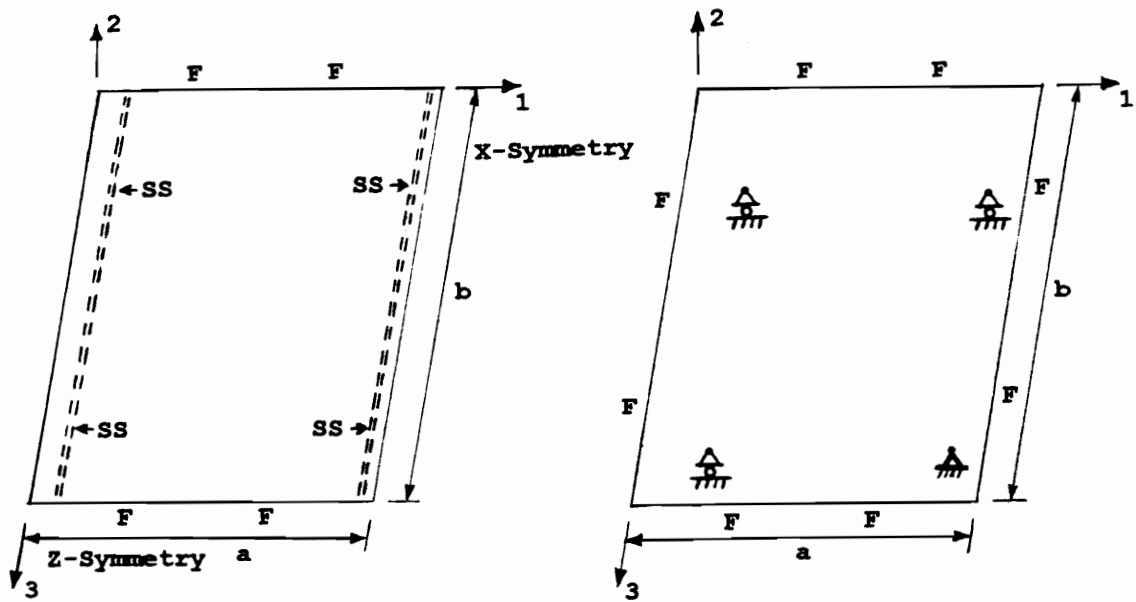
Panel decks can be modeled as plates using the S9R5 and the S8R shell elements in ABAQUS. These elements were used because they are good general purpose shell elements capable of modeling orthotropic materials. The S9R5 is a *thin* shell element and is used when the span-to-depth ratio is sufficient that shear stresses are not considered a factor. For solid wood, a ratio exceeding 16:1 is usually considered sufficient (Superfeský et. al., 1977). However, for *anisotropic sandwich* composites such as plywood, where plies alternate and properties vary significantly, transverse (rolling) shear forces can be significant for members which would normally be considered as *thin* shells. The S8R is a *thick* shell element and is used when shear is considered a factor. Although ABAQUS can be used to provide an estimate of interlaminar shear stresses in composite shells, the estimates of transverse and rolling shear flexibility were limited to evaluating both plywood and OSB assuming uniformity through the cross section.

Geometric inputs to the models include nodal coordinates and panel thickness. Nodal coordinates were assigned based on the pallet configuration. Panel thickness was determined by measuring thickness at numerous locations and calculating the average which was input to the models. Because these models are linear, a minimum of 3 integration points are required through the cross section (thickness), although 5 points were generally used.

Orthotropic material properties required include E_1 , E_2 , ν_{12} , G_{12} , G_{13} , and G_{23} . E_1 and E_2 were determined experimentally. Utilizing equations given previously in Chapter 2, Poisson's ratio (ν_{12}) was determined using either Equation 2.2 for plywood or Equation 2.3 for OSB. Values for G_{12} , G_{13} , and G_{23} were obtained from literature (Bodig and Jayne, 1982).

To determine the mesh fineness required to model panel decks, two test cases were evaluated. These test cases are shown in Figure 3.2. Test cases considered were for the stack condition because convergence requirements are more severe in this condition than for pallets (panels) supported in a rack.

The first case was for a panel simply supported along two opposing sides and along the mid-span. The remaining 2-sides were free. This simulates the deck of a stringer



Test Case 1: Panel Simply Supported along Two Sides and Middle as Shown.

Test Case 2: Panel Simply Supported at Four Points as Shown.

SS - Simply Supported
 F - Free Edge
 a - Panel Width (Length)
 b - Panel Length (Width)

Figure 3.2. Test Cases used to Determine Mesh Fineness Required to Model Panel Decks.

pallet supported in the stack condition. Symmetry was utilized in this test case which considers the entire panel.

The second test case was a panel supported at 4 corners which simulates the deck support for block pallets. Symmetry was not used in this test case. Simply supporting the panel at nine points which simulates a nine block pallet presented a problem. There is a Saint Venant's effect associated with the interior point supports. This generally became an issue with block pallet models and is discussed further in Chapter 5. Nonetheless, the four corner support example was considered sufficient for determining mesh fineness.

In these test cases, a panel was analyzed using finite element meshes of various fineness (coarseness). The 40 x 48 inch plywood panel shown in Figure 3.3 was used. The panel had a thickness of 0.719 inches and orthotropic properties as given in Figure 3.3. The panel was analyzed using meshes of S9R5 shell elements in ABAQUS as shown in Figure 3.4. For Test Case 1, the number of elements comprising the mesh was increased sequentially from 3 to 80 (3, 8, 24, and 80). For Test Case 2, mesh fineness was increased from 9 to 100 (9, 16, 36, and 100) elements. A uniform load of 0.1 psi was applied to the panel.

Complete results for these test cases are presented by Mackes (1998, Volume I, Section 1). A summary of results

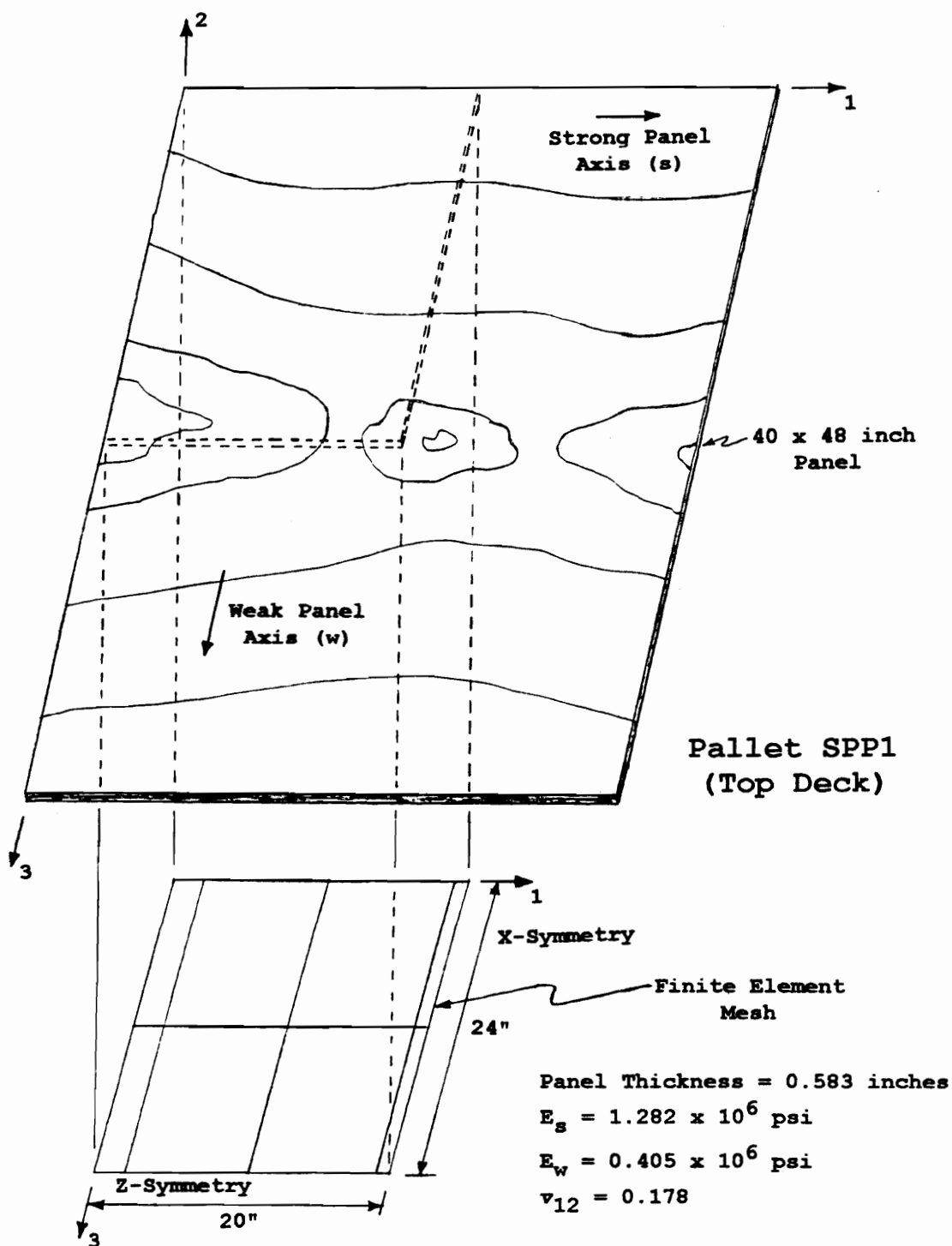
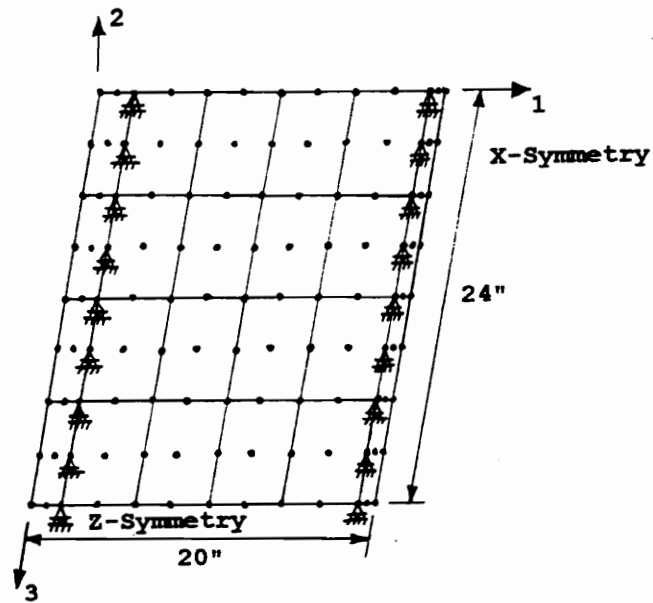
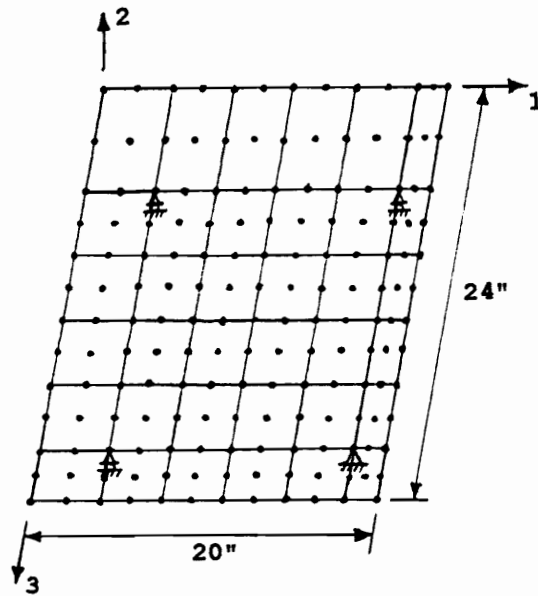


Figure 3.3. Plywood Panel used to Analyze Mesh Fineness Required to Model Panel Decks.



Test Case 1: Mesh of 24
S9R5 Shell Elements



Test Case 2: Mesh of 36
S9R5 Shell Elements

Figure 3.4. Examples of Finite Element
Meshes used to Analyze Plywood Panel.

can be found in Table 3.1. Given the criteria for acceptable error levels (less than 15 percent is considered acceptable), acceptable precision was achieved with an 8 element mesh for Test Case 1, while 36 elements were required for Test Case 2. Generally, stringer pallet models are less complex, requiring fewer elements, than block pallet models.

3.1.2 Modeling Panels Using a Grid

In this research, panels of simplified PC models were modeled using grids comprised of B33 beam elements in ABAQUS. An example of a grid is shown in Figure 3.5. This grid is comprised of 19 horizontal and 19 vertical members. This particular grid was used to model block pallets (see Chapter 5). The grid members were assigned a width based on tributary area. Tributary area is a concept where members are assigned properties based on their relationship in space to adjacent members. For grid members comprising a panel, the width assigned to a member is one-half the combined sum of distance to adjacent grid members, with the sum of all member widths equaling panel width. This technique can also be used to distribute a uniform load to the grid.

To show that a grid can adequately model a panel, the panel described in Section 3.1.1 was modeled using grids of various mesh fineness. Grids having 7 x 7, 13 x 13, and 25

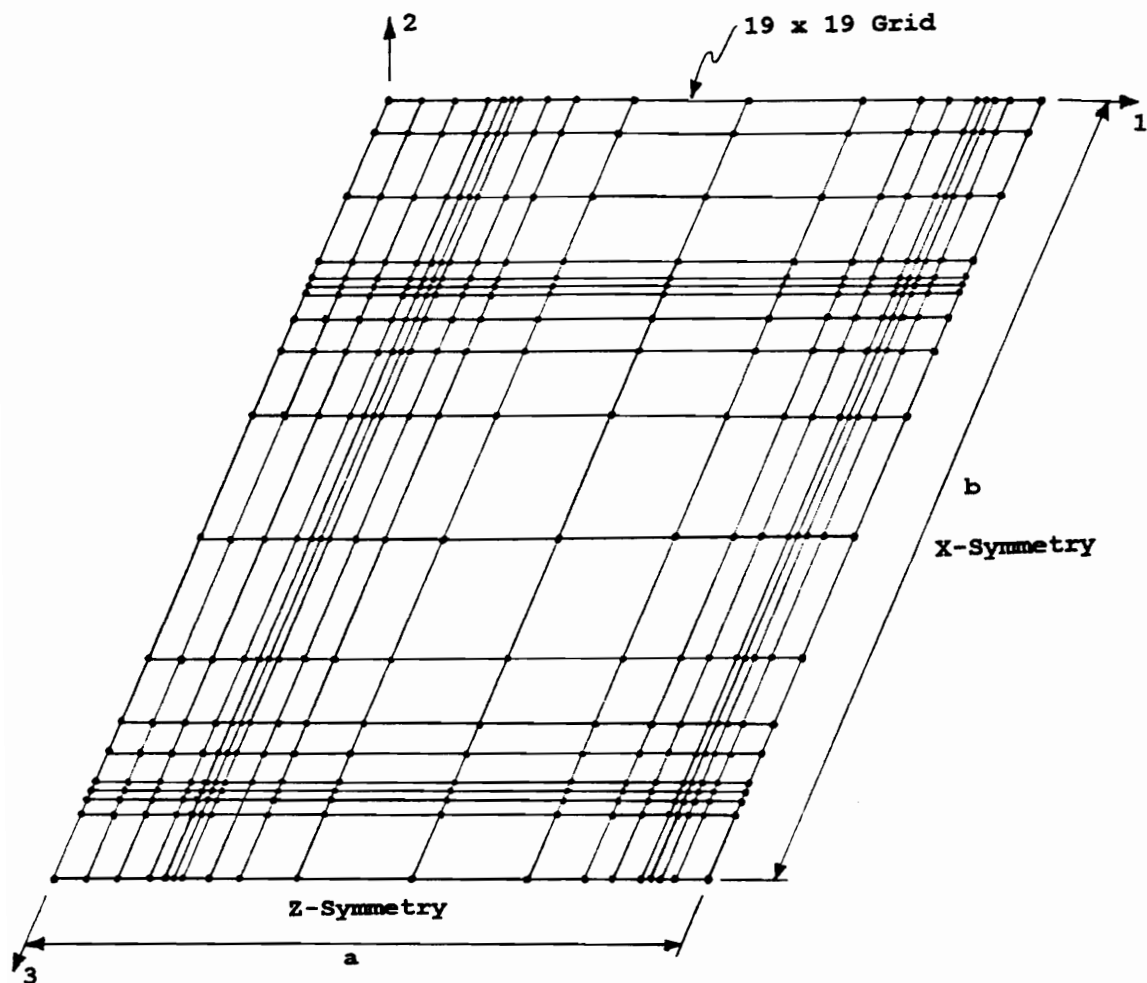
Table 3.1. Summary of Results for Finite Element Meshes of various Fineness used to Predict the Behavior of Panel Decks.

NUMBER OF ELEMENTS	MAXIMUM DEFLECTION		MAXIMUM STRESS (S11)		MAXIMUM STRESS (*S33)	
	LOCATION	(in.)	LOCATION	(psi)	LOCATION	(psi)
Test Case 1:						
3	11	-0.0142	20	524.5	20	30.71
8	11	-0.0245	20	528.3	20	31.29
24	11	-0.0246	20	529.6	189	29.77
80	10	-0.0250	20	529.5	63	32.02
**CS		-0.0246		528.0		
Test Case 2:						
9	221	-0.0549	410	219.3	231	198.0
16	221	-0.0799	389	387.2	231	453.8
36	221	-0.0806	389	326.2	231	383.1
100	221	-0.0807	389	311.8	231	373.8

Notes: * Global S33 direction in table corresponds to local S22 in ABAQUS output.

**** Classical Beam Solution**

The classical plate solution for test case 2 is complex and is not presented. However, test case 2A is presented by Mackes (1998, Volume 1) pages 1.15 through 1.17 to show that the model works properly.



- - Node
- - Beam Element Connecting Two Nodes

Note: Grid is comprised of 361 Nodes
and 684 Beam Elements.

**Figure 3.5. Grid of Beam Elements
Simulating a Panel Deck.**

x 25 members were used. The details of this analysis are presented by Mackes (1998, Volume 1, Section 2). Results for the grid models are compared to those for plate models in Figures 3.6 and 3.7. Generally as mesh fineness increased, the agreement between the grid and plate solutions improved, although there were exceptions. For Test Case 1, adequate precision was achieved only if it is assumed that normal stresses in the S33 direction do not govern. Because the magnitude of S11 stresses are considerably greater than S33 stresses, this assumption is valid. Otherwise, adequate precision can be achieved with even the coarsest grid meshes used in this evaluation.

The grid solution converges to a plate solution where Poisson's ratio of the plate equals zero. Because the Poisson's ratio is not zero for either plywood or OSB panels, this does present a inherent source of error in using grids. However, it is possible to adjust maximum deflections and stresses for this factor. An example of stress adjustment is presented by Mackes (1998, Volume I, Section 3). However, these adjustments are not currently used in PDS-Panel because it is a reliability-based design program and this factor is simply incorporated into the beta value selected for use in the program.

Selecting the proper number and location of grid members was an integral part of model simplification. A

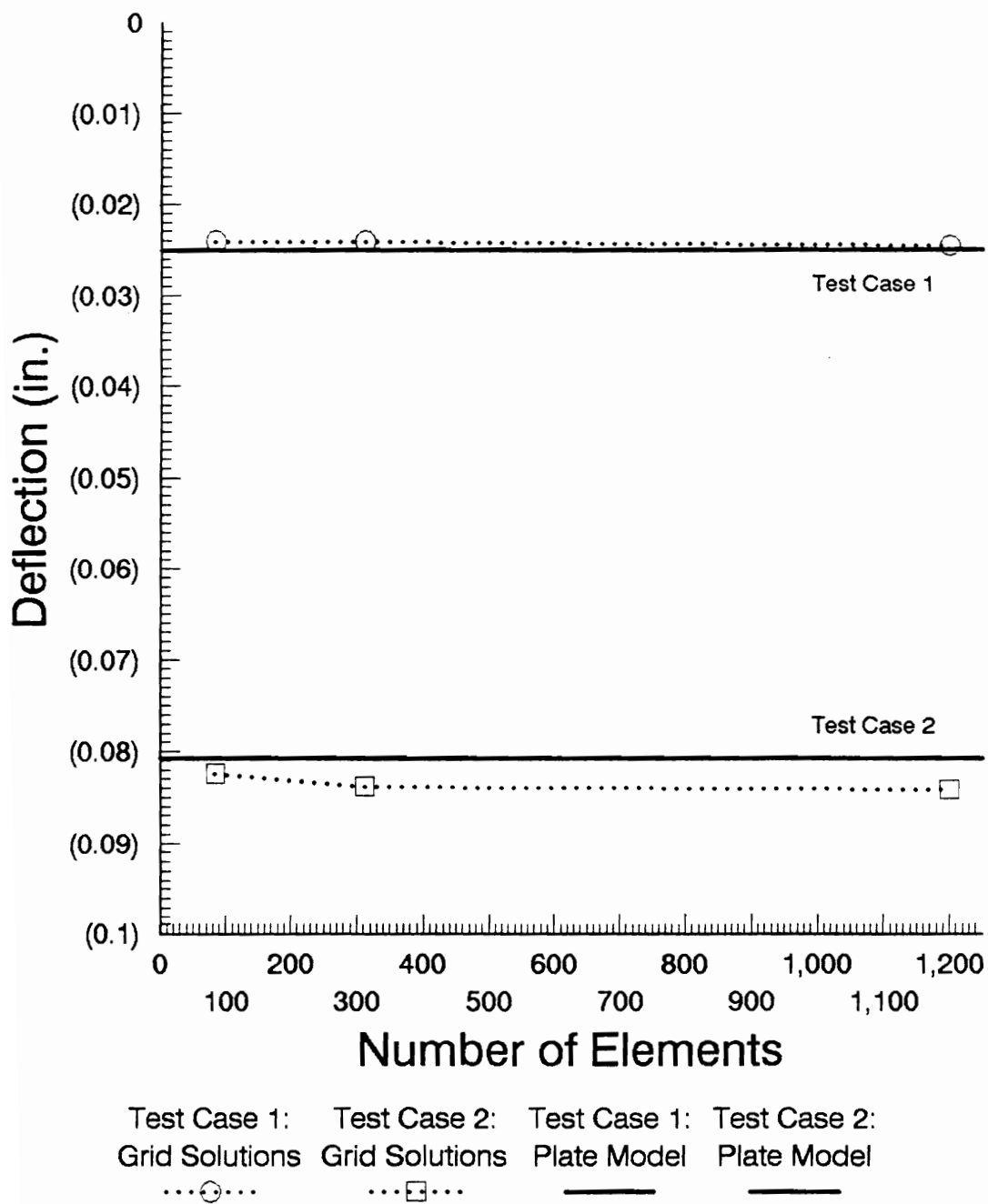
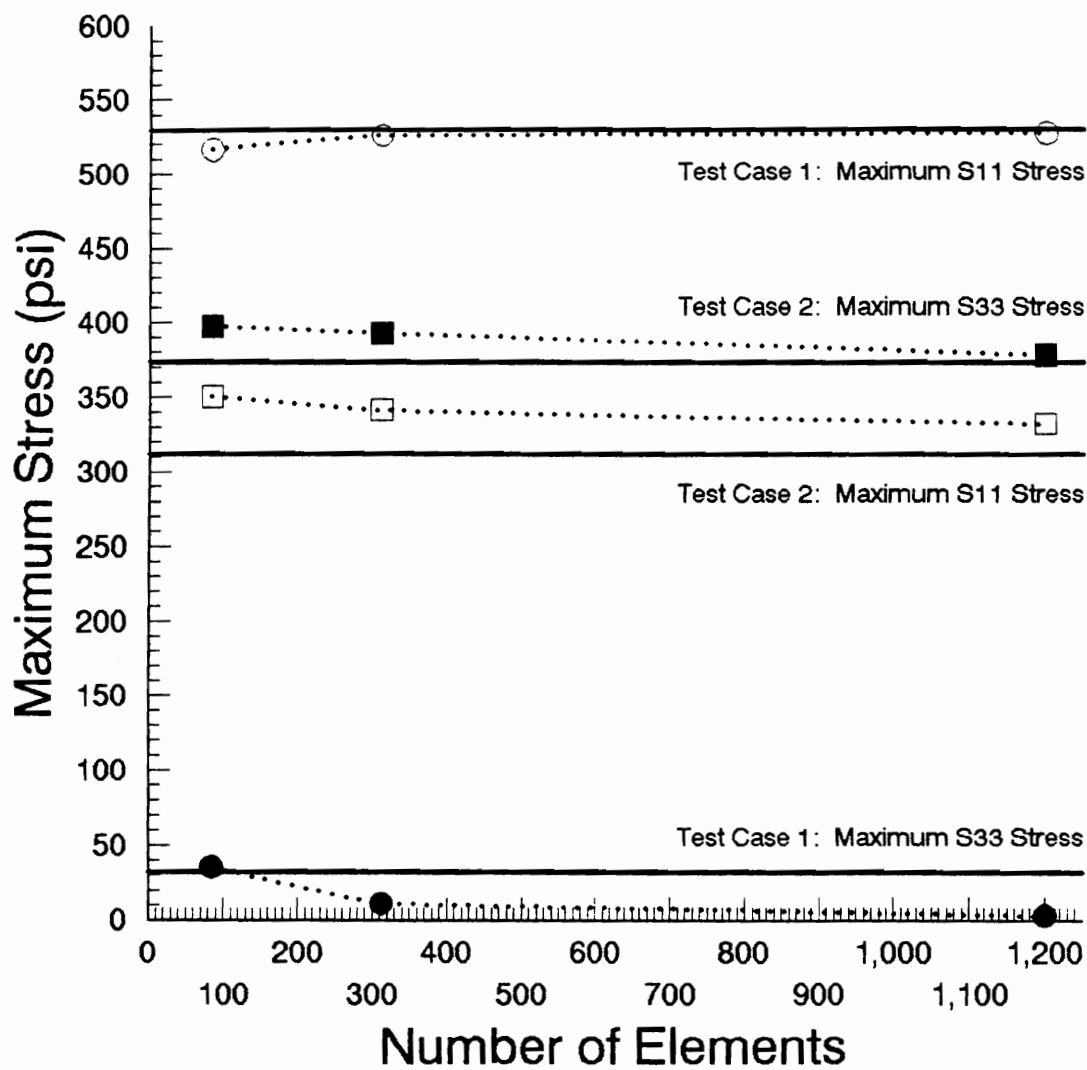


Figure 3.6. Comparison of Finite Element Plate Model to Grid Model: Maximum Deflection.



Test Case 1:	Test Case 1:	Test Case 1:	Test Case 1:
S11 Grid Solutions	S33 Grid Solutions	S11 Plate Solution	S33 Plate Solution
..○..	..●..	_____	_____
Test Case 2:	Test Case 2:	Test Case 2:	Test Case 2:
S11 Grid Solutions	S33 Grid Solutions	S11 Plate Solution	S33 Plate Solution
..□..	..■..	_____	_____

Figure 3.7. Comparison of Finite Element Plate Model to Grid Model: Maximum Normal Stresses.

detailed discussion of this selection process is discussed for the PC-based RAS model in Chapter 4 and PC-based models for all support conditions of block pallets in Chapter 5.

3.2 Strip-Type Decking

Strip-type decking is used in numerous pallet designs considered in this research. Strip-type decking can be of lumber or composites, such as strips of plywood or OSB. Partial four-way stringer pallets with lumber bottom decks, the lower deck of both unidirectional base and perimeter base pallets, and leading edge reinforcement boards found on the top deck are examples of pallet designs considered which have strip-type decking.

Strip-type deck members can be modeled using the B33 beam element shown in Figure 2.20. Cross-sectional dimensions (length and width) of the deck member(s) are required as input to the models. The cross-section of the members are assumed to be rectangular. In addition they are assumed to be homogeneous. The modulus of elasticity along the length of the member is also required as input to the model. Stress output from ABAQUS includes normal stress in the 1-direction (S_{11}) and shear stresses in the 1,2 plane (S_{12}). Transverse shear deformations are ignored. The deflection in the global 1- and global 2-directions (u_x and u_y , respectively) are reported by ABAQUS.

A beam example is shown in Figure 3.8. This beam was modeled with various numbers of B33 elements to determine the mesh fineness required to adequately model strip-type deck members. Details of this test case are given by Mackes (1998, Volume I, Section 4). Figure 3.9 shows that a minimum of 3 elements along the length of the beam are required for stress convergence to the classical solution when symmetry is used. Therefore, a minimum of 3 elements, exploiting symmetry, were used to model strip-type decking.

3.3 Stringers

As with strip-type decks, pallet stringers can be modeled using beam elements. The beam element selected for use was the B33 elements in ABAQUS. Because the length to depth ratios of the stringers spanning a rack support do not normally exceed 16:1, shear through the thickness is considered using the B33 element for stringer members which function in bending. In this research, two types of stringers were modeled, notched and unnotched stringers.

In addition to providing support when acting in the racked-across-stringer condition, stringers act as a spacer between the top and bottom decks in all important support conditions. Load is not normally applied directly to the stringer. Load is transferred to the stringer from the top and/or bottom decks. In actual pallet structures, contact

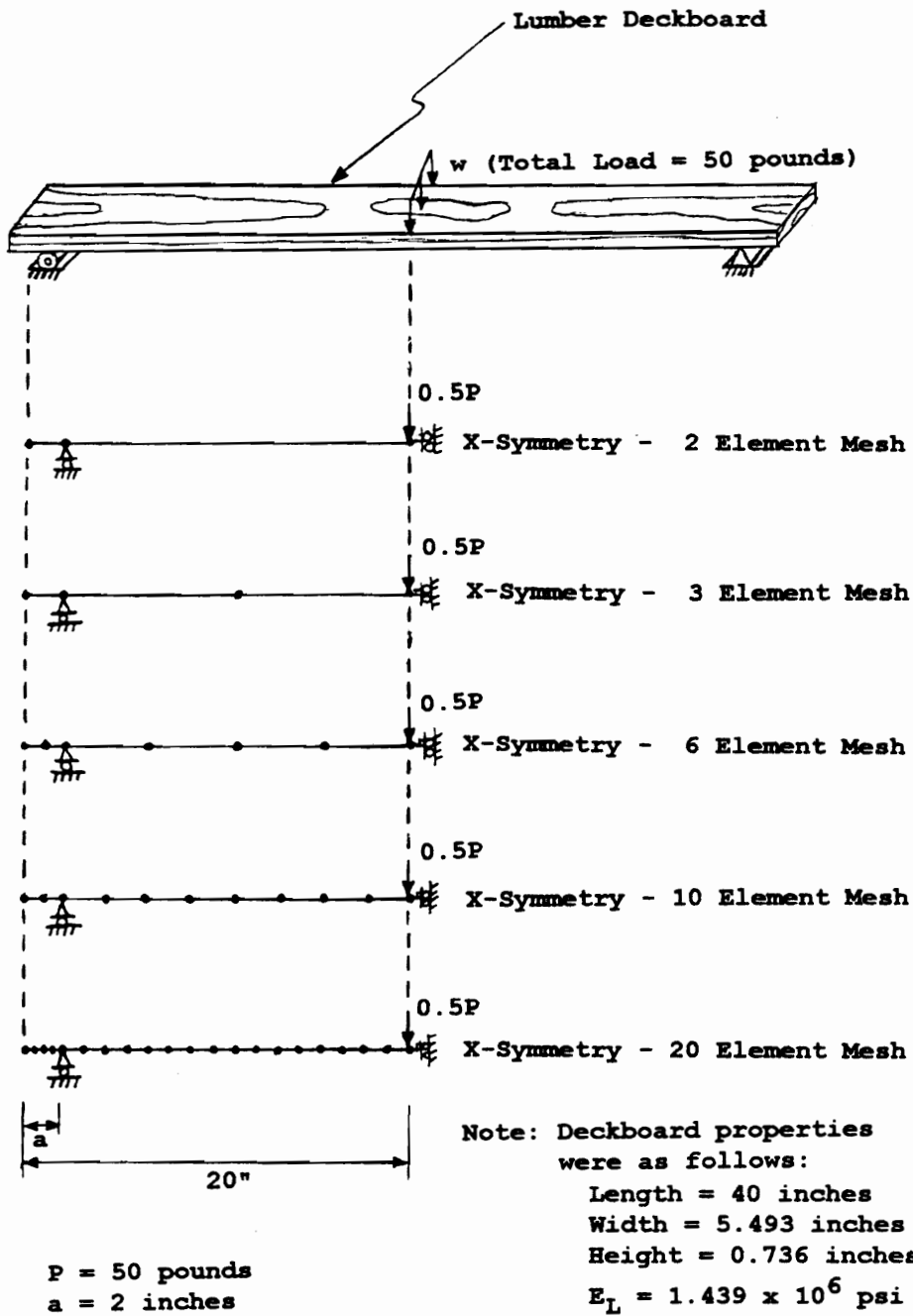
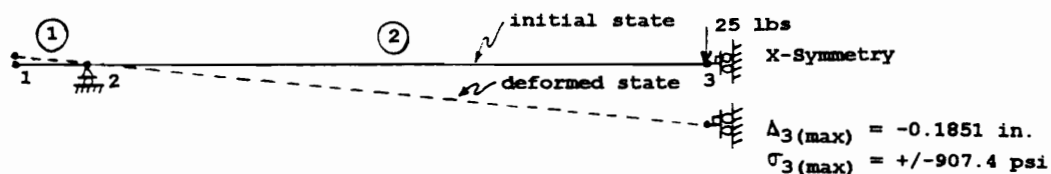
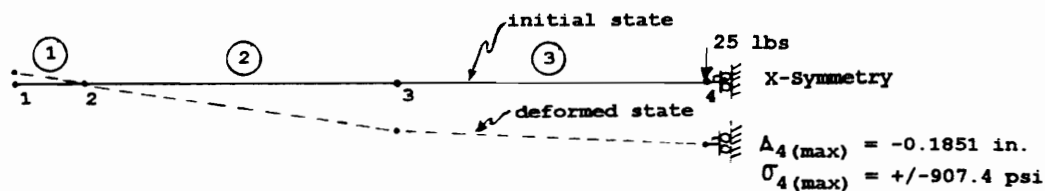


Figure 3.8. Lumber Bottom Deck Example.

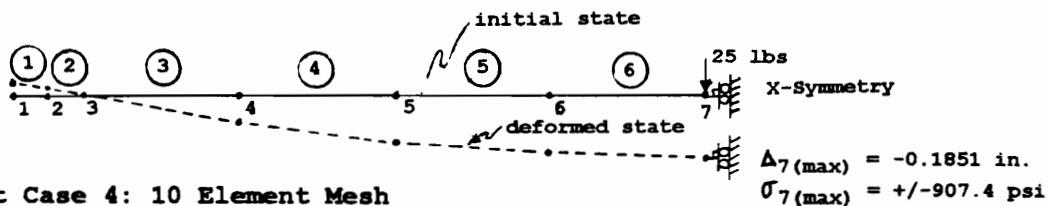
Test Case 1: 2 Element Mesh



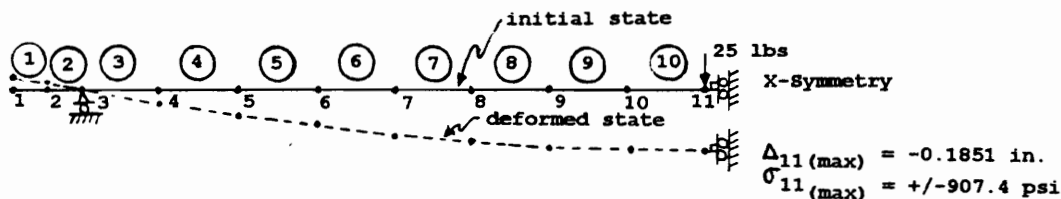
Test Case 2: 3 Element Mesh



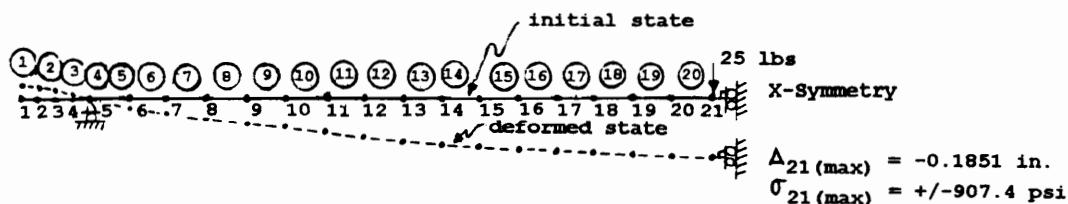
Test Case 3: 6 Element Mesh



Test Case 4: 10 Element Mesh



Test Case 5: 20 Element Mesh



Classical Solution: Continuum

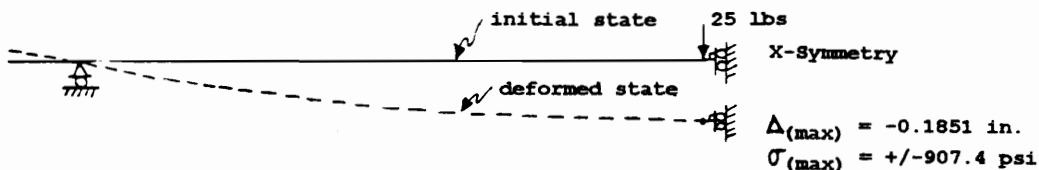
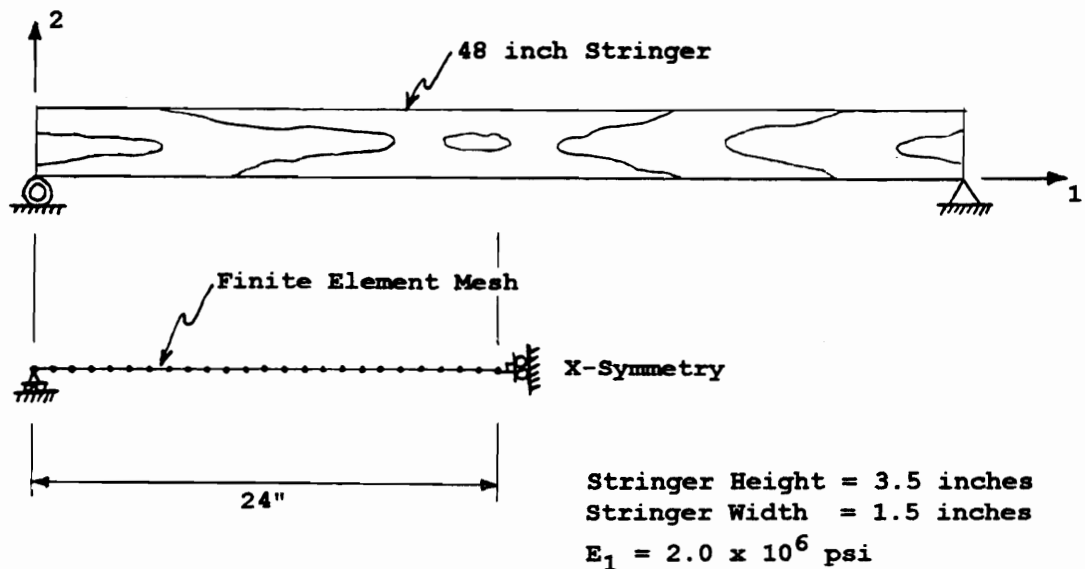


Figure 3.9. Deformed States and Maximum Predicted Stress for Test Cases of Lumber Bottom Deck Example.

between the decks and stringers are more or less continuous along the length of the stringer and load is transferred as such. However, in the models, this contact was not continuous, because the nodes of the deck were linked to the nodes of the stringer through contact elements at a finite number of locations. As a result, the loads applied to the stringer at these locations were concentrated. Therefore, in addition to checking convergence requirements for stress and deflection, it was necessary to determine how many nodes spaced evenly along the stringers were required to simulate a uniform load transfer between the stringers and deck surfaces.

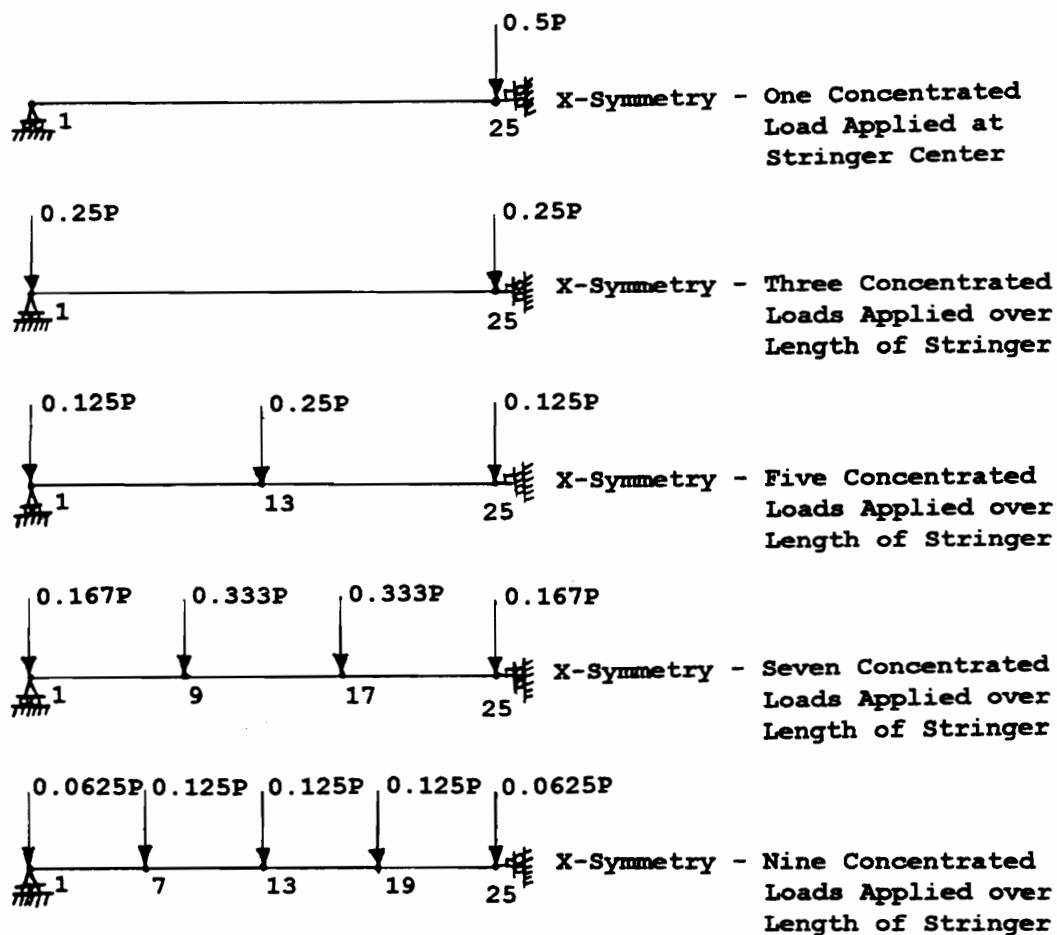
To determine this number, the stringer in Figure 3.10 was analyzed. The 48 inch beam was modeled using 24 B33 elements, exploiting quarter symmetry. The width of the stringer was 1.5 inches and the height was 3.5 inches. The finite elements mesh was loaded with up to 5 concentrated loads as shown in Figure 3.11. The finite element input and output files to ABAQUS are presented by Mackes (1998, Volume I, Section 5). A summary of results presented in Table 3.2 suggest that at least 5 nodes spaced evenly along the length of the stringer were necessary, when using symmetry, to simulate a uniform load applied to the structure. Therefore, at least 5 nodes and 4 beam elements, exploiting symmetry, were used to model stringers along the length.



- - Node
- - Beam Element Connecting Two Nodes

Note: Beam is comprised of 25 Nodes and 24 Beam Elements.

Figure 3.10. Stringer Analyzed to Determine the Number of Concentrated Loads Required to Simulate a Uniform Load.



Note: Loads assigned based tributary area.

Figure 3.11. Finite Element Mesh Simulating Stringer Bending Behavior Loaded with up to Nine Concentrated Loads.

Table 3.2. Comparison of Finite Element Results for Uniform Load Simulation Test Cases to Classical Solution.

TEST CASE NO.	NUMBER OF CONC. LOADS	FE SOLUTION	CLASSICAL SOLUTION	PERCENT DIFFERENCE
Maximum Deflection:		(in.)	(in.)	(%)
1	1	-0.0103	-0.0064	60.94
2	2	-0.0052	-0.0064	-18.75
3	3	-0.0061	-0.0064	-4.69
4	4	-0.0063	-0.0064	-1.56
5	5	-0.0064	-0.0064	0.00
6	UDL	-0.0064	-0.0064	0.00
Maximum Normal Stress:		(psi)	(psi)	(%)
1	1	188.01	94.04	99.93
2	2	94.04	94.04	0.00
3	3	94.04	94.04	0.00
4	4	94.04	94.04	0.00
5	5	94.04	94.04	0.00
6	UDL	94.07	94.04	0.03

Note: The maximum normal stress reported is absolute in terms of magnitude.

3.3.1 Unnotched Stringers

In the plate models, unnotched stringers were modeled using assemblies of B33 beam elements in ABAQUS. These elements were arranged to model two features of the stringer, the bending behavior and the cross-sectional characteristics of the stringer which acts as a spacer between the top and bottom decks of the pallet.

Bending behavior was modeled using an assembly of beam elements oriented along the length of the stringer as shown in Figure 3.12. This was generally assumed to be the longitudinal axes of the wood comprising the member. A minimum of five beam elements were used to model each stringer. These elements were given the cross-sectional geometric properties (width and height) and modulus of elasticity along the length of the stringer.

Members simulating cross-sectional characteristics of the stringers were assembled as shown in Figure 3.13. These members were assigned an arbitrarily high stiffness. Therefore, the cross-sectional members did not bend or distort in shape. Distortion, including compression perpendicular-to-grain, and bending which occurred in the stringers were incorporated into the spring elements which model contact with the top or bottom deck.

Bending and cross-sectional members were then assembled into a stringer as shown in Figure 3.14. To check that the

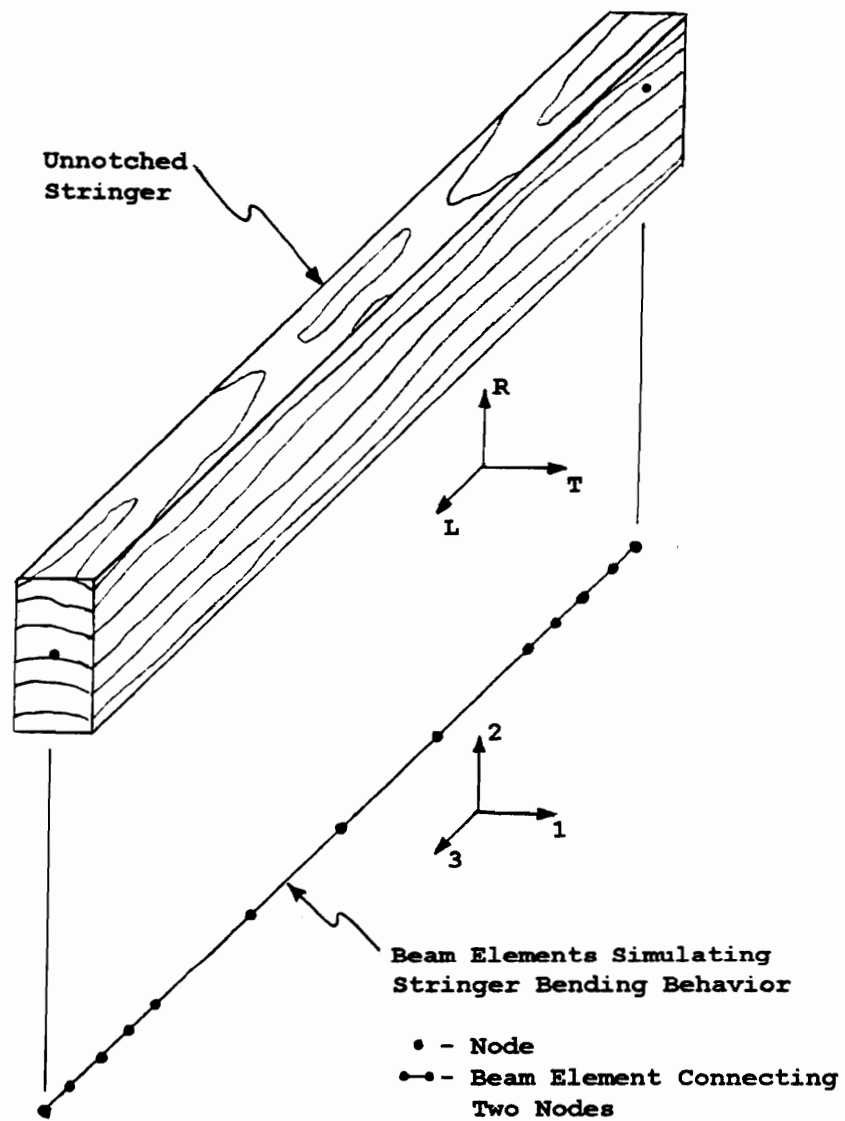


Figure 3.12. Assembly of Beam Elements used to Predict Stringer Bending Behavior.

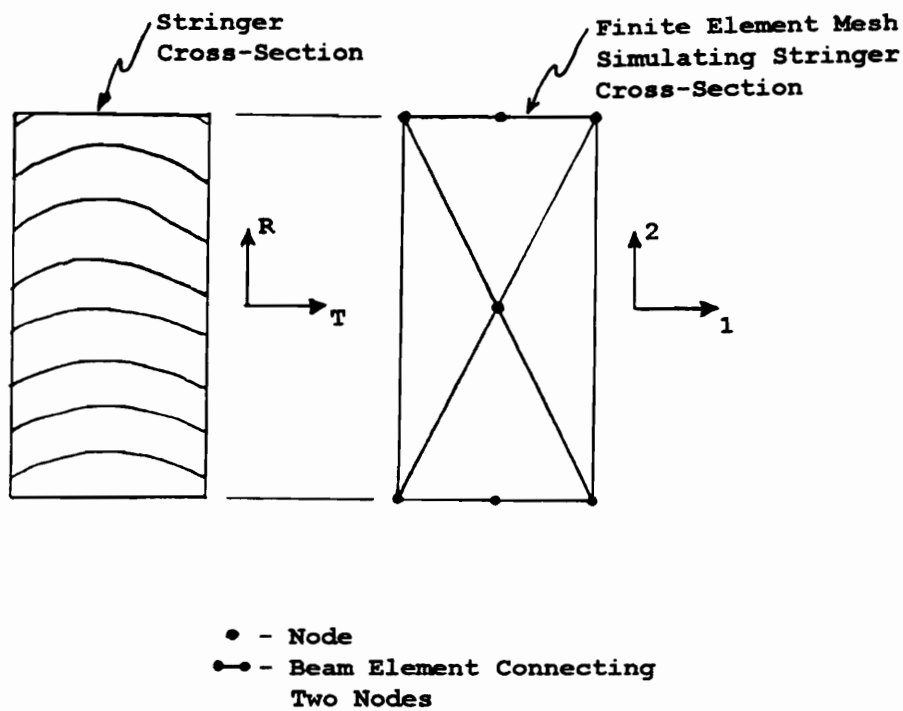


Figure 3.13. Assembly of Beam Elements used to Model Stringer Cross-Sectional Properties.

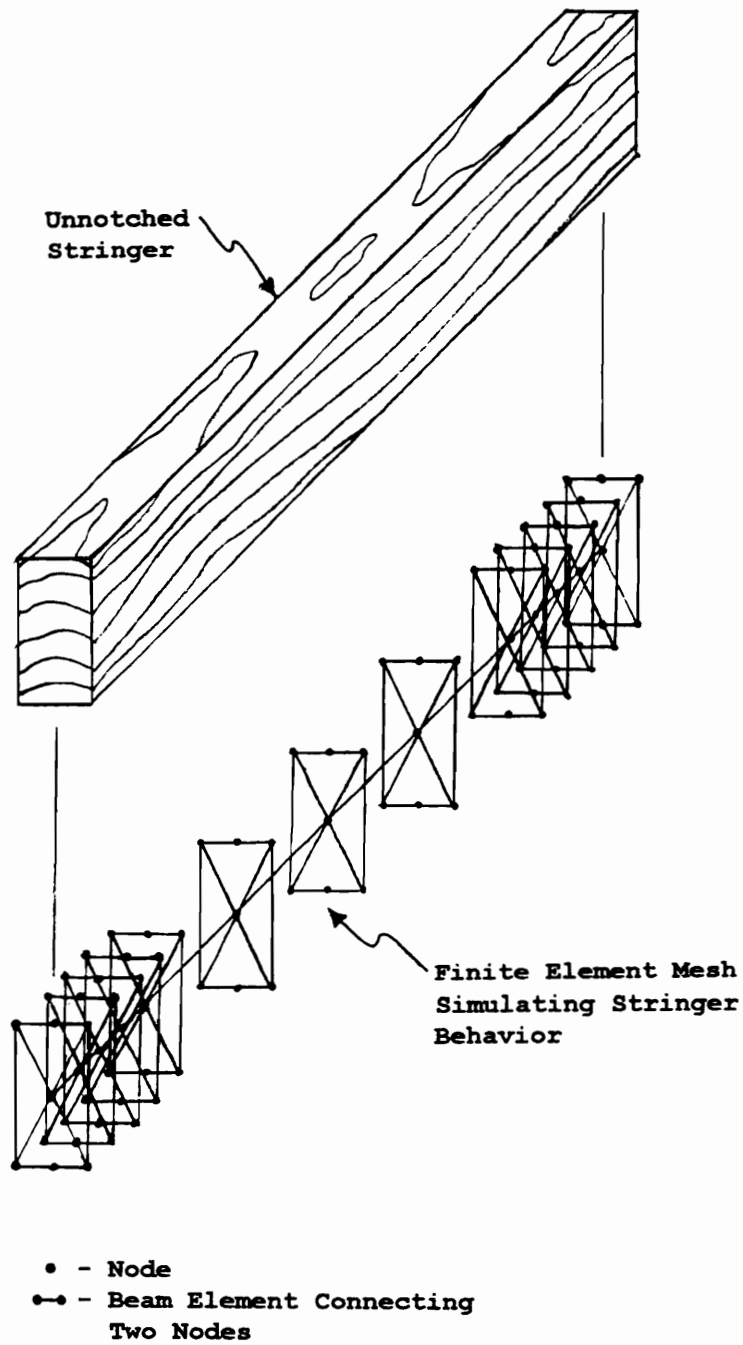


Figure 3.14. Assembly of Beam Elements used to Simulate Stringers in Three-Dimensional Plate Model.

cross-sectional members had no unintended effects on bending stiffness, a test case was run. One 48 inch stringer was tested in two-point bending in accordance with ASTM standard D 198-84 (ASTM, 1994). The member was loaded to 200 pounds at a rate of 0.100 in per minute. The modulus of elasticity was calculated as the slope of the load-deflection curve. A finite element model was setup to simulate the test and deflection was predicted at 200 pounds of load based on the modulus of elasticity determined from the test. Details of this evaluation are presented by Mackes (1998, Volume I, Section 6).

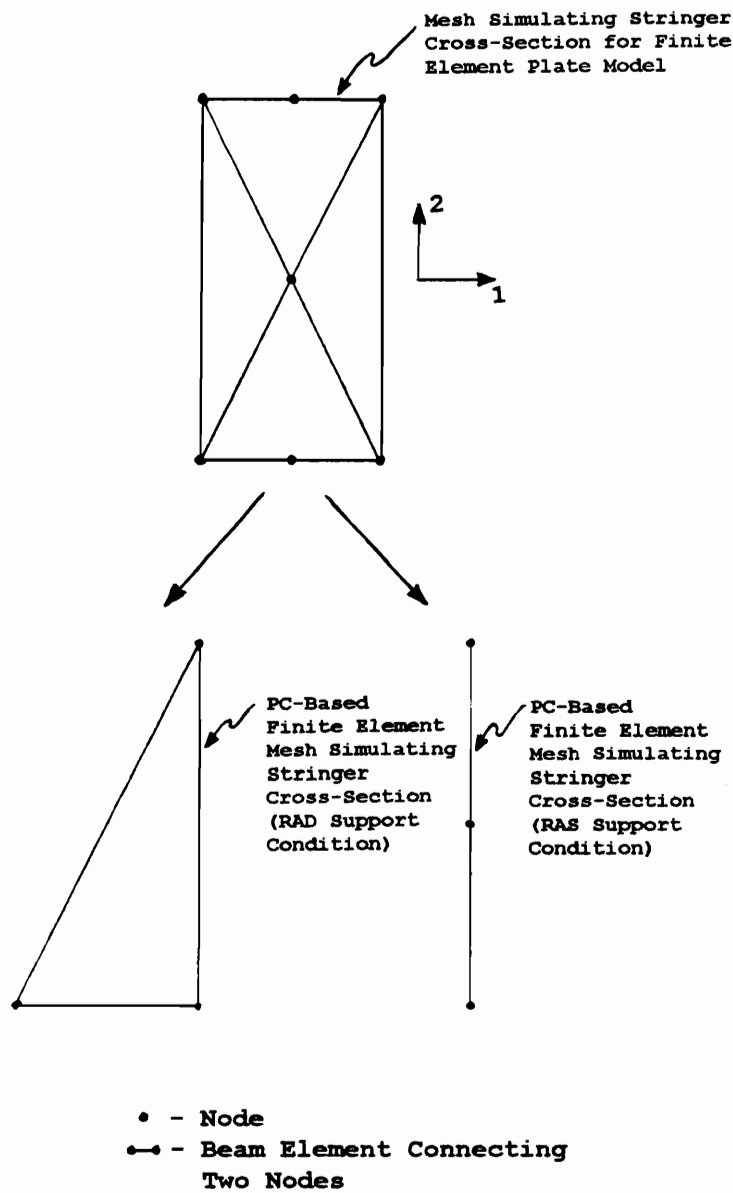
A summary of results presented in Table 3.3 reveal that the finite element solution is comparable to that calculated using classical beam theory. Maximum stresses are identical, while the finite element model is slightly stiffer, with the maximum deflection being 2.7 percent less than the classical beam solution. Nonetheless, this indicates that the stringer assembly works as intended with a small difference in deflection predictions.

In simplified PC models, stringer bending components are essentially the same as those for the plate models. However, the number of cross-sectional members are reduced to that shown in Figure 3.15. For the RAS support condition, the top and bottom nodes of the stringer are actually shared with the corresponding top and bottom deck

Table 3.3. Comparison of Finite Element Solution to Classical Solution for Element Assemblage used to Simulate Stringers - Test Case S-13.

PARAMETER	FINITE ELEMENT SOLUTION	CLASSICAL SOLUTION	PERCENT DIFFERENCE (%)
S11 Stress (maximum, psi)	816.3	816.3	0.0
Deflection (maximum, in.)	-0.0527	-0.0540	-2.4

Note: Both maximum stress and deflection occurred at mid-span.



Note: PC-Based model for the stack
support condition does not
require stringer elements.

Figure 3.15. Assembly of Beam Elements used
to Model Stringers in PC-Based Pallet Models.

nodes. This has an adverse impact on model behavior, but became necessary because of PC memory limitations. Stringer simplification is discussed further in chapter 4.

3.3.2 Notched Stringers

Notched stringers were modeled much the same way as unnotched stringers in the plate models. Beam elements with modified bending properties were used to model the notched section of the stringer. The properties assigned to this section were based on the conjugate beam method. An example of this method is presented by Mackes (1998, Volume I, Section 7). The example is for a notched stringer as shown in Figure 3.16. A comparison of deflection results for the conjugate beam method and the finite element method is given in Table 3.4. Both stresses and deflections predicted by the two methods are essentially the same.

To ensure that this methodology works on stringers used to construct pallets, 9 spruce-pine-fir stringers were evaluated. The modulus of elasticity was first determined for each stringer using a 2-point bending test in accordance with ASTM D 198-84 (ASTM, 1994). A summary of results for this evaluation can be found in Mackes (1998, Volume I, Section 8). Members were then notched using a band saw. These stringers had minimal radii at the notch corners. The notched stringers were again loaded up to 25 pounds at a

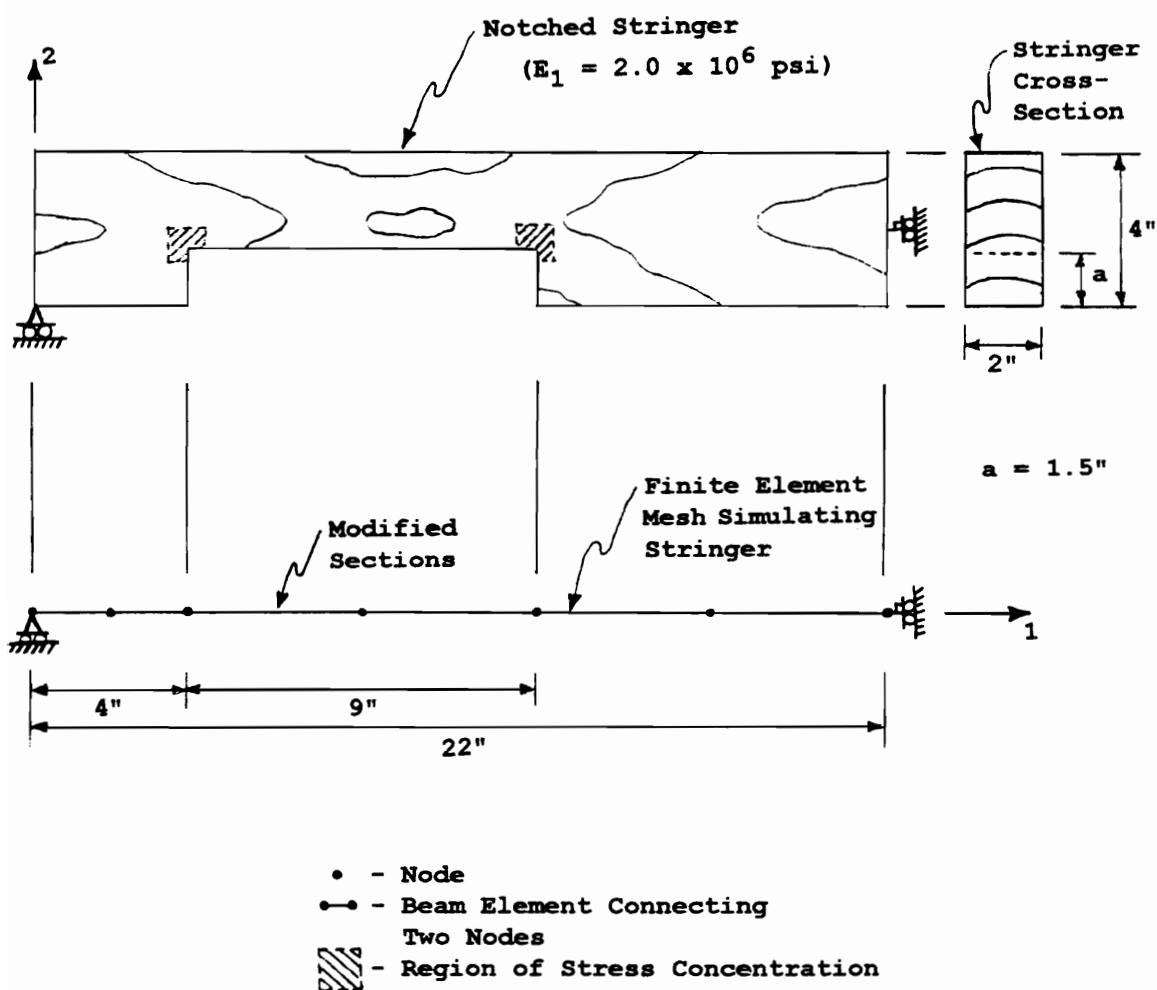


Figure 3.16. Notched Stringer used in Conjugate Beam Example.

Table 3.4. Comparison of Finite Elements Results to those obtained using the Conjugate Beam Method.

LOCATION (node)	FINITE ELEMENT SOLUTION	CONJUGATE BEAM SOLUTION	PERCENT DIFFERENCE (%)
Maximum Deflection:			
	(in.)	(in.)	
7	-0.005439	-0.005439	0.0
Maximum S11 Normal Stress:			
	(psi)	(psi)	
5 (compression)	-145.09	-145.03	0.0

rate 0.010 inch per minute to obtain an experimental deflection. Experimental deflections were compared to values obtained using the finite element method.

An example of model formulation, along with the ABAQUS input and output files for stringer S-1 are also given in Volume I, Section 8 of Mackes (1998). Results for all 9 stringers tested are presented in Table 3.5. Differences between experimental and predicted results range up to 10.3 percent. Part of this difference may be due to inconsistencies between actual notch dimensions and those assumed in the finite element model. Because the notches were cut with a band saw, they had a tendency to be somewhat irregular dimensionally. The method used to determine modulus of elasticity may also explain part of this difference. It was assumed that the modulus of elasticity of the wood in the unnotched member remained unchanged when the member was notched. This is true assuming the member was fairly uniform, which is not usually true in the case of wood. Nonetheless, the mean difference between experimental and predicted deflections was 2.7 percent, which suggests that this method can be used to predict the behavior of notched stringers used in this research.

The methodology used to model notched stringers in simplified models was that utilized in the current version of PDS-STRINGER for pallets with lumber decks. This

Table 3.5. Predicted versus Measured Deflections
for Notched Stringers.

STRINGER NO.	PREDICTED DEFLECTION (in.)	MEASURED DEFLECTION (in.)	PERCENT DIFFERENCE (%)
S-1	-0.0107	-0.0106	0.9
S-2	-0.0137	-0.0132	3.8
S-3	-0.0151	-0.0148	2.0
S-4	-0.0126	-0.0120	5.0
S-5	-0.0131	-0.0122	7.4
S-6	-0.0139	-0.0146	-4.8
S-7	-0.0111	-0.0104	6.7
S-8	-0.0139	-0.0126	10.3
S-9	-0.0146	-0.0152	-3.9
MEAN	-0.0132	-0.0128	2.7

methodology is based on work by Gerhardt (1985). The methodology involving modified sections was not utilized in simplified models because the radius used at notch corners varies significantly in commercial pallets. It is not clear how these variations affect stresses and stress concentrations in the stringers, particularly in the vicinity of the notch corner as indicated in Figure 3.16. Consequently, it is uncertain whether the stresses predicted by the finite element model utilizing modified sections are adequate. Therefore, the decision was made to utilize the current methodology used in PDS based on work by Zalph (1989) which has gained acceptance through years of use.

3.4 Blocks

Blocks were assumed to behave as rigid bodies which act as spacers between the top and bottom decks. They were constructed using either assemblages of beam and plate (shell) elements or only beam elements. All elements (no matter what the element type) comprising the blocks were assigned an arbitrarily high stiffness. Block compression, both global and localized at contact points with the top and bottom decks, was modeled using the contact (spring) elements. In the pallet models, blocks rotate as rigid bodies restrained only by the spring elements which simulate nail joints and contact locations.

The spring elements which were used to attach blocks to the top and bottom decks have zero-length. Therefore, both deck and block nodes share the same geometric location at points of attachment. Geometrically, this introduces a source of error into the model because top and bottom block surfaces do not physically occur at the same locations as the neutral planes (1-3 planes) of the top and bottom deck surfaces respectively. Attempting to model the actual geometric block height and deck thickness would have required a significant modification adding considerably to model size and complexity. Therefore, the height of blocks in the model were extended to the neutral planes of both the top and bottom deck surfaces as is currently done in PDS. For example, if a pallet was comprised of two 23/32 inch plywood decks and 4 inch high blocks, block height in the model is effectively 4.719 inches.

An example of a block used in the plate model is shown in Figure 3.17. The top and bottom surface of the block was comprised of shell elements. The mesh selected for the top and bottom block surface precisely matched the corresponding deck surface at points of attachment. S9R5 shell elements in ABAQUS were generally used instead of S8R shell elements because the additional node proved useful for spring attachment to the decks. The interior block support structure was comprised of B33 elements. Nodes of the top

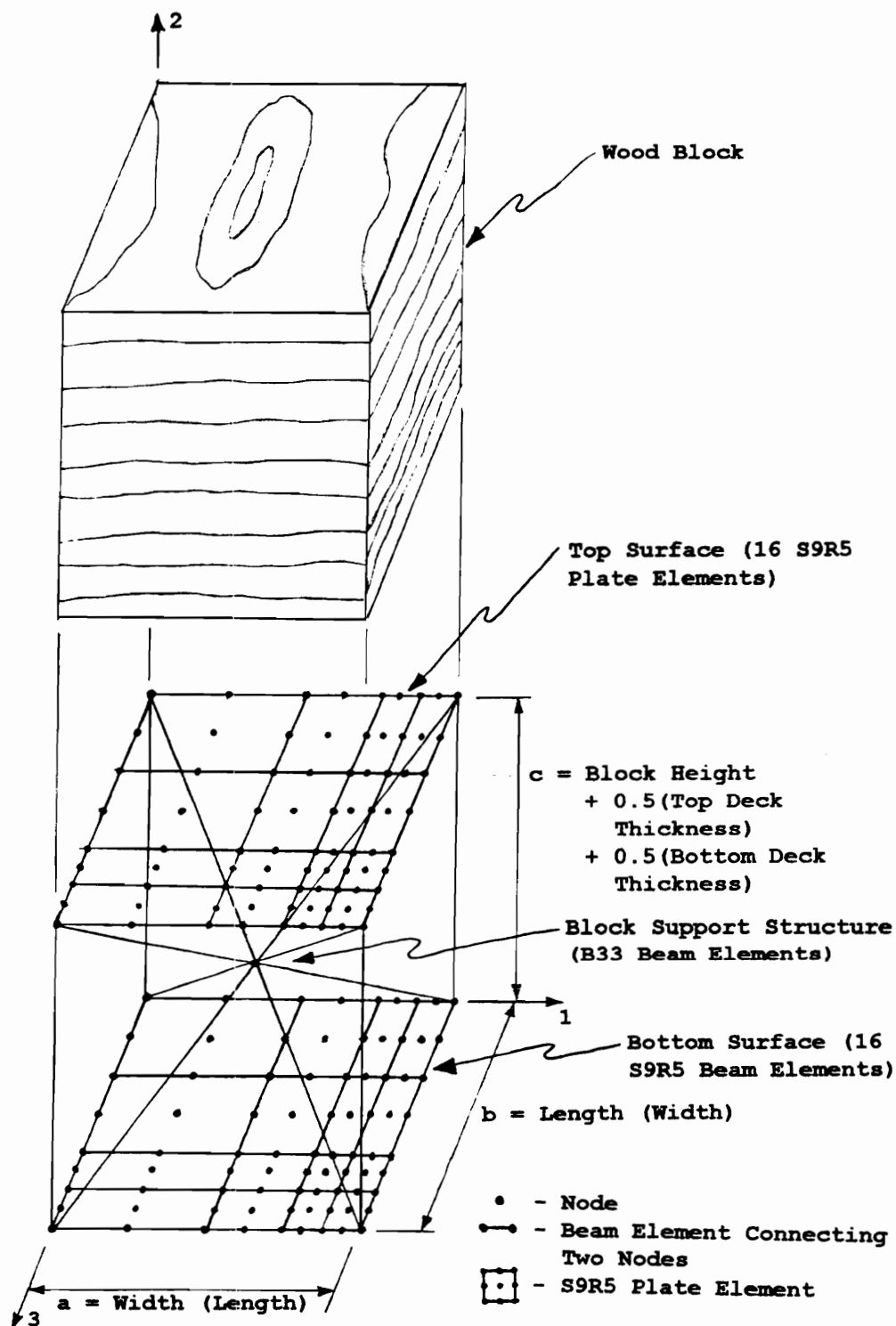


Figure 3.17. Assembly of Elements used to Simulate Blocks in Plate Models.

and bottom block surfaces which shared geometric coordinates with nodes of the top or bottom decks were attached using zero-length spring elements which function either as nail joints or contact locations. Spring elements can also be *dummied* out when not required.

The simplified blocks shown in Figure 3.18 functioned much the same way. The upper block surface was modeled using a grid framework of beam elements (B33) in place of shell elements. The bottom block surface was configured in one of three ways as shown in Figure 3.18:

- Type 1. The bottom block surface modeled using a grid framework of beam elements attached to a grid framework of beam elements simulating a full panel base with or without cut-outs.
- Type 2. The bottom block surface modeled using two lines of beam elements oriented perpendicular to each other attached to beam elements simulating a perimeter base, or a full panel base with or without cut-outs.
- Type 3. The bottom block surface modeled using one line of beam elements attached to beam elements simulating a unidirectional base.

Only Type 2 and Type 3 blocks are used in PDS-PANEL because the solution times required for models which use Type 1 blocks and a full grid simulating the bottom deck are too long. The Type 2 blocks are used to model pallets having a panel base either with or without cut-outs.

As with the plate model, the interior block support structure was comprised of beam elements, modified as needed

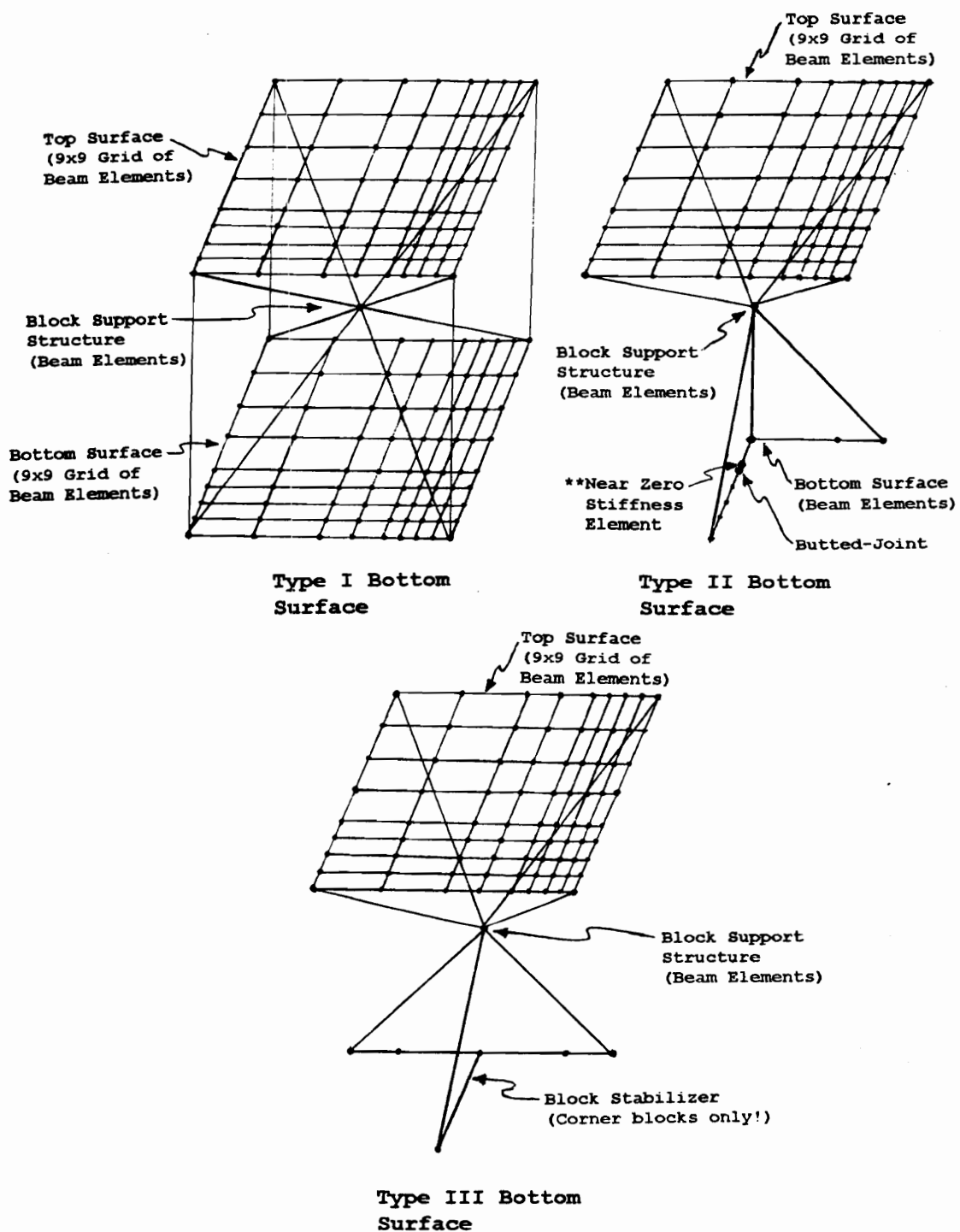


Figure 3.18. Assembly of Beam Elements used to Model Blocks in PC-Based Pallet Models.

to accommodate the different bases (bottom decks). The block stabilizer, shown in Figure 3.18 (Type 3 blocks only), was required for the corner blocks of unidirectional pallets modeled with Type 3 blocks to prevent excessive block rotation about the X-axis (1-direction).

3.5 Joints and Contact Zones

A critical aspect of pallet modeling involves successfully modeling non-rigid (flexible) nail joints and contact zones between the decks and spacers. Two types of resistance are thought to affect nail joints in pallets, shank withdrawal/head embedment (combined) stiffness and lateral stiffness. The contact springs between the decks and spacers of the pallets must account for both global and localized compression of the pallet members under load. Lateral frictional forces (resistance) which develop due to member contact were neglected.

Nails joints and contact zones can be modeled using zero-length spring elements in ABAQUS. Both SPRING1 and SPRING2 element types shown in Figure 2.23 were used. Although spring elements in ABAQUS can be used to model both linear and nonlinear behavior, only linear behavior was considered in this research. Linear behavior of springs was defined in terms of a spring constant (k). For displacement springs, the spring constant has the units force per unit

displacement. Other than the spring constant, the only additional inputs to ABAQUS required are defining the node(s) to which the spring is attached and the direction of spring action.

Generally, displacement springs were used in this research. However, for PC stringer pallet models, it is advantageous to replace several displacement springs with one rotational spring. The spring constant for this rotational spring is called the rotation modulus (k_r). The rotation modulus (k_r) has the units moment per unit rotation (i.e. inch pounds per radian) and is discussed further in Section 3.5.1.3.

3.5.1 Withdrawal/Head Embedment

The withdrawal and head embedment stiffness of a nail joint can be represented as one combined zero-length spring. For the models developed in this research, these springs were normally oriented in the 2-direction. Because no rational prediction methodology (formula) exists for estimating the stiffness values of these springs, they were determined experimentally.

A combined value for withdrawal/head embedment can be determined using the setup shown in Figure 3.19. A section of deckboard material was nailed to a stringer or block. The deckboard was loaded in double shear which acts to both

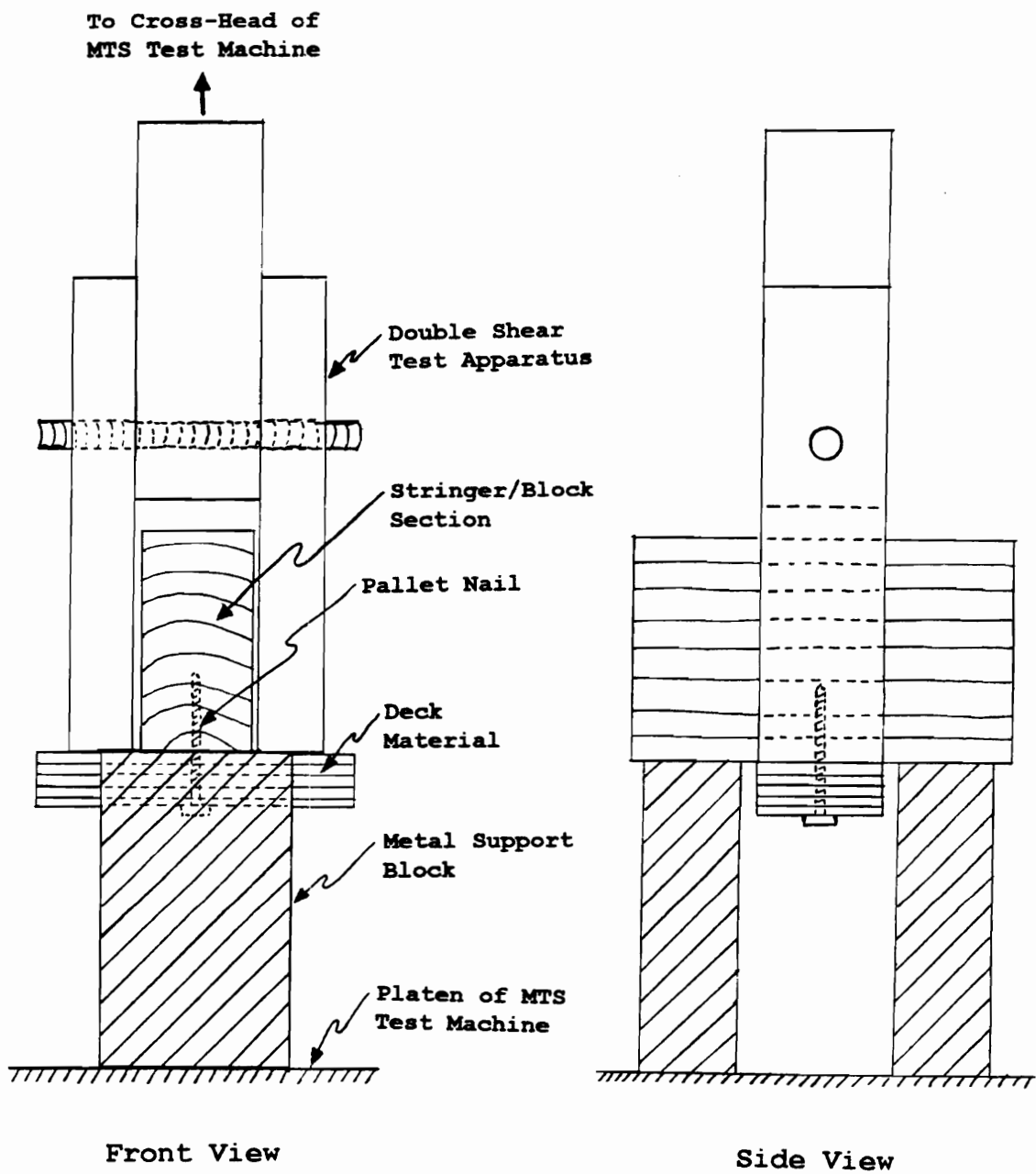


Figure 3.19. Setup used to determine a Stiffness Value for Withdrawal/Head Embedment Combined.

withdraw the shank and embed the head of the nail. As the system was loaded, a plot of load (P) versus deformation ($\Delta_{w/he}$) was recorded. An example of a plot is shown in Figure 3.20. The initial portion of the plot (up to 100 pounds) was of most importance because this is the load range that a nail will experience in a pallet under normal working conditions. Stiffness can be determined from the plot using the following equation:

$$k_{w/he} = P/\Delta_{w/he} \quad [3.1]$$

The units associated with $k_{w/he}$ are pounds per inch. Values obtained using this method were approximate because deckboard bending was also included in the deformation recorded. Therefore, the stiffness values calculated for $k_{w/he}$ are lower than actual.

Spring constants for withdrawal (k_w) and head embedment (k_{he}) can be determined more precisely separately. Once determined, these individual values can then be combined into a single value using the following equation:

$$k_{w/he} = (1/k_w + 1/k_{he})^{-1} \quad [3.2]$$

Methods for determining withdrawal and head embedment stiffness separately are discussed in subsequent sections. The rotation modulus is also discussed further in Section 3.5.1.3.

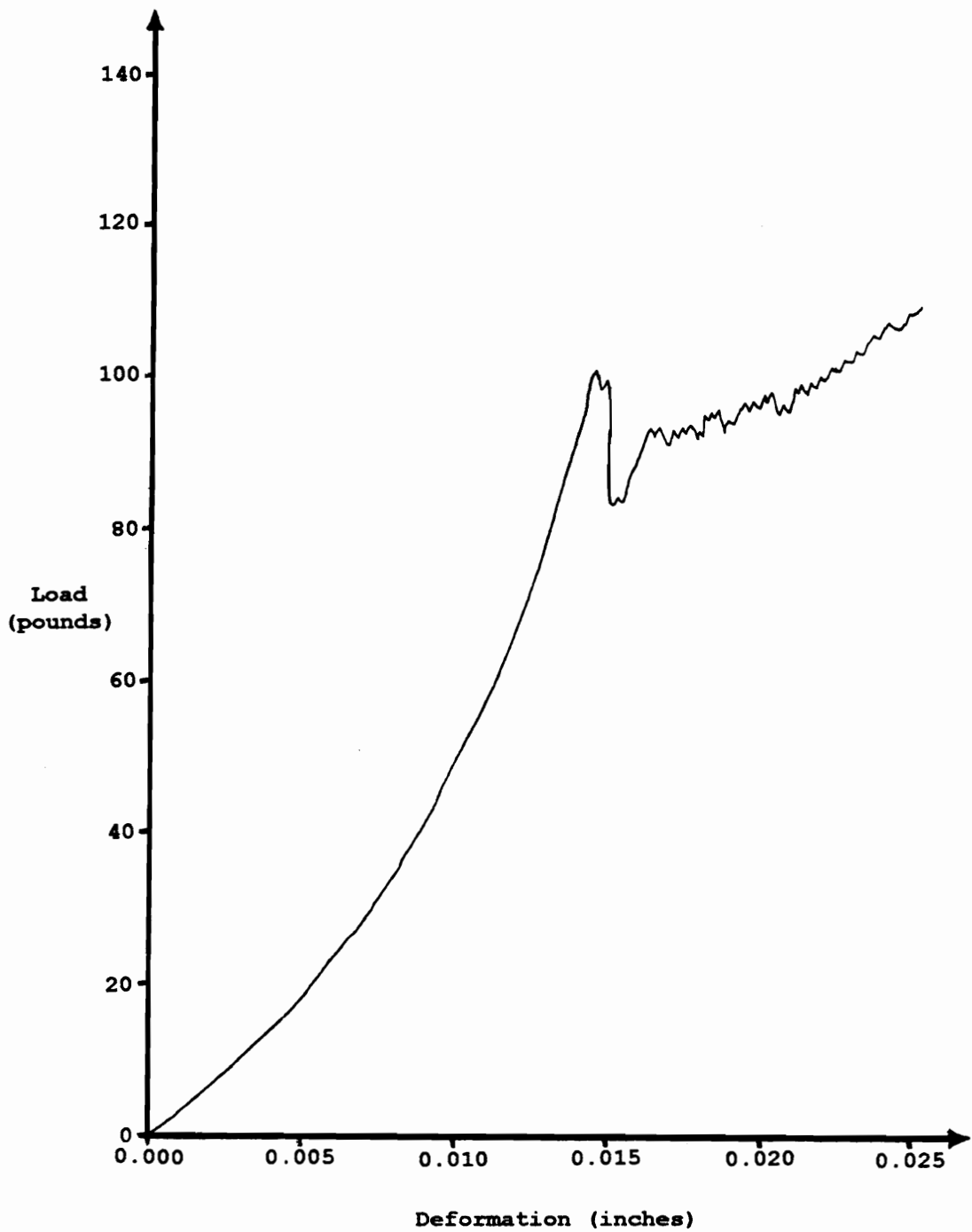


Figure 3.20. Plot of Load versus Withdrawal/
Head Embedment Deformation (Δ_w/h_e) .

3.5.1.1 Withdrawal Stiffness

Determination of withdrawal spring constant, K_w , was done experimentally. A schematic diagram of the test setup is presented in Figure 3.21. Three wood species, oak, southern yellow pine, and spruce, were selected for testing. Southern yellow pine and spruce members had a nominal cross-section of 2 by 4 inches, while the oak members had an actual cross-section of 2 by 4 inches. Two different nail types were used. One nail was 2 inches in length with a flat head and the other 2.25 inches with a countersinking head. Complete specifications for these two nail types are presented by Mackes (1998, Volume I, Section 9).

Nails were driven vertically into the test material (wood member). The nail along with the wood member was then placed in the test fixture. As the nail was loaded in withdrawal at a rate of 0.100 inch per minute, a plot of load versus deformation was recorded. Although nails were loaded in withdrawal until they were extracted from the wood, only the initial part of the load deformation curve was considered. Figure 3.22 shows a typical load deformation plot for a 2 inch nail loaded in withdrawal from a spruce member.

Deformation was measured at 100 pounds of load (P). Although somewhat arbitrary, this load level was used because it is a reasonable load that a given nail in a

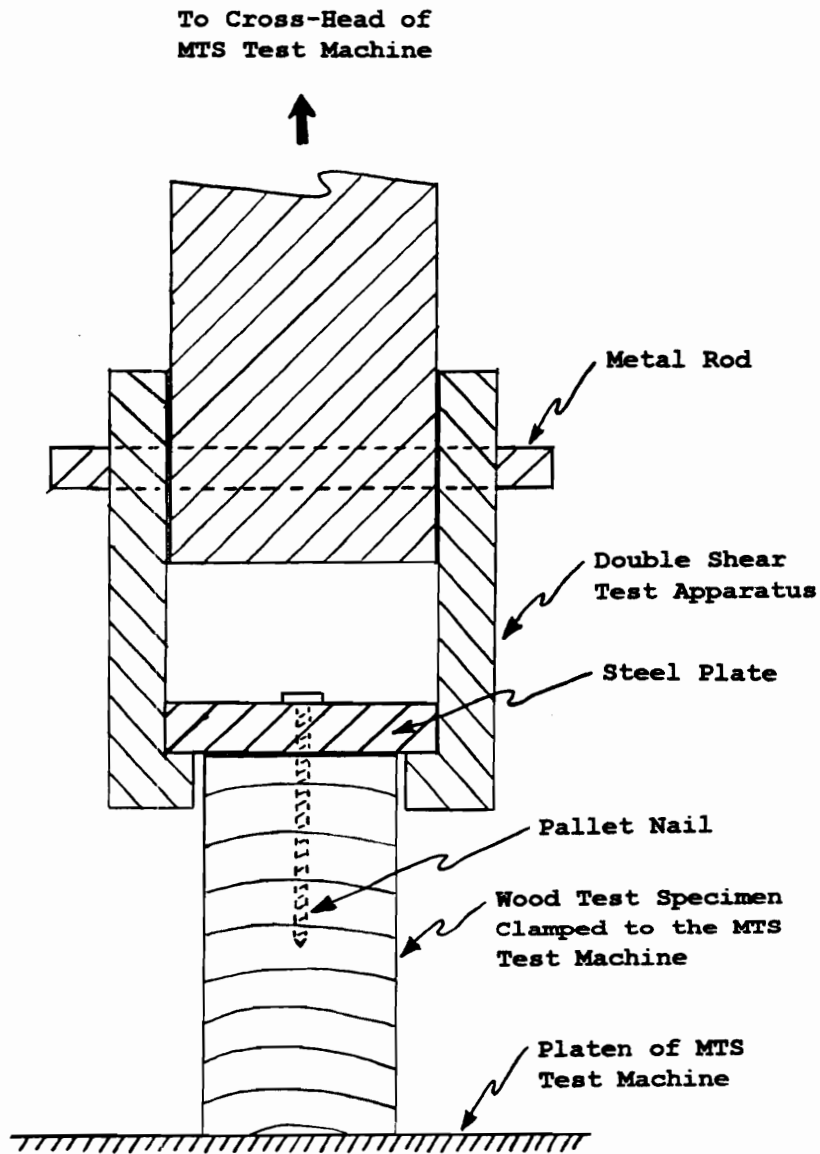


Figure 3.21. Schematic Diagram of Test Setup used to determine Withdrawal Stiffness.

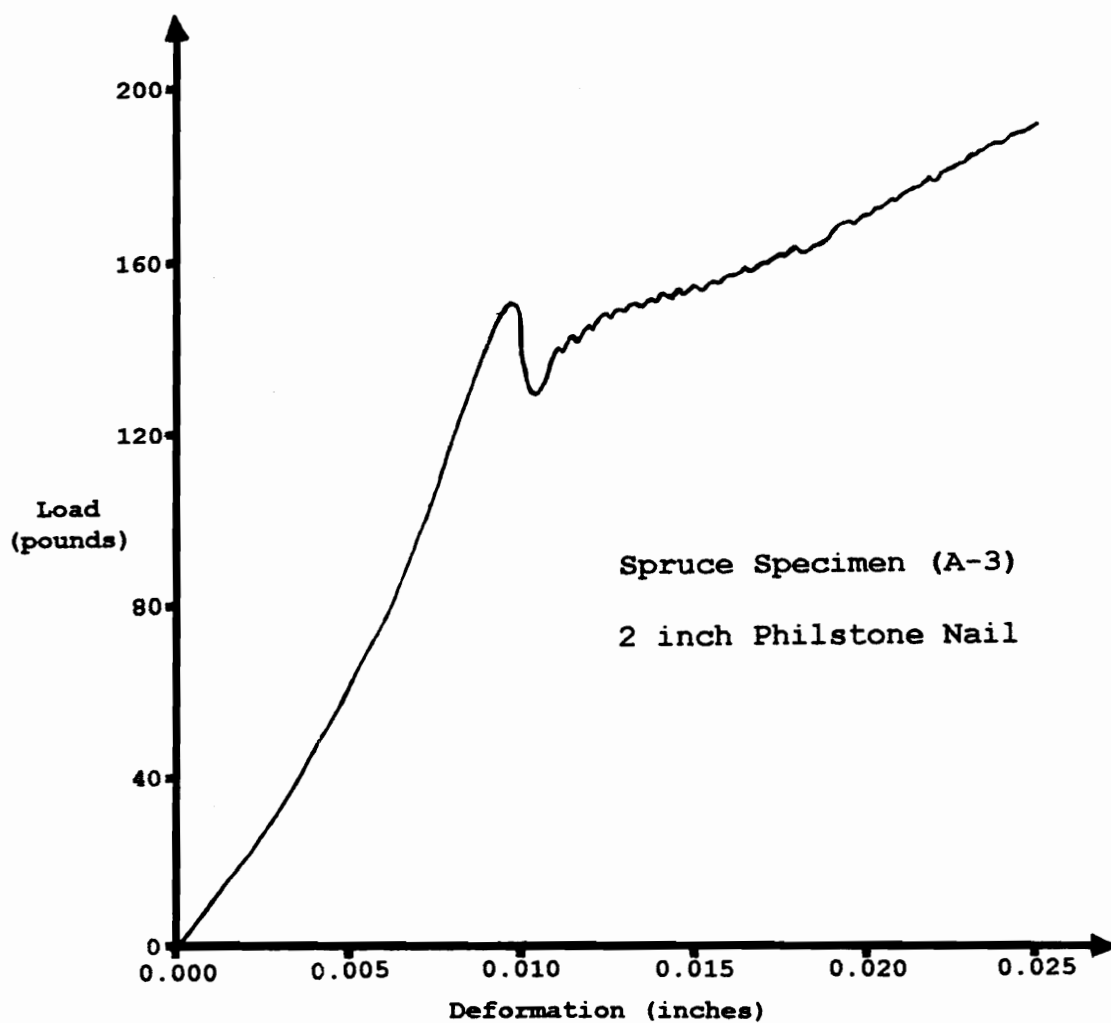


Figure 3.22. Plot of Load versus Withdrawal Deformation (Δ_w).

pallet might be subjected to. The measured deformation (Δ_w) was adjusted for settlement of the test setup. Complete data is given by Mackes (1998, Volume I, Section 10). The equation used for calculating k_w is as follows:

$$k_w = P/\Delta_w \quad [3.3]$$

The units of k_w are pounds per inch. Table 3.6 gives a summary of k_w values reported for use in PDS-PANEL. These values are the average of test values for both 2 and 2.25 inch long nails.

3.5.1.2 Head Embedment Stiffness

The spring constant for head embedment, k_{he} , can be determined experimentally using the test setup shown schematically in Figure 3.23. To determine k_{he} , the same two nail types selected for determining k_w were used. Both the 2 and 2.25 inch long nails were driven through plywood and OSB panels of varying thickness. Plywood Panels of various thickness, including 15/32, 19/32, and 23/32 inch, were tested, along with 7/16 and 23/32 inch thick OSB panels. Specimens were placed in the test apparatus and loaded at a rate of 0.100 inch per minute. As they were loaded, a plot of load versus deformation was recorded.

Several load deformation plots are shown in Figure 3.24. Note that the plots are initially linear, then begin to yield nonlinearly. The amount of load applied before

Table 3.6. Withdrawal Stiffness for
Selected Wood Species.

MATERIAL TYPE	MATERIAL DIMENSIONS (in)	SPRING CONSTANT (k) [(lb/in) /nail]
OAK	2" X 4"	12750
SYP	2" X 4"	13550
SPRUCE	2" X 4"	10500

Note: Withdrawal spring constants are the average for 2 inch and 2,25 inch nail data.

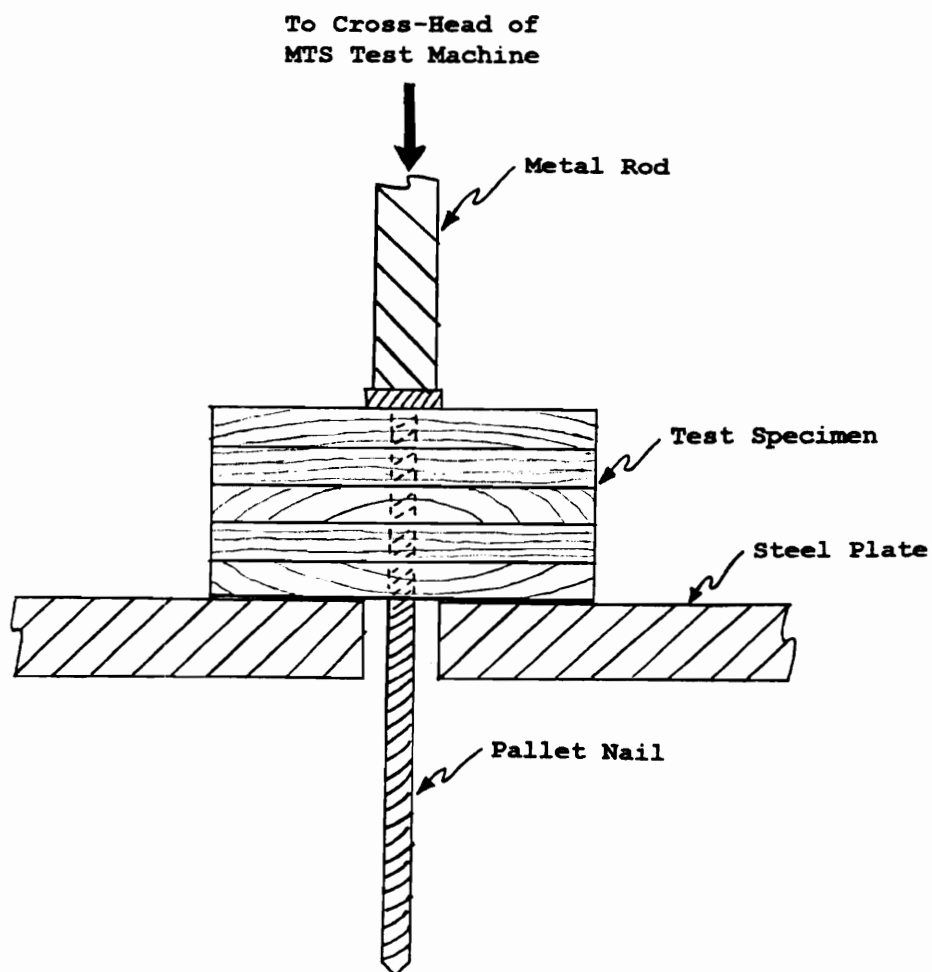


Figure 3.23. Schematic Diagram of Test Setup used to determine Head Embedment Stiffness.

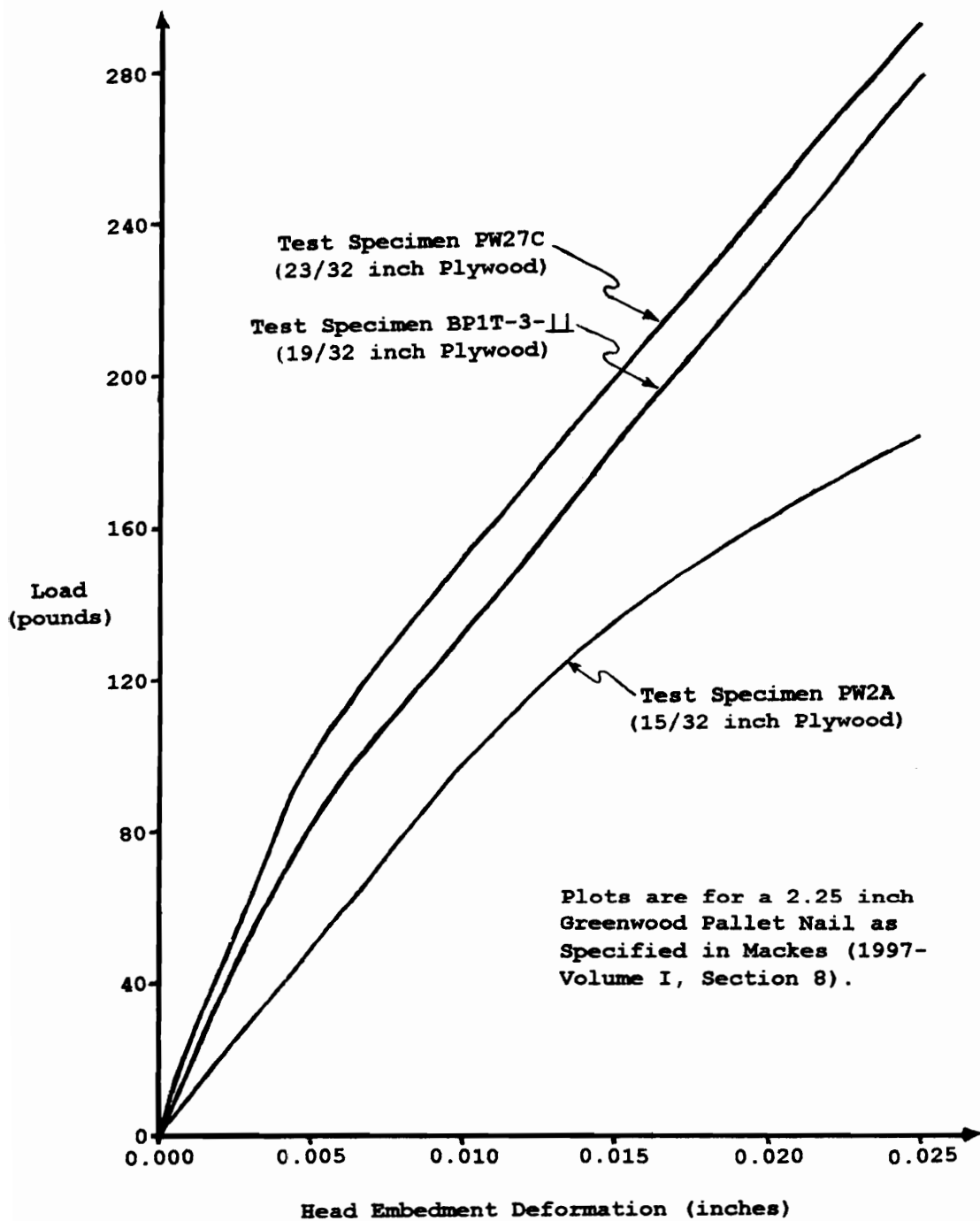


Figure 3.24. Plots of Load versus Head Embedment Deformation (Δ_{he}).

nonlinear yielding occurs was dependent on panel thickness. The length of the linear region increases with panel thickness. This is probably related to the length of the nail in contact with the panel resisting head embedment. When a threshold is reached the nail begins to embed. However, for pallets under normal load conditions, the initial part of the plot is probably of most importance in determining k_{he} .

Deformations (Δ_{he}) were measured at 100 pounds of load (P) for panels with a thickness of 19/32 and 23/32 inch and at 50 pounds of load for 7/16 and 15/32 inch thick panels. Although still somewhat arbitrary, deformation was measured at only 50 pounds for thinner panels because they support less load when assembled into pallets. Therefore, the load a given nail in a pallet constructed with these panels will experience is less. The equation used to calculate k_{he} was:

$$k_{he} = P/\Delta_{he} \quad [3.4]$$

As with k_w , the units of k_{he} are pounds per inch. Table 3.7 presents a summary of values submitted for use in PDS-PANEL. OSB values for 15/32 and 19/32 inch panels are estimated by interpolating between the values for 7/16 and 23/32 inch panel. All k_{he} values reported for OSB are rounded off to the nearest 1000 pounds per inch. Complete data are given by Mackes (1998, Volume I, Section 11).

Table 3.7. Head Embedment Stiffness for
Selected Pallet Deck Materials.

MATERIAL TYPE	MATERIAL THICKNESS (in)	SPRING CONSTANT (K) [(lb/in)/nail]
OAK	3/4	41400
SYP	1 (nom.)	74200
PLYWOOD	15/32	12900
	19/32	19100
	23/32	27000
OSB	7/16	5000
	15/32	*7000
	19/32	*9000
	23/32	11000

* Assigned a value based on existing data
by interpolation.

Note: OSB spring constants are for 2.25 inch
nail data. All other spring constants
are an average of 2 inch and 2.25 inch
nail data.

Plywood values reported are an average of results for both 2 and 2.25 inch long nails. OSB values are those for the 2.25 inch nail. These values were selected for OSB because the difference between the 2 and 2.25 inch nails was significant with stiffness being higher for the 2 inch nail. This was probably because the 2 inch nail had a flat head, while the 2.25 inch nail had a countersinking head. Also, if the OSB had a screen side, results varied depending on whether the screen side was up or down. Generally, results for OSB were more variable and joint stiffness less certain; therefore, the most conservative values obtained from testing were selected for use in PDS-PANEL.

3.5.1.3 Rotation Modulus

For simplified stringer pallet models, it is convenient to replace the combined withdrawal/head embedment spring with a single rotational spring. This is done as shown in Figure 3.25. The spring constant assigned to this rotational spring is called the rotation modulus. The model shown in this figure is for the top deck attachment to an edge stringer of a pallet.

The rotation modulus was calculated by applying a load ($P = 100$ pounds) and moment ($M = 100$ pounds/inch) at joint 2 of model #1 in Figure 3.26. For the example given, there were 11 nails along the 48 inch length of the stringer. The

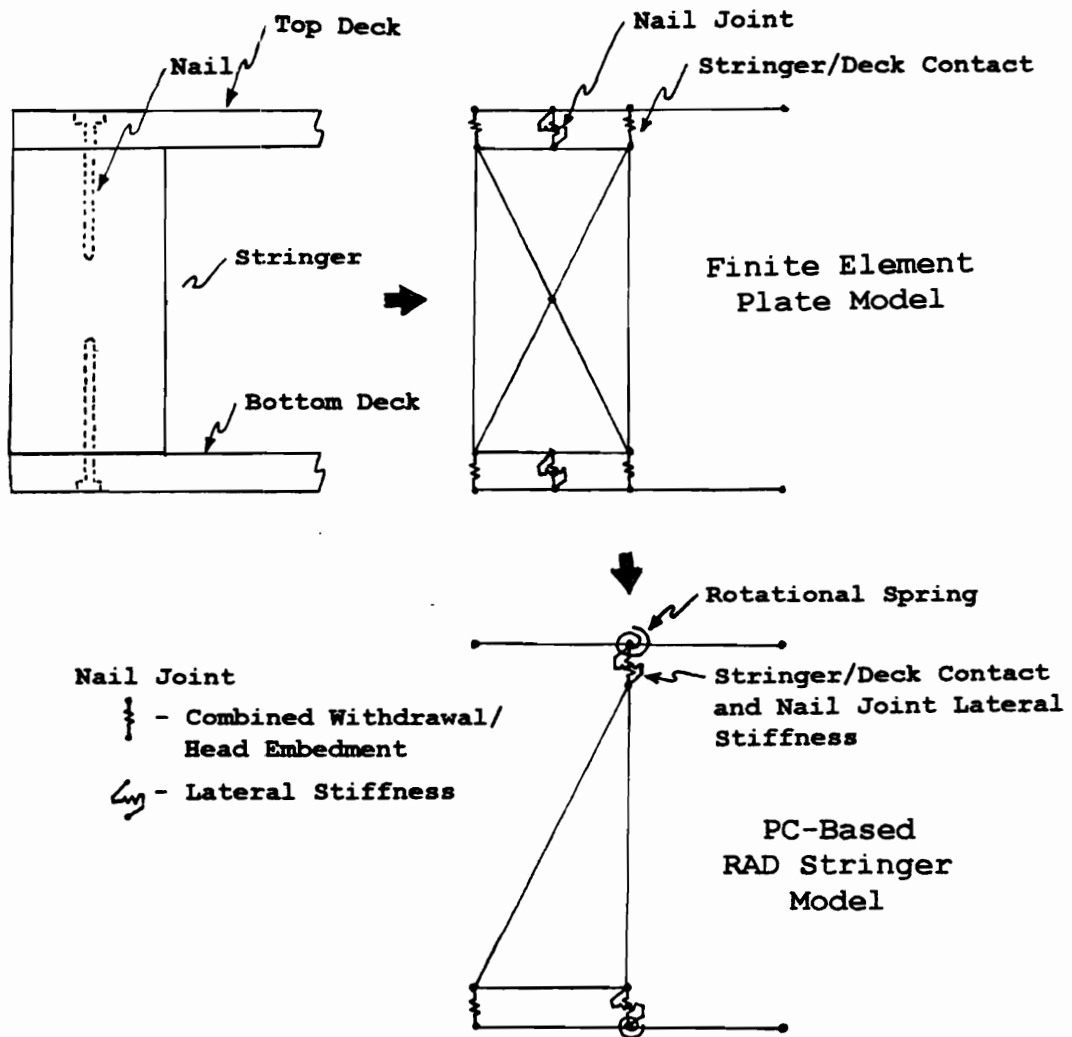
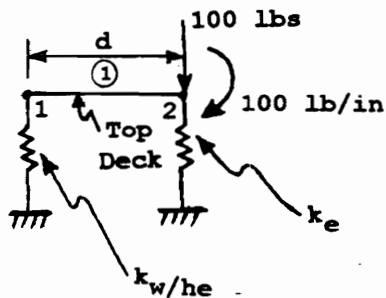


Figure 3.25. Replacement of the Combined Withdrawal/Head Embedment Spring with a Rotation Spring in Stringer Pallet Nail Joints.



k_w/he = Withdrawal/Head
 Embedment Stiffness
 k_e = Stringer/Top Deck
 Contact Stiffness
 d = Distance between the Nail
 Joints and Stringer Edge

Example:

Top Deck (Panel) Properties:

$E = 1.282 \times 10^6$ psi
 $b = \text{Length (Width)} = 48''$
 $h = \text{Thickness} = 0.583''$

$k_e = 60000 \text{ (lb/in)/in} \times 48 \text{ in} = 2.88 \times 10^6 \text{ lb/in}$
 $k_w/he = 5400 \text{ (lb/in)/nail} \times 11 \text{ nails} = 59,400 \text{ lb/in}$
 $d = 0.75 \text{ in}$

Finite Element Solution:

Rotation (rad) = -3.1255×10^{-3} rad
 Rotation Modulus = $31995 \text{ (in}\cdot\text{lb/rad)}/11 \text{ nails}$
 = $2909 \text{ (in}\cdot\text{lb/rad)}/\text{nail}$

Figure 3.26. Finite Element Model used to
 determine Rotation Modulus for Top Deck
 Attachment to Edge Stringer.

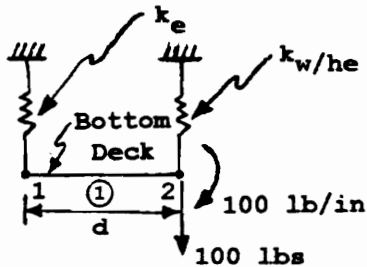
thickness of the top deck was 0.583 inches and the modulus of elasticity of the top deck in the 1-direction was 1.282×10^6 . The withdrawal/head embedment stiffness, k_w/h_e , was assumed to be 5,400 pounds/inch for each nail or a total of 59,400 pounds/inch. The stringer/top deck contact stiffness, k_e (discussed in section 3.5.3), was assumed to equal 60,000 (pounds/inch)/inch of stringer, or 2.88×10^6 pounds/inch.

Rotation at joint 2 can be determined using ABAQUS. The ABAQUS input and output for this example are given by Mackes (1998, Volume I, Section 12). The rotation at joint 2 was -3.1255×10^{-3} radians. The rotation modulus was then calculated using the equation:

$$\text{Rotation modulus} = M/\theta \quad [3.5]$$

M is the moment applied at joint 2 and θ is the rotation at joint 2. For the example given, the rotation modulus equaled 31,995 inch•pound/radian over the stringer length with 11 nail joints or 2,909 (inch•pound/radian) for each nail joint.

The model for the bottom deck attachment to stringers is shown in Figure 3.27. Although it is similar to the top deck model, it differs in one respect. Because contact between the bottom deck and stringer can potentially occur at any location across the width of the stringer (see Section 3.5.3.3), the point of rotation in the model was



$k_{w/he}$ = Withdrawal/Head
 Embedment Stiffness
 k_e = Stringer/Bottom Deck
 Contact Stiffness
 d = Distance between the Nail
 Joints and Stringer Edge

Example:

Bottom Deck (Panel) Properties:

$E = 1.282 \times 10^6$ psi
 b = Length (Width) = 48"
 h = Thickness = 0.583"

$k_e = 60000 \text{ (lb/in)/in} \times 48 \text{ in} = 2.88 \times 10^6 \text{ lb/in}$
 $k_{w/he} = 5400 \text{ (lb/in)/nail} \times 11 \text{ nails} = 59,400 \text{ lb/in}$
 $d = 0.75 \text{ in}$

Finite Element Solution:

Rotation (rad) = $+5.3700 \times 10^{-3}$ rad
 Rotation Modulus = $18622 \text{ (in}\cdot\text{lb/rad)}/11 \text{ nails}$
 = $1693 \text{ (in}\cdot\text{lb/rad)}/\text{nail}$

Figure 3.27. Finite Element Model used to
 determine Rotation Modulus for Bottom Deck
 Attachment to Edge Stringer.

always assumed to occur at joint 2. This tends to be conservative. For properties used with the top deck example, this model yields a lower rotation modulus of 1693 inch•pound/radian for each nail joint. Guidelines for determining which model should be used are also presented by Mackes (1998, Volume I, Section 12).

3.5.2 Lateral Stiffness

In this research, lateral stiffness (restraint) was applied using zero-length springs. The zero-length springs were oriented laterally in either the global 1- or global 3-direction. They attached 2 nodes, one deck node and one spacer node, sharing the same coordinates in the initial, undeformed state.

Other than identifying which node(s) the spring element was attached to and the direction of spring action, the only other input required was the spring constant, k_1 . In this research, k_1 was normally assigned a value utilizing the lateral stiffness prediction routine used in PDS. This routine is based on a methodology outlined in the Wood Handbook (1987) and discussed in detail by McLain (1975). When values from the PDS prediction routine were unavailable, a modified version of the procedure discussed by McLain (1975) was used. This modified procedure and

examples of lateral stiffness prediction are presented by Mackes (1998, Volume I, Section 13).

3.5.3 Spacer/Deck Contact

One prerequisite for precisely predicting pallet behavior is adequately modeling the contact regions between the decks and spacers. The amount of contact between the decks and spacers varies depending on numerous factors discussed below.

The perpendicular-to-grain modulus of elasticity values of both the deck and spacer were considered in modeling the localized effects of deck/spacer contact. In the undeformed state, the surfaces of both the deck and spacer were assumed to be smooth. Spacers were assumed to have sharp corners and edges. The latter assumption was often violated because stringer edges often had a radius.

Deck stiffness (modulus of elasticity) and lateral stability provided by nail joints both have an impact on gap formation, which directly relates to the amount of surface contact between the deck and spacer. Although the approach used to model stringer pallets does not directly incorporate deck stiffness, it does consider the lateral stability provided by nail joints attached to the deck. Both deck stiffness and lateral stability provided by nail joints were considered for block pallets.

The load type (uniform, line load, etc.) and magnitude of load also have an impact on the size and location of gap formation between decks and spacers. Gap formation is typically non-linear. As load increases, the gaps which can occur between the decks and spacers increase nonlinearly. Because linear analyses were used, the gaps that occurred in the models were unaffected by changes in load.

Contact between the decks and the spacers were modeled using zero-length springs oriented in the global 2-direction. Primary model inputs for these spring elements were definition of nodal attachment, direction of spring action, and spring constant, k_c . For stringer pallets, k_c values were determined using cross-sectional models. For block pallets, k_c values were based on tributary area, with contact between the decks and spacers determined iteratively. A discussion of these two differing approaches for determining k_c are presented in sections 3.5.3.1 and 3.5.3.2.

3.5.3.1 Stringer/Deck Contact

Several factors potentially influence the k_c value for stringer/deck contact, including the following:

1. Global stringer compression (GSC)
2. Localized stringer compression (crushing) at the point of contact (LSC)

3. Stringer bending (SB)
4. Stringer shear distortion (SSD)
5. Global deckboard compression (GDC)
6. Localized deck compression (crushing) at the point of contact (LDC)

The global compression of the deck (GDC) was not significant relative to the other factors and was neglected. The approaches used to model the stringer/deck contact for both the stack, RAD, and RAS support conditions are discussed in subsequent sections.

3.5.3.1.1 Stringer/Deck Contact in the Stack Support Condition

For plate models in the stack support condition, stringer/deck contact elements were assigned a stiffness value based on the combined value (k_c) for all factors considered. The k_c value was calculated as:

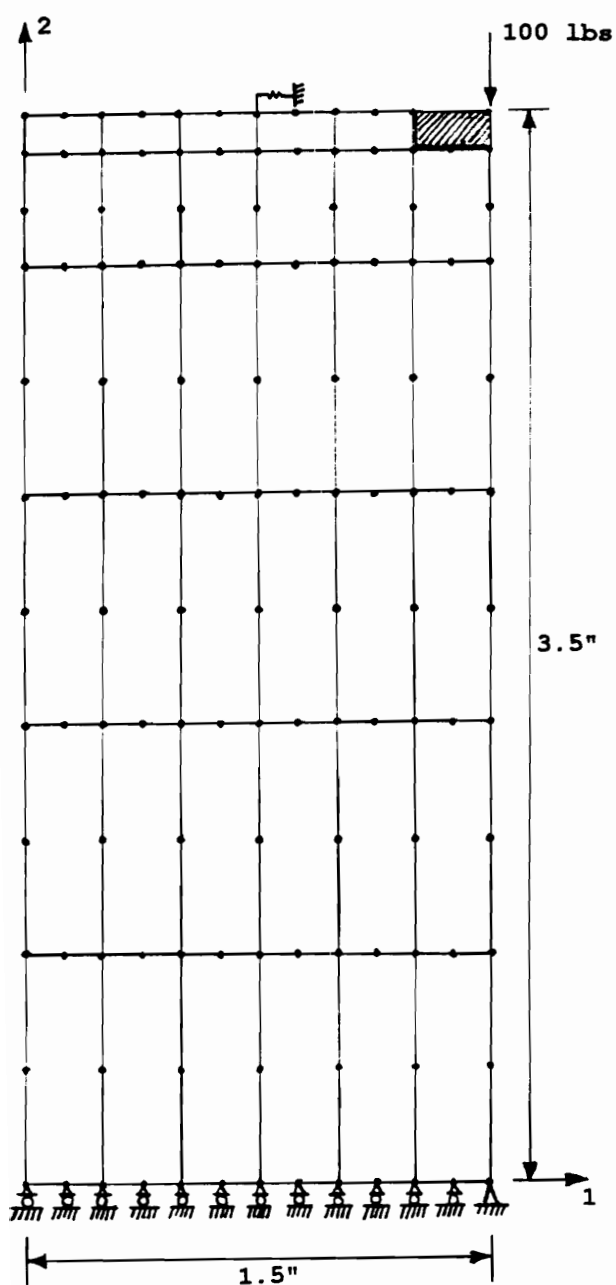
$$k_c = (1/k_{GSC} + 1/k_{LSC} + 1/k_{SB} + 1/k_{SSD} + 1/k_{LDC})^{-1} \quad [3.6]$$

The values for k_{GSC} , k_{LSC} , k_{SB} and k_{SSD} can be predicted as a combined value (k_{CS}). Therefore,

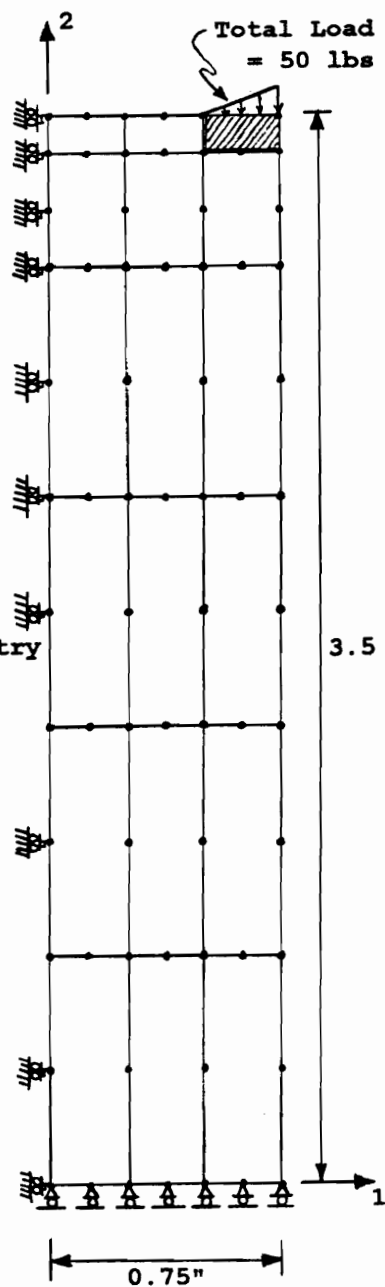
$$k_c = (1/k_{CS} + 1/k_{LDC})^{-1} \quad [3.7]$$

Values required for determining k_c were all predicted using finite element models.

The k_{CS} value can be determined using the finite element model shown in Figure 3.28. Elements comprising



Edge Stringer Model



Interior Stringer Model

- - CPS8 Element in ABAQUS
- ▨ - Section A (See Mackes, 1998 - Volume I, Section 14)
- ~| - Lateral Restraint of Nail Joint

Figure 3.28. Finite Element Models used to Predict Stringer Contact (k_{CS}) Stiffness.

this model were CPS8 solid orthotropic elements in ABAQUS. This model also considered shear distortion of the stringer, but this factor was not considered to be significant. The lateral spring attached to the top of the stringer in the model represents the lateral restraint of the nail joints. Input values to the model included the modulus of elasticity in both the 1- and 2-directions (E_1 and E_2) and the associated Poisson's ratio (ν_{12}). The 1-direction of the model was assumed to correspond with the radial direction of the wood comprising the stringer. The 2-direction was assumed to correspond with the tangential direction and the 3-direction with the longitudinal direction. E_R , E_T , and ν_{12} were determined from literature (Bodig and Jayne, 1982). A unit section width of one inch was used along the length of the stringer.

Ideally, the load should be applied to the member over an area which corresponds to the contact region. Unfortunately, in actual pallet structures, this region of contact can be quite variable. Therefore, it was necessary to assume the amount of contact based on observations of gap formation in stringer pallet joints. Generally, these assumptions resulted in conservative (lower than actual) stiffness values. For contact between the edge stringer and the top deck where gap formation was most notable, the load was applied at node 525. For interior stringer members

where no gap formation was observed to occur, the load was applied over a region of 0.25 inches. The load applied to the member was tapered as shown in Figure 3.28. The tapered load was thought to better simulate the actual condition.

With regard to model output, the primary value of interest was the deformation at node 525 of the model pictured in Figure 3.28. Contact model examples, along with ABAQUS input and output files, are presented by Mackes (1998, Volume I, Section 14). The deformation pattern predicted for the edge stringer example is shown in Figure 29. A k_{CS} value can be calculated based on the load (P) and the deflection at node 525 (Δ_{525}) as follows:

$$k_{CS} = P/\Delta_{525} \quad [3.8]$$

The units associated with k_{CS} are pounds per inch.

The value for k_{LDC} can be determined using the finite element model shown in Figure 3.30. This model was also comprised of CPS8 solid orthotropic elements. Symmetry was used during model development. The 2-direction of the model was assumed to correspond to the radial direction of the wood comprising the deck. The 1-direction normally corresponded to the strong axis of the panel or the longitudinal axis of a solid wood deckboard. E_R and the required Poisson's ratio were obtained from literature (Bodig and Jayne, 1982). The load was applied over a region of contact which corresponded to those assumed for the

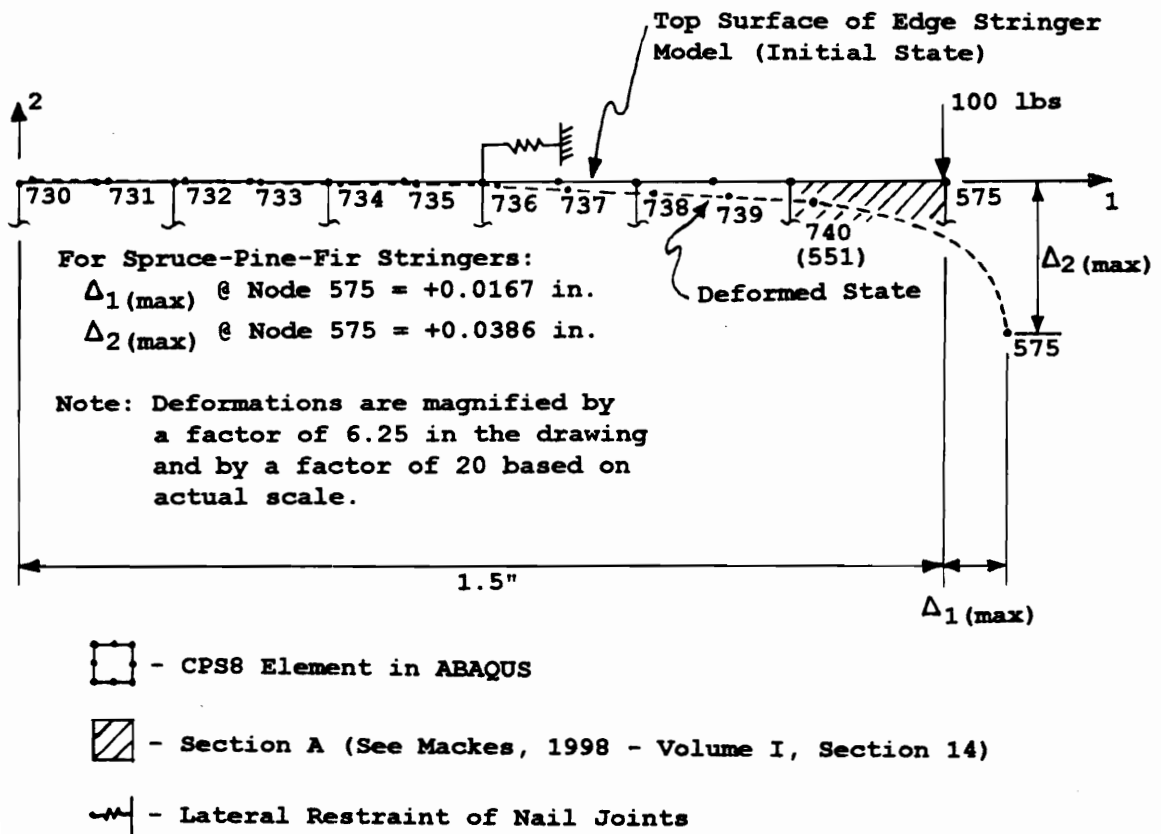
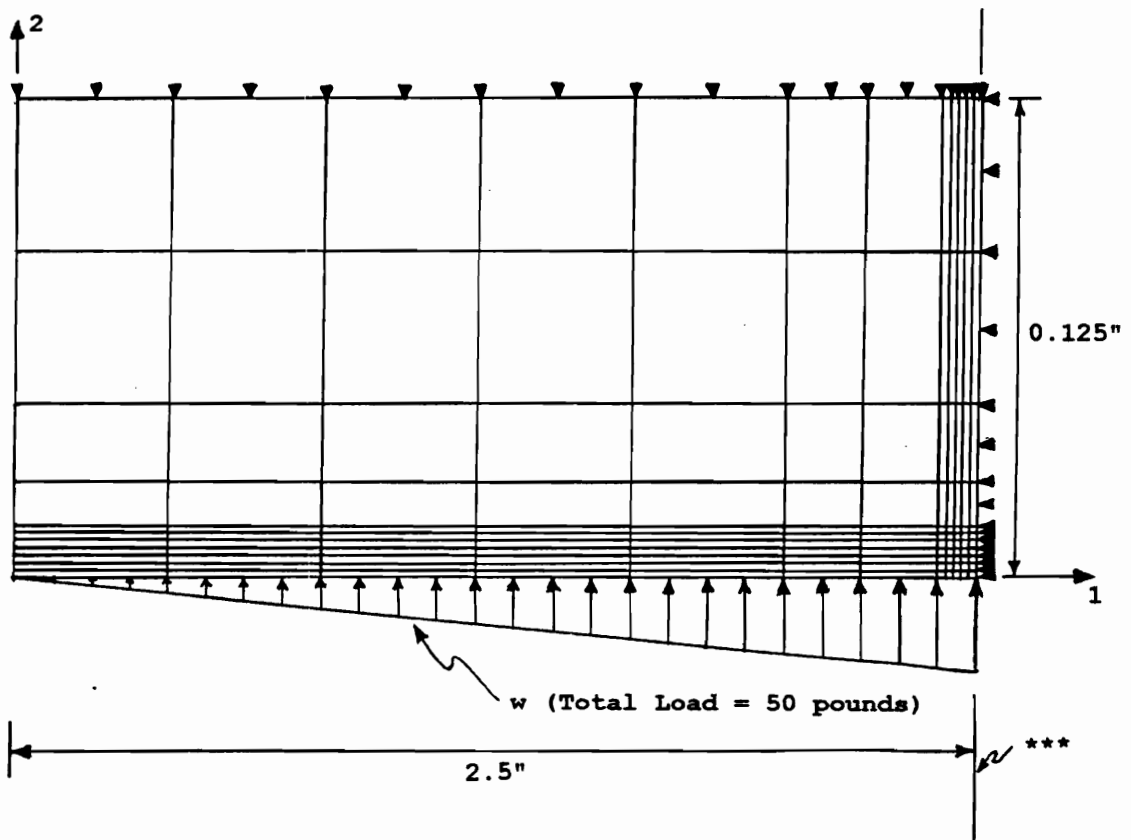


Figure 3.29. Deformation Pattern Predicted by Finite Element Model used to Predict Edge Stringer Contact (k_{CS}) Stiffness.



□ - CPS8 Solid Element

Boundary Conditions

▼ - Restrained in 2-Direction

◄ - Indicates a Line (Boarder) of X-Symmetry

*** Note: Nodes which occur along the line of X-Symmetry are effectively restrained in the 1 and 6 degrees of freedom.

Figure 3.30. Finite Element Model used to Determine k_{LDC} Value.

stringer. The value for k_{LDC} was calculated based on load (P) and predicted deformation using the equation:

$$k_{LDC} = P/\Delta_{525} \quad [3.9]$$

Stiffness values for k_{CS} and k_{LDC} were then used to calculate an overall value for k_C using Equation 3.1.2.

To simplify this process for pc-based models, multiple regression analyses were performed. Complete documentation of these analyses are included in Volume I, Section 15 of Mackes (1998). In these analyses only the k_{CS} values were considered, with the k_{LDC} values being neglected. The following factors were considered for both edge and interior stringers in the regression analyses:

1. 3 stringer widths (1, 1.5 and 3.5 inches)
2. 3 stringer heights (2.5, 3.5, and 5.5 inches)
3. 3 modulus of elasticity (E_T) values in the 2-direction (0.05×10^6 , 0.75×10^6 , and 0.1×10^6 psi)

Because there was potential for bending and shear distortion in the cross-sectional (1-2) plane of edge stringers, the modulus of elasticity (E_R) in the 1-direction was considered for these members. Two levels of this factor (0.1×10^6 and 0.2×10^6 psi) were used.

Based on this analysis the following equation was the best fit for determining the spring constant of edge stringer contact (k_{esc}):

$$k_{esc} = 983.2 + 47.9048SW - 79.6151SH + 0.0188E_T + 0.00104 E_R \quad [3.10]$$

Equation 3.10 uses literature values for E_R and E_T at a 12 percent moisture content basis. This equation was converted to an equation based on specific gravity assuming a correlation between modulus of elasticity and specific gravity (G). The equation, derived based on specific gravity (oven-dry volume basis), is:

$$k_{esc} = 983.2 + 47.9048SW - 79.6151SH + 3684.71G \quad [3.11]$$

Because all values in PDS-PANEL are input on a "green" basis, an adjustment to Equation 3.11 was necessary. This adjustment was accomplished by reducing the modulus of elasticity (perpendicular-to-grain) and subsequently the constant assigned to specific gravity by 23 percent (Wood Handbook, 1987). The following equation results:

$$k_{esc} = 983.2 + 47.9048SW - 79.6151SH + 2837.23G \quad [3.12]$$

A similar equation can be derived for determining the spring constant of interior stringer contact (k_{isc}):

$$k_{isc} = 3537.3 + 582.9SW - 715.5SH + 9064.86G \quad [3.13]$$

These latter two equations form the basis for predicting the stringer/deck contact stiffness used in PC-based models for stringer pallets in the stack support condition.

3.5.3.1.2 Stringer/Deck Contact in the RAD Support Condition

Stringer/deck contact points are shown for the RAD support condition in Figure 3.31. The points of contact considered are:

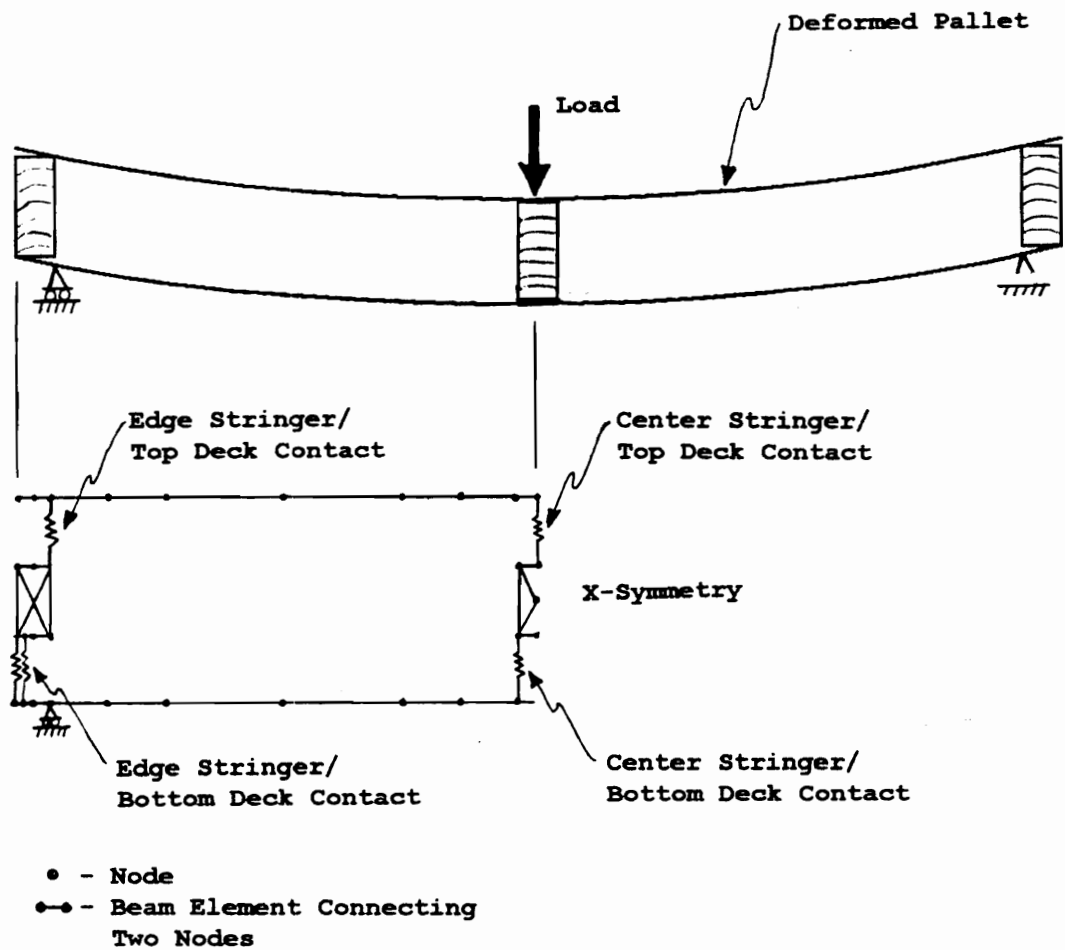
1. Edge stringer to top deck (ESTD)
2. Edge stringer to bottom deck (ESBD)
3. Interior (Center) stringer to top deck (ISTD)
4. Interior (Center) stringer to bottom deck (ISBD)

Generally, the global effects of the stringer were neglected in the rack support conditions because they were not significant. This includes global stringer compression, stringer bending, and stringer shear distortions. It must be noted that even though stringer bending was neglected, the stringer was still free to rotate as a rigid body restrained primarily by the nail joints.

Localized deformations were considered for determining the stiffness of contact elements in the RAD support condition. The k_{ESTD} value was calculated as the localized edge stringer compression (LESC) caused by the downward force on the top deck plus the localized compression of the top deck (LDC). This equation takes the form:

$$k_{ESTD} = (1/k_{LESC} + 1/k_{LDC})^{-1} \quad [3.14]$$

The k_{ESBD} value was calculated as the localized compression of the edge stringer (LESC) caused by the upward movement of



Note: Nail Joints are not Shown.

Figure 3.31. Contact Points of Stringers and Decks for the RAD Support Condition.

the lower deck due to deck deflection minus the downward movement of the block causing localized deckboard compression (LDC). This equation takes the form:

$$k_{ESBD} = (1/k_{LESC} - 1/k_{LDC})^{-1} \quad [3.15]$$

The equations for k_{ISTD} and k_{ISBD} are:

$$k_{ISTD} = (1/k_{IESC/TD} + 1/k_{LDC})^{-1} \quad [3.16]$$

$$k_{ISBD} = (1/k_{IESC/BD} + 1/k_{LDC})^{-1} \quad [3.17]$$

The $k_{IESC/TD}$ is the localized compression of the interior stringer caused by the top deck and $k_{IESC/BD}$ is that caused by the bottom deck. The models used to predict localized deflections in both stringers and decks are presented by Mackes (1998, Volume I, Section 16).

To adequately model contact between the edge stringer and bottom deck, it was necessary to consider all potential contact configurations. Several possibilities are shown in Figure 3.32. Figure 3.33 further illustrates this phenomenon by showing profiles of contact between the edge stringer and lower pallet deck. They were generated iteratively using pallet section models discussed further in Section 3.5.4. Based on these figures, it should be apparent that contact between the stringer and lower deck can potentially occur at any point between the exterior or interior edge of the stringer. Therefore, a methodology was

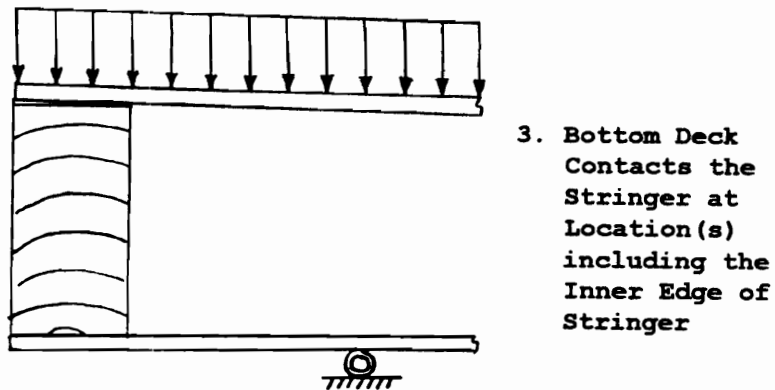
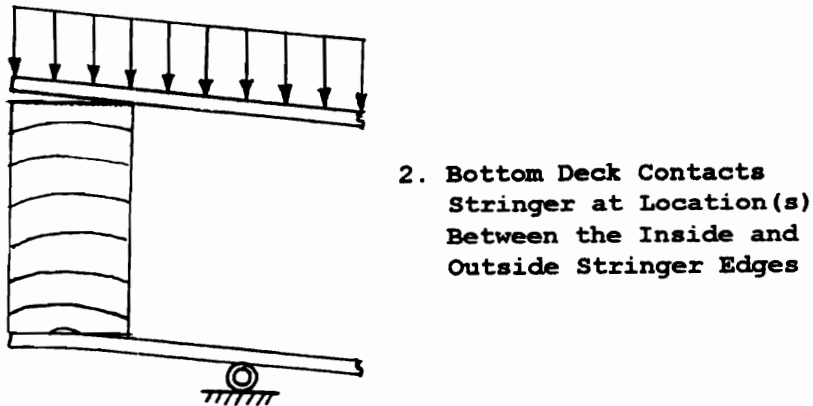
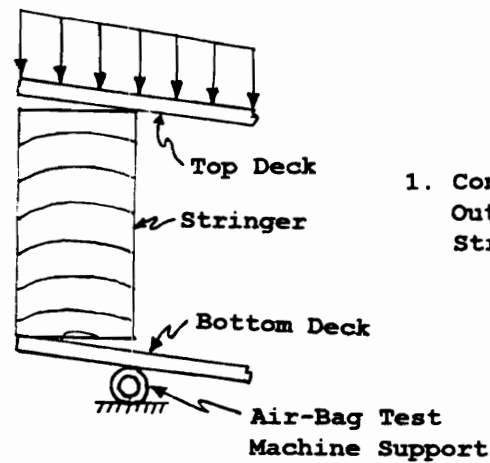
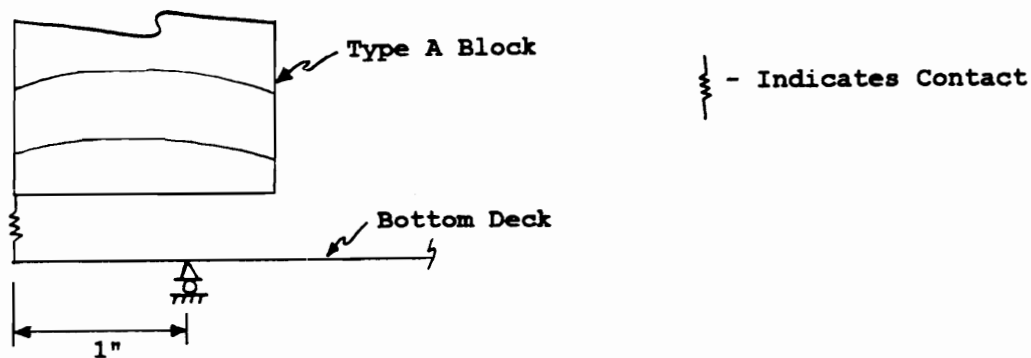
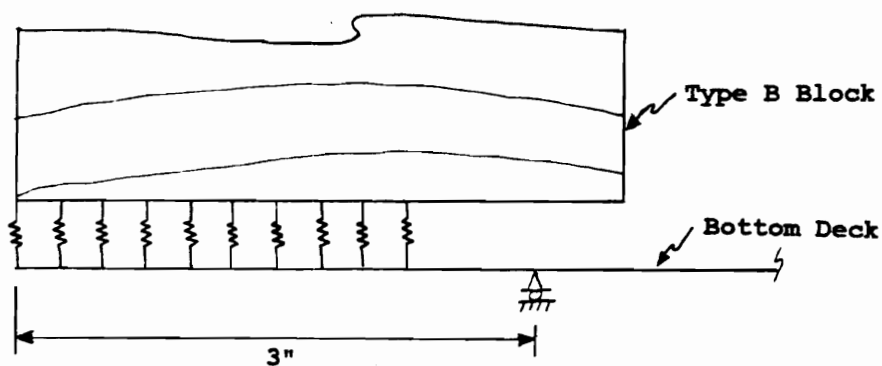


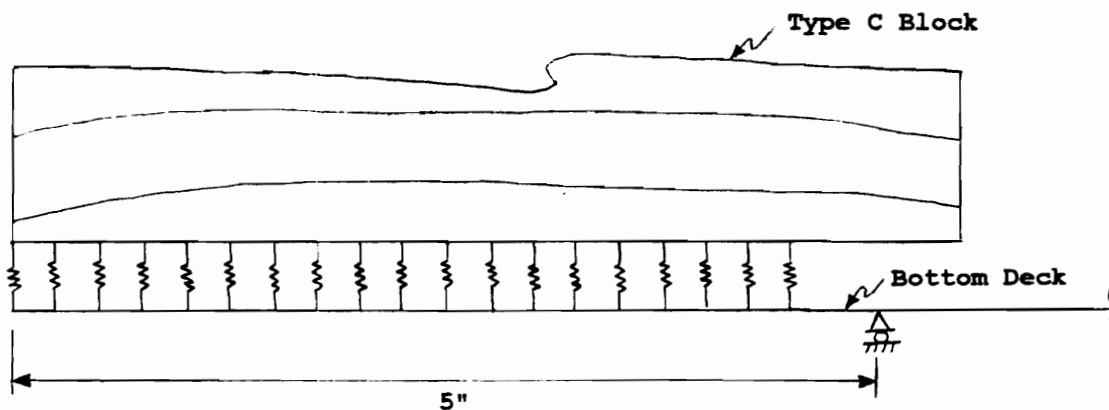
Figure 3.32. Potential Contact Configurations between Edge Stringer and Bottom Deck.



Test Specimen FA1-46



Test Specimen FB1-42



Test Specimen FC1-38

Figure 3.33. Profiles of Contact between the Edge Stringer and Bottom Deck.

devised for allowing the contact point to float across the base of the stringer. This methodology is based on the analysis of edge stringer/bottom deck interfaces conducted using pallet section models.

To make this methodology of practical use, the distance (D) of the contact spring from the outside edge of the stringer was predicted based on a multiple regression analysis. Factors considered for predicting D are:

1. OH = Portion of the pallet overhanging the support
2. SW = Stringer width
3. EI = EI of lower deck expressed on a per foot basis

Details of this regression analysis are given by Mackes (1998, Volume I, Section 17).

Based on the multiple regression analysis, the best fit for predicting D of a full uniformly loaded pallet is:

$$\text{LOG (PBW)} = -1.26174 + 0.187756(\text{OH}) \quad [3.18]$$

PBW is the fractional percentage of stringer width for locating the contact spring from the outside edge of the stringer. BW and EI were dropped from the model as insignificant. Equation 3.18 can be expressed as follows:

$$\text{PBW} = 10^{[-1.26174+0.187756(\text{OH})]} \quad [3.19]$$

The equation with the best fit for line loaded pallets is:

$$\begin{aligned} \text{PBW} = & -0.271217 + 0.052872(\text{OH}) - 1.66 \text{ E-}7(\text{EI}) \\ & + 0.112912(\text{BW}) \end{aligned} \quad [3.20]$$

For both full uniformly and line loaded pallets, D was calculated using:

$$D = PBW * BW \quad [3.21]$$

Partial uniform loads were not considered in this analysis, but are thought to behave somewhere between full uniformly loaded and line loaded pallets depending on the degree of partiality. In this research the line load equation was used for partial uniform loads because it yields more conservative predictions.

3.5.3.1.3 Stringer/Deck Contact in the RAS Support Condition

Because interior stringers deflect more than the edge stringers, the deflection pattern of the pallet at mid-span, shown in Figure 3.34, appears similar to that for patterns observed in the RAD support condition. Because of this similarity, spring constants used for contact elements in the RAD support condition were used for elements in the RAS support condition. However, in the vicinity of supports it was necessary to have the stringer fully in contact with the lower deck. The configuration of contact elements for both the plate and PC-based stringer pallet models in the RAS support condition are discussed further in Chapter 4.

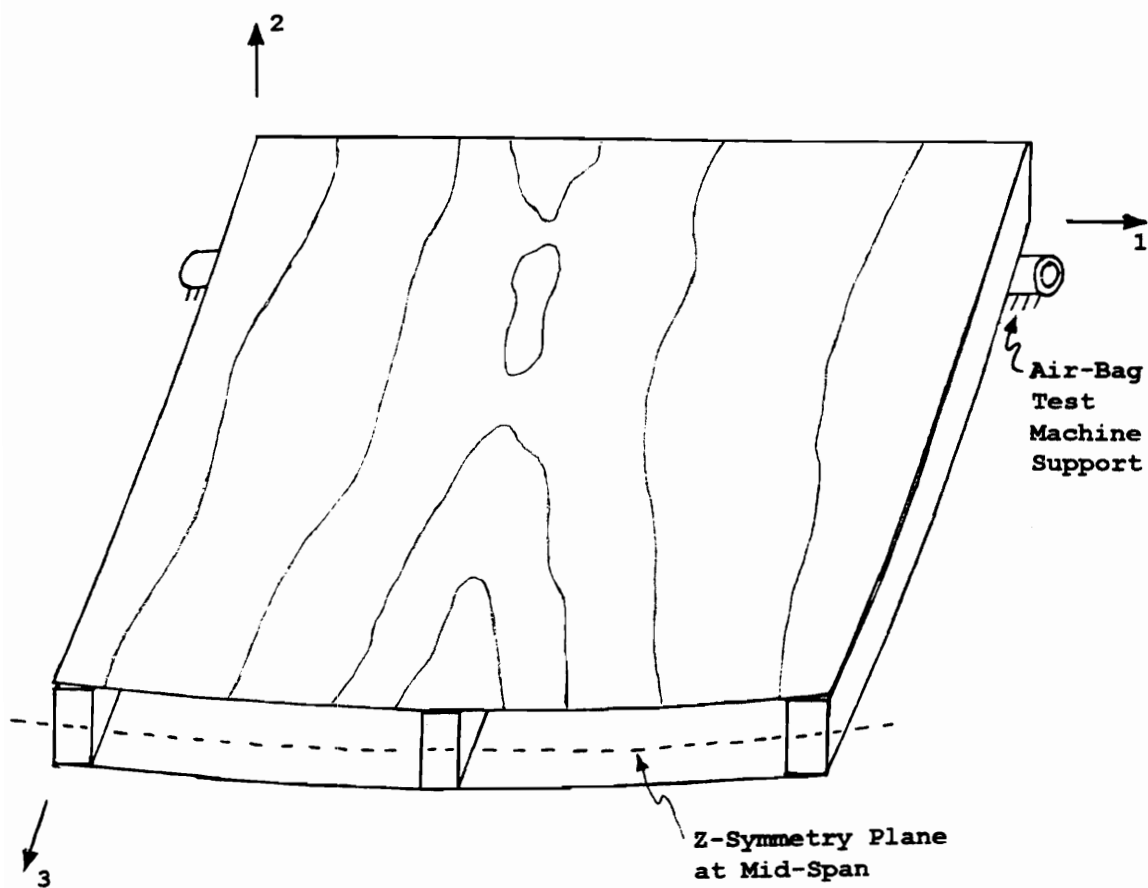


Figure 3.34. Deformation Pattern
at Mid-Span for Stringer Pallets
in the RAS Support Condition.

3.5.3.2 Block/Deck Contact

The approach used to calculate k_C for block pallets is based on tributary area and modulus of elasticity for blocks in compression (E_C). E_C values for the block material used were determined experimentally. Six blocks of 3 different material types were tested in compression. The three material types tested were solid oak, solid pine, and plywood composite blocks. Block dimensions were measured using hand-held calipers and moisture content was measured using a moisture meter. Blocks were subjected to a load of 12000 pounds applied uniformly over the surface of the block using an MTS testing machine. The equations used to calculate E_C is:

$$E_C = (P \cdot L) / (A \cdot \Delta_C) \quad [3.22]$$

Where P equals the applied load, L equals the block height, A equals the area of the block over which the load was applied (width * length), and Δ_C equals the deformation at load P .

Load deflection curves (plots) were recorded by the MTS machine at the time of testing. Results from these tests are given by Mackes (1998, Volume I, Section 18). A summary of these results are presented in Table 3.8. Values given in this table were adjusted to a 12 percent and green moisture condition based on effects reported in Table 4-11 of the Wood Handbook (Wood Handbook, 1987). For plate

Table 3.8. Mean Modulus of Elasticity (E_{\perp})
Values for Blocks in Compression
Perpendicular-to-Grain.

BLOCK TYPE	MEAN E_{\perp} (12% BASIS) (E6 psi)	MEAN E_{\perp} (GRN BASIS) (E6 psi)
Plywood Composite	0.0371	0.0286
Solid Oak	0.0552	0.0425
Solid Pine	0.0211	0.0163

models, the appropriate mean E_c value for the block material was used to calculate k_c for input to ABAQUS. For simplified models, a mean E_c (green basis) of 0.03×10^6 was used to calculate k_c .

A k_c value was calculated separately for each spring element. Prior to calculating k_c , it was necessary to calculate the deformation (Δ_p) at load P:

$$\Delta_p = (P \cdot L) / (A \cdot E) \quad [3.23]$$

Load P was applied arbitrarily. For the stack support condition, L is the block height. L equals one-half the block height for the rack support conditions. A is the region of the block represented by the spring based on the concept of tributary area. The equation used to calculate k_c is:

$$k_c = P / \Delta_p \quad [3.24]$$

The units of k_c are pounds per inch.

For block pallets supported in the rack condition, the contact point between the edge blocks and lower deck can occur at any location along the base of the block. The possible configurations, shown in Figure 3.35, are similar to those that occur with stringer pallets. Because of these similarities, Equations 3.19 and 3.20 derived for use with stringer pallets were also used for block pallets.

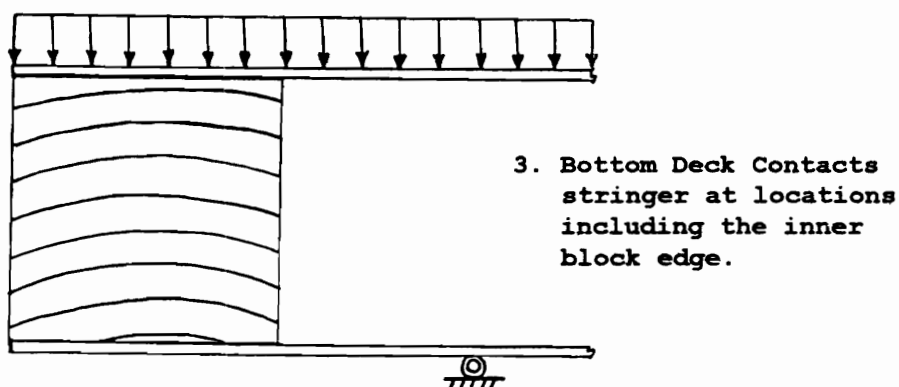
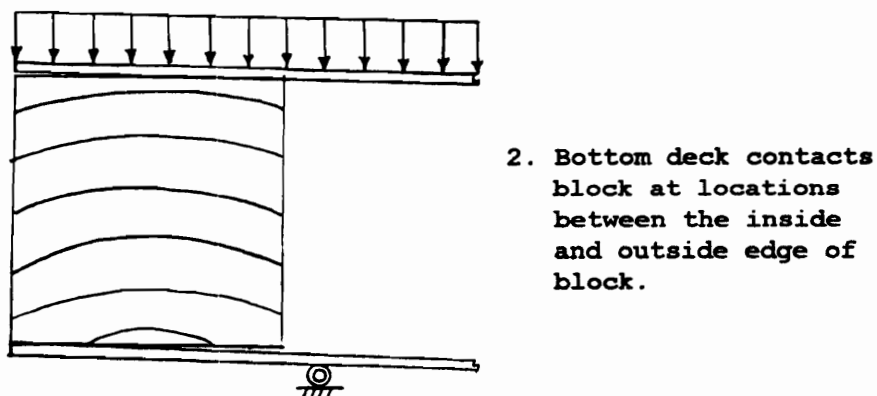
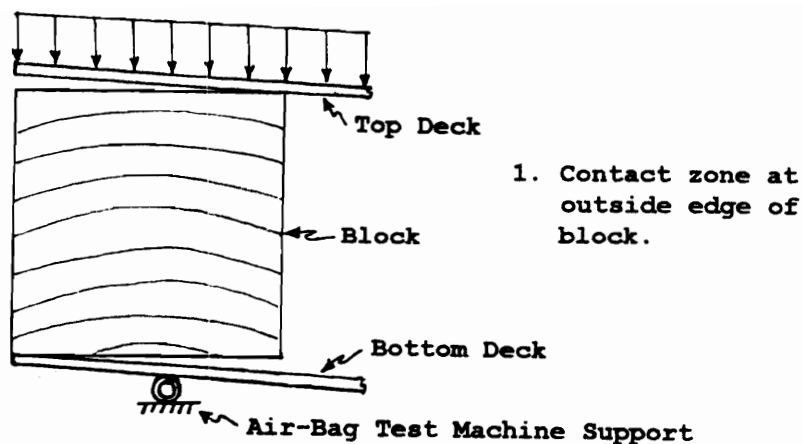
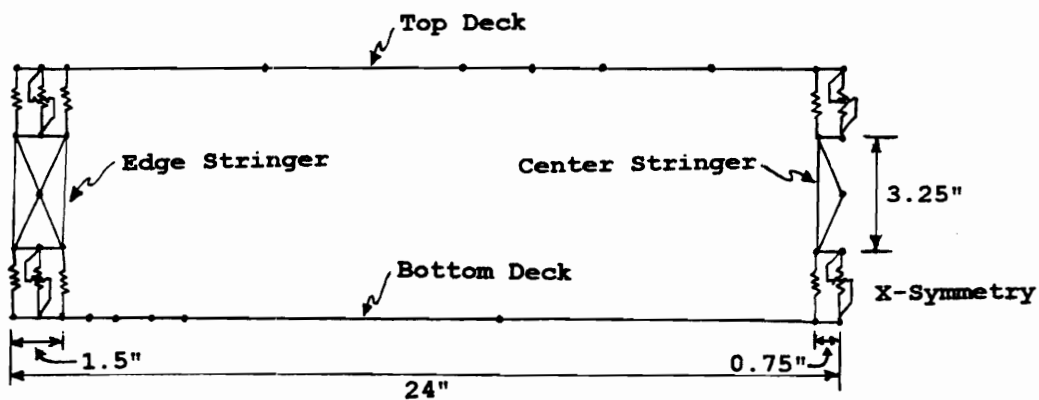


Figure 3.35. Potential Contact Configurations between the Edge Blocks and Bottom Deck in both the RAL and RAW Support Conditions.

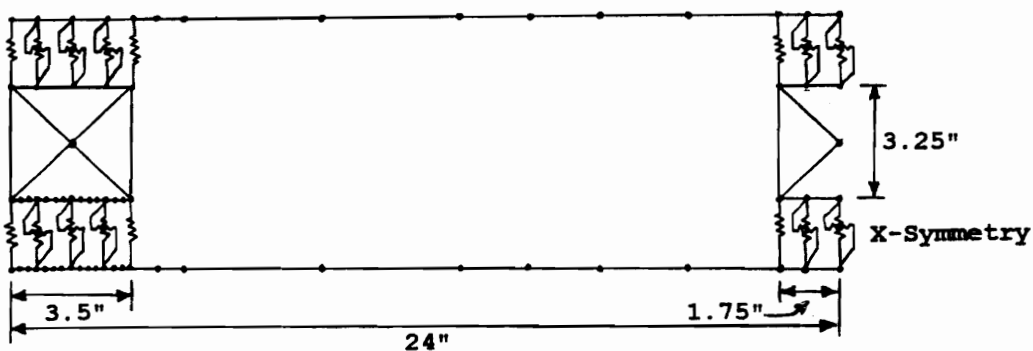
3.5.4 Pallet Section Models

To verify that the methodologies proposed for modeling joints and contact zones simulate actual conditions found in pallets, data from bending tests conducted using yellow-poplar pallet sections were compared to the proposed finite element model. Although the models used in this analysis were two-dimensional in nature, three-dimensional elements in space were used. This facilitated the development of three-dimensional plate models.

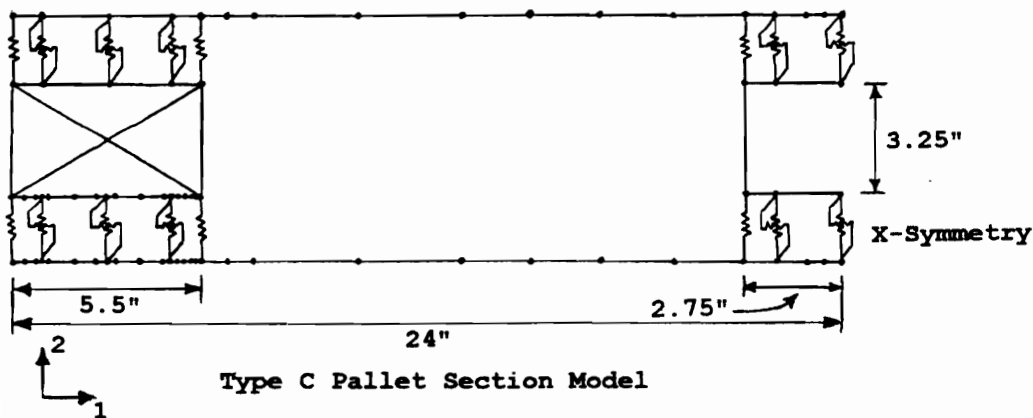
Figure 3.36 shows several pallet section models. B33 beam elements were used to model the top and bottom decks. The stiffness assigned to these elements was based on bending tests conducted on the members in accordance with ASTM Standard D 143-83 (ASTM, 1994) prior to building the pallet sections. Spacers (stringers or blocks) were also comprised of B33 elements. These elements were assigned arbitrarily high stiffness values. The models shown predicted the behavior of pallet sections constructed with 1.5 inch (Type A) spacers, 3.5 inch (Type B) spacers, and 5.5 inch (Type C) spacers. Deckboards were either relatively stiff with a target thickness of 0.75 inches or flexible (F) having a target thickness of 0.459 inches. Complete geometric and material property data for pallet section components are given by Mackes (1998, Volume I, Section 19).



Type A Pallet Section Model



Type B Pallet Section Model



Type C Pallet Section Model



- - Node
- - Beam Element Connecting Two Nodes
-  - Nail Joint
-  - Potential Contact Element

Figure 3.36. Pallet Section Models.

The joints of the pallet sections were constructed with helically threaded hardened steel pallet nails. Type A pallet sections were constructed with two nails per joints, Type B sections with 3 nails, and Type C sections with 5 nails. Nail joint configurations are shown in Figure 3.37. Nail joints were modeled using zero-length springs, with springs representing combined nail shank withdrawal and head embedment oriented in the 2-direction and springs representing lateral stiffness oriented in the 1-direction. Springs representing combined shank withdrawal and head embedment were assigned a value of 12,000 (pounds per inch) per nail (Saminghe, 1987). Springs representing lateral stiffness were assigned a stiffness of 8238 (pounds per inch) per nail using PDS prediction techniques.

Deck/spacer contact was modeled using zero-length springs oriented in the 2-direction. Spring constants for these elements were determined using the contact models for stringer pallets discussed in Section 3.5.3.1. The spring constants assigned to contact elements are given for each section model type in Volume I, Section 20 of Mackes (1998).

Pallet sections were tested in both the Stack support condition and the RAD support condition. Loads were applied to the pallet sections in the stack support condition as shown in Figure 3.38 and the RAD support condition as shown in Figure 3.39. Pallet sections were tested in the RAD

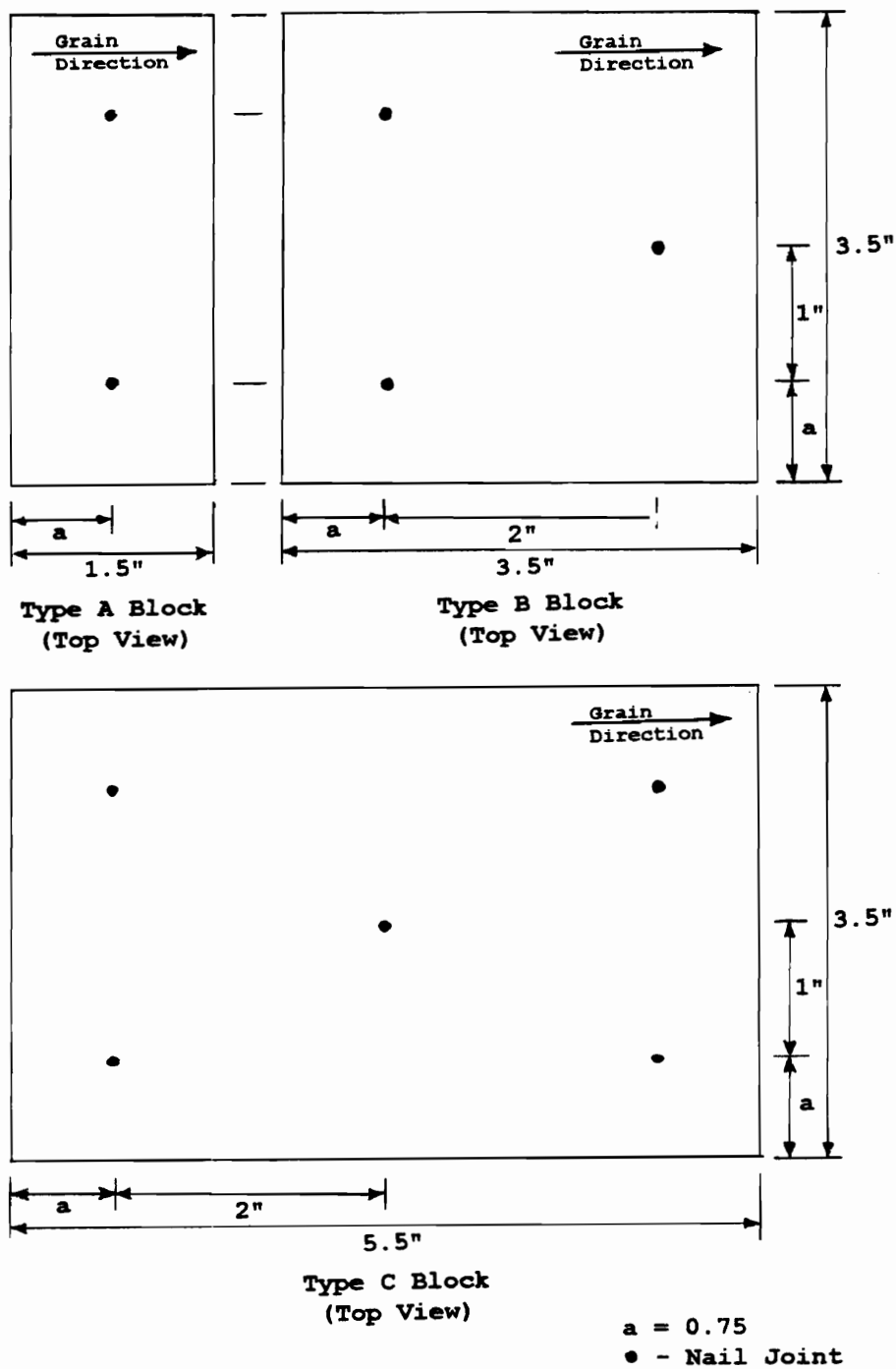
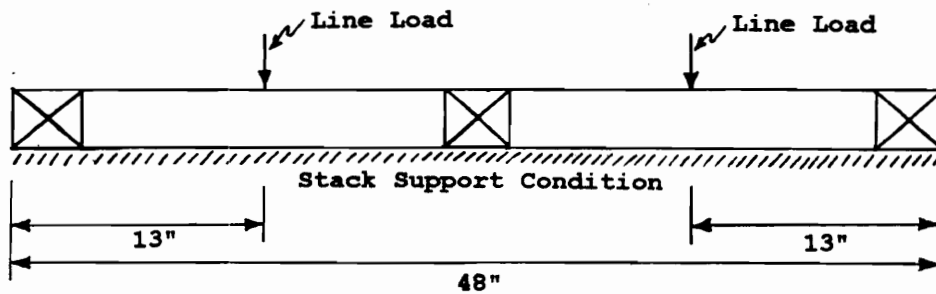
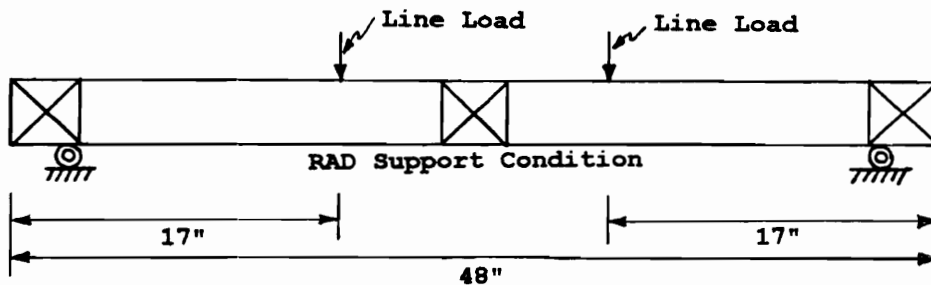


Figure 3.37. Nail Joint Configurations for Pallet Section Models.



Type B Pallet Section

Figure 3.38. Application of Load to Pallet Sections in the Stack Support Condition.



Type B Pallet Section

Figure 3.39. Application of Load to Pallet Sections in the RAD Support Condition.

support conditions using test spans of 38, 42, and 46 inches. Type C sections were also tested at a span of 34 inches. Three replications of each section type utilizing two different deckboard thicknesses were built and tested. Therefore, a total of 78 tests were conducted.

Experimental results were compared to finite element results. Examples of ABAQUS input and output files are presented by Mackes (1998, Volume I, Section 21). Table 3.9 gives a summary of results for Type A pallet sections, Table 3.10 for Type B sections, and Table 3.11 for Type C sections. Generally differences between predicted and experimental deflections were less than 10 percent. One notable exception was for Type C sections tested over a span of 34 inches, where differences for two specimens were considerably greater than 10 percent. Upon further investigation, it was discovered that the blocks of these sections cracked during testing and this probably accounts for the majority of the difference. These results indicate that the methodologies developed and used for modeling joints and contact zones work as intended.

3.6 Cut-outs

Two types of cut-outs were considered in this research, hand-holds and wheel openings. Hand-holds could occur in both the top and bottom deck of reversible pallets having a

Table 3.9. Comparison of Predicted Deflections to Experimental Results for Type A Pallet Sections.

DECK TYPE	REP. NO.	SUPPORT CONDITION	PREDICTED DEFLECTION (in.)	MEASURED DEFLECTION (in.)	PERCENT ERROR (%)
F	1	RAD-46	-0.631	-0.666	-5.55
F	1	RAD-42	-0.539	-0.572	-6.12
F	1	RAD-38	-0.448	-0.486	-8.48
F	1	STACK	-0.223	-0.223	0.00
F	2	RAD-46	-0.585	-0.608	-3.93
F	2	RAD-42	-0.490	-0.492	-0.41
F	2	RAD-38	-0.399	-0.416	-4.26
F	2	STACK	-0.227	-0.221	2.64
F	3	RAD-46	-0.682	-0.684	-0.29
F	3	RAD-42	-0.587	-0.576	1.87
F	3	RAD-38	-0.491	-0.488	0.61
F	3	STACK	-0.193	-0.188	2.59
S	1	RAD-46	-0.464	-0.438	5.60
S	1	RAD-42	-0.362	-0.343	5.25
S	1	RAD-38	-0.277	-0.264	4.69
S	1	STACK	-0.191	-0.196	-2.62
S	2	RAD-46	-0.490	-0.474	3.27
S	2	RAD-42	-0.387	-0.391	-1.03
S	2	RAD-38	-0.301	-0.295	1.99
S	2	STACK	-0.173	-0.181	-4.62
S	3	RAD-46	-0.465	-0.449	3.44
S	3	RAD-42	-0.367	-0.350	4.63
S	3	RAD-38	-0.285	-0.270	5.26
S	3	STACK	-0.149	-0.156	-4.70

Table 3.10. Comparison of Predicted Deflections to Experimental Results for Type B Pallet Sections.

DECK TYPE	REP. NO.	SUPPORT CONDITION	MODEL B6 DEFLECTION (in.)	MEASURED DEFLECTION (in.)	PERCENT CHANGE (%)
F	1	RAD-46	-0.525	-0.551	-4.95
F	1	RAD-42	-0.477	-0.447	6.29
F	1	RAD-38	-0.412	-0.392	4.85
F	1	STACK	-0.168	-0.171	-1.79
F	2	RAD-46	-0.496	-0.501	-1.01
F	2	RAD-42	-0.449	-0.418	6.90
F	2	RAD-38	-0.387	-0.360	6.98
F	2	STACK	-0.153	-0.153	0.00
F	3	RAD-46	-0.589	-0.576	2.21
F	3	RAD-42	-0.539	-0.515	4.45
F	3	RAD-38	-0.468	-0.446	4.70
F	3	STACK	-0.186	-0.189	-1.61
S	1	RAD-46	-0.568	-0.528	7.04
S	1	RAD-42	-0.426	-0.388	8.92
S	1	RAD-38	-0.348	-0.320	8.05
S	1	STACK	-0.137	-0.134	2.19
S	2	RAD-46	-0.533	-0.488	8.44
S	2	RAD-42	-0.398	-0.381	4.27
S	2	RAD-38	-0.324	-0.313	3.40
S	2	STACK	-0.125	-0.129	-3.20
S	3	RAD-46	-0.501	-0.486	2.99
S	3	RAD-42	-0.372	-0.346	6.99
S	3	RAD-38	-0.302	-0.280	7.28
S	3	STACK	-0.114	-0.116	-1.75

Table 3.11. Comparison of Predicted Deflections to Experimental Results for Type C Pallet Sections.

DECK TYPE	REP. NO.	SUPPORT CONDITION	MODEL C6 DEFLECTION (in.)	MEASURED DEFLECTION (in.)	PERCENT CHANGE
F	1	RAD-46	-0.494	-0.482	2.43
F	1	RAD-42	-0.466	-0.423	9.23
F	1	RAD-38	-0.425	-0.396	6.82
F	1	RAD-34	-0.359	-0.346	3.62
F	1	STACK	-0.130	-0.139	-6.92
F	2	RAD-46	-0.503	-0.472	6.16
F	2	RAD-42	-0.475	-0.431	9.26
F	2	RAD-38	-0.433	-0.408	5.77
F	2	RAD-34	-0.365	-0.374	-2.47
F	2	STACK	-0.148	-0.156	-5.41
F	3	RAD-46	-0.470	-0.425	9.57
F	3	RAD-42	-0.442	-0.395	10.63
F	3	RAD-38	-0.401	-0.374	6.73
F	3	RAD-34	-0.338	-0.344	-1.78
F	3	STACK	-0.141	-0.150	-6.38
S	1	RAD-46	-0.418	-0.440	-5.26
S	1	RAD-42	-0.363	-0.370	-1.93
S	1	RAD-38	-0.305	-0.298	2.30
S	1	RAD-34	-0.244	-0.246	-0.82
S	1	STACK	-0.089	-0.105	*-17.98
S	2	RAD-46	-0.397	-0.401	-1.01
S	2	RAD-42	-0.343	-0.334	2.62
S	2	RAD-38	-0.286	-0.270	5.59
S	2	RAD-34	-0.228	-0.224	1.75
S	2	STACK	-0.090	-0.105	*-16.67
S	3	RAD-46	-0.374	-0.351	6.25
S	3	RAD-42	-0.321	-0.306	4.67
S	3	RAD-38	-0.267	-0.248	7.12
S	3	RAD-34	-0.212	-0.214	-0.94
S	3	STACK	-0.077	-0.078	-1.30

* - The spacers (blocks) between the top and bottom decks split during testing.

full panel deck top and bottom, and only the top deck of nonreversible pallets, such as stringer pallets with a lumber deck bottom, unidirectional base block pallets, and perimeter-base block pallets. Wheel openings were allowed to occur in the bottom deck of pallets where the bottom deck was comprised of a panel.

Because of computer memory limitations, primarily with respect to PC's, and criteria established for maximum allowable solution times, the finite element meshes used to model cut-outs were quite coarse. One result of using these coarse meshes was that stress concentrations which may occur in the vicinity of the cut-out were not modeled very accurately. Therefore, it was assumed that they did not govern failure. For hand-holds this assumption is probably reasonable. However, for bottom deck wheel openings this assumption may not always be valid.

To evaluate models simulating the behavior of panels with cut-outs, bending tests were conducted. Prior to putting cut-outs in test panels, the modulus of elasticity values both parallel- and perpendicular-to-grain were determined for each test panel. These values were determined by testing panels in two-point flexure as described in ASTM D 3043-87 (ASTM, 1994), Method B. Two rigid line loads were applied to the panel using the air-bag test machine. For 23/32 inch panels with face plies

parallel-to-grain the test span between supports was 36 inches and 24 inches with face plies oriented perpendicular-to-grain. For 15/32 inch panels, a test span of 24 inches between supports was used when face plies were oriented parallel-to-grain and an 18 inch span when face plies were oriented perpendicular-to-grain. The following equation was used to calculate EI:

$$EI = (P * A) / (48 * \Delta_p) * (3L^2 - 4A^2) \quad [\text{Eq. 3.25}]$$

P is the applied load. L is the test span and A is equal to one-third the test span. The Δ_p value is the deflection at mid-span when load P is applied.

The EI values determined from full panel tests were then adjusted for membrane (plate) action. Adjustments resulted in values more comparable to those obtained from 2 inch strip data. Adjustment factors were determined by comparing EI values from panel tests to EI values for the same material tested as 2 inch strips. These comparisons are presented for plywood by Mackes (1998, Volume I, Section 22). A summary of adjustment factors for both plywood and OSB are presented in Table 3.12.

3.6.1 Top Deck Hand-Holds

Top deck hand-holds were simulated in plate models by assigning arbitrarily thin geometric properties and low stiffness to elements located in the area of the hand-hold.

Table 3.12. Adjustment of EI Values
determined using 40 x 48 inch Panels
for Membrane (Plate) Action.

FACE-PLY DIRECTION (EXAMPLE)	PLYWOOD EI ADJUSTMENT (%)	OSB EI ADJUSTMENT (%)
15/32 inch Plywood:		
Parallel-to-Grain	-20.4	-24.7
Perpendicular-to-Grain	-24.2	-37.8
23/32 inch Plywood:		
Parallel-to-Grain	-24.4	-13.6
Perpendicular-to-Grain	-27.5	-22.8

Both geometric and material properties were assigned near zero values to avoid singularity errors. The finite element mesh selected for modeling the panels with hand-holds is shown in Figure 3.40. It was comprised of 36 S9R5 general shell elements and contains 169 nodes.

To verify that this concept models the behavior of panels with hand-holds, hand-holds were cut in 9 plywood panels having a thickness of 15/32 inches. The panels were tested on the air-bag testing machine in bending using a two-point flexure test. Panels were tested with face plies spanning both parallel- and perpendicular-to-grain supported along two opposing sides and along the middle as shown in Figure 3.41. Additional details regarding this testing can be found in Volume I, Section 23 of Mackes (1998). After testing, the panels were used to construct pallets.

Mean experimental (measured) deflections were compared to those obtained using the finite element model in Table 3.13. Finite element deflections were generated using mean geometric and material properties for the ten panels as determined by Mackes (1998, Volume I, Section 23). These property values are presented along with an example of the finite element input and output files. Because the differences between finite element solutions and mean experimental values are less than 5.1 percent, the model was assumed to predict panel behavior adequately.

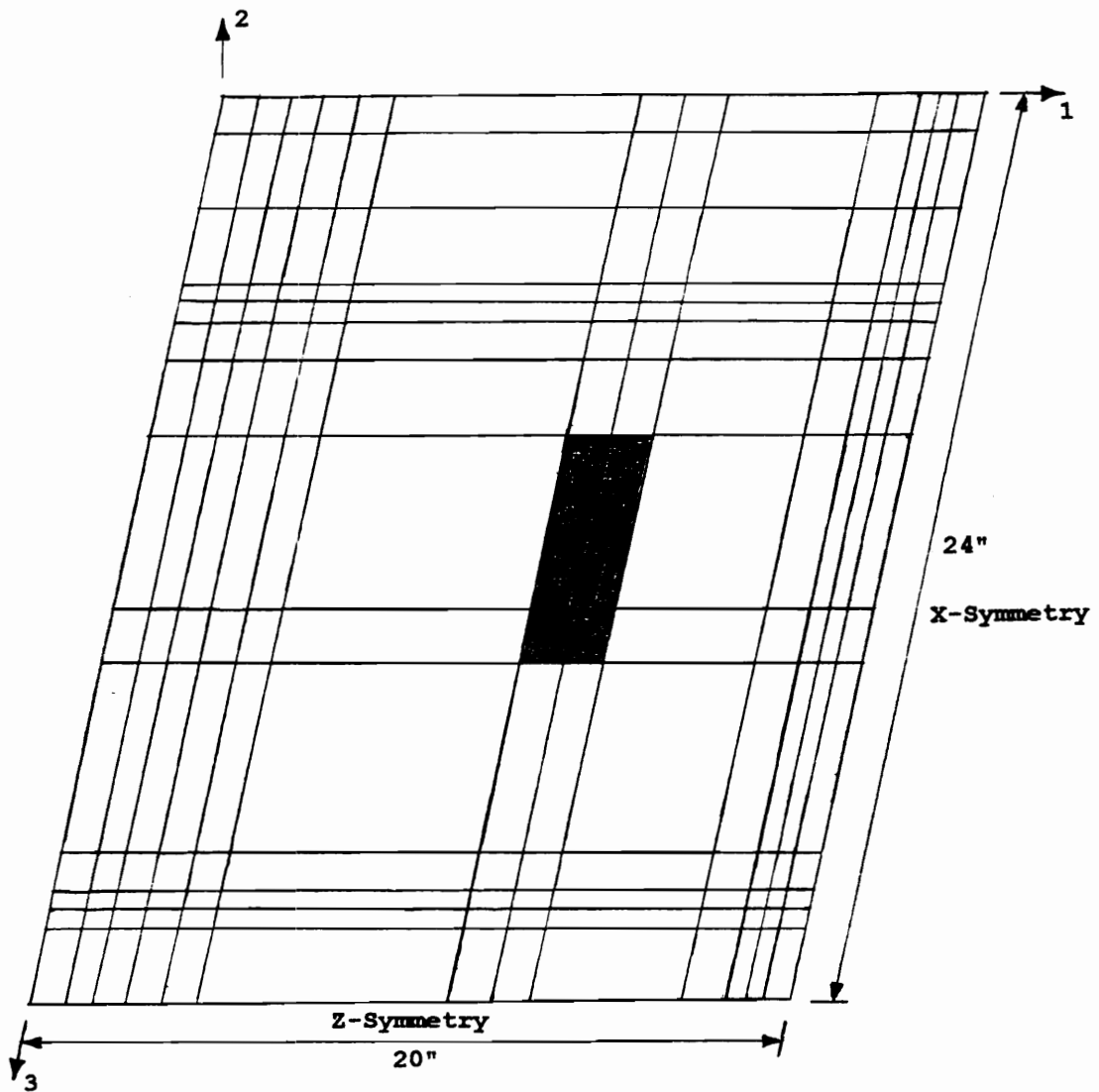


Figure 3.40. Finite Element Mesh used to Simulate a Panel with Hand-Holds in a Block Pallet Plate Model.

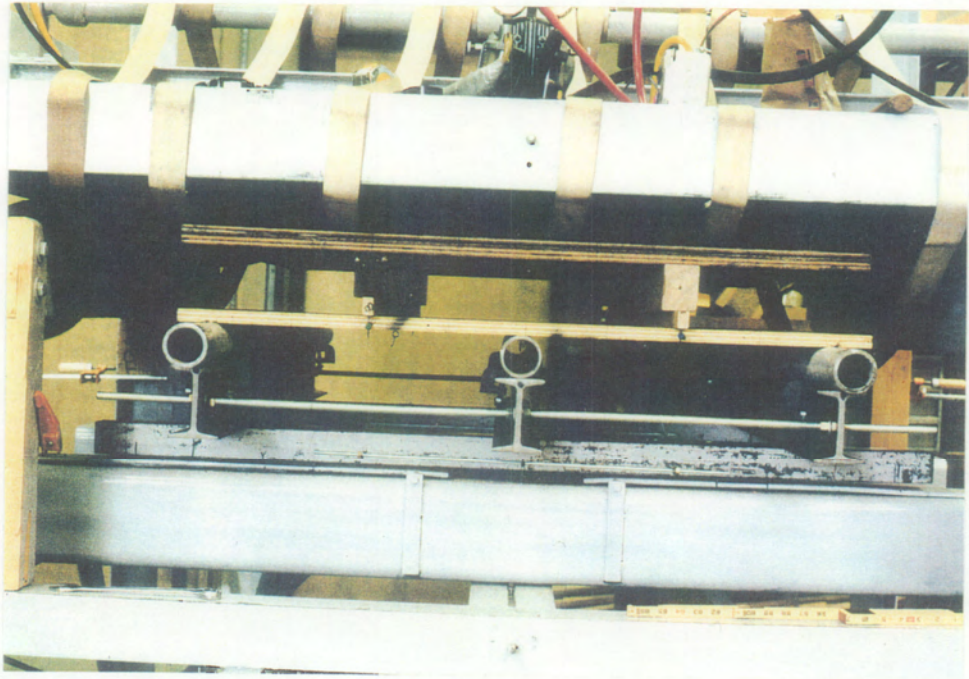


Figure 3.41. Setup for Testing Panels in Bending on the Air-Bag Testing Machine at VPI & SU.

Table 3.13. Predicted (Finite Element) versus Measured Deflections for Panels with Hand-Holds.

FACE-PLY DIRECTION (EXAMPLE)	FINITE ELEMENT DEFLECTION (in.)	MEAN MEASURED DEFLECTION (in.)	PERCENT DIFFERENCE (%)
Parallel-to-Grain	-0.166	-0.175	-5.1
Perpendicular-to-Grain	-0.307	-0.315	-2.5

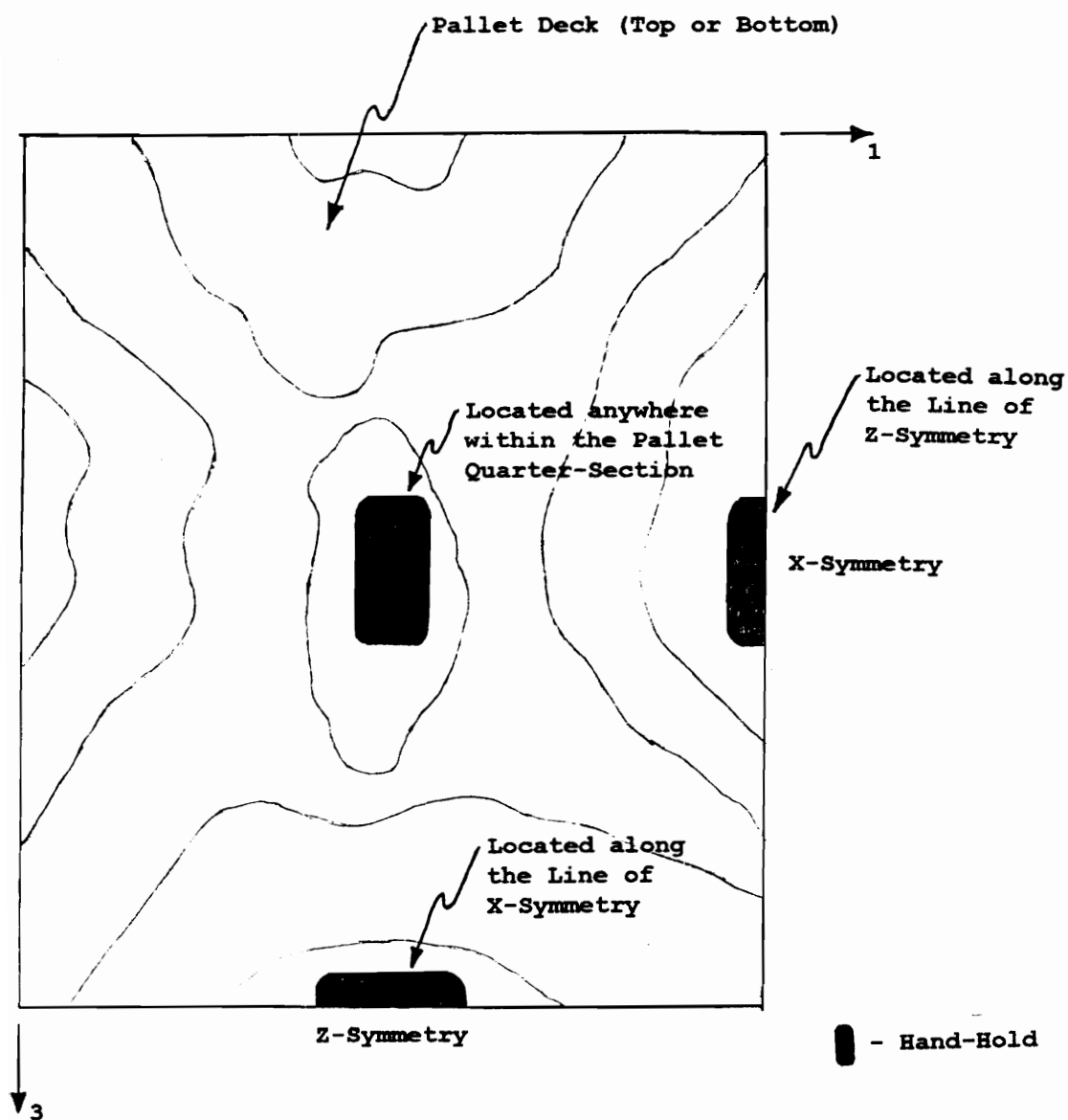
- Notes: 1. Predicted (Finite Element) deflections were generated using mean panel properties as determined by Mackes (1998, Volume I, Section 23).
2. Measured deflections are the mean of 9 panels tested in two-point flexure (see Mackes, 1998, Volume I, Section 23 for additional details).
3. Deflections reported are maximum values predicted or measured at mid-span.

To check that solutions obtained with this model had converged, mesh fineness was doubled and comparisons were made. Details of the evaluation are presented by Mackes (1998, Volume I, Section 24) and a summary of comparisons are presented in Table 3.14. Comparisons reveal that agreement both in terms of maximum stress and deflection values are very good. However, further evaluation also reveals differences in the regions around the corners of the hand-holds. Mesh refinement increased the stress magnitudes predicted at these locations which can be attributed to the occurrence of stress concentrations. If the assumption is made that these locations do not govern failure when the panel is incorporated into the pallet structure, the 36 element mesh was sufficient. Because most hand-holds are relatively small and have round corners which act to reduce stress concentrations, this assumption seems justified.

In simplified PC models, hand-holds were allowed in selected locations which are shown in Figure 3.42. Hand-holds were incorporated into the finite element mesh of simplified models by adjusting the width of grid members which comprise the deck at the hand-hold location. Schemes used to achieve this are presented for stringer pallets in Chapter 4 and Section 5.4.3.1 for block pallets. For panels tested with hand-holds, the simplified mesh was as shown in Figure 3.43. An example of the finite element (ABAQUS)

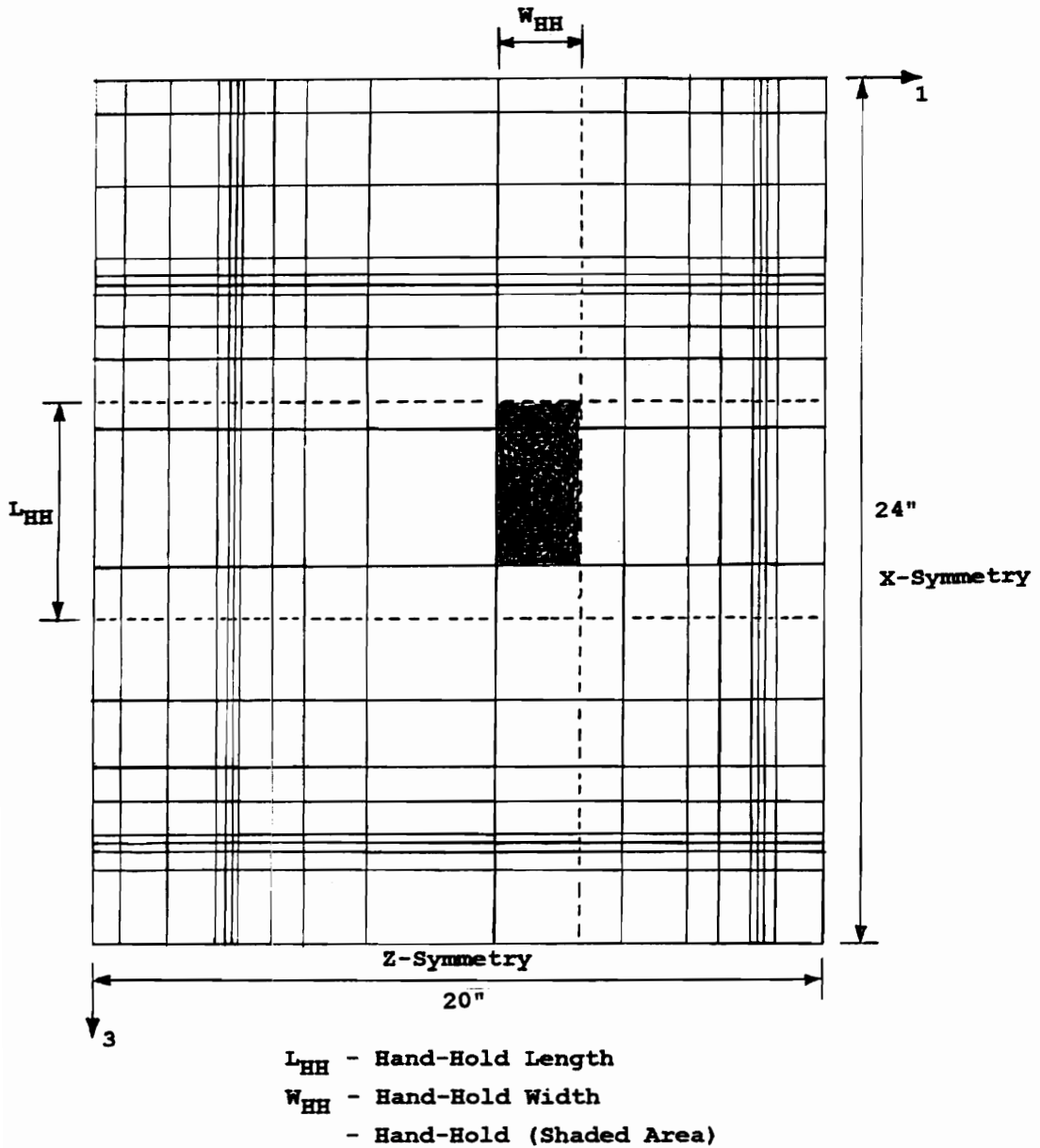
Table 3.14. Comparison of Finite Element Solutions
for 25 and 100 Element Plate Models
Checking Solution Convergence.

PARAMETER	FINITE ELEMENT SOLUTION (25 Element Plate Model)	FINITE ELEMENT SOLUTION (100 Element Plate Model)	PERCENT DIFFERENCE (%)
Parallel-to-Grain Example:			
S33 Stress (maximum, psi)	1639.0	1622.0	1.0
Deflection (maximum, in.)	-0.1659	-0.1665	-0.4
Perpendicular-to-Grain Example:			
S11 Stress (maximum, psi)	1171.0	1138.0	2.9
Deflection (maximum, in.)	-0.3070	-0.3079	-0.3



Note: Hand-holds at allowable locations can vary in length and width.

Figure 3.42. Allowable Locations for Hand-Hold Placement.



19 x 19 Grid Model Emulating
the Top Deck of Specimen BPU-7

Note: Grid Members in the vicinity of
hand-hold have modified widths
based on hand-hold size.

**Figure 3.43. The Simplified Finite
Element Mesh Adapted to Model
Hand-Holds in Block Pallets.**

input and output files for this model can be found in Volume I, Section 25 of Mackes (1998). A comparison of results presented in Table 3.15 indicates that predictions generated with the simplified model are reasonably close to those of the plate model. This suggests that the simplified approach used for modeling hand-holds is adequate.

3.6.2 Bottom Deck Wheel Openings

In plate models, wheel openings were modeled by assigning near zero thickness and stiffness to the shell elements in the region of the cut-out. An example of a finite element mesh exhibiting wheel openings is shown in Figure 3.44. As with hand-holds, the assumption was made that stress concentrations in the vicinity around the corners of wheel openings did not govern panel failure. This was assumed because of computer memory and solution time limitations imposed for development of simplified models.

The capability of this technique to model the behavior of panels with wheel openings was validated by comparing finite element results to experimental values. Nine 15/32 inch thick OSB panels were tested in flexure. Details of this evaluation, including ABAQUS input and output files, are given by Mackes (1998, Volume I, Section 26). Results from this analysis are presented in Table 3.16. Deflection

Table 3.15. Comparison of Finite Element Solutions
for Grid Model to Plate (Shell) Model for Panels
with Hand-Holds.

PARAMETER	FINITE ELEMENT SOLUTION (Grid Model)	FINITE ELEMENT SOLUTION (Plate Model)	PERCENT DIFFERENCE (%)
Parallel-to-Grain Example:			
S33 Stress (maximum, psi)	1639.0	1639.0	0.0
Deflection (maximum, in.)	-0.1698	-0.1659	2.4
Perpendicular-to-Grain Example:			
S11 Stress (maximum, psi)	1243.0	1171.0	6.1
Deflection (maximum, in.)	-0.3437	-0.3070	12.0

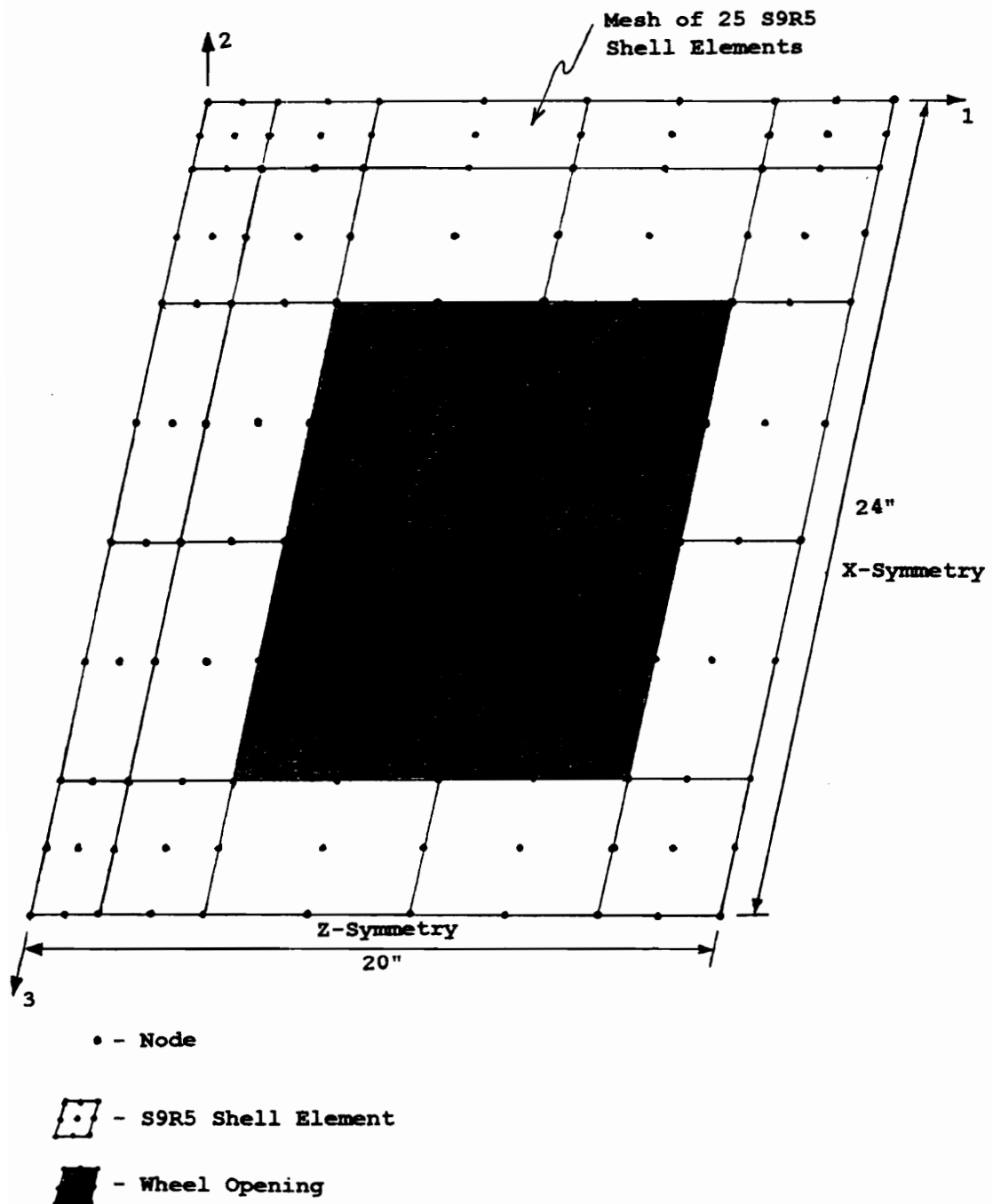


Figure 3.44. Mesh of Shell Elements which Simulate the Bottom Deck of a Pallet with Wheel Openings.

Table 3.16. Predicted (Finite Element) versus Measured Deflections for Panels with Wheel Openings.

FACE-PLY DIRECTION (EXAMPLE)	FINITE ELEMENT DEFLECTION (in.)	MEAN MEASURED DEFLECTION (in.)	PERCENT DIFFERENCE (%)
Parallel-to-Grain	-0.073	-0.076	-3.9
Perpendicular-to-Grain	-0.114	-0.108	5.6

- Notes: 1. Predicted (Finite Element) deflections were generated using mean panel properties as determined by Mackes (1998, Volume I, Section 26).
2. Measured deflections are the mean of 9 panels tested in two-point flexure (see Mackes, 1998, Volume I, Section 26 for additional details).
3. Deflections reported are maximum values predicted or measured at mid-span.

differences are less than 6 percent, which is evidence that this approach models panel behavior satisfactorily.

Wheel openings in simplified models are limited to one opening per quarter-panel. The opening is incorporated into the mesh by adjusting the width of grid members accordingly. Schemes used to achieve this are discussed further for stringer pallet models in Chapter 4 and in Section 5.4.3.2 for block pallet models.

For the panels tested with wheel openings, the simplified mesh is as shown in Figure 3.45. Details of test cases considered, along with ABAQUS input and output files, are presented in Volume I, Section 27 of Mackes (1998). A summary of results, presented in Table 3.17, reveals that the simplified predictions are again reasonably close to plate model predictions with differences of 5 percent or less. This suggests that the approach performs adequately.

3.7 Summary

In Chapter 3, the strategies developed for modeling pallet components, including panel decks, lumber decks, stringers, and blocks, and features such as leading edge boards and cut-outs were discussed. The finite elements and methodologies used to model nail joints and contact zones between components were also presented. Strategies were developed for both three-dimensional plate models and

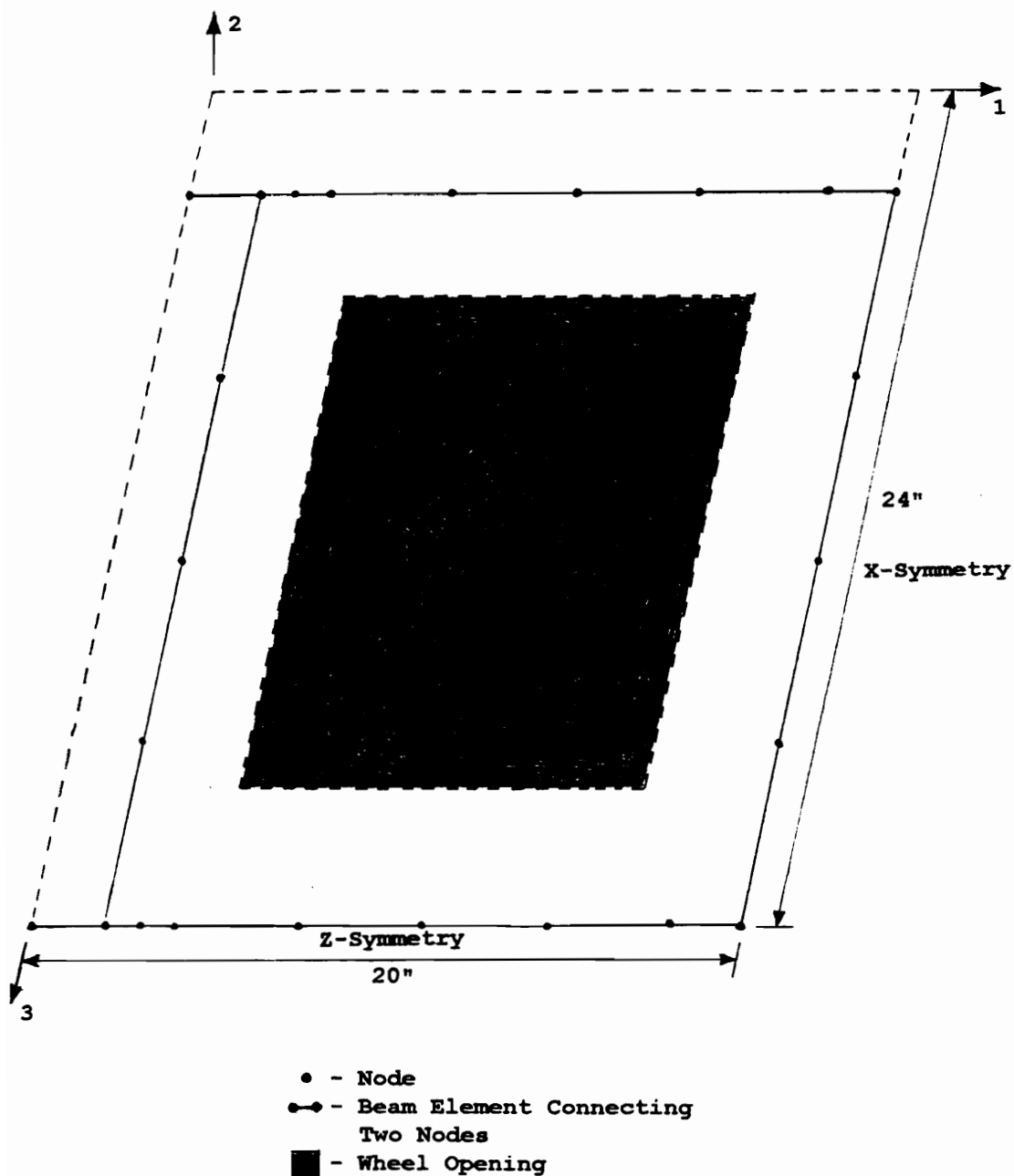


Figure 3.45. Mesh of Beam Elements which can be used to Simulate the Bottom Deck of a Pallet with Wheel Openings.

Table 3.17. Comparison of Finite Element Solutions
for Grid Model to Plate (Shell) Model for Panels
with Wheel Openings.

PARAMETER	FINITE ELEMENT SOLUTION (Grid Model)	FINITE ELEMENT SOLUTION (Plate Model)	PERCENT DIFFERENCE (%)
Parallel-to-Grain Example:			
S33 Stress (maximum, psi)	1039.0	1094.0	-5.0
Deflection (maximum, in.)	-0.0700	-0.0704	-0.6
Perpendicular-to-Grain Example:			
S11 Stress (maximum, psi)	708.0	718.9	-1.5
Deflection (maximum, in.)	-0.1180	-0.1135	4.0

simplified PC models. Based primarily on comparisons to experimental data and observations, the strategies developed in this chapter to model pallet components, nail joints, contact zones, and other pallet features considered perform adequately, providing the basis for modeling complete pallets as discussed in subsequent Chapters. Stringer pallet models are discussed in Chapter 4 and block pallet models in Chapter 5.

4.0 Modeling Stringer Pallets

Stringer pallets were modeled using ABAQUS (Hibbitt, Karlsson, and Sorenson, Inc., 1989). Three-dimensional plate models were developed to evaluate pallet behavior under load. Finite element model results were compared to experimental results obtained using a uniform load testing machine to validate model performance. Sensitivity studies were conducted with three-dimensional plate models. These studies were used to identify pallet characteristics (degrees of freedom) which have significant impact on behavior. Identifying these characteristics formed a basis for development of PC-compatible models with reduced degrees of freedom.

4.1 Development of Plate Models for Stringer Pallets

To evaluate stringer pallet behavior, three-dimensional plate models were assembled using the modeling techniques discussed in Chapter 3. The Pallet assembly format used to construct models was very systematic. The bottom deck was built first, followed by spacers (stringers), and then the top deck. Finally, the nail joints and contact elements which tie pallet members together were added.

Initially, two principal stringer pallet models were built and refined:

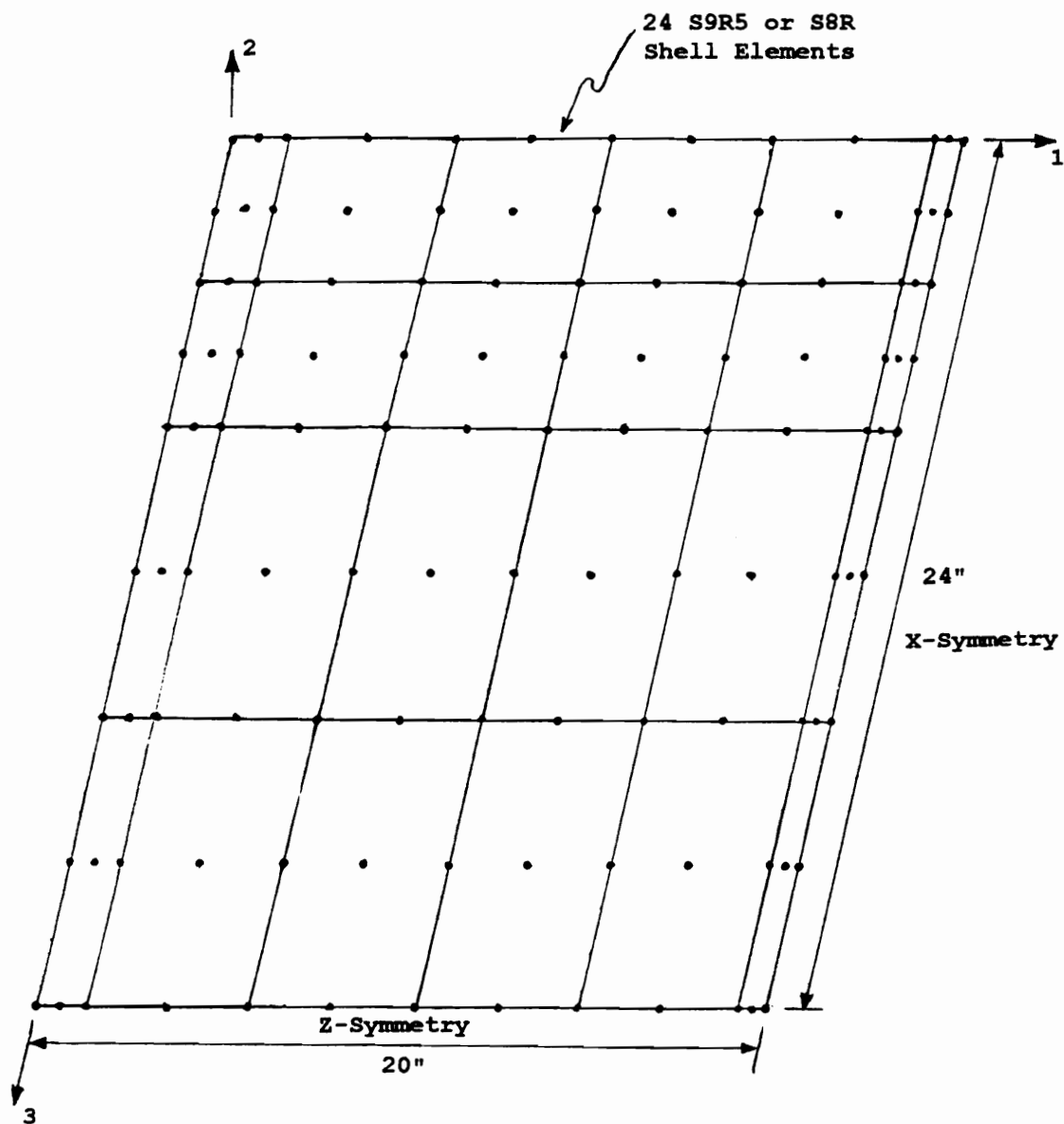
1. Two-way entry, reversible three stringer (un-notched) pallet with panel decks top and bottom.

2. Partial four-way entry, three stringer (notched) pallet with panel deck top and lumber deck bottom.

Plate models were later developed to analyze additional pallet geometries, including 4- and 5-stringer pallets and features such as leading edge board reinforcement and cut-outs.

4.1.1 Stringer Pallets with Panel Decks Top and Bottom

Plate models were programmed using a framework compatible with ABAQUS. Pallet components and joint characteristics were generally modeled as discussed in Section 3.5. Shell (plate) element mesh configurations used to evaluate deck behavior were derived systematically. An example of this process is presented by Mackes (1998, Volume II, Section 1). This approach began with a known solution, modifying it one factor (step) at a time until a satisfactory mesh configuration was developed. Each step was carefully checked to verify that accuracy was maintained. An example of the deck configuration used to model 3-stringer pallets is shown in Figure 4.1. For reversible stringer pallets, the bottom deck had the same configuration as the top deck. Stringers were assembled as shown in Figure 3.14. The configuration of nail joints and contact elements used for a three-stringer pallet are shown in Figure 4.2.



Top Panel Deck of Model
Simulating Pallet SPP3-1

Figure 4.1. Mesh Configuration
used to Simulate the Panel Decks
of Three-Stringer Pallets.

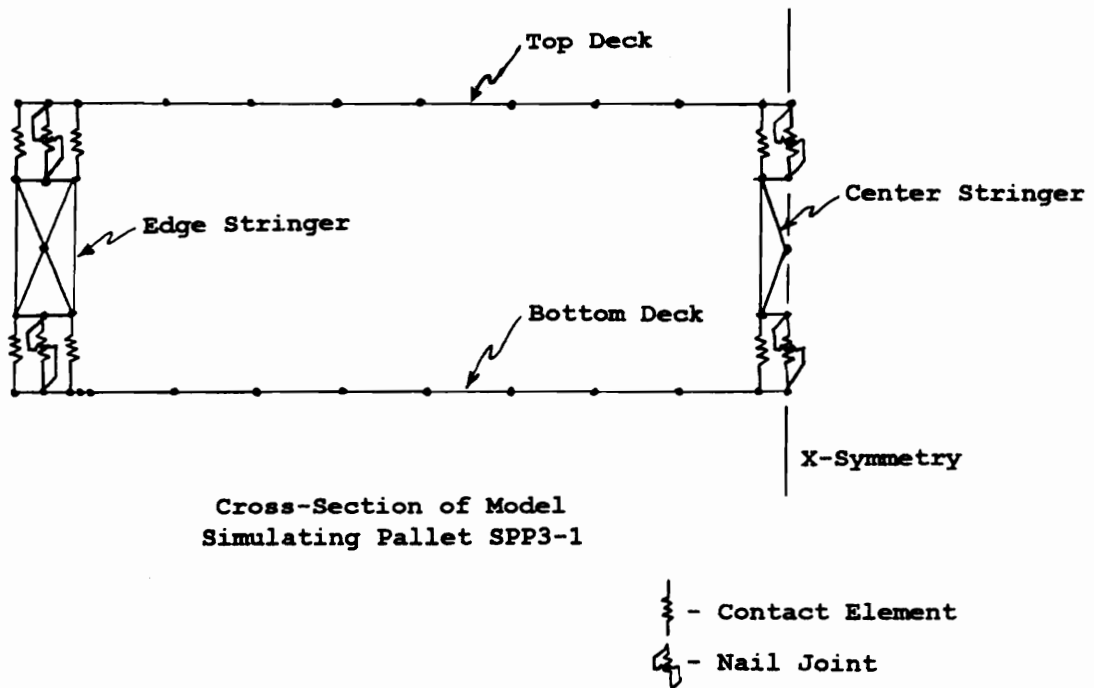


Figure 4.2. Element Configuration used to Simulate Nail Joints and Contact Regions of Three-Stringer Pallets.

When all the pallet members were assembled, the model appeared as shown in Figure 4.3. The model shown is for a reversible 3-stringer pallet. An example of ABAQUS program code for this model can be found in Volume II, Section 2 of Mackes (1998). By changing input coordinates of the pallet members, this model can be used to predict the behavior of 3-stringer pallets having any practical length and width. Stringers of any height can also be modeled. Altering the properties of panels and stringers, as well as joints and contact elements, is also easily achieved.

Modeling 4- and 5-stringer pallets was achieved by modifying the 3-stringer model. To predict the behavior of 4- and 5-stringer pallets an additional stringer was added to the model exploiting symmetry. To accommodate this additional stringer, modifications to the top and bottom decks were required. These modifications are shown in Figure 4.4. All stringers were active if a 5-stringer pallet was being modeled. For a 4-stringer pallet, the center stringer was not active and elements in this stringer assembly were assigned near zero geometric and material values. Modifications required to model pallet features such as leading edge board reinforcement and cut-outs were relatively minor. An example of the deck mesh used to model pallets with lead edge boards is shown in Figure 4.5.

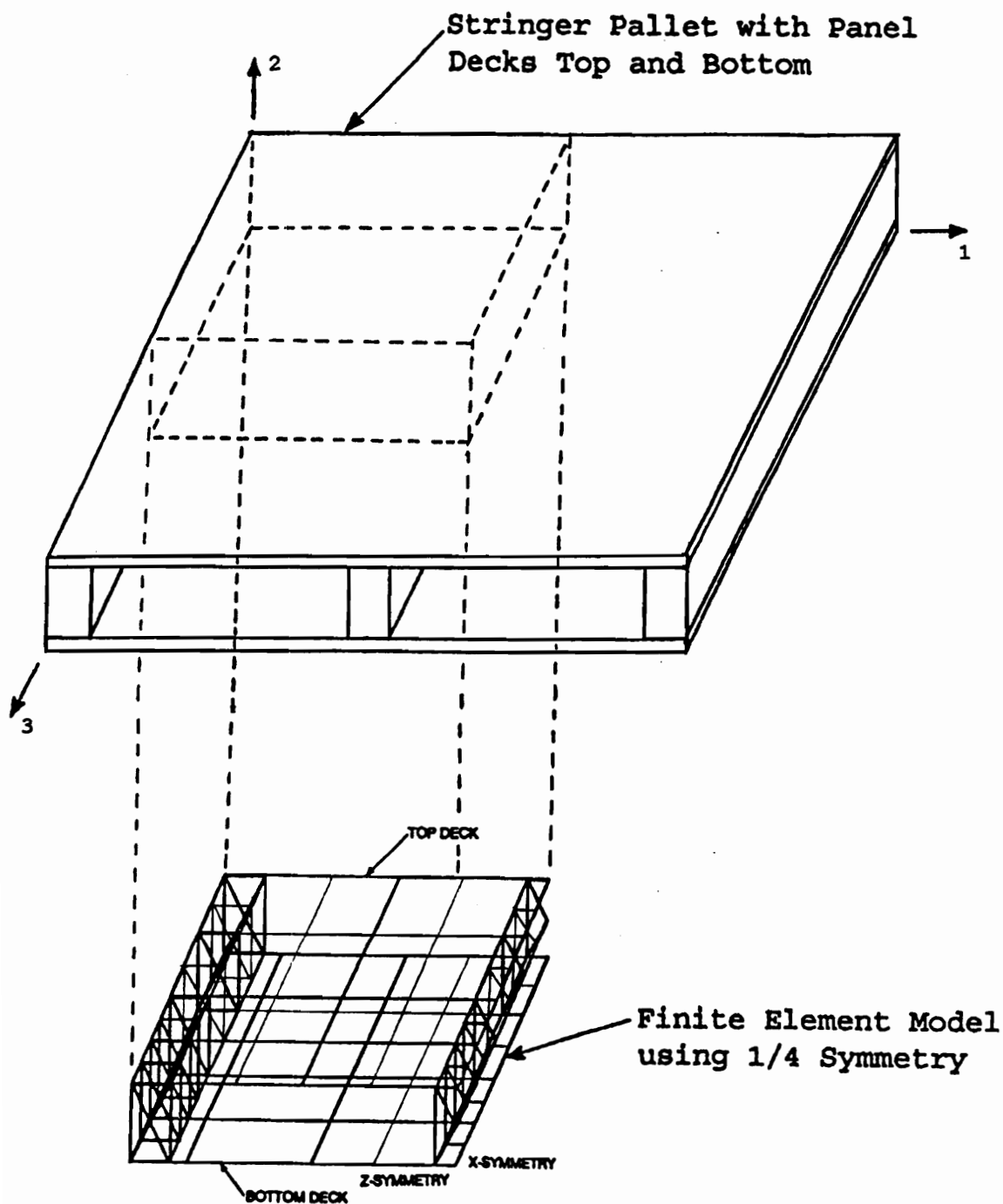


Figure 4.3. Finite Element Model
used to Predict the Behavior
of Three-Stringer Pallets.

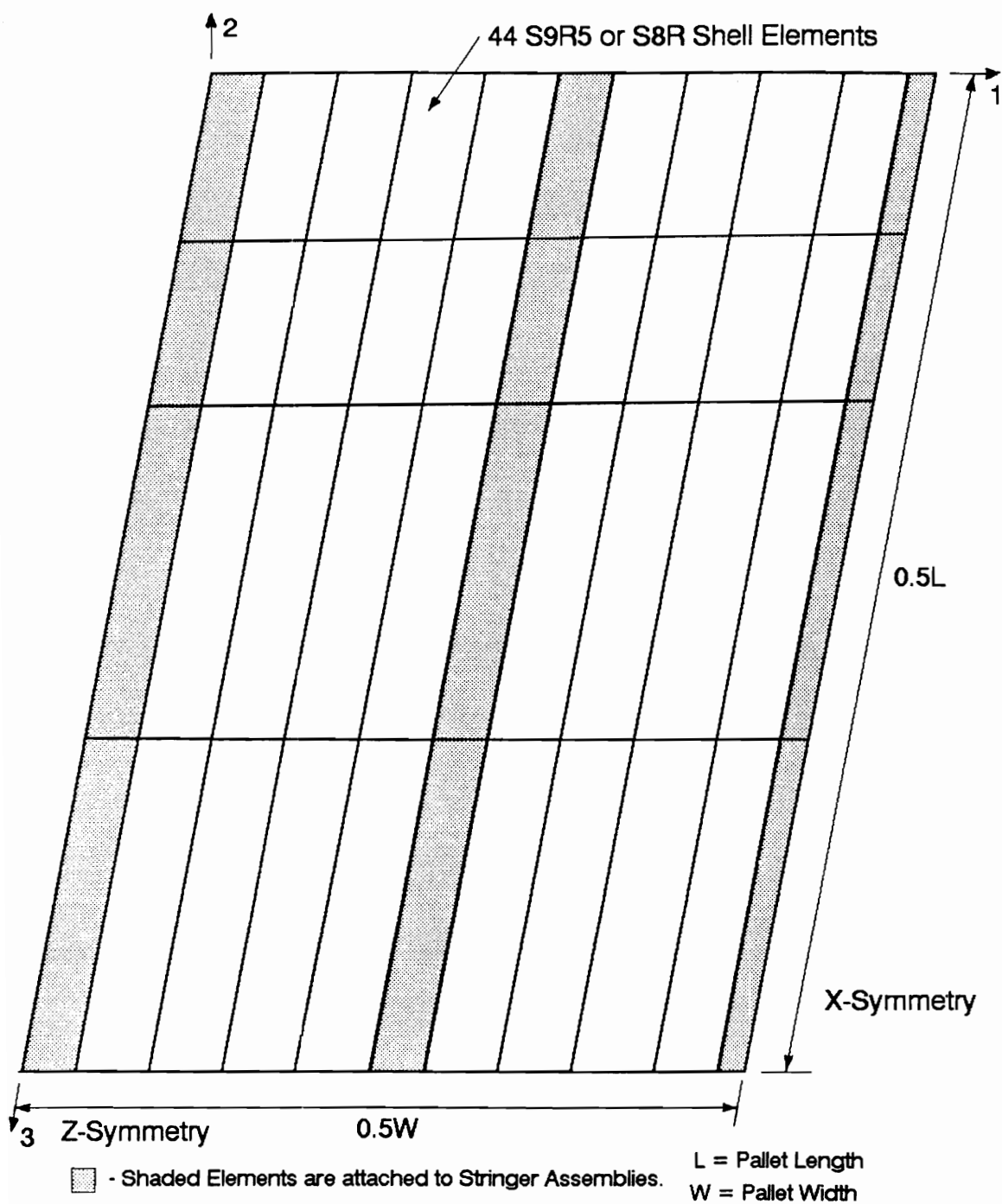


Figure 4.4. Finite Element Mesh used to Simulate the Deck Behavior of Four- and Five-Stringer Pallets.

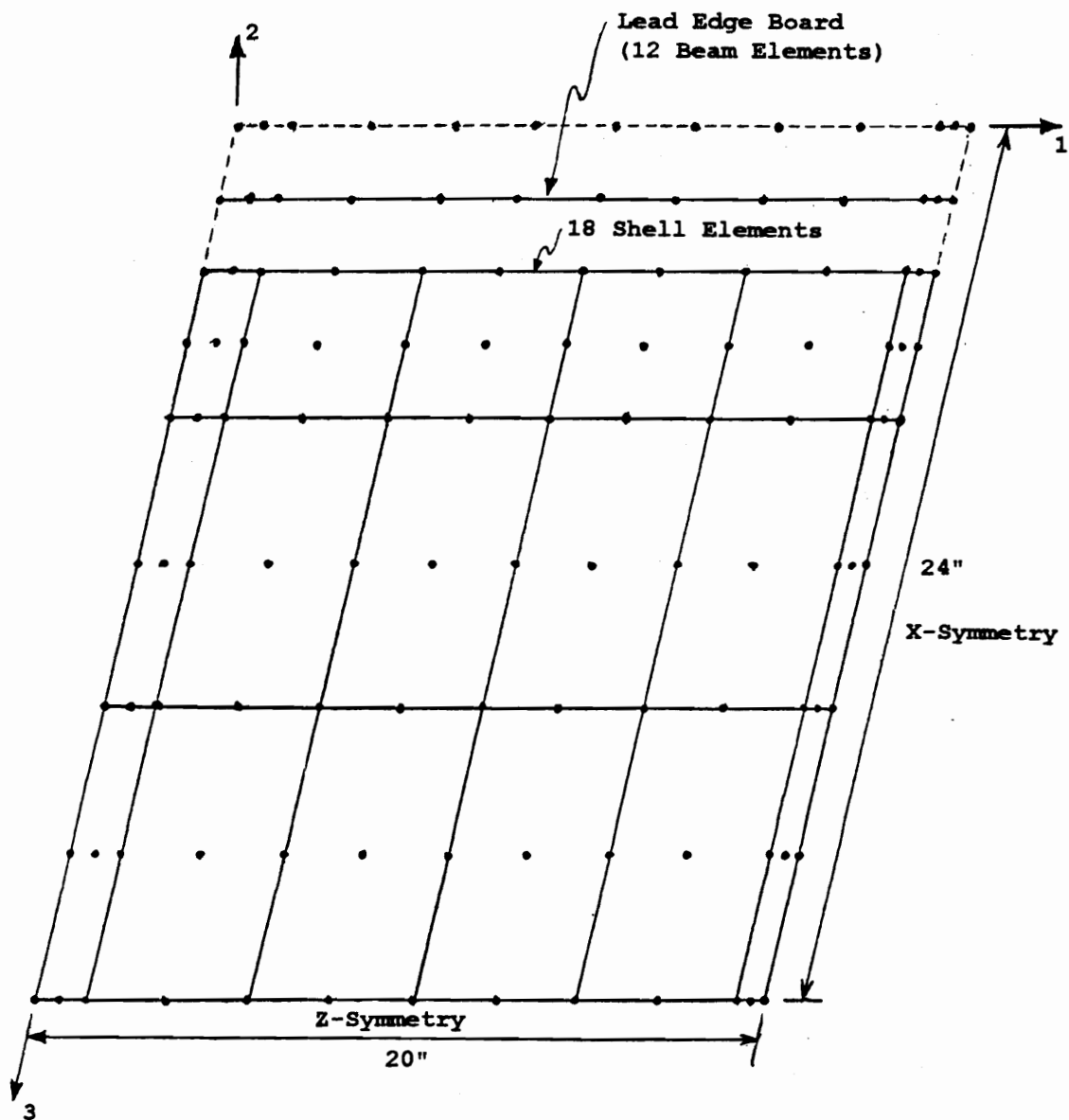


Figure 4.5. Finite Element Mesh used to Simulate Panel Decks with Lead Edge Boards.

Examples of the meshes used to model cut-outs can be found in Section 3.6.

4.1.2 Stringer Pallets with Panel Deck Top and Lumber Deck Bottom

For stringer pallets with a lumber bottom deck, deckboards were modeled using beam elements as shown in Figure 4.6. The configuration of unnotched stringers was essentially unchanged from those used to model pallets with panel decks top and bottom, although it was necessary to move stringer cross-sectional members or add members at locations which correspond to those of deckboards so they could be attached using nail joint and contact elements. Notched stringers required more significant modification involving the use of modified stringer bending members outlined in Section 3.3.1. The configuration of the top panel deck is unchanged.

4.2 Validation of Stringer Pallet Plate Models

To verify that the plate models predicted pallet behavior adequately, pallet deflections determined using plate models were compared to experimental values obtained by physically testing pallets on the pneumatic pressure bag (air-bag) test machine. Pallets were tested nondestructively in the stack, RAD, and RAS support conditions. To predict pallet deflections it was necessary

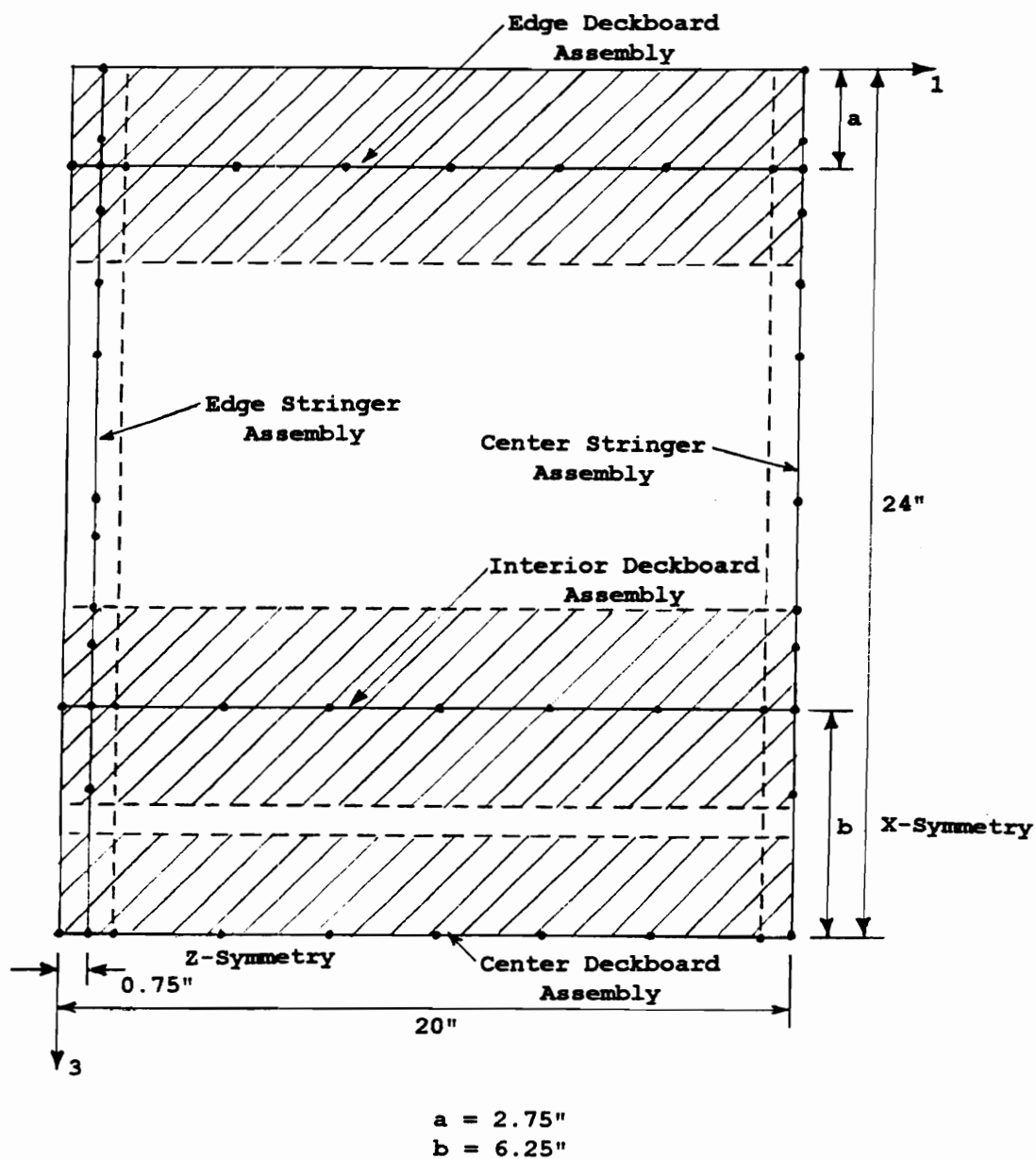


Figure 4.6. Finite Element Mesh used to Simulate the Bottom Deck Behavior of Stringer Pallets with Bottom Decks comprised of Five Lumber Deckboards.

to know important geometric and material properties of the members comprising the pallets. Where possible, these properties were determined prior to full-pallet testing. However, for panel decks, material properties were determined after full-pallet testing because it was necessary to cut the panels into 2 inch strips to determine them.

4.2.1 Determining Pallet Member Properties

Important material and geometric properties of pallet components are required as input to the stringer pallet plate models. Primary geometric input properties required for panel decks are thickness, length, and width. Panel material properties required include moduli of elasticity (both strong and weak panel axis), Poisson's ratio (1-2 plane), and moduli of rigidity (G_{12} , G_{13} , and G_{23}). Geometrically, the length and cross-sectional properties (width and height) are required for strip-type decking and the bending members of stringers. The only material property required as input to ABAQUS for these members is the modulus of elasticity along the length. This is normally the longitudinal direction of solid wood members and the strong panel axis of plywood and OSB strips.

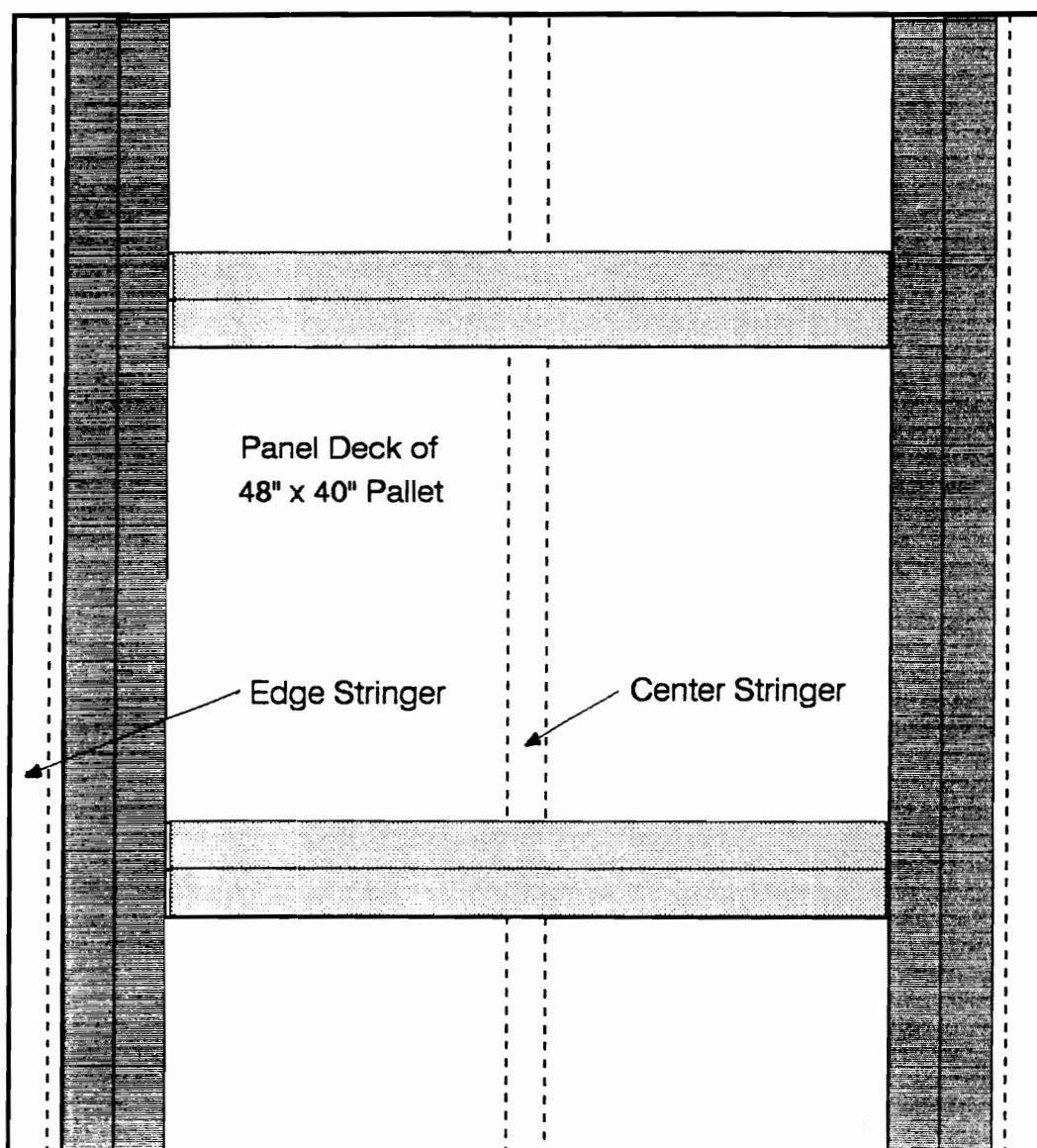
Geometric properties were measured using hand-held calipers accurate to 0.0005 inches. Material properties

were determined experimentally. Test procedures used to determine material properties are described in subsequent sections. Properties were assigned to nail joints and contact regions using the methodologies discussed in Section 3.5.

4.2.1.1 Panel Moduli of Elasticity (E_{PS} and E_{PW})

Moduli of elasticity were determined for both the strong (S) and weak (W) axes of 40 inch x 48 inch panels used in stringer pallets. For pallet models which utilized plate theory an estimate of true E was required. Modulus of elasticity values determined from full-panel tests were effective values because a plate effect (membrane action) was incorporated into the values. Therefore, 2 inch wide strips of deck material were evaluated using a center point load, static bending test to estimate E_{PS} and E_{PW} . Static bending tests were conducted in accordance with ASTM Standard D 3043-87 (ASTM, 1994).

Because strip testing was conducted after the conclusion of pallet testing, it was necessary to remove deck material from the pallets which effectively destroyed them. The pattern of material removal from SPP3, SOO3, and SPL3 type pallets is shown in Figure 4.7. This pattern of removal was also used for S4PP pallets tested in the stack support condition. However, for S4PP pallets tested in the





-  - Specimens with Face Plies oriented Parallel-to-Grain.
-  - Specimens with Face Plies oriented Perpendicular-to-Grain.

Figure 4.7. The Pattern used for Removal of Test Specimens from Panel Decks for the Determination of Material Properties.

RAD support condition all available material was cut into 2 inch wide by 40 inch long strips and for the RAS support condition, into 2 inch wide by 48 long inch strips. Modulus of elasticity values for the panel axis not tested were estimated based on full-panel testing conducted prior to pallet fabrication. Adjustments to full-panel test results are discussed by Mackes (1998, Volume I, Section 22).

The length of 2 inch wide strip specimens varied with panel direction and thickness. For specimens oriented in the strong panel axis, the minimum length specified in ASTM Standard D 3043-87 (ASTM, 1994) is 48 times the panel thickness plus 2 inches. For specimens oriented in the weak panel axis, minimum length is 24 times the thickness plus 2 inches. Minimum lengths of 2 inch wide strip specimens used in bending tests are given in Table 4.1.

The 2 inch wide strips were tested to a maximum load of 10 pounds which was in the elastic range. Therefore, plots of load versus deflection are linear. A typical plot is shown in Figure 4.8. Using these plots, the deflection (Δ_p) at maximum load P (10 pounds) can be determined. With this information, it was possible to calculate an E value using:

$$E = (P \cdot L^3) / (48 \cdot \Delta_p \cdot I) \quad [\text{Eq. 4.1}]$$

where, L is the test span and I is moment of inertia of the panel deck calculated as:

Table 4.1. Minimum Specimen (Strip) Lengths used to Determine Modulus of Elasticity Values for Plywood and Oriented Strand Board (OSB) Panels.

PANEL THICKNESS (inch)	STRIP LENGTH (inch)
*Parallel-to-Grain Orientation:	
15/32	24.50
19/32	30.50
23/32	36.50
*Perpendicular-to-Grain Orientation	
15/32	13.25
19/32	16.25
23/32	19.25

* Note: Orientation of Face Plies.

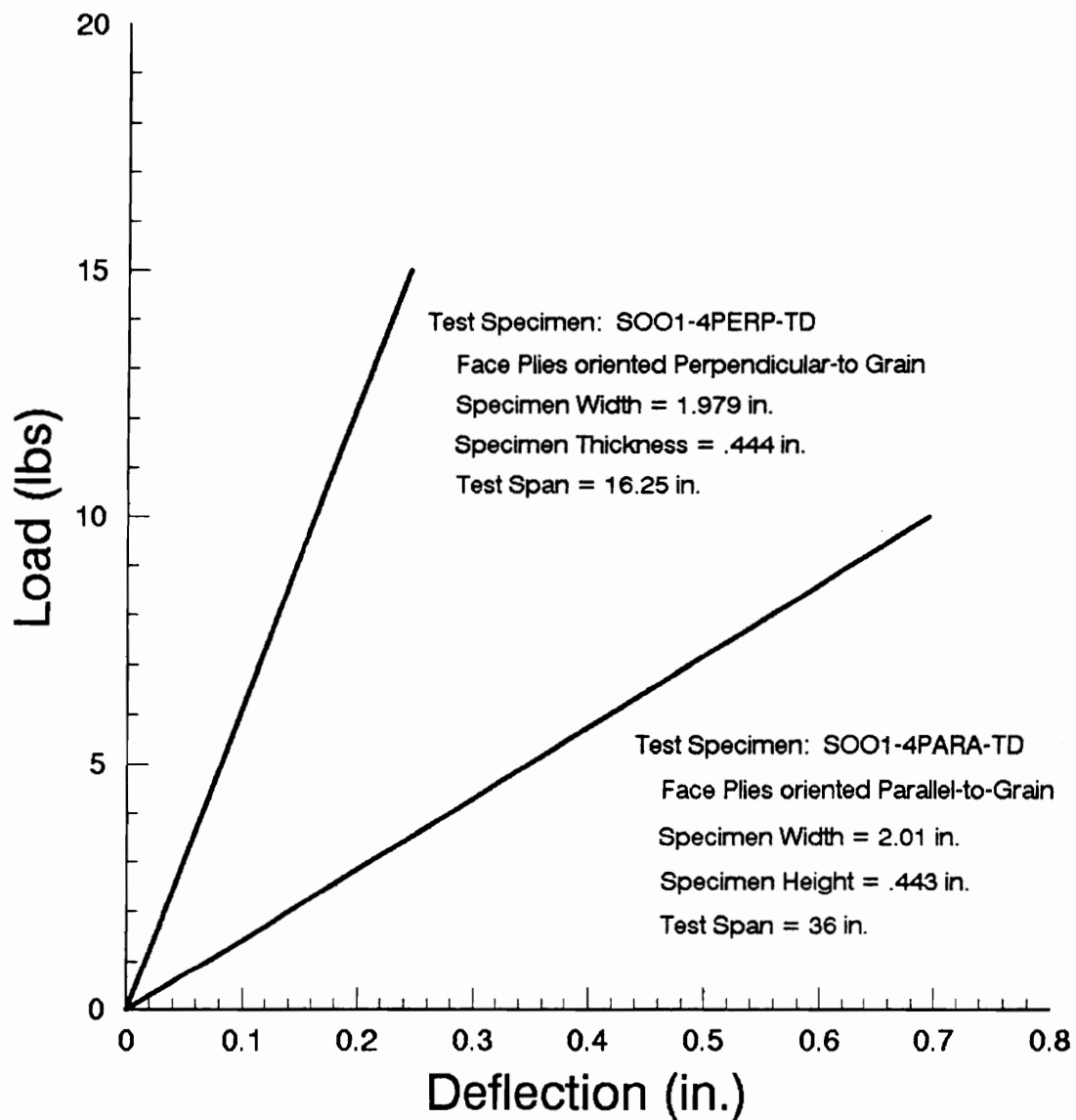


Figure 4.8. Typical Plot of Load versus Deflection for 2 inch Strips of OSB Tested in Bending in the Elastic Range.

$$I = (b \cdot h^3) / 12 \quad [\text{Eq. 4.2}]$$

The strip width (b), which was approximately 2 inches, and height (h) were measured using hand-held calipers.

An overall E_{PS} or E_{PW} value can be determined by averaging the values obtained from testing of individual strips. A summary of E_{PS} and E_{PW} values is presented for panels used to assemble stringer pallets in Volume II, Section 3 of Mackes (1998).

4.2.1.2 Stringer Modulus of Elasticity (E_S)

Stringer modulus of Elasticity (E_S) was determined using a static bending test in accordance with ASTM Standard D 198-84 (ASTM, 1994). The load was applied to stringers at two points equidistance from the supports (reactions). The distance from the reaction to the load point was equal to one third of the span. Stringers were loaded in the linear range at low load levels to avoid damage. The maximum load applied to stringers was 200 pounds, which is well within the elastic (linear) range of stringer deflection.

Nominal 2 x 4 spruce-pine-fir stringers were used to fabricate pallets. Stringers were tested prior to pallet fabrication. E_S values were determined for notched stringers before they were notched. These stringers were again tested after being notched, but at a lower load level (maximum of 50 pounds) to avoid damage. As stringers were

loaded, a plot of load versus deflection was plotted using an x-y recorder. A typical plot is shown in Figure 4.9 and response was linear as expected. Using the plots, the deflection (Δ_P) at load P (200 pounds) can be determined. With this information, E_S can be calculated using:

$$E_S = ((P*a) / (24*\Delta_P*I)) * (3*L^2 + 4*a^2) \quad [\text{Eq. 4.3}]$$

where, L is the test span (which was 45 inches), "a" equals one-third the test span (15 inches), and I is moment of inertia of the stringer, calculated using Equation 4.2. The stringer width (b) and height (h) were measured using hand-held calipers. E_S values for the stringers tested are presented in Volume II, Section 4 of Mackes (1998).

4.2.1.3 Bottom Deckboard Modulus of Elasticity

Modulus of Elasticity (E_{DB}) was determined for bottom deckboards using a single point loading, static bending test in accordance with ASTM Standard D 143-83 (ASTM, 1994). Load was applied to deckboards at mid-span. As with stringers, deckboards were loaded in the linear range (at low load levels) to avoid damage. Fifteen 1 inch by 6 inch nominal southern yellow pine deckboards were used in fabricating SPL type pallets. Deckboards were tested prior to pallet fabrication.

As deckboards were loaded to 50 pounds, a plot of load versus deflection was plotted using an x-y recorder. A

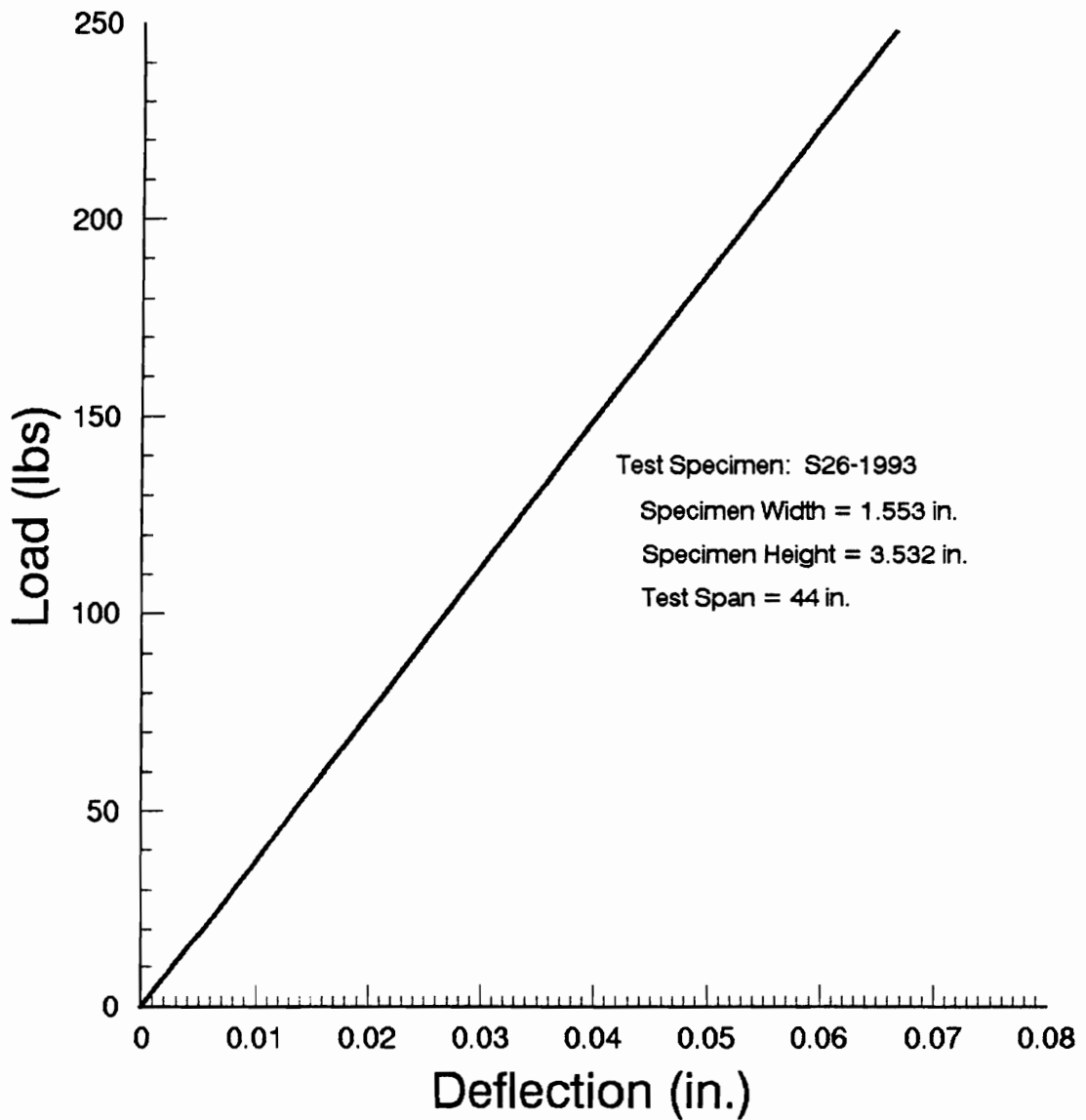


Figure 4.9. Typical Plot of Load versus Deflection for a Spruce-Pine-Fir Stringer in Bending in the Elastic Range.

typical plot is shown in Figure 4.10 and response was linear as expected. Using the plots, the deflection (Δ_P) at load P (25 pounds) was determined. With this information, E_{DB} can be calculated as:

$$E_{DB} = (P \cdot L^3) / (48 \cdot \Delta_P \cdot I) \quad [\text{Eq. 4.4}]$$

where, L is the test span (which was 36 inches) and I is moment of inertia of the deckboard, calculated using Equation 4.2. The deckboard width (b) and height (h) were measured using hand-held calipers. E_{DB} values for the deckboards tested are presented by Mackes (1998, Volume II, Section 5).

4.2.2 Preparation of Pallets

Prior to pallet assembly, components were clearly identified and marked. The location of each component placed in the pallet was then recorded. Figure 4.11 shows the location of pallet components used to assemble test pallet SPP3-1. Complete records of component locations for all stringer pallets tested are presented by Mackes (1998, Volume II, Section 6).

Pallet components were assembled into three basic stringer pallet types:

1. Three-stringer reversible pallet with panel decks top and bottom (SPP3 and S003 pallet types).
2. Four-stringer reversible pallet with panel decks top and bottom (S400 pallet types).

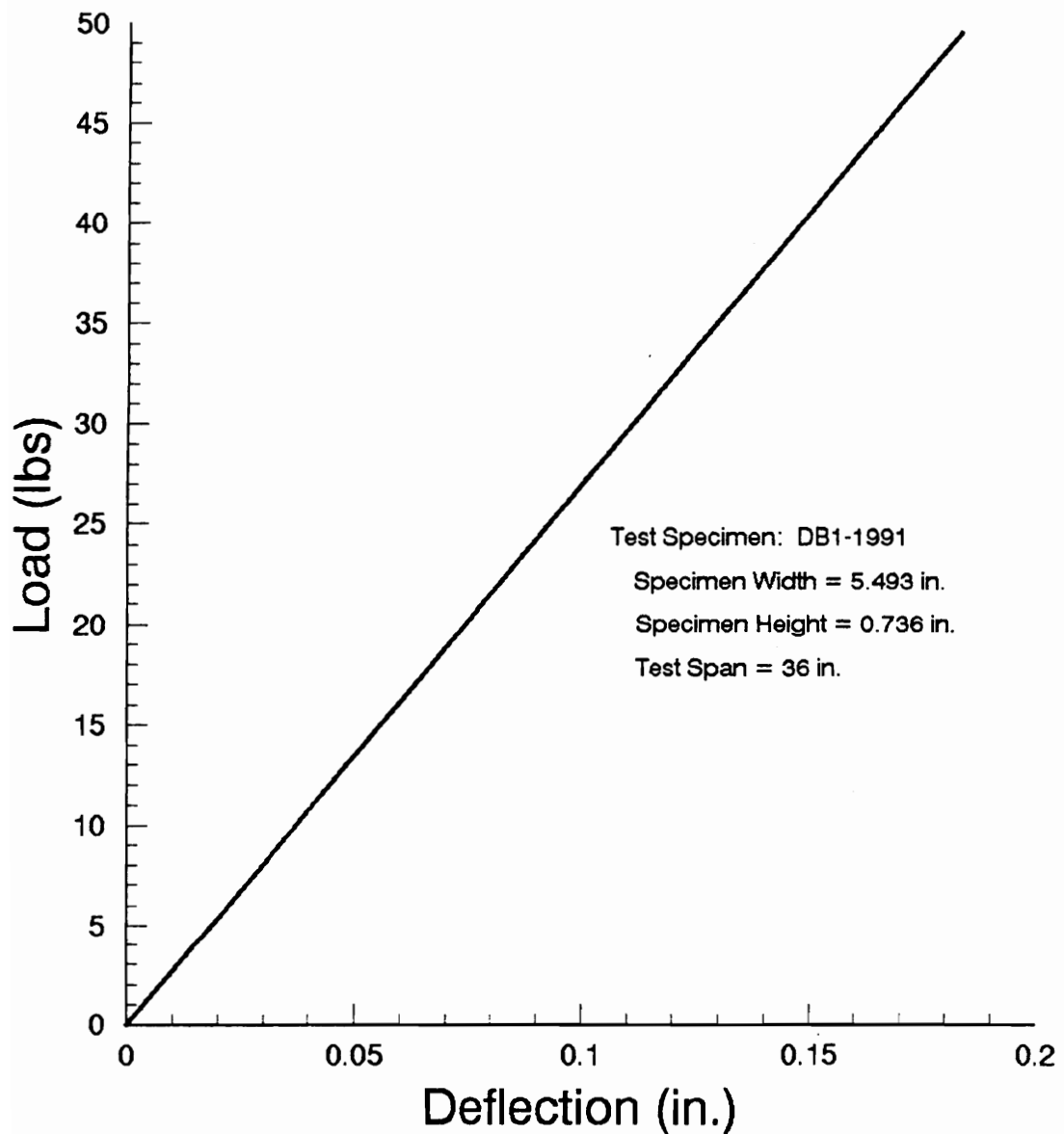
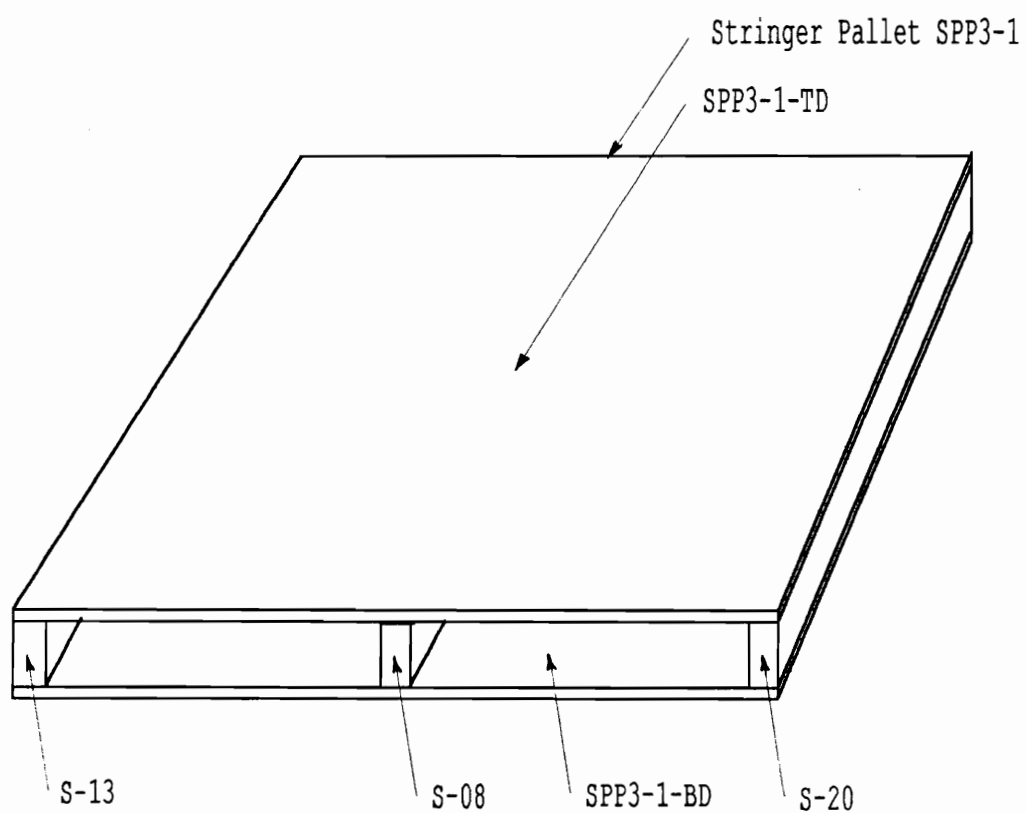


Figure 4.10. Typical Plot of Load versus Deflection for a Southern Yellow Pine Deckboard in Bending in the Elastic Range.



**Figure 4.11. Location of Pallet Components
Comprising Test Pallet SPP3-1.**

3. Three-stringer non-reversible pallet with a panel top deck top and a lumber deck bottom (SPL3 pallet type).

The size of all pallets built and tested was 48 by 40 inches, with the 48 inch direction of the pallet oriented along the length of the stringer. For panel types SPP3, SOO3, and SPL3, the strong axis of the panel was oriented in the 40 inch width direction of the pallet spanning across the stringers. For S400 type pallets, several replications were built with the weak panel axis spanning across the stringers.

Panels used for SPP3 and SPL3 pallets were cut from 4 by 8 foot sheets of 19/32 inch southern yellow pine plywood identified as loblolly pine. OSB panels used to fabricate SOO3 and S400 type pallets were comprised of either cottonwood or southern yellow pine flakes. Panels for SOO3 type pallets were cut from 15/32 inch sheets of OSB, tempered on both sides. This OSB is comprised primarily of southern yellow pine flakes and generally has higher stiffness properties than the OSB used in S400 pallet fabrication. The 40 inch lumber deckboards, comprising the bottom deck of SPL type pallets, were cut from nominal 1 x 6 boards of southern yellow pine.

The 48 inch stringers used in pallet fabrication were cut from nominal 2 x 4's of spruce-pine-fir. An attempt was made to minimize the use of members with excessively large

knots and wane. However, both knots and wane were present in the stringers, particularly in S400 pallet stringers. Although not ideal for research, the use of stringers with defects such as knots and wane better reflects the actual condition of pallets used in the field. Where possible, an attempt was made to account for the effect of these defects on results.

Pallet assembly was accomplished using pallet nails hand driven into members using hammers. Nails selected for use in assembling SPP3, SOO3, and SPL3 type pallets were 2 inch long Philstone nails. S400 pallets were assembled with 2.25 inch long Greenwood nails. Properties for these nail types are given in Volume I, Section 9 of Mackes (1998). Figure 4.12 shows the nailing pattern used to assemble SPP3, SOO3, and SPL3 pallets. The nailing pattern used to assemble S400 pallets was similar, except that only nine nails were used to attach the panel to each stringer as opposed to eleven.

4.2.3 Pallet Testing

A pneumatic pressure-bag (air-bag) test machine was used to experimentally measure the deflection of pallets under load. The procedure used to operate the air-bag test machine is presented by Mackes (1998, Volume II, Section 7). All three replications of each pallet type were tested in

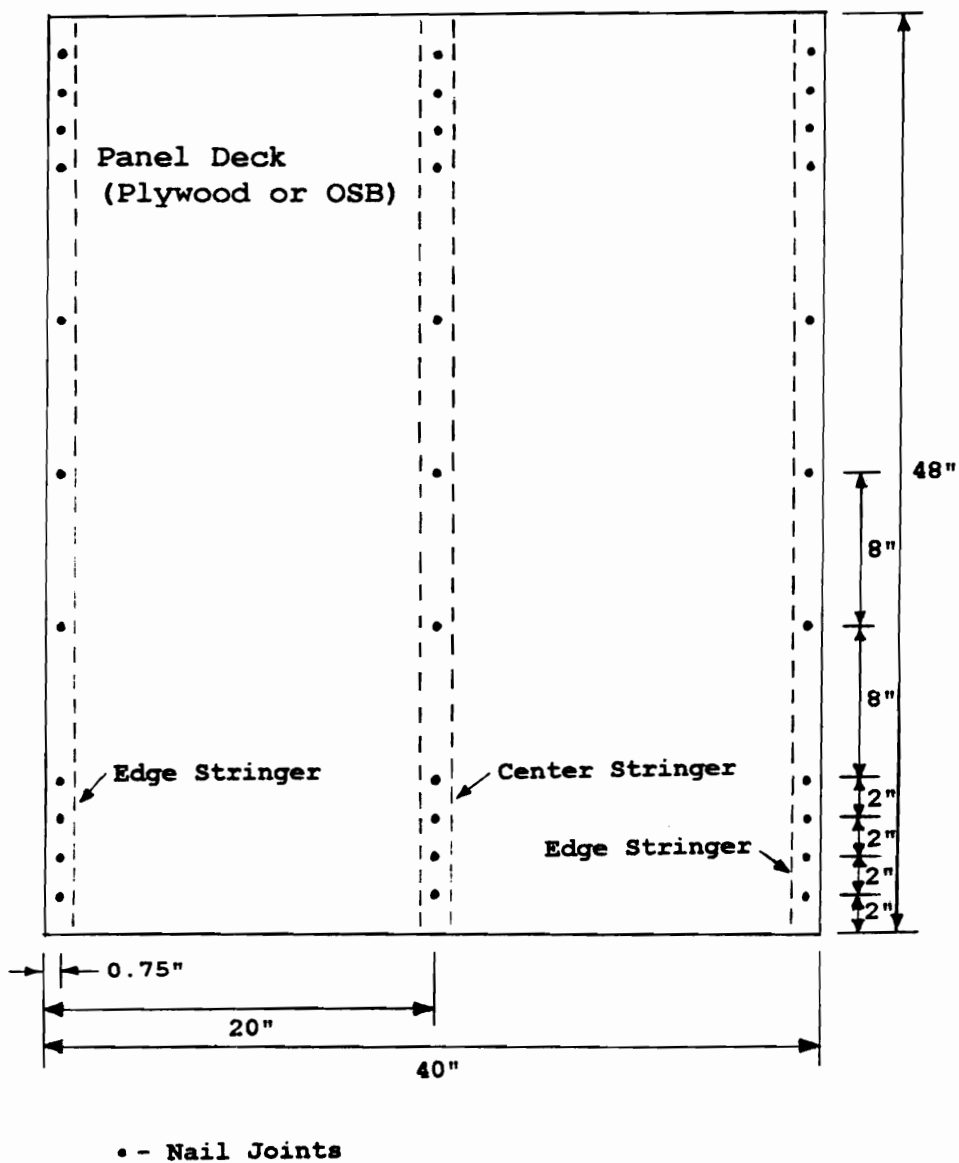


Figure 4.12. Nailing Pattern used to attach Panel Decks to Stringers in Pallet Assembly.

the stack, RAD, and RAS support conditions using the air-bag testing machine. Figure 4.13 shows a pallet as it undergoes testing in the air-bag testing machine. Because each pallet was used in multiple tests, they were stressed at relatively low loads in the elastic range of both individual pallet members and unit (pallet) as a whole to avoid damage. During testing, a plot of load versus deformation was observed on the monitor of the data acquisition computer to ensure that pallets were stressed in the linear range.

For each support condition, each pallet was loaded three times, the first two times to work pallet joints and the third time to obtain deflection readings. The rate of loading was 0.10 inch per minute. This is equivalent to 18 liters of air per minute entering the air-bag. A discussion of pallet testing for each support condition is presented in subsequent sections.

4.2.3.1 Stack Support Condition

To test pallets in the stack support condition using the air-bag test machine, the machine was fitted with steel I-beams that support the pallet under each stringer. Therefore, a three stringer pallet required three I-beams, a four stringer pallet required four, and so on. The center LVDT was attached to the test setup (I-beam) at the pallet center to monitor deformation of the support structure,

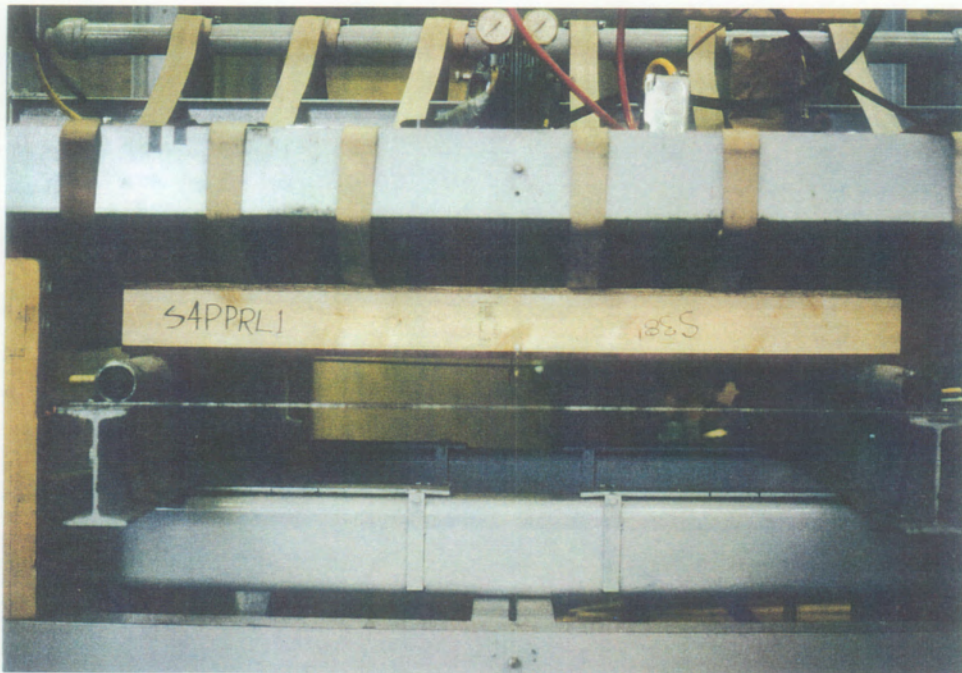


Figure 4.13. Stringer Pallet being
Tested in Flexure (RAS Support Condition)
using the Pneumatic Pressure-Bag
Test Machine at VPI & SU.

including I-beam bending. Pallet deflections recorded by the LVDT's on the test machine were adjusted for this factor which is discussed further in Section 4.2.4.

In the stack support condition, panel decks were uniformly loaded by contacting the surface of the air-bag directly to the surface of the panel. A schematic of the test setup is shown in Figure 4.14. SPP3, SPL3, and S003 pallet types were uniformly loaded to 2.604 pounds per square inch which is a total load of 5000 pounds. S400 pallets were uniformly loaded to 1 psi or a total load of 1920 pounds.

Deflections were measured at mid-span between the stringers one-quarter of the panel length in from the edge. For reversible pallets, with panel decks top and bottom, it was necessary to drill holes in the bottom panel to allow clear access to the top deck for LVDT attachment. Therefore, only the top decks of reversible pallets were tested. Because only three LVDT's could be monitored by the data acquisition computer at a given time, each pallet was tested twice with deflection readings for one side of the pallet collected on the first run and the other side on the second.

In addition to uniform load testing, some panel decks were line-loaded. Pallet type P(JC) was loaded with two line loads of 52.083 pounds per inch each (5000 pounds)

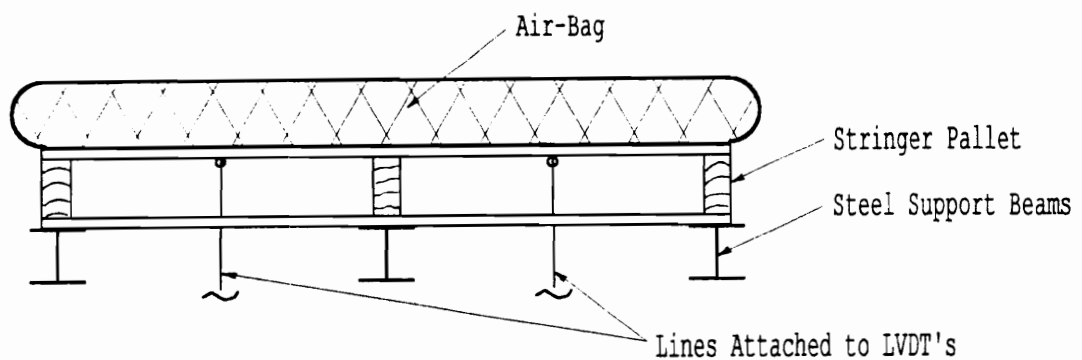


Figure 4.14. Schematic of Test Setup contained within the Metal Support Frame of the Air-Bag Test Machine used to Evaluate the Panel Deck Behavior of Stringer Pallets in the Stack Support Condition.

applied at the mid-spans between stringers. Line loads were also used to evaluate the bottom deck of non-reversible stringer pallets having a bottom deck comprised either of lumber or a panel with wheel openings.

Line loads were applied to the pallet deck by inserting a platen which had two wooden members attached to it acting as line loads between the air-bag and pallet. A schematic of this test setup is shown in Figure 4.15. Line loads were applied at the mid-spans between the stringers. Deflection measurements were recorded at mid-span between stringers at each edge. As with uniform load tests, only one LVDT was available along each edge. Rather than continuing to conduct two tests on each pallet, a yoke was used as shown in Figure 4.15 to obtain an average value for both sides, conducting only one test.

4.2.3.2 Rack-Across-Deck (RAD) Support Condition

In the RAD support condition, the lower pallet deck was simply supported along the 48 inch sides (oriented along the length of stringers) and free along the other two sides.

Test spans were as follows:

1. SPP3 Pallets: Span = 36 inches
2. SOO3 Pallets: Span = 37 inches
3. SPL3 Pallets: Span = 34 inches
4. S400 Pallets: Span = 36 inches

Because pallets were 40 inches wide, they did overhang the supports.

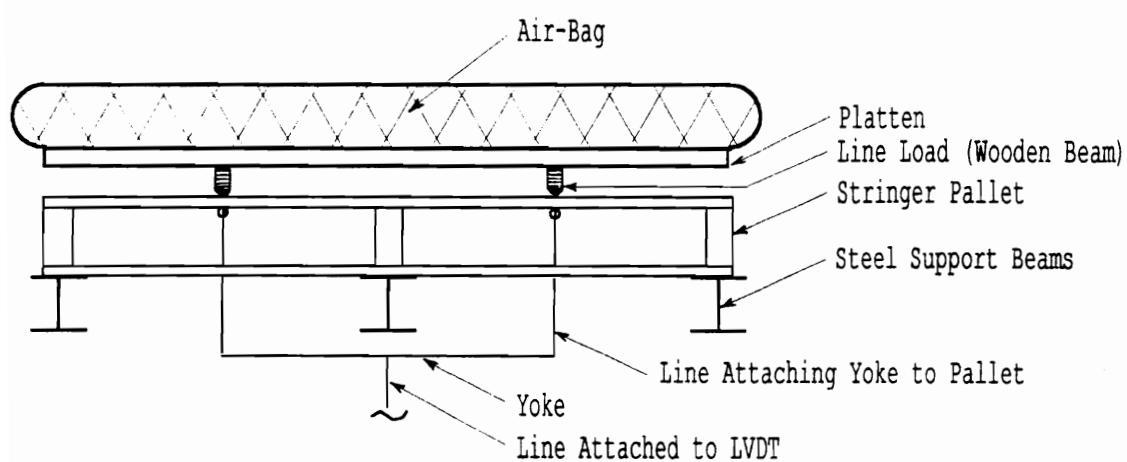


Figure 4.15. Schematic of Test Setup used to evaluate Lumber and Composite (Plywood and OSB) Strip-Type Bottom Deck Behavior of Stringer Pallets in the Stack Support Condition.

A uniformly distributed load was applied to the top deck of the pallets. Plywood pallets (SPP3 and SPL3) were uniformly loaded to 2000 pounds and SOO3 pallets were loaded to 1000 pounds. S400 Pallets were loaded to 300 pounds. Deflection values were measured at the mid-span along each free edge and at the pallet center.

During testing, gaps formed in the joints of all stringer pallets tested. Gaps occurred as shown in Figure 4.16. For edge stringers and interior stringers away from the center, load was transferred from the top deck to the inner edge of the stringer where the deck contacts the stringer. Then load was transferred to the bottom outside stringer edge and to the bottom deck. For center stringers, load transferred from the top deck to the middle of the upper stringer surface, down to the bottom outside stringer edges and finally to the bottom deck. Although load transferred through the stringers, they acted primarily as spacers between the decks in the RAD support condition.

4.2.3.3 Rack-Across-Stringer (RAS) Support Condition

In the RAS support condition, the lower pallet deck was simply supported along the 40 inch sides (oriented across the stringers) and free along the other two sides. Test spans were:

1. SPP3 Pallets: Span = 44 inches
2. SOO3 Pallets: Span = 44 inches

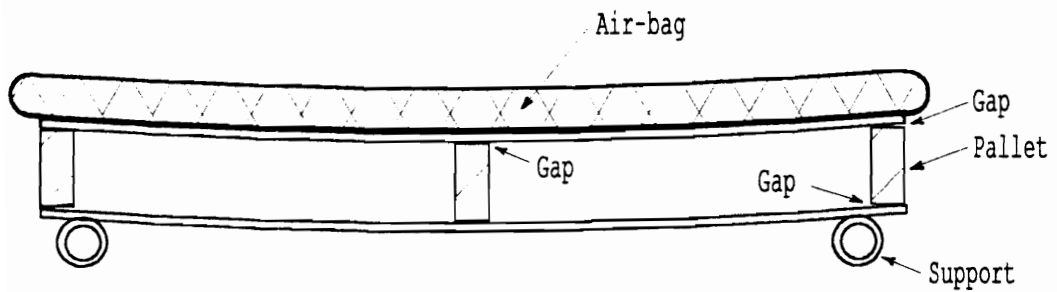


Figure 4.16. Gap Formation in the Joints of Stringer Pallets tested in the RAD Support Condition.

3. SPL3 Pallets: Span = 42 inches
4. S400 Pallets: Span = 44 inches

Because pallets were 48 inches long, they did overhang the supports by either 2 or 3 inches.

A uniformly distributed load of up to 2 psi (3840 pounds of total load) was applied to SPP3 pallets. For SPL3 and OSB pallet types, the uniformly distributed load applied was in the range of 1 to 1.5 psi. As with RAD testing, deflection values were measured at mid-span along each free edge and at the pallet center.

No gap formation was observed to occur along the length of the pallet (48 inch direction), with the deck fully in contact with the stringers. However, because the center stringer deflected more than the edge stringer at mid-span, gap formation was observed across the pallet width and was most evident at mid-span. Gaps which formed, although not as pronounced, appeared similar to those observed in the RAD support condition shown in Figure 4.16.

4.2.4 Data Analysis and Results

As pallets were uniformly loaded in the test machine, load versus deflection data were recorded by a data acquisition computer. Data were adjusted for support settlement based on support conditions as outlined in Section 2.1.3.1. Further discussion of data adjustments is given by Mackes (1998, Volume II, Section 8).

Load versus deflection plots were generated from adjusted data. Typical plots for the three principle support conditions tested are shown in Figure 4.17. Initially at low load levels, plots were non-linear. This was attributed to several factors including pallet joint settlement, support settlement not considered in the data adjustment, and warped pallets. For several pallets tested, warpage was significant and portions of the pallet were not initially in contact with the support, resulting in plots that were extremely non-linear at low load levels. Initial non-linear data were discarded. Otherwise, plots were very linear as expected.

Using a linear regression analysis, the slope for the linear region of load versus deflection plots was determined. Based on the slope, deflection was calculated at selected load levels within the range of physical testing for comparison to plate model predictions. Details of stringer pallet testing and this calculation procedure are given in Volume II, Section 8 of Mackes (1998).

A summary of results for the stack support condition is presented in Table 4.2. Included in this table are comparisons of deflection predictions generated using stringer pallet plate models and experimentally measured values. Maximum differences between predicted and experimental values were less than 15 percent. Mean

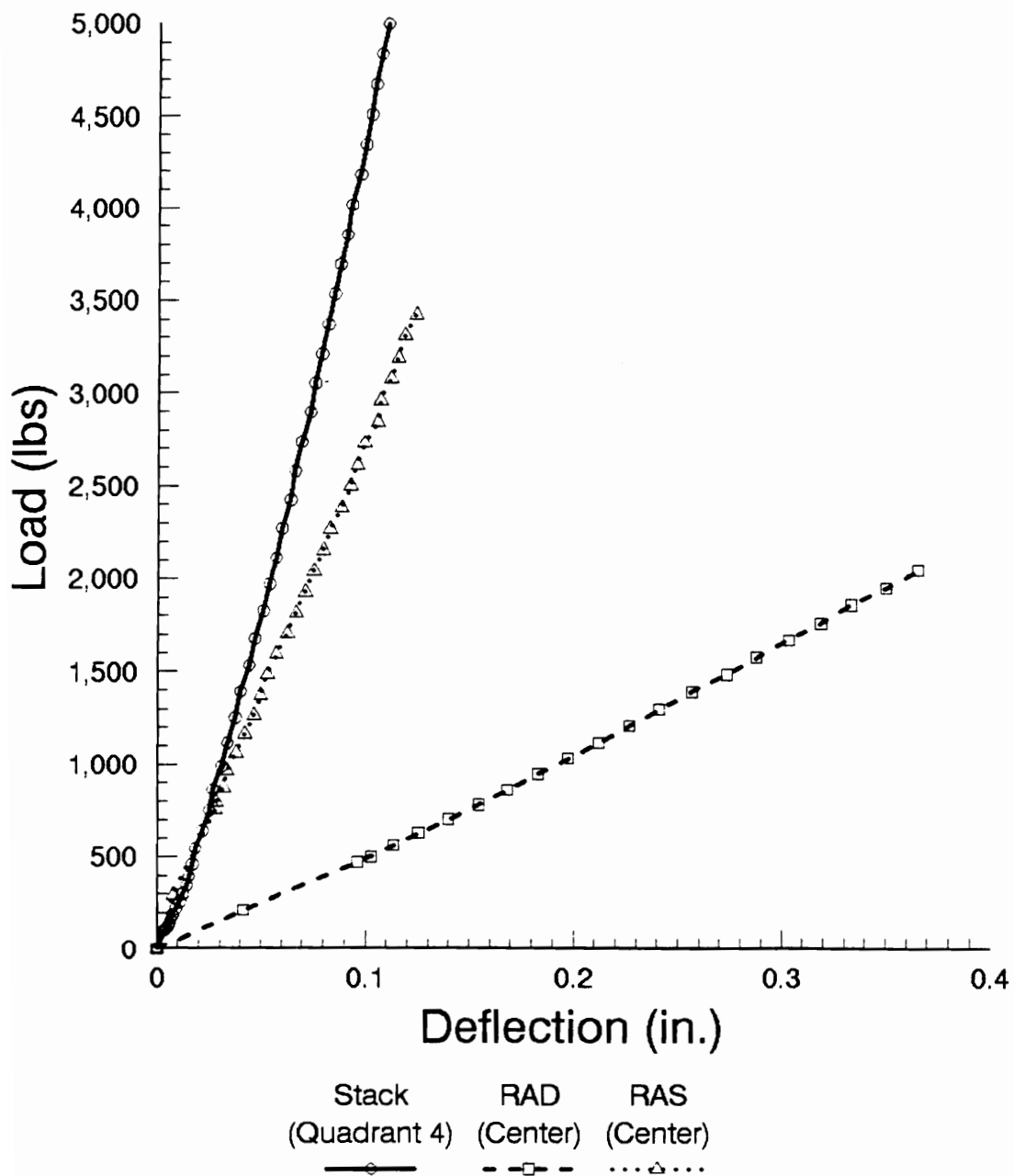


Figure 4.17. Plots of Load versus Deflection for Test Pallet SPP3-1 loaded in the Stack, Rad, and RAS Support Conditions.

Table 4.2. Comparison of Stringer Pallet Plate Model Predictions to Experimentally Measured (ABTM) Deflections in the Stack Support Condition.

PALLET ID. NUMBER	PREDICTED DEFLECTION (in.)	ABTM DEFLECTION (in.)	PERCENT DIFFERENCE (%)
SPP3-1	-0.072	-0.078	-7.7
SPP3-2	-0.048	-0.042	14.3
SPP3-3	-0.052	-0.059	-11.9
MEAN	-0.057	-0.060	-3.9
SOO3-1	-0.188	-0.203	-7.4
SOO3-2	-0.187	-0.198	-5.6
S003-3	-0.189	-0.195	-3.1
MEAN	-0.188	-0.199	-5.4
SPL3-1	-0.083	-0.079	5.1
SPL3-2	-0.076	-0.080	-5.0
SPL3-3	-0.070	-0.063	11.1
MEAN	-0.076	-0.074	3.2
S400-7	-0.206	-0.209	-1.4
S400-8	-0.248	-0.244	1.6
S400-9	-0.220	-0.208	5.8
MEAN	-0.225	-0.220	2.0
P(JC)-1	-0.155	-0.159	-2.5

Notes: Experimental deflections measured at mid-span between stringers 12 inches from edge of pallet. Corresponding nodes of finite element models were as follows [refer to model drawings presented in Volume II, Section 9 of Mackes (1998)]:

SPP3 and S003 Models - Node #297

SPL3 Models - Node #187

S400 and P(JC) Models - Node #500

Loads were as follows (P = Total Load):

SPP3, SOO3, and SPL3 Pallets: UDL = 2.604 psi
(P = 5000 lbs)

S400 Pallets: UDL = 1.000 psi (P = 1920 lbs)

P(JC) Pallet: Two Line-Loads - 52.083 lb/in.
(P = 5000 lbs)

differences for replicated samples were 5.4 percent or less. Similar comparisons for the RAD and RAS support conditions are given in Table 4.3 and 4.4 respectively. In the RAD support condition maximum differences between predicted and experimental deflections were less than 9 percent, with mean differences of 5.5 percent or less. In the RAS support condition, agreement was again good, with maximum differences of 12.1 percent or less and mean differences not exceeding 8 percent. These results suggest that stringer pallet plate models satisfactorily predict behavior in the three principle support conditions.

4.3 Stringer Pallet Sensitivity Studies

Sensitivity studies are presented for the principle support conditions considered in this research, the stack, RAD, and RAS support conditions. These studies were conducted to systematically determine which geometric and material properties significantly influence pallet behavior. The approach used involved varying the property of interest, with all other properties remaining unchanged. To determine the effect of a given property, the property value was reduced by a factor of 0.5 and increased by a factor of 2.0. The percentage of change was then calculated for both maximum S11 normal stress and deflection (D2). These sensitivity studies provided a rational basis for reducing

Table 4.3. Comparison of Stringer Pallet Plate Model Predictions to Experimentally Measured (ABTM) Deflections in the RAD Support Condition.

PALLET ID. NUMBER	PREDICTED DEFLECTION (in.)	ABTM DEFLECTION (in.)	PERCENT DIFFERENCE (%)
34 inch Test Span:			
SPL3-1	-0.205	-0.222	-7.7
SPL3-2	-0.179	-0.185	-3.2
SPL3-3	-0.154	-0.163	-5.5
MEAN	-0.179	-0.190	-5.5
36 inch Test Span:			
SPP3-1	-0.337	-0.335	0.6
SPP3-2	-0.206	-0.218	-5.5
SPP3-3	-0.233	-0.251	-7.2
MEAN	-0.259	-0.268	-3.5
S400-4	-0.287	-0.313	-8.3
S400-5	-0.281	-0.279	0.7
S400-6	-0.274	-0.279	-1.8
MEAN	-0.281	-0.290	-3.3
37 inch Test Span:			
SOO3-1	-0.191	-0.190	0.5
SOO3-2	-0.195	-0.187	4.3
SOO3-3	-0.190	-0.179	6.1
MEAN	-0.192	-0.185	3.6

Notes: Each experimental (ABTM) deflection measurement and corresponding finite element prediction reported is the mean of three values, one taken along each pallet edge at mid-span and the third at the pallet center.

Loads were as follows (P = Total Load):

SPL3 Pallets: UDL = 1.000 psi (P = 1920 lbs)
SPP3 Pallets: UDL = 1.000 psi (P = 1920 lbs)
S400 Pallets: UDL = 0.125 psi (P = 240 lbs)
SOO3 Pallets: UDL = 0.250 psi (P = 480 lbs)

Table 4.4. Comparison of Stringer Pallet Plate Model Predictions to Experimentally Measured (ABTM) Deflections in the RAS Support Condition.

PALLET ID. NUMBER	EDGE AT MID-SPAN			PALLET CENTER		
	FE D (in.)	ABTM D (in.)	DIF (%)	FE D (in.)	ABTM D (in.)	DIF (%)
42 inch Test Span:						
SPP3-3	-0.035	-0.038	-7.9	-0.051	-0.052	-1.9
44 inch Test Span:						
SPP3-1	-0.038	-0.040	-5.0	-0.074	-0.069	7.2
SPP3-2	-0.040	-0.036	11.1	-0.075	-0.068	10.3
MEAN	-0.039	-0.038	2.6	-0.075	-0.069	8.0
SOO3-1	-0.036	-0.038	-5.3	-0.084	-0.086	-2.3
SOO3-2	-0.042	-0.043	-2.3	-0.081	-0.087	-6.9
SOO3-3	-0.042	-0.044	-4.5	-0.093	-0.089	4.5
MEAN	-0.040	-0.042	-4.0	-0.086	-0.087	-1.5
S400-1	-0.066	-0.066	0.0	-0.065	-0.067	-3.0
S400-2	-0.065	-0.058	12.1	-0.086	-0.081	6.2
S400-3	-0.065	-0.065	0.0	-0.084	-0.083	1.2
MEAN	-0.065	-0.063	3.7	-0.078	-0.077	1.7

- Notes: 1. FE D - Deflection predicted using finite element plate model.
 ABTM D - Experimental deflection measured using the air-bag test machine.
 DIF - Difference between predicted and experimental deflections.
2. Experimental (ABTM) deflection measurements and corresponding finite element predictions reported are the mean of the two values taken along each pallet edge at mid-span and the value taken at the pallet center.
3. A full uniformly distributed load of 1.0 psi was applied (total applied load = 1920 lbs).

the degrees of freedom required to predict pallet behavior in simplified PC-based pallet models.

4.3.1 Stack Support Condition

Sensitivity studies were conducted using stringer pallet plate models. Both top and bottom decks of pallets were evaluated to determine which geometric and material properties significantly affected behavior. Test Case SPP3-1 data were used to evaluate panel deck behavior. A summary of results for geometric and material properties evaluated are presented in Table 4.5. Generally, only the properties of the pallet deck being evaluated had a significant impact on model solutions. Therefore, in the stack support condition, bottom deck properties were not significant (important) if the top deck was being evaluated and vice versa.

As expected, the thickness of panel decks evaluated in the stack support condition was important. Modulus of elasticity for the panel axis oriented in the 1-direction (bridging across the stringers) was also important. Modulus of elasticity for the panel axis oriented in the 3-direction (along the length of the stringer) was not as significant. Poisson's ratio (ν_{12}) does have some effect, although it was not as great as for block pallets. G_{12} , G_{13} , and G_{23} were not significant.

**Table 4.5. Sensitivity of the Stringer Pallet
Plate Model to Changes in Geometric and Material
Properties in the Stack Support Condition.**

PROPERTY ALTERED	0.5 X ACTUAL PROPERTY VALUE				2.0 X ACTUAL PROPERTY VALUE			
	MAXIMUM S11 (psi)	CHANGE (%)	MAXIMUM D2 (in)	CHANGE (%)	MAXIMUM S11 (psi)	CHANGE (%)	MAXIMUM D2 (in)	CHANGE (%)
Top Deck Properties (loaded surface):								
T	5420.0	247.0	-0.4567	516.3	418.0	-73.2	-0.0135	-81.8
E1	1502.0	-3.8	-0.1366	84.3	1611.0	3.1	-0.0403	-45.6
E3	1561.0	-0.1	-0.0734	-0.9	1570.0	0.5	-0.0751	1.3
V12	1560.0	-0.1	-0.0735	-0.8	1571.0	0.6	-0.0746	0.7
G	1564.0	0.1	-0.0750	1.2	1561.0	-0.1	-0.0736	-0.7
Bottom Deck Properties (no load applied directly to surface):								
T	1562.0	0.0	-0.0741	0.0	1562.0	0.0	-0.0741	0.0
E1	1562.0	0.0	-0.0741	0.0	1562.0	0.0	-0.0741	0.0
E3	1562.0	0.0	-0.0741	0.0	1562.0	0.0	-0.0741	0.0
V12	1562.0	0.0	-0.0741	0.0	1562.0	0.0	-0.0741	0.0
G	1562.0	0.0	-0.0741	0.0	1562.0	0.0	-0.0741	0.0
Stringer Properties:								
ES	1562.0	0.0	-0.0741	0.0	1562.0	0.0	-0.0741	0.0
CS	1562.0	0.0	-0.0741	0.0	1562.0	0.0	-0.0741	0.0
Deck Spacing:								
DS	1562.0	0.0	-0.0741	0.0	1562.0	0.0	-0.0741	0.0

Notes: 1. Property data are for Test Pallet SPP3-1.

Top Deck Properties (loaded surface):

Panel Thickness (T) = 0.0592 in.

E1 = 1.284 E+6 psi; E3 = 0.0405 E+6 psi

V12 = 0.178; G12 = G13 = G23 = 0.5 E+6 psi

Bottom Deck Properties:

Panel Thickness (T) = 0.0574 in.

E1 = 1.140 E+6 psi; E3 = 0.0380 E+6 psi

V12 = 0.172; G12 = G13 = G23 = 0.5 E+6 psi

Edge Stringer (ES) and Center Stringer (CS) Properties:

ES: W = 1.485 in.; H = 3.443 in.; E1 = 1.871 E+6 psi

CS: W = 1.486 in.; H = 3.484 in.; E1 = 1.740 E+6 psi

Deck Spacing (DS): DS = 4.094 in.

2. For Test Pallet SPP3-1 property data,

Maximum Predicted Stress (S11) = +/-1562 psi

Maximum Predicted Deflection (D2) = -0.0741 in.

3. Absolute maximum stress magnitudes are reported in table.

Sensitivity to changing joint and contact properties is presented in Table 4.6. Withdrawal/head embedment was significant. Lateral stiffness was not significant in the plate model. However, prior to removing lateral stiffness for the simplified stack models, this factor was evaluated further using the pallet section model shown in Figure 4.18. Details of this evaluation are given in Volume II, Section 10 of Mackes (1998). Results of this study are summarized in Table 4.7. Based on this highly refined model, lateral stiffness still did not have a significant effect on either maximum stress or deflection predictions. Therefore, lateral stiffness was not considered in the simplified stack models. Contact stiffness was important with regards to deflection, particularly when the top deck was extremely stiff. However, contact stiffness was not as significant with regard to stress magnitudes. This was particularly true when the strong panel axis was oriented in the 1-direction (bridging across the stringers).

An evaluation of spring attachment between the stringers and bottom deck was done to determine the effect of the stringers and bottom deck on behavior when the top deck was loaded in the stack support condition. Results of this evaluation are presented in Table 4.8. Fixing the joints which attach the stringer to the bottom deck had no significant effect on behavior. Therefore, by incorporating

Table 4.6. Sensitivity of the Stringer Pallet Plate Model to Changes in Stringer/Deck Contact and Nail Joint Properties in the Stack Support Condition.

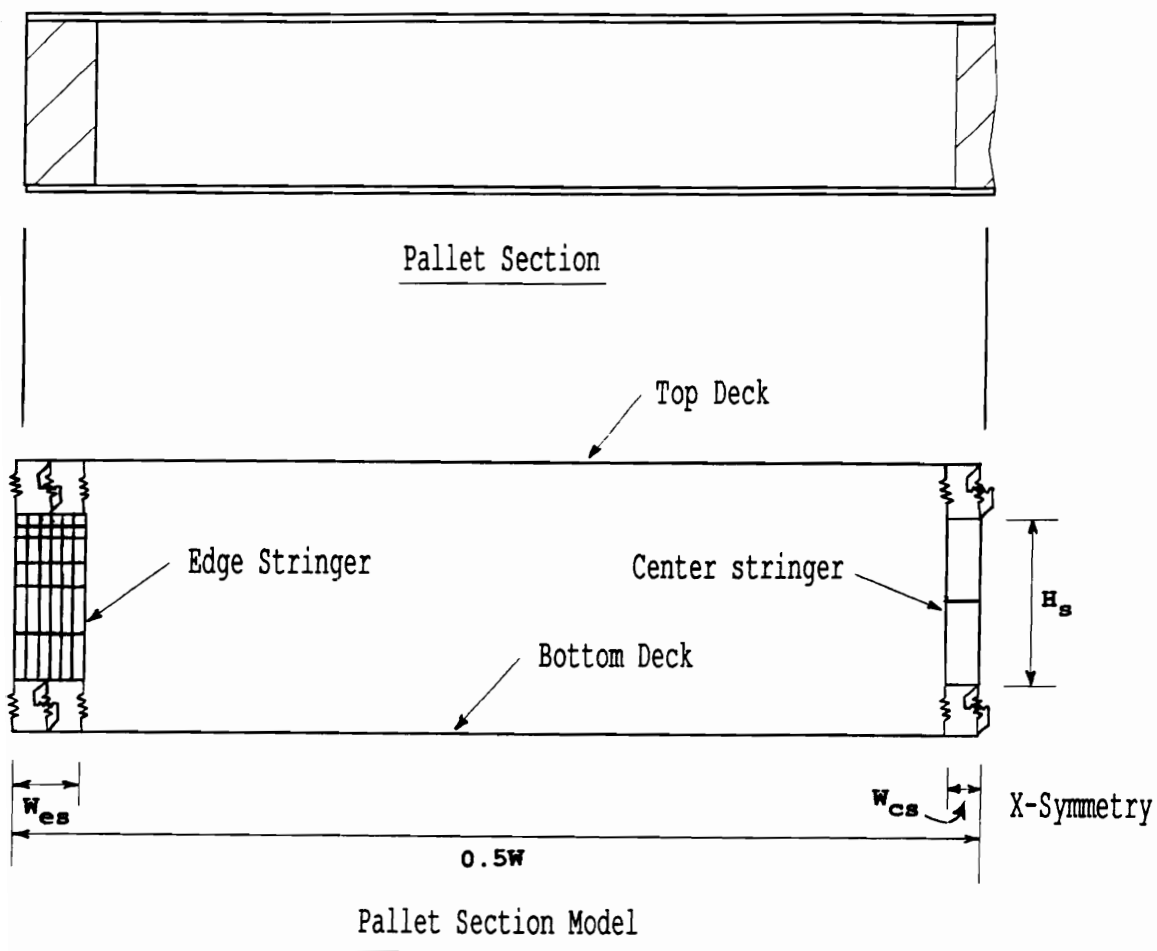
PROPERTY ALTERED	0.5 X ACTUAL PROPERTY VALUE				2.0 X ACTUAL PROPERTY VALUE			
	MAXIMUM S11 (psi)	CHANGE (%)	MAXIMUM D2 (in)	CHANGE (%)	MAXIMUM S11 (psi)	CHANGE (%)	MAXIMUM D2 (in)	CHANGE (%)
Stringer/Top Deck Contact Properties:								
ES	1605.0	2.8	-0.0790	6.6	1527.0	-2.2	-0.0707	-4.6
CS	1604.0	2.7	-0.0755	1.9	1549.0	-0.8	-0.0734	-0.9
Withdrawal/Head Embedment Siffness Properties:								
ES	1567.0	0.3	-0.0745	0.5	1557.0	-0.3	-0.0737	-0.5
CS	1548.0	-0.9	-0.0741	0.0	1588.0	1.7	-0.0741	0.0
Lateral Stiffness Properties:								
LS1	1562.0	0.0	-0.0741	0.0	1562.0	0.0	-0.0741	0.0
LS3	1562.0	0.0	-0.0741	0.0	1562.0	0.0	-0.0741	0.0

- Notes:**
1. TD - Top Deck
ES - Edge Stringer
CS - Center Stringer
 2. Property data are for Test Pallet SPP3-1.


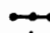


Stringer/Top Deck Contact Stiffness Properties:
ES/TD Contact Stiffness = 3172 (lb/in.)/in.
CS/TD Contact Stiffness = 9033 (lb/in.)/in.

Withdrawal/Head Embedment (W/H) Stiffness Properties:
ES W/H = 5400 (lb/in.)/nail
CS W/H = 5400 (lb/in.)/nail

Lateral Stiffness (LS) Properties:
LS in 1-Direction (LS1) = 6280 (lb/in.)/nail
LS in 3-Direction (LS3) = 6280 (lb/in.)/nail
 3. A summary of model sensitivity to stringer/bottom deck contact stiffness is presented in Table 4.8.
 4. For Test Pallet SPP3-1 property data,
Maximum Predicted Stress (S11) = +/-1562 psi
Maximum Predicted Deflection (D2) = -0.0741 in.
 5. Absolute maximum stress magnitudes are reported in table.



Where: W = Pallet Width
 W_{es} = Edge Stringer Width
 W_{cs} = Center Stringer Width
 H_s = Stringer Height

-  - CPS8 Elements
-  - Beam Elements
-  - Contact Elements and Nail Joints
-  - Lateral Elements

Note: Nodes of elements are not shown.

Figure 4.18. Pallet Section Model used to Evaluate the Effects of Lateral Stiffness in the Stack Support Condition.

Table 4.7. Summary of an Evaluation conducted to determine the Effects of Lateral Stiffness on the Behavior of Stringer Pallets in the Stack Support Condition.

Run No.	Lateral Siffness (lb/in)	*MAXIMUM S11 STRESS (psi)	PERCENT CHANGE (%)	MAXIMUM DEFLECTION (in)	PERCENT CHANGE (%)
Example 1:					
	(per nail)				
LS1-1	0.0	3340.0	0.2	-0.2247	0.9
LS1-2	4119.0	3335.0	0.1	-0.2232	0.2
LS1-3	8238.0	3333.0	0.0	-0.2227	0.0
LS1-4	16476.0	3332.0	0.0	-0.2222	-0.2
LS1-5	1.0 E+10	3330.0	-0.1	-0.2215	-0.5
Example 2:					
	(per 48 in)				
LS2-1	0.0	600.0	0.0	-0.0290	0.3
LS2-2	10500.0	600.1	0.0	-0.0289	0.0
LS2-3	21000.0	600.1	0.0	-0.0289	0.0
LS2-4	42000.0	600.2	0.0	-0.0289	0.0
LS2-5	1.0 E+10	600.4	0.0	-0.0286	-1.0
Example 3:					
	(per 48 in)				
LS3-1	0.0	1029.0	0.0	-0.0776	0.0
LS3-2	10500.0	1029.0	0.0	-0.0775	0.0
LS3-3	21000.0	1029.0	0.0	-0.0774	0.0
LS3-4	42000.0	1030.0	0.1	-0.0773	0.0
LS3-5	1.0 E+10	1031.0	0.2	-0.0767	-0.9

Notes: 1. Example #1: Yellow-Poplar Pallet Section
Concentrated Load @ Mid-span = 120 lbs
Experimental Deflection (Maximum) = 0.227 in.

Example #2: SPP3-1 Stringer Pallet
UDL = 48 lbs/in (Total Load = 1920 lbs)
Experimental Deflection (Maximum) = 0.030 in.

Example #3: S003-1 Stringer Pallet
UDL = 48 lbs/in (Total Load = 1920 lbs)
Experimental Deflection (Maximum) = 0.078 in.

2. Absolute maximum stress magnitudes are reported.

Table 4.8. Sensitivity of the Stringer Pallet Plate Model to Changes in Stringer/Bottom Deck Contact Stiffness Properties in the Stack Support Condition.

PROPERTY ALTERED	MAXIMUM S11 (psi)	CHANGE (%)	MAXIMUM D2 (in)	CHANGE (%)
Stringer/Bottom Deck Contact Properties:				
0.5 x Actual	1563.0	0.0	-0.0750	0.5
1.0 x Actual	1563.0	0.0	-0.0746	0.0
2.0 x Actual	1563.0	0.0	-0.0744	-0.3
AHS	1562.0	-0.1	-0.0741	-0.7

Notes:

1. Property data are for Test Pallet SPP3-1.

Stringer/Bottom Deck (S/BD) Contact Properties:

Edge S/BD Contact Stiffness = 61200 (lb/in.)/in.

Center S/BD Contact Stiffness = 61200 (lb/in.)/in.

2. For Test Pallet SPP3-1 property data,
Maximum Predicted Stress (S11) = +/-1562 psi
Maximum Predicted Deflection (D2) = -0.0741 in.
3. Absolute maximum stress magnitudes are reported in Table.
4. AHS - Arbitrarily high stiffness values used for all S/BD contact elements.

bottom deck and stringer response into contact springs, top deck behavior could be adequately modeled with the bottom deck and stringer assemblages removed. This also applied when modeling the bottom deck in the stack support condition, which was modeled with the top deck and stringer assemblages removed.

4.3.2 RAD Support Condition

As for pallets supported in the stack support condition, sensitivity studies were conducted for the RAD support condition using the stringer pallet plate model to determine which geometric and material properties significantly affected behavior. Test Case SPP3-1 data were used to evaluate the panel deck behavior of stringer pallets. A summary of results for the geometric and material properties evaluated are presented in Table 4.9.

Panel thickness and modulus of elasticity of the panel axis oriented in the 1-direction (bridging across the stringers) were important. The modulus of elasticity for the panel axis oriented in the 3-direction (along the length of the stringer) and Poisson's ratio (ν_{12}) were not as significant because of the stiffening effect of the center stringer on the system. Stringer are relatively stiff, preventing the panel(s) from bending along the length of the stringer (3-direction) effectively retarding the formation

**Table 4.9. Sensitivity of the Stringer Pallet
Plate Model to Changes in Geometric and Material
Properties in the RAD Support Condition.**

PROPERTY ALTERED	0.5 X ACTUAL PROPERTY VALUE				2.0 X ACTUAL PROPERTY VALUE			
	MAXIMUM NS (psi)	CHANGE (%)	MAXIMUM D2 (in)	CHANGE (%)	MAXIMUM NS (psi)	CHANGE (%)	MAXIMUM D2 (in)	CHANGE (%)
Top Deck Properties (loaded surface):								
T	*2507.0	141.8	-0.5411	63.4	595.0	-54.8	-0.0965	-70.9
E1	1599.0	21.4	-0.4169	25.9	*1376.0	32.7	-0.2379	-28.2
E3	1320.0	0.2	-0.3320	0.2	1315.0	-0.2	-0.3301	-0.3
V12	1321.0	0.3	-0.3321	0.3	1307.0	-0.8	-0.3276	-1.1
G	1320.0	0.2	-0.3316	0.1	1317.0	0.0	-0.3306	-0.2
Bottom Deck Properties (no load applied directly to surface):								
T	2024.0	53.7	-0.6057	82.9	662.0	-49.7	-0.1023	-69.1
E1	*1244.0	20.0	-0.4178	26.1	1765.0	34.0	-0.2461	-25.7
E3	1309.0	-0.6	-0.3318	0.2	1332.0	1.1	-0.3302	-0.3
V12	1306.0	-0.8	-0.3320	0.2	1353.0	2.7	-0.3279	-1.0
G	1326.0	0.7	-0.3313	0.0	1311.0	-0.5	-0.3309	-0.1
Stringer Properties:								
ES	1330.0	1.0	-0.3333	0.6	1307.0	-0.8	-0.3308	-0.1
CS	1305.0	-0.9	-0.3329	0.5	1319.0	0.2	-0.3311	0.0
Deck Spacing:								
DS	1411.0	7.1	-0.3668	10.7	1279.0	-2.9	-0.3199	-3.4

Notes: 1. Property data are for Test Pallet SPP3-1.

See Table 4.5 for actual property values assigned to members.

2. Maximum Predicted Normal Stress (NS):

NS (Bottom Deck) = +1317. psi

NS (Top Deck) = -1037. psi

Maximum Predicted Deflection (D2) = -0.3312 in.

3. Absolute maximum stress magnitudes are reported in table.

4. "*" - indicates maximum stress (S11) occurred in top deck instead of bottom deck.

of plate (membrane) action in the panel. Although the stringers act as spacers and stiffen the system, models in the RAD support condition were not sensitive to stringer stiffness (modulus of elasticity) along the length. G_{12} , G_{13} , and G_{23} were also not significant.

An evaluation was performed to determine the effect of changing the spacing between decks on stress and deflection predictions. The results of this evaluation are also presented in Table 4.9. Dramatic changes in the spacing between the decks did significantly affect model behavior. Therefore, it is important that the deck spacing used in the simplified RAD models be reasonably accurate.

Results for model sensitivity to changing joint and contact properties are presented in Table 4.10. Both withdrawal/head embedment and lateral stiffness across the stringers are significant in the plate model. However, the model was not particularly sensitive to lateral stiffness along the stringers and contact stiffness. Therefore, the contact elements can be assigned arbitrary stiffnesses based on tributary area without significantly affecting stress and deflection predictions.

4.3.3 RAS Support Condition

Sensitivity studies conducted for the RAS support condition were similar to RAD evaluations. Test Case SPP3-1

**Table 4.10. Sensitivity of the Stringer Pallet Plate
Model to Changes in Stringer/Deck Contact and Nail
Joint Properties in the RAD Support Condition.**

PROPERTY ALTERED	0.5 X ACTUAL PROPERTY VALUE				2.0 X ACTUAL PROPERTY VALUE			
	MAXIMUM NS (psi)	CHANGE (%)	MAXIMUM D2 (in)	CHANGE (%)	MAXIMUM NS (psi)	CHANGE (%)	MAXIMUM D2 (in)	CHANGE (%)
Stringer/Deck Contact Stiffness Properties:								
ES	1324.0	0.5	-0.3335	0.7	1314.0	-0.2	-0.3299	-0.4
CS	1316.0	-0.1	-0.3311	0.0	1318.0	0.1	-0.3312	0.0
Withdrawal/Head Embedment Siffness Properties:								
ES	1392.0	5.7	-0.3663	10.6	1231.0	-6.5	-0.2947	-11.0
CS	1317.0	0.0	-0.3312	0.0	1317.0	0.0	-0.3312	0.0
Lateral Stiffness Properties:								
LS1-ES	1342.0	1.9	-0.3435	3.7	1304.0	-1.0	-0.3244	-2.1
LS1-CS	1317.0	0.0	-0.3312	0.0	1317.0	0.0	-0.3312	0.0
LS3	1317.0	0.0	-0.3312	0.0	1317.0	0.0	-0.3312	0.0

Note:

1. Property data are for Test Pallet SPP3-1.

See Table 4.6 for actual withdrawal/head embedment and lateral stiffness properties.

Stringer/Top (TD) and Bottom Deck (BD) Contact Stiffness Properties:

Edge Stringer (ES)/BD Contact Stiffness = 174500. (lb/in.)/in.

Edge Stringer (ES)/TD Contact Stiffness = 61200. (lb/in.)/in.

Center Stringer (CS)/BD Contact Stiffness = 61200. (lb/in.)/in.

Center Stringer (CS)/TD Contact Stiffness = 112600. (lb/in.)/in.

2. Maximum Predicted Normal Stress (NS):

NS (Bottom Deck) = +1317. psi

NS (Top Deck) = -1037. psi

Maximum Predicted Deflection (D2) = -0.3312 in.

3. Absolute maximum stress magnitudes are reported in table.

data were again used in the evaluation. Results for geometric and material properties evaluated are presented in Table 4.11. Modulus of elasticity for stringers along their length significantly impacted model predictions. Panel thickness and modulus of elasticity for the panel axis oriented in the 3-direction (along the length of the stringers) were also important. Modulus of elasticity for the panel axis oriented in the 1-direction (bridging across the stringers) and Poisson's ratio (ν_{12}) were not as significant. G_{12} , G_{13} , and G_{23} were again not important.

Results of an evaluation performed to determine the effect of changing the spacing between decks on model predictions are also presented in Table 4.11. Even slight changes in the spacing between the decks significantly affected model results. In the RAS support condition, composite action between stringers and decks is significant, with stringers functioning as supports in addition to acting as deck spacers; therefore, accurately simulating deck spacing is crucial.

Results for model sensitivity to changing joint properties are presented in Table 4.12. Both withdrawal/head embedment and lateral stiffness were significant, influencing the distribution of load to the stringers. The model was also sensitive to lateral stiffness along the stringers. However, the model was not

**Table 4.11. Sensitivity of the Stringer Pallet
Plate Model to Changes in Geometric and Material
Properties in the RAS Support Condition.**

PROPERTY ALTERED	0.5 X ACTUAL PROPERTY VALUE				2.0 X ACTUAL PROPERTY VALUE			
	MAXIMUM NS (psi)	CHANGE (%)	D2 (in)	CHANGE (%)	MAXIMUM NS (psi)	CHANGE (%)	D2 (in)	CHANGE (%)
Top Deck Properties (loaded surface):								
T	1200.0	1.8	-0.0756	1.7	923.0	-21.7	-0.0585	-21.3
E1	1177.0	-0.2	-0.0743	0.0	1156.0	-2.0	-0.0733	-1.3
E3	1198.0	1.6	-0.0755	1.6	1159.0	-1.7	-0.0730	-1.7
V12	1180.0	0.1	-0.0744	0.1	1173.0	-0.5	-0.0740	-0.4
G	1195.0	1.4	-0.0755	1.6	1150.0	-2.5	-0.0725	-2.4
Bottom Deck Properties (no load applied directly to surface):								
T	1252.0	6.2	-0.0788	6.1	943.0	-20.0	-0.0597	-19.7
E1	1188.0	0.8	-0.0750	0.9	1160.0	-1.6	-0.0733	-1.3
E3	1199.0	1.7	-0.0755	1.6	1160.0	-1.6	-0.0731	-1.6
V12	1179.0	0.0	-0.0744	0.1	1174.0	-0.4	-0.0741	-0.3
G	1193.0	1.2	-0.0753	1.3	1153.0	-2.2	-0.0728	-2.0
Stringer Properties:								
ES	1502.0	27.4	-0.1305	75.6	1040.0	-11.8	-0.0659	-11.3
CS	*992.0	17.3	-0.1873	152.1	*822.0	-2.8	-0.0290	-61.0
Deck Spacing:								
DS	1386.0	17.6	-0.0896	20.6	*791.0	-5.9	-0.0453	-39.0

Notes: 1. Property data are for Test Pallet SPP3-1.

See Table 4.5 for actual property values assigned to members.

2. Maximum Predicted Normal Stress (NS):

NS (Center Stringer) = +1179. psi

NS (Top Deck) = -846. psi

Maximum Predicted Deflection (D2) = -0.0743 in.

3. Absolute maximum stress magnitudes are reported in table.

4. "*" - indicates maximum stress (S11) occurred in top deck instead of center stringer.

5. Deformation (D2) values reported are for the bottom deck at the pallet center.

Table 4.12. Sensitivity of the Stringer Pallet Plate Model to Changes in Stringer/Deck Contact and Nail Joint Properties in the RAS Support Condition.

PROPERTY ALTERED	0.5 X ACTUAL PROPERTY VALUE				2.0 X ACTUAL PROPERTY VALUE			
	MAXIMUM S11 (psi)	CHANGE (%)	MAXIMUM D2 (in)	CHANGE (%)	MAXIMUM S11 (psi)	CHANGE (%)	MAXIMUM D2 (in)	CHANGE (%)
Stringer/Deck Contact Stiffness Properties:								
ES	1180.0	0.1	-0.0744	0.1	1178.0	-0.1	-0.0743	0.0
CS	1179.0	0.0	-0.0743	0.0	1178.0	-0.1	-0.0743	0.0
Withdrawal/Head Embedment Stiffness Properties:								
ES	1191.0	1.0	-0.0751	1.1	1181.0	0.2	-0.0732	-1.5
CS	1178.0	-0.1	-0.0743	0.0	1179.0	0.0	-0.0743	0.0
Lateral Stiffness Properties:								
LS1-ES	1179.0	0.0	-0.0744	0.1	1178.0	-0.1	-0.0743	0.0
LS1-CS	1179.0	0.0	-0.0743	0.0	1179.0	0.0	-0.0743	0.0
LS3	1297.0	10.0	-0.0831	11.8	1028.0	-12.8	-0.0632	-14.9

Note:

- Property data are for Test Pallet SPP3-1.

See Table 4.6 for actual withdrawal/head embedment and lateral stiffness properties.

Stringer/Top (TD) and Bottom Deck (BD) Contact Stiffness Properties:

Edge Stringer (ES)/BD Contact Stiffness = 174500. (lb/in.)/in.
 Edge Stringer (ES)/TD Contact Stiffness = 61200. (lb/in.)/in.
 Center Stringer (CS)/BD Contact Stiffness = 61200. (lb/in.)/in.
 Center Stringer (CS)/TD Contact Stiffness = 112600. (lb/in.)/in.

- Maximum Predicted Normal Stress (NS):

NS (Center Stringer) = +1179. psi
 NS (Top Deck) = -846. psi
 Maximum Predicted Deflection (D2) = -0.0743 in.

- Absolute maximum stress magnitudes are reported in table.

sensitive to contact stiffness. Therefore, as for the RAD support condition, contact elements could be assigned arbitrary stiffnesses based on tributary area without significantly affecting results.

4.4 Development of PC Compatible Stringer Pallet Models

PC compatible stringer models were developed for use on a 286 or more powerful PC capable of running the current versions of PDS. These programs were required to provide solutions in less than 2 minutes, without the use of extended memory. Developing PC models which were compatible with the current versions of PDS was also a consideration. PC models, with reduced degrees of freedom (DOF), were simplified from plate models. Maximum DOF reduction was achieved by developing separate models for each principle support condition, stack, RAD, and RAS. For the stack and RAS conditions, additional efficiency was gained by using separate models for various load conditions.

4.4.1 Stack Support Condition

Separate models were used to predict stringer pallet behavior in the stack support condition based on the load condition. The PC model for full uniformly and line loaded pallets could be reduced to a two-dimensional model, while partial uniformly loaded pallets were simulated using a three-dimensional grid model. Although the grid model could

be used to model full uniformly loaded and line loaded stringer pallets in the stack support condition, this model was considerably larger with added DOF's, requiring additional solution time. Because the full uniformly loaded condition is the most common, evaluating this load condition with a more reduced model is considerably more efficient. Stack models are discussed further in subsequent sections.

4.4.1.1 Full Uniform and Line Load Model

The PC model developed to predict behavior for full uniformly and line loaded pallets was two-dimensional. Reducing the model to two-dimensions was based on the assumption that the stresses for the panel axis oriented in the 3-direction (along the length of stringers) did not govern. Sensitivity studies indicate that stresses oriented in this direction are small compared to those oriented perpendicular to the stringers (1-direction). Therefore, this assumption appears valid.

Figure 4.19 shows a two-dimensional cross-section of a stringer pallet section. The effect of rigid body stringer rotation in the stack support condition was minimal for the test cases evaluated. If it is assumed that no rigid body rotation of the stringers occurs, all connections between the stringer and lower deck could be assigned arbitrarily high stiffness. Then by incorporating the stringer and

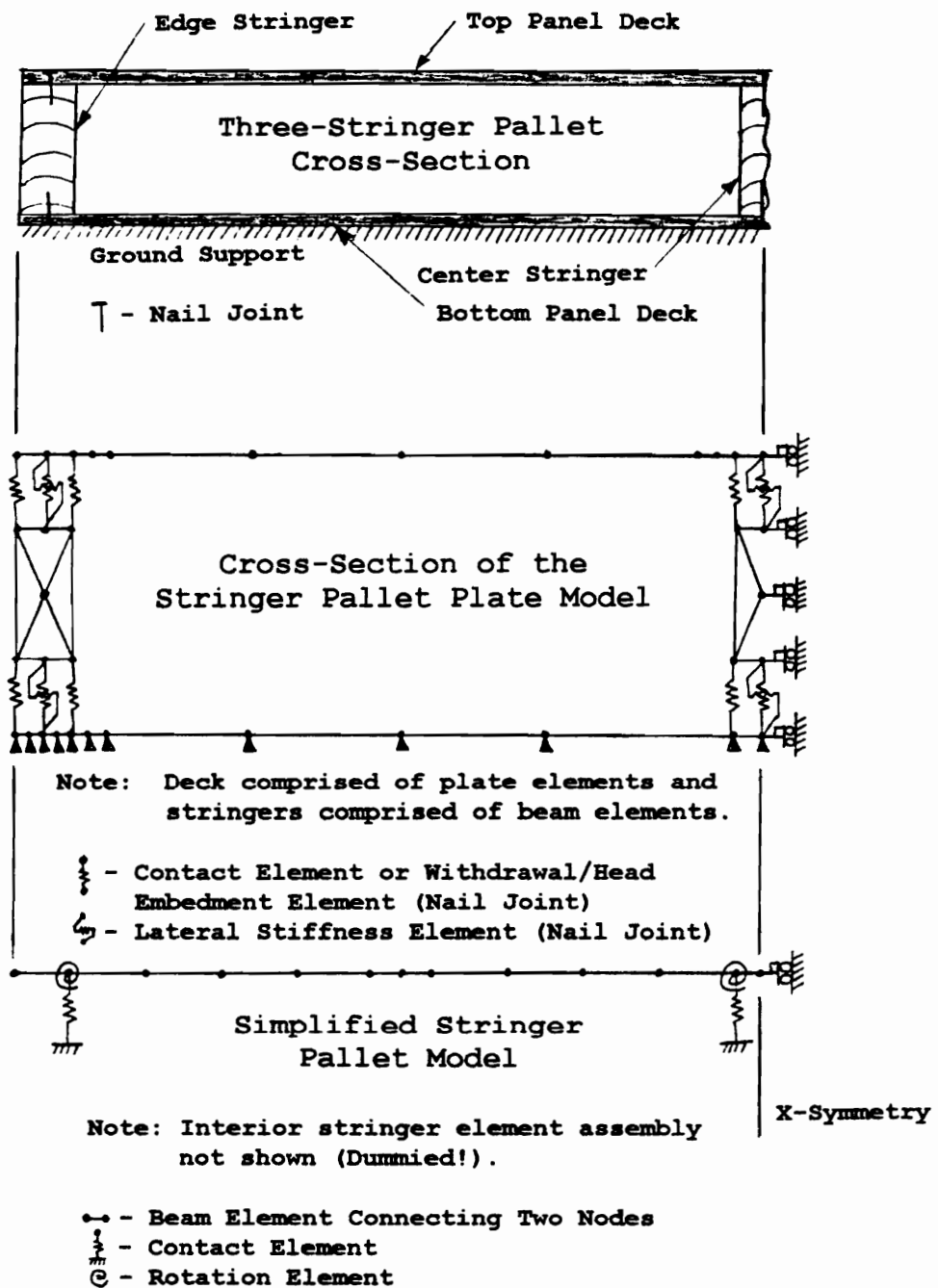


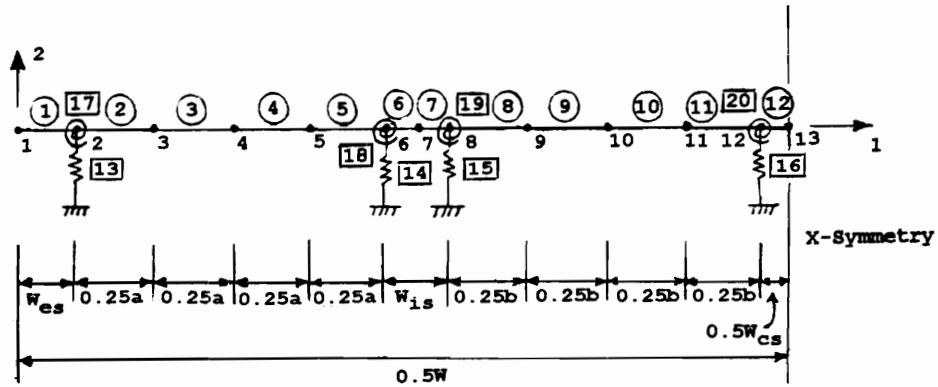
Figure 4.19. Two-Dimensional Cross-Section of a Three-Stringer Pallet, Cross-Section of the Stringer Pallet Plate Model, and the corresponding Simplified Model.

lower deck response into the edge effect factor, these members could be dropped from the model as shown in Figure 4.19. Therefore, only the deck being evaluated, the top deck in Figure 4.19, was used to model behavior in the stack support condition.

Reducing the model as such has one unintended consequence. Because lateral displacements due to flexure were ignored in theory, this effectively eliminated lateral stability (stiffness) imposed by nail joints from the model. Fortunately, sensitivity studies presented in Section 4.3.1 indicate that this factor is not significant in the stack support condition. Therefore, lateral spring elements were removed from the simplified stack models.

The final version of the simplified stack model is shown in Figure 4.20. In addition to modeling full uniformly and line loaded pallets, this model can also be used to model lumber bottom decks and lead edge boards. The top deck of the pallet was modeled using beam elements and the joint and contact zones were modeled using spring elements. Node locations were as indicated in Figure 4.20. X-symmetry was used in the model.

Geometric inputs to the model included deck thickness and width. For panel decks, average panel thickness was used and the primary material property required was the appropriate modulus of elasticity (E) for the panel



Where: W = Pallet Width
 W_{es} = Edge Stringer Width
 W_{is} = Interior Stringer Width
 W_{cs} = Center Stringer Width
 a = Distance from Inside Edge of Edge Stringer to Outside Edge of Interior Stringer
 b = Distance from Inside Edge of Interior Stringer to Edge of Center Stringer

—•— •— - Beam Element Connecting Two Nodes
 —•— - Contact Element (Spring)
 —•— - Rotation Element (Spring)

Figure 4.20. Simplified Model Simulating the Behavior of Full Uniformly or Line Loaded Stringer Pallets in the Stack Support Condition.

orientation being modeled which will normally (but not necessarily) be the strong panel axis. Lumber bottom decks were modeled by summing the width of the deckboards. Average deckboard thickness and modulus of elasticity along the length (which is normally the longitudinal direction) were used as inputs to the model.

The withdrawal/head embedment stiffness of the nail joint was considered in this model using rotational springs. Rotation moduli assigned to these springs were determined using the methodology outlined in Section 3.5.1.3. Spring constants were assigned to contact elements using the equations given in Section 3.5.3.1.2. For three-stringer pallets, the rotational and contact springs for the second (interior) stringer were assigned near zero stiffness (i. e., dummied). Center stringer elements were dummied for four-stringer pallets. All stringer elements were active when modeling five-stringer pallets. Lateral stiffness was not considered in the model. Assignment of stiffness (spring constants) to joint and contact elements is discussed thoroughly by Mackes (1998, Volume II, Section 11).

Although the model was not designed to function iteratively, it was necessary to check deflections after generating a solution to ensure that all contact elements were properly activated or dummied. Figure 4.21 illustrates

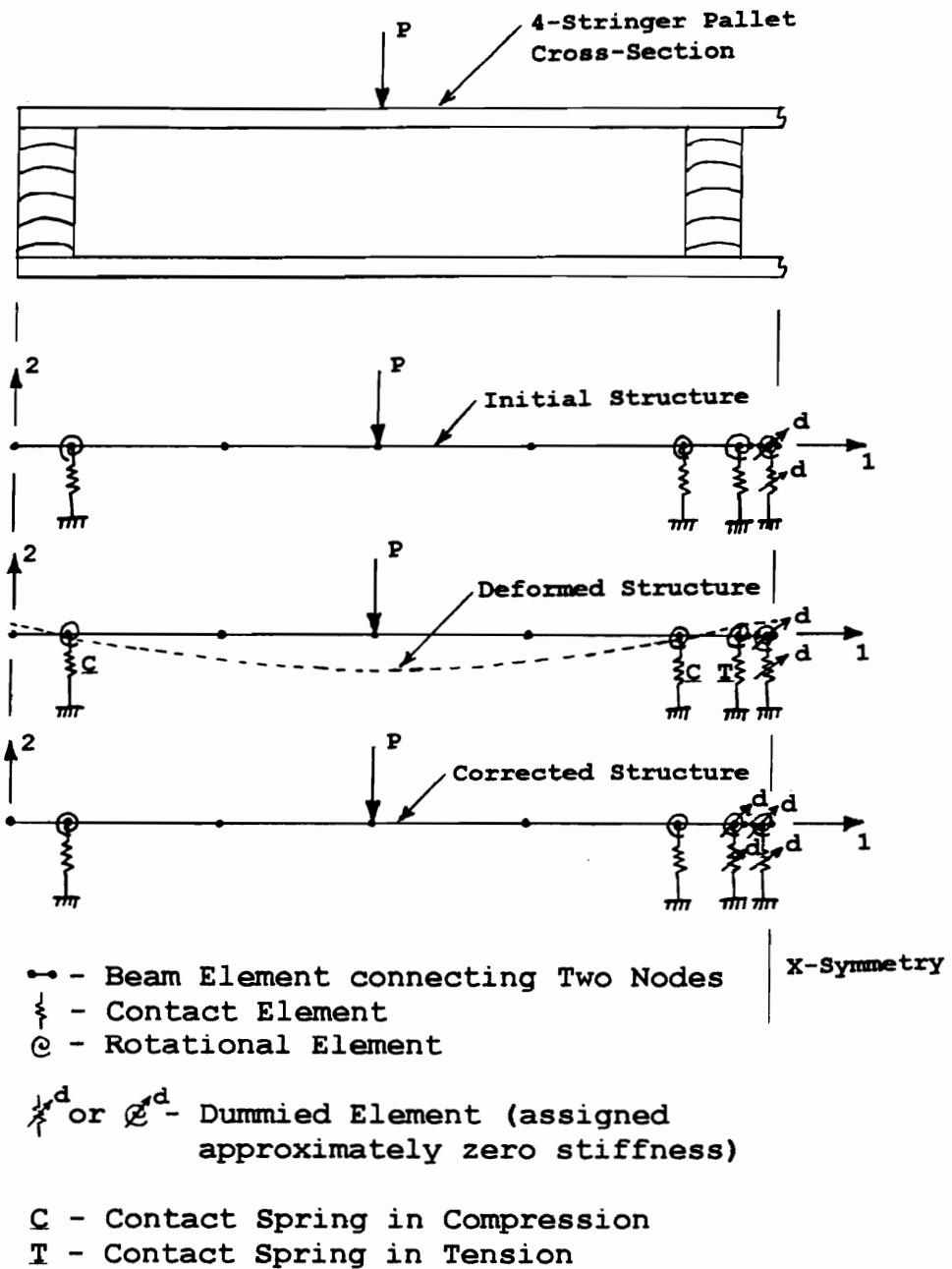
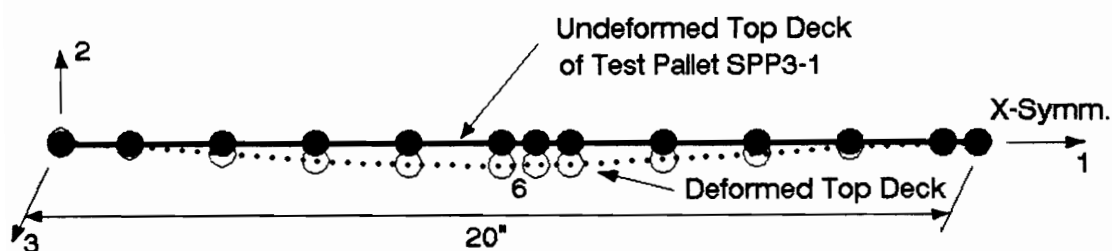


Figure 4.21. Schematic of Methodology used to ensure that Contact Elements are properly Activated or Dummied.

this condition. Initially all the contact elements for stringers being considered are assumed to be active in the model. Based on a check of the initial solution, inactive contact elements are then dummied and the model is rerun generating a new solution.

To verify that the simplified stack model yields reliable results, deflections and maximum stresses obtained using this model were compared to those generated using the corresponding plate model. An example of the ABAQUS input code, along with results for test cases evaluated, are presented in Volume II, Section 12 of Mackes (1998). The predicted deflection pattern for Test Pallet SPP3-1 is shown in Figure 4.22. The S11 stress profile predicted for this test case is shown in Figure 4.23. The predicted deflection pattern and stress profile were as expected.

Results for the simplified stack model are summarized and compared to plate model results in Table 4.13. Agreement between simplified and plate model predictions was good. Except for S400 type pallets, differences between maximum S11 stress predictions were less than 6 percent and differences in maximum deflection predictions were less than 3 percent. Differences in maximum S11 stress predictions for type S400 pallets were up to 14.4 percent. Differences were greater for this pallet type because the panel decks were oriented with the weak axis of the panels spanning the



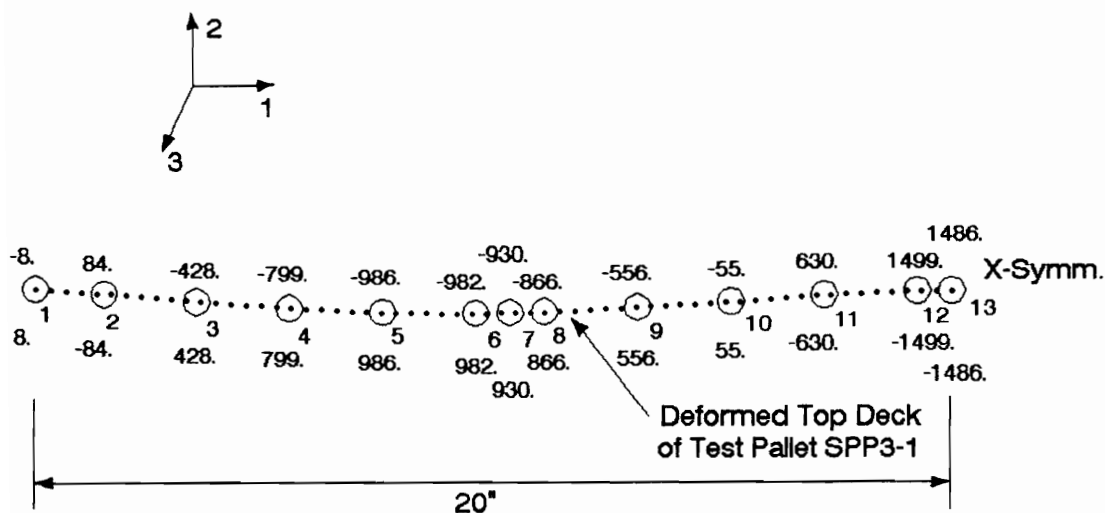
Notes: 1. Maximum Deflection @ Node 6 = -0.0735 in.

2. Deflections are magnified 6.8 times

● or ○ - Nodes

— or ---- - Beam Elements

Figure 4.22. Deflection Pattern predicted for the Top Deck of Test Pallet SPP3-1 by the Simplified Stringer Model for Full-Uniformly Loaded Pallets in the Stack Support Condition.



- Notes:
1. Stress magnitudes are maximum values averaged at each node.
 2. Units of stress magnitude are psi.
 3. Maximum Stress occurs at Node 12 and has a magnitude of +/-1499. psi.
 4. Deflections are magnified 6.8 times.

○ - Nodes
 ---- - Beam Elements

Figure 4.23. Stress (S-11) Profile predicted for the Top Deck of Test Pallet SPP3-1 by the Simplified Stringer Model for Full-Uniformly Loaded Pallets in the Stack Support Condition.

Table 4.13. Comparison of Plate (P) and Simplified (S) Model Maximum Stress (S11) and Deflection Predictions for Full Uniformly and Line Loaded Stringer Pallets in the Stack Support Condition.

PALLET ID. NUMBER	MAXIMUM S11 STRESS			MAXIMUM DEFLECTION (D)		
	S-SK S11 (psi)	P-SK S11 (psi)	PERCENT ERROR (%)	S-SK D (in.)	P-SK D (in.)	PERCENT ERROR (%)
SPP3-1	1499	1562	-4.0	-0.074	-0.074	0.0
SPP3-2	1616	1693	-4.5	-0.049	-0.049	0.0
SPP3-3	1588	1663	-4.5	-0.053	-0.054	-1.9
MEAN	1568	1639	-4.4	-0.059	-0.059	-0.6
SOO3-1	2560	2656	-3.6	-0.193	-0.194	-0.5
SOO3-2	2503	2598	-3.7	-0.192	-0.194	-1.0
S003-3	2642	2742	-3.6	-0.194	-0.196	-1.0
MEAN	2568	2665	-3.6	-0.193	-0.195	-0.9
SPL3-1	1533	1623	-5.5	-0.082	-0.084	-2.4
SPL3-2	1596	1690	-5.6	-0.077	-0.079	-2.5
SPL3-3	1582	1682	-5.9	-0.069	-0.071	-2.8
MEAN	1570	1665	-5.7	-0.076	-0.078	-2.6
S400-7	446	506	-11.9	-0.203	-0.209	-2.9
S400-8	453	529	-14.4	-0.241	-0.248	-2.8
S400-9	485	557	-12.9	-0.217	-0.223	-2.7
MEAN	461	531	-13.1	-0.220	-0.227	-2.8
P(JC)-1	3029	3096	-2.2	-0.149	-0.155	-3.9

Note: Loads were as follows (P = Total Load):

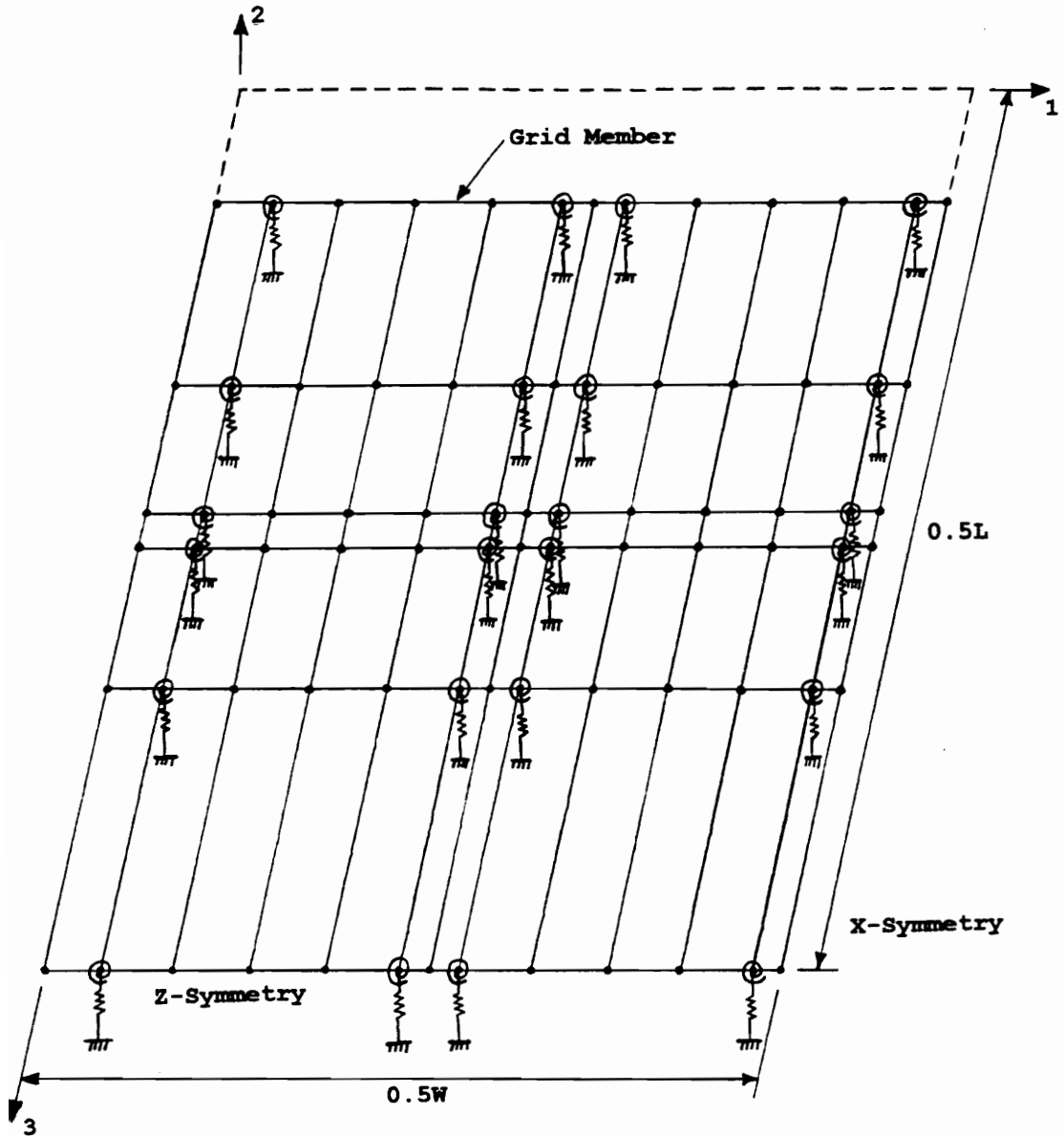
SPP3 Pallets: UDL = 2.604 psi (P = 5000 lbs)
SOO3 Pallets: UDL = 2.604 psi (P = 5000 lbs)
SPL3 Pallets: UDL = 2.604 psi (P = 5000 lbs)
S400 Pallets: UDL = 1.000 psi (P = 1920 lbs)
P(JC) Pallet: Two Line Loads - 52.083 lb/in.
each (P = 5000 lbs)

stringers. Because the panel axis spanning the stringers was relatively weak, the contribution of the strong panel axis was significant. This contribution was considered in plate model results and neglected in results generated by the simplified model.

4.4.1.2 Partial Uniform Load Model

The two-dimensional stack model for full uniform and line loaded stringer pallets is inadequate for simulating partial uniform loads in the 3-direction along the length of stringers. To resolve this inadequacy, a grid model was used. The grid model developed is shown in Figure 4.24. It had six members oriented in the 1 direction (bridging across stringers) and 11 members oriented in the 3-direction (along the length of stringers).

Grid members were comprised of beam members. Grid members oriented in the 1-direction were located and assigned a section width based on the configuration of the partial load. Procedures for locating these members are discussed by Mackes (1998, Volume II, Section 13). Grid members oriented in the 3-direction were assigned a section width based on tributary area as shown in Figure 4.25. The grid model was designed so that when the partial load approaches a full load, the solutions generated converge to



L = Pallet Length

W = Pallet Width

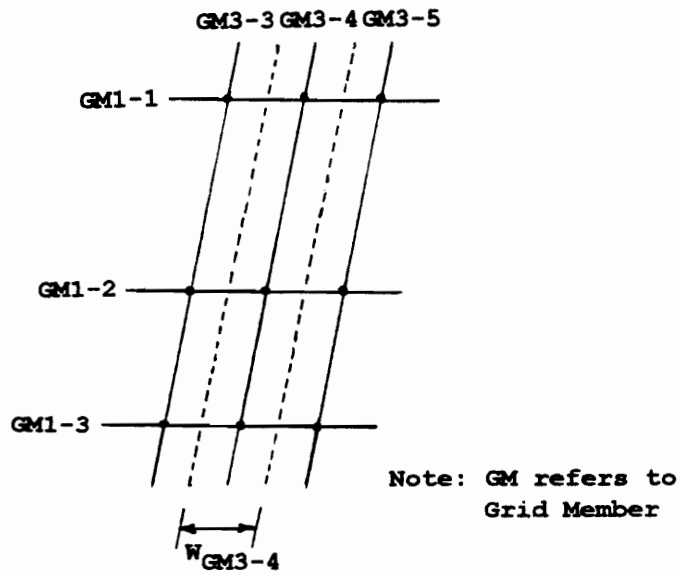
●—● - Beam Element Connecting Two Nodes

⊥ - Contact Element

⊙ - Rotational Element

Note: See Mackes (1998, Volume II, Section 13) for procedure used to locate grid members.

Figure 4.24. Grid Model Simulating the Behavior of Partial Uniformly Loaded Stringer Pallets in the Stack Support Condition.



W_{GM3-4} = Width assigned to Grid Member (GM) 3-4

$W_{GM3-4} = 0.5(\text{distance between GM3-3 and GM3-4})$
 $+ 0.5(\text{distance between GM3-4 and GM3-5})$

Figure 4.25. Tributary Area Technique used to assign Width to the Grid Members of the Partial Uniform Load Stack Model for Stringer Pallets oriented in the 3-Direction.

those of the 2-dimensional full uniform stack model. When a full uniform load was applied, they gave the same solution.

Cross-sectional members oriented in the 1-direction were similar to the 2-dimensional stack model. Lateral joint stiffness was not an important factor. Nail joint stiffness was represented using rotational springs. A rotation modulus was calculated based on the number of nails, nail stiffness, deck stiffness and contact stiffness as outlined in Section 3.5.1.3. This value was then divided by the length of deck in contact with the stringer. The result was rotational stiffness per unit length. Rotational stiffness for a grid member was obtained by multiplying this value by the section width. Contact elements were also assigned stiffness based on section width. The contact stiffness per unit width was determined using the methodology discussed in Section 3.5.3.1. As with the 2-dimensional stack model, it was necessary to check deflections after generating a solution to ensure that all the contact elements were properly activated or dummied.

Comparisons between simplified and plate model predictions are presented for selected partial uniform load test cases in Table 4.14. More complete ABAQUS results for these test cases are given in Volume II, Section 13 of Mackes (1998). Normal stresses in the 1-direction (S11) show good agreement with differences of less than 5 percent.

Table 4.14. Comparison of Finite Element Solutions
for Partial Uniformly Stringer Pallets
in the Stack Support Condition.

PARAMETER	FINITE ELEMENT SOLUTION GRID MODEL SG-STK	FINITE ELEMENT SOLUTION PLATE MODEL SP-STK	PERCENT DIFFERENCE (%)
Test Case #1:			
S11 Stress (maximum, psi)	471.9	493.8	-4.4
Deflection (maximum, in.)	-0.0206	-0.0198	4.0
Test Case #2:			
S11 Stress (maximum, psi)	492.0	487.7	0.9
Deflection (maximum, in.)	-0.0220	-0.0218	0.9

Notes: Test Case #1: 48 inch by 40 inch 3-stringer pallet
with a 22 inch by 28.875 inch partial
uniform load.

Test Case #2: 48 inch by 40 inch 3-stringer pallet
with a 44 inch by 28.875 inch partial
uniform load.

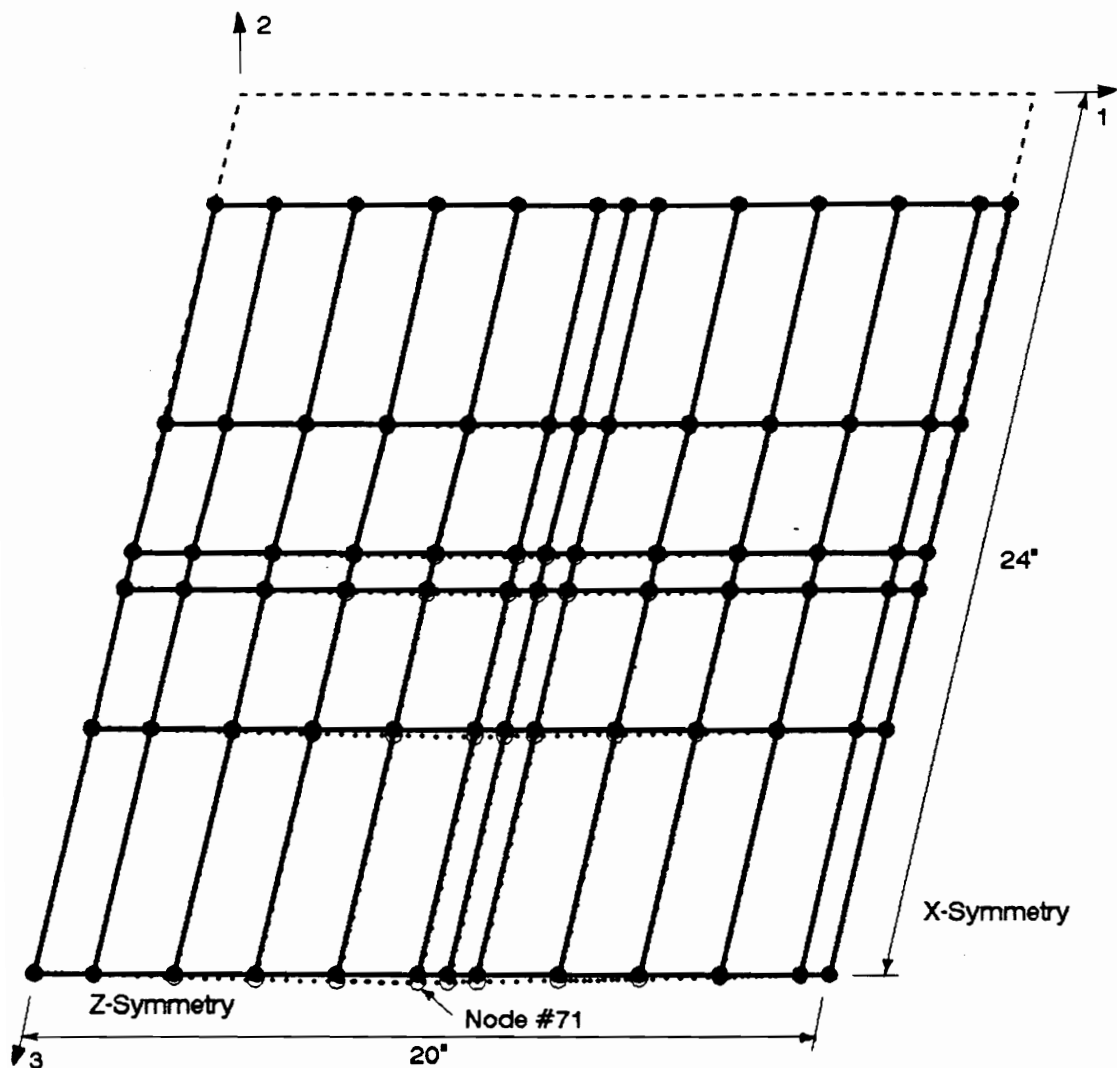
As with the full uniform and line load stack model, it was assumed that S33 stresses do not govern pallet failure. Agreement between predicted maximum deflections were also quite good with differences of less than 1 percent. The predicted deflection pattern for Test Case SPP3-1 is shown in Figure 4.26 and appears as expected. The same is true for the S11 stress profile, shown for Test Case SPP3-1 in Figure 4.27.

An analysis was performed to determine which degrees of freedom could be held fixed and effectively eliminated from the simplified grid model without affecting model performance. This analysis is presented by Mackes (1998, Volume II, Section 14), with a summary presented in Table 4.15. This analysis indicated that the grid essentially behaves as modeled by Holzer (1985).

4.4.2 RAD Support Condition

The simplified PC-based model for the RAD support condition was reduced to a two-dimensional model based on the assumption that the stringers are relatively stiff and minimize panel bending along the length of the stringer. Therefore, it was assumed that normal stresses oriented in this direction did not govern pallet failure.

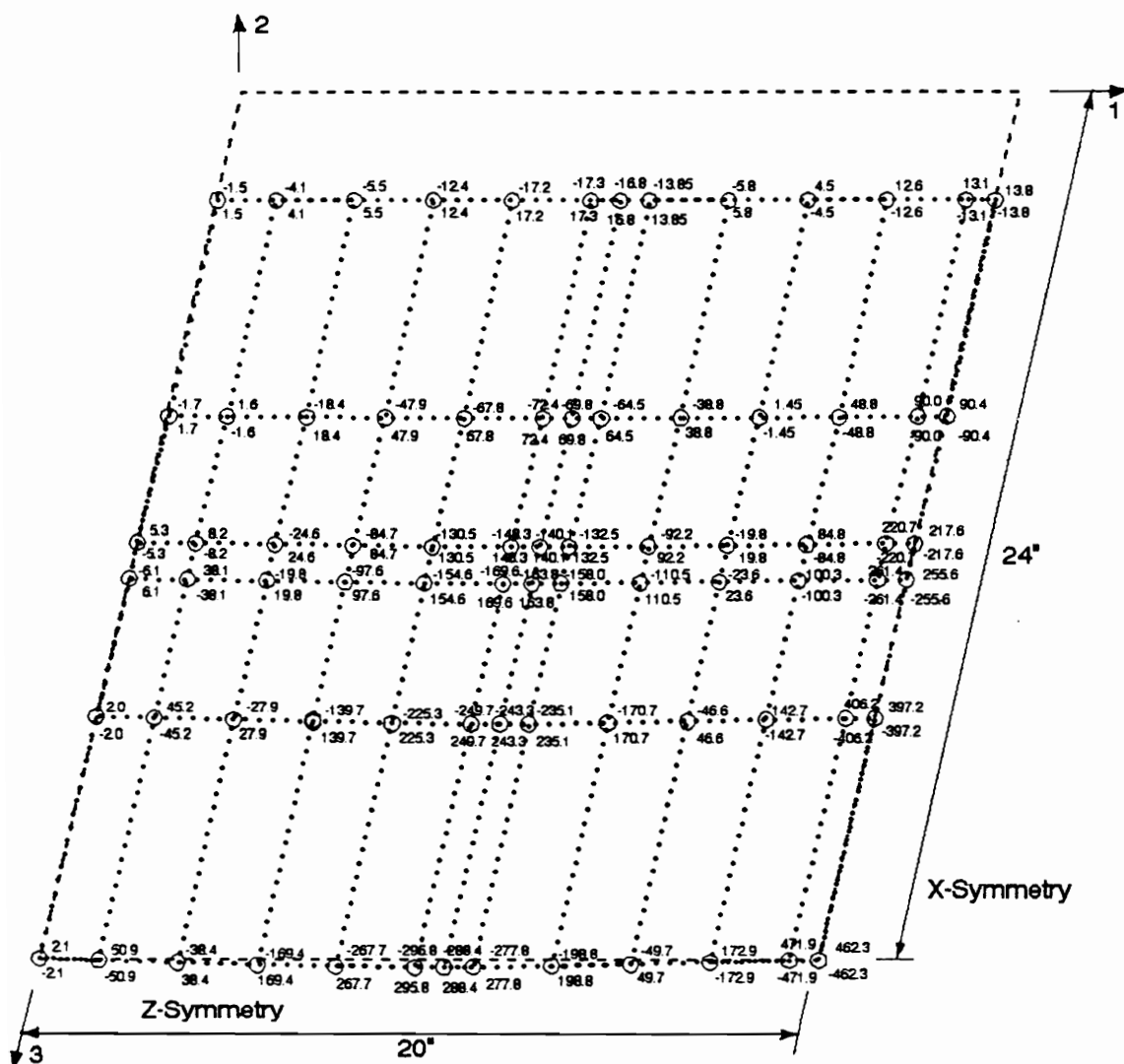
Figure 4.28 shows a cross-section of a stringer pallet. By incorporating stringer response into connections with the



- - Initial Undeformed Grid
- - Deformed Grid
- - Perimeter of Pallet Deck

Notes: 1. Maximum Deflection At Node #71 = -0.0206 inches
 2. Deflection is magified by a factor of 10.
 3. Partial Uniform Load = 1 psi (Total Load = 635.25 lbs)

Figure 4.26. Deflection Pattern predicted for the Top Deck of Test Pallet SPP3-1 by the Simplified Partial Uniform Load Model for Stringer Pallets in the Stack Support Condition.



..... - Deformed Grid

----- - Undeformed Perimeter of Pallet Deck

Notes: 1. Maximum S11 Stress At Node #77 = +/-471.9 psi

2. Partial Uniform Load = 1 psi (Total Load = 635.25 lbs)

3. Units of Stress are psi.

Figure 4.27. S11 Stress Profile predicted for the Top Deck of Test Pallet SPP3-1 by the Simplified Partial Uniform Load Model for Stringer Pallets in the Stack Support Condition.

Table 4.15. Summary of Sensitivity Study Results for the Partial Uniform Load Grid Model used to analyze Stringer Pallets in the Stack Support Condition.

RUN NUMBER	MAXIMUM S11 STRESS (psi)	PERCENT CHANGE (%)	MAXIMUM DEFLECTION (in.)	PERCENT CHANGE (%)
#1	471.9	***	-0.0206	***
#2	471.9	0.0	-0.0206	0.0
#3	471.9	0.0	-0.0206	0.0
#4	375.0	-20.5	-0.0160	-22.3
#5	471.9	0.0	-0.0206	0.0

Notes: Test Case #1: 48 inch by 40 inch 3-stringer pallet with a 22 inch by 28.875 inch partial uniform load.

Run #1: No additional restraint.

Run #2: 1st degree of freedom restrained for each node.

Run #3: 1st and 3rd degrees of freedom restrained for each node.

Run #4: 1st, 3rd, and 4th degrees of freedom restrained for each node.

Run #5: 1st, 3rd, and 5th degrees of freedom restrained for each node.

It was assumed that the 2nd and 6th degrees of freedom significantly impacted behavior.

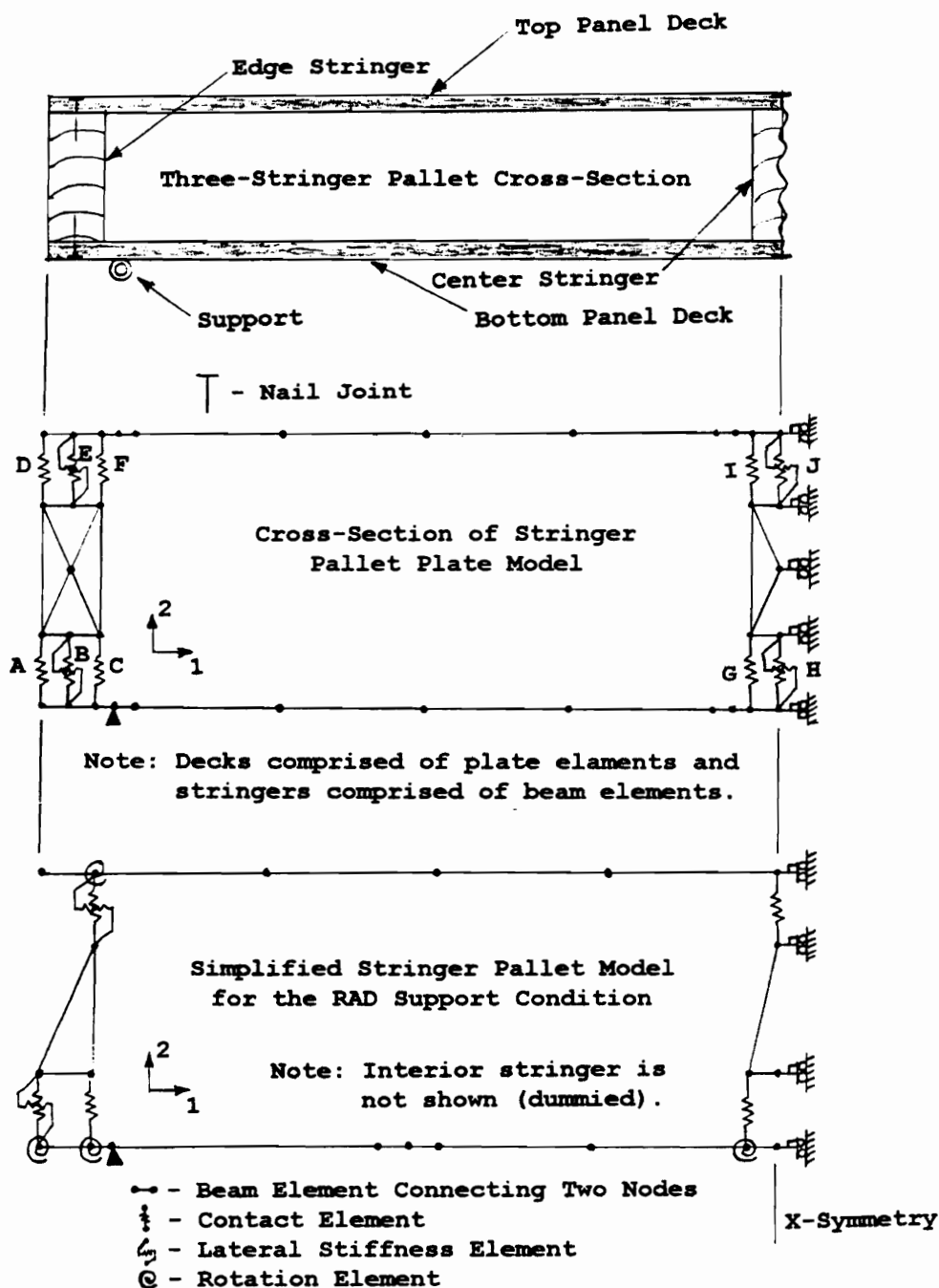
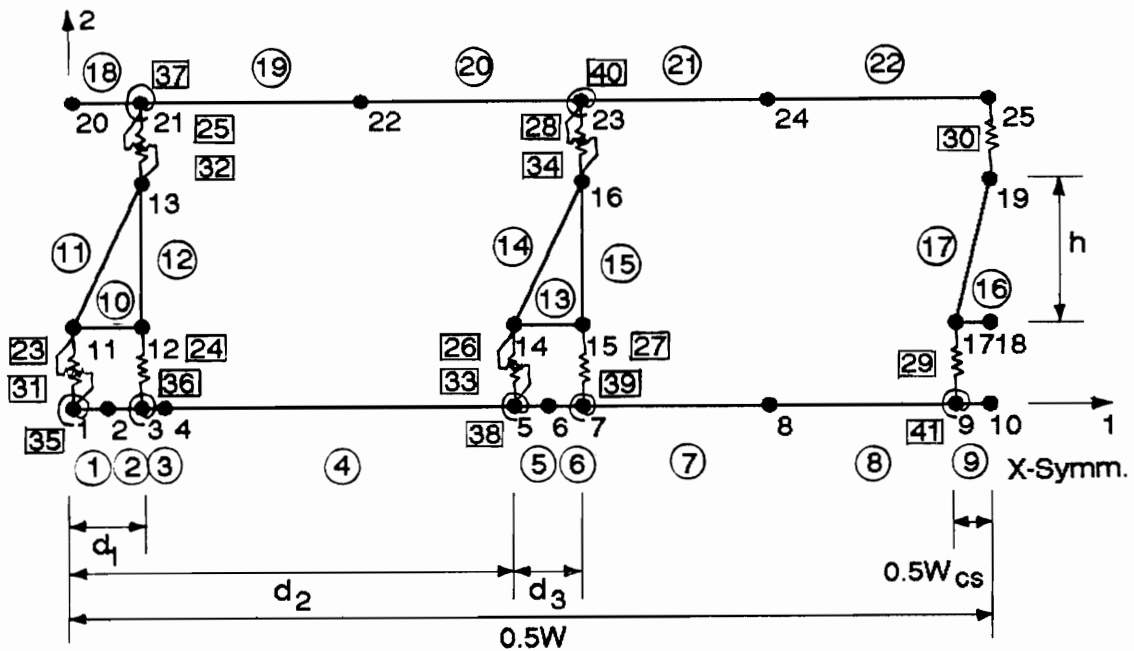


Figure 4.28. Two-Dimensional Cross-Section of a Three-Stringer Pallet, Cross-section of the Stringer Pallet Plate Model, and the Corresponding Simplified RAD Model.

decks, stringer members (elements) can be assigned an arbitrarily high stiffness. Stringers can then be represented using beam elements as shown in the cross-section of the stringer pallet plate model.

Again referring to the cross-section of the plate model, if the contact element (spring) attaching the nodes at location D was always assumed to be in tension which indicates that there was a gap forming here rather than contact, the stringer node at this position and all associated elements can be removed from the model. This assumption appears valid based on observations of gap formation which occurred as pallets were loaded. The stringer node at position G was always assumed to be in contact with the bottom deck and the stringer node at position J with the top deck. The element at position I was assumed to always be in tension based on gap formation observations; therefore, it and associated nodes and elements were removed from the model. By using a rotation modulus to simulate withdrawal/head embedment stiffness and relocating lateral stiffness elements, the elements at positions B, E, and H were removed from the model. The simplified stringer pallet model shown in Figure 4.28 resulted.

The simplified RAD model proposed for use in PDS-Panel is shown in Figure 4.29. This model was designed to



Where: W = Pallet Width
 W_{cs} = Center Stringer Width
 d_1 = Block Width in Contact with Deck (Calculated using Equations given in Section 3.5.3.1.2) or Width of Edge Stringer
 d_2 = Distance from Pallet Edge to Outer Edge of Interior Stringer
 d_3 = Block Width in Contact with Deck (Calculated using Equations given in Section 3.5.3.1.2) or Width of Interior Stringer
 h = Stringer Height

Nodes 2, 4, 6, and 8 are potential support locations.

Nodes 22 and 24 can be positioned to accommodate line loads.

— — Beam Element Attaching Two Nodes (Elements 1 through 22)
 | — Contact Element (Elements 23 through 30)
 ⚡ — Lateral Stiffness Element (Elements 31 through 34)
 © — Rotational Element (Elements 35 through 41)

Figure 4.29. Simplified RAD Model for Stringer Pallets.

accommodate both uniformly distributed loads and line loads. Partial uniform loads were directly modeled in the width direction across the stringers. However, a modified load had to be used in the direction along the length of stringers as shown in Figure 4.30. Although this approach does not accurately simulate the actual condition, the resulting inaccuracy was minimal because the stringers act to redistribute load in the actual structure, particularly to the bottom deck. Cut-outs, such as hand-holds and bottom deck wheel openings, were modeled by adjusting the panel length along the stringer proportionately to the size of the cut-out.

The lower (nodes 1 through 10) and upper decks (nodes 20 through 25) were comprised of beam elements. These elements were assigned geometric and material property values consistent with the deck being modeled. Geometric properties required included thickness and length along the stringers (3-direction). The primary material property required was modulus of elasticity in the width direction across the stringers (1-direction). For lumber decks, the width of the deckboards were summed to obtain a deck length along the stringers and an average modulus of elasticity value was used for the deckboard stiffness.

As in the stack model, stringer elements were activated or dummied appropriately to reflect the number of stringers

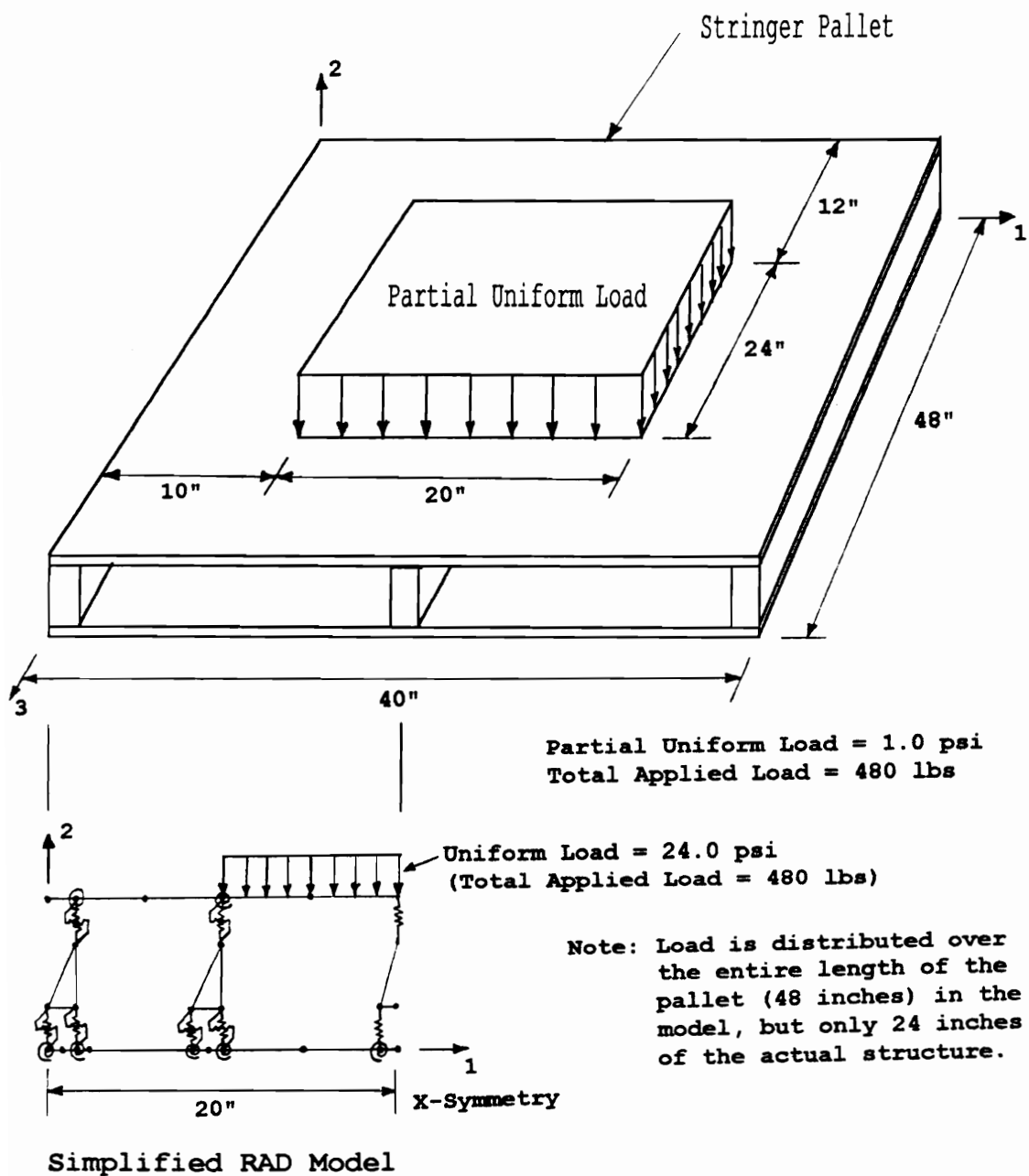


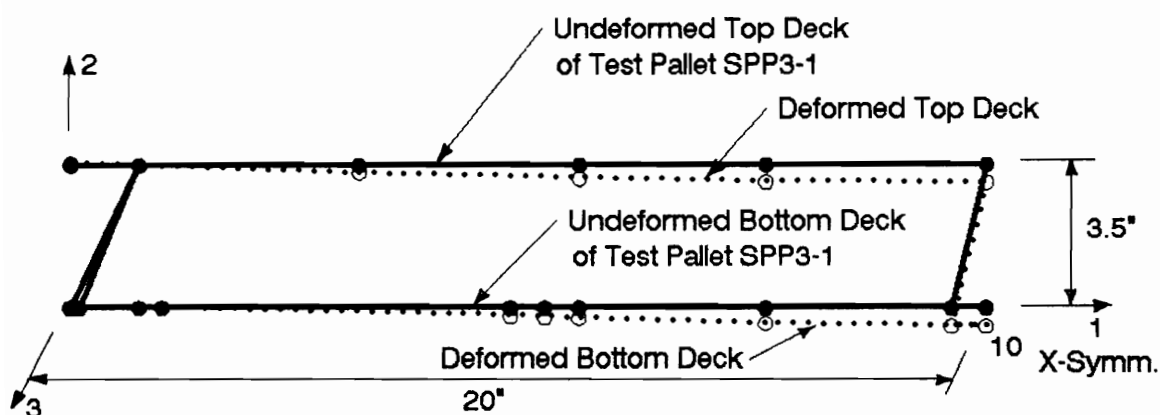
Figure 4.30. Partial Uniformly Loaded Stringer Pallet and the Simplified RAD Model Simulating its Behavior.

(2, 3, 4, or 5) in the pallet. Active stringer (beam) elements were assigned arbitrarily high stiffness.

Nail joints were represented by rotational and lateral stiffness elements. Models used to determine rotation moduli have been discussed previously in Section 3.5.1.3. Lateral stiffness values were determined using current PDS prediction techniques (NWPCA, 1988).

Based on sensitivity studies, the maximum stress predicted by the model was not especially sensitive to contact stiffness. Therefore, the contact elements were assigned conservative values which are summarized by Mackes (1998, Volume II, Section 15). The location of contact nodes between the edge stringer and lower deck were determined using the methodology discussed previously in Section 3.5.3.1.2.

An example of the ABAQUS input program for the simplified RAD model simulating stringer pallets is given in Volume II, Section 16 of Mackes (1998), along with results for numerous test cases. The deflection pattern and stress profile predicted by this model for Test Case SPP3-1 are shown in Figures 4.31 and 4.32. These results were as expected. Comparisons of simplified RAD and plate model solutions are presented in Table 4.16. Differences between predicted deflections were less than 2 percent. For SPP3 type pallets, differences in maximum predicted S11 stress



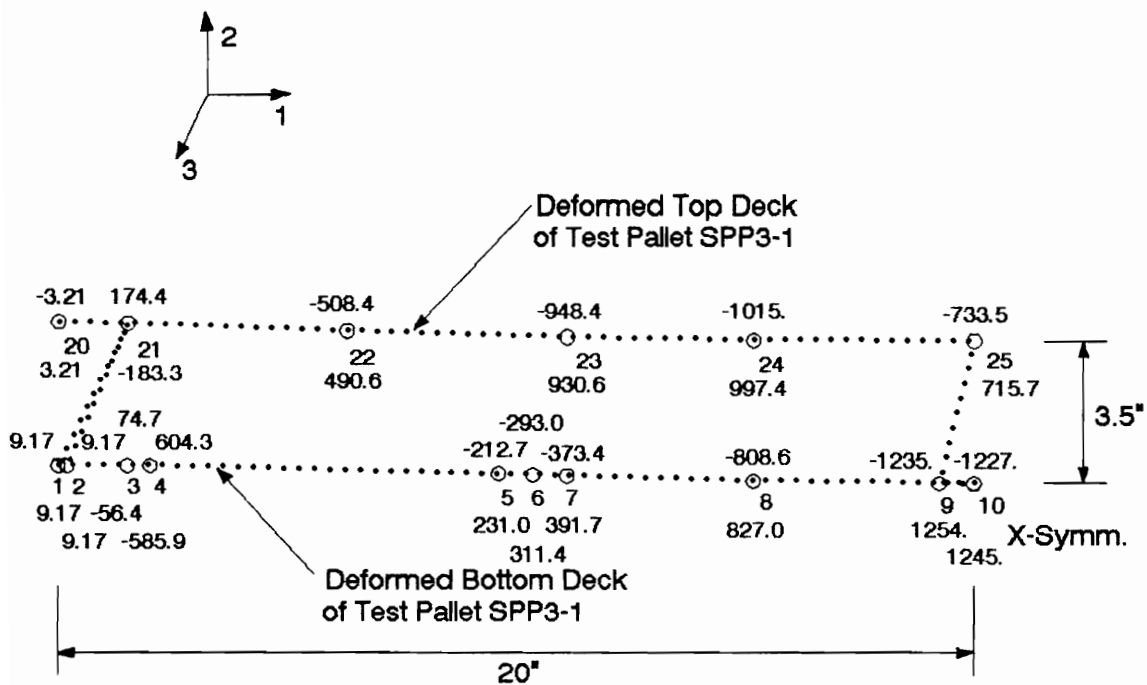
Notes: 1. Maximum Deflection occurs at Node 10
and equals -0.3396 inches.

2. Deflections are to scale.

● or ○ - Nodes

— or ---- - Beam Elements

Figure 4.31. Deflection Pattern predicted for Test Pallet SPP3-1 by the Simplified Model for Stringer Pallets loaded in the RAD Support Condition.



- Notes:
1. Stress magnitudes are maximum values averaged at each node.
 2. Units of stress magnitude are psi.
 3. Maximum Stress occurs at Node 9 and has a magnitude of +1254. psi.
 4. Deflections are to scale.

○ - Nodes
 ---- - Beam Elements

Figure 4.32. Stress (S11) Profile predicted for Test Pallet SPP3-1 by the Simplified Model for Stringer Pallets loaded in the RAD Support Condition.

Table 4.16. Comparison of Maximum Stresses (S11) and Deflections predicted using Plate Models to Values obtained using the Simplified Model for Stringer Pallets in the RAD Support Condition.

PALLET ID. NUMBER	MAXIMUM S11 STRESS			MAXIMUM DEFLECTION (D)		
	S-RD S11 (psi)	P-RD S11 (psi)	PERCENT ERROR (%)	S-RD D (in.)	P-RD D (in.)	PERCENT ERROR (%)
34 inch Test Span:						
SPL3-1	1620	1868	-13.3	-0.209	-0.205	2.0
SPL3-2	1746	1981	-11.9	-0.182	-0.181	0.6
SPL3-3	1833	1876	-2.3	-0.160	-0.157	1.9
MEAN	1733	1908	-9.2	-0.184	-0.181	1.5
36 inch Test Span:						
SPP3-1	1254	1336	-6.1	-0.340	-0.338	0.6
SPP3-2	1458	1530	-4.7	-0.209	-0.207	1.0
SPP3-3	1382	1457	-5.1	-0.235	-0.233	0.9
MEAN	1365	1441	-5.3	-0.261	-0.259	0.8
S400-4	197	268	-26.5	-0.287	-0.288	-0.3
S400-5	177	242	-26.9	-0.281	-0.283	-0.7
S400-6	183	235	-22.1	-0.274	-0.275	-0.4
MEAN	186	248	-25.2	-0.281	-0.282	-0.5
37 inch Test Span:						
SOO3-1	483	549	-12.1	-0.192	-0.191	0.5
SOO3-2	447	514	-13.1	-0.197	-0.196	0.5
SOO3-3	501	570	-12.1	-0.192	-0.191	0.5
MEAN	477	544	-12.4	-0.194	-0.193	0.5

Note: Loads were as follows (P = Total Load):

SPP3 Pallets: UDL = 2.604 psi (P = 5000 lbs)
SOO3 Pallets: UDL = 2.604 psi (P = 5000 lbs)
SPL3 Pallets: UDL = 2.604 psi (P = 5000 lbs)
S400 Pallets: UDL = 1.000 psi (P = 1920 lbs)
P(JC) Pallet: Two Line-Loads - 52.083 lb/in.
each (P = 5000 lbs)

were 6.1 percent or less and 13.1 percent or less for S003 type pallets. For SPL3 type pallets, differences ranged between 2.3 and 13.3 percent, averaging 9.2 percent. This range occurred because maximum stress occurred in the bottom lumber deck where average values for deckboard stiffness were used in the simplified model as opposed to experimentally determined stiffness values being assigned to the individual deckboards in the plate model. Differences in maximum predicted S11 stresses for S400 type pallets were considerably greater, up to 26.9 percent, averaging 25.2 percent.

In the RAD support condition, differences between simplified and plate model stress predictions were generally higher than those experienced for the stack condition. This occurred because the spans were greater in the RAD support condition, resulting in more panel action, increasing stresses at certain joints. This was particularly true for S400 type pallets where the decks were oriented with the weak panel axis spanning across the stringers. The contribution of the strong panel axis had significant influence resulting in lower maximum stresses for the simplified model where this factor was not considered.

Additional pallets were tested to further evaluate the prediction capabilities of the simplified RAD model with changing span. Two 48 inch by 40 inch pallets were

constructed, one with Plywood decks and one with OSB decks. Pallets were tested at spans of 32 and 36 inches using a uniformly distributed load of 1.0 psi for the plywood pallet and 0.25 psi for the OSB pallet. Because insufficient data was collected for input to the plate model, simplified model results are compared directly to experimental deflections in Table 4.17. Agreement between predicted and experimental deflections was good, with differences of 6.5 percent or less.

4.4.3 RAS Support Condition

Separate simplified PC-based models were developed for line loaded and uniformly loaded stringer pallets. The relatively simple line load model was two-dimensional, while the model used to predict the behavior of both full and partial uniformly loaded pallets was a considerably more complex three-dimensional grid model. Discussion of these two models in subsequent sections focuses on pallets with unnotched stringers. This is because notched stringers are modeled in PDS-PANEL using the current PDS prediction methodology based on work by Zalph (1989).

4.4.3.1 Line Load Model

The model used to predict the behavior of line loaded stringer pallets in the RAS support condition was reduced to a two-dimensional model based on assumptions that the line

Table 4.17. Summary of Results for 4-Stringer
Pallets Tested in the RAD Support Condition.

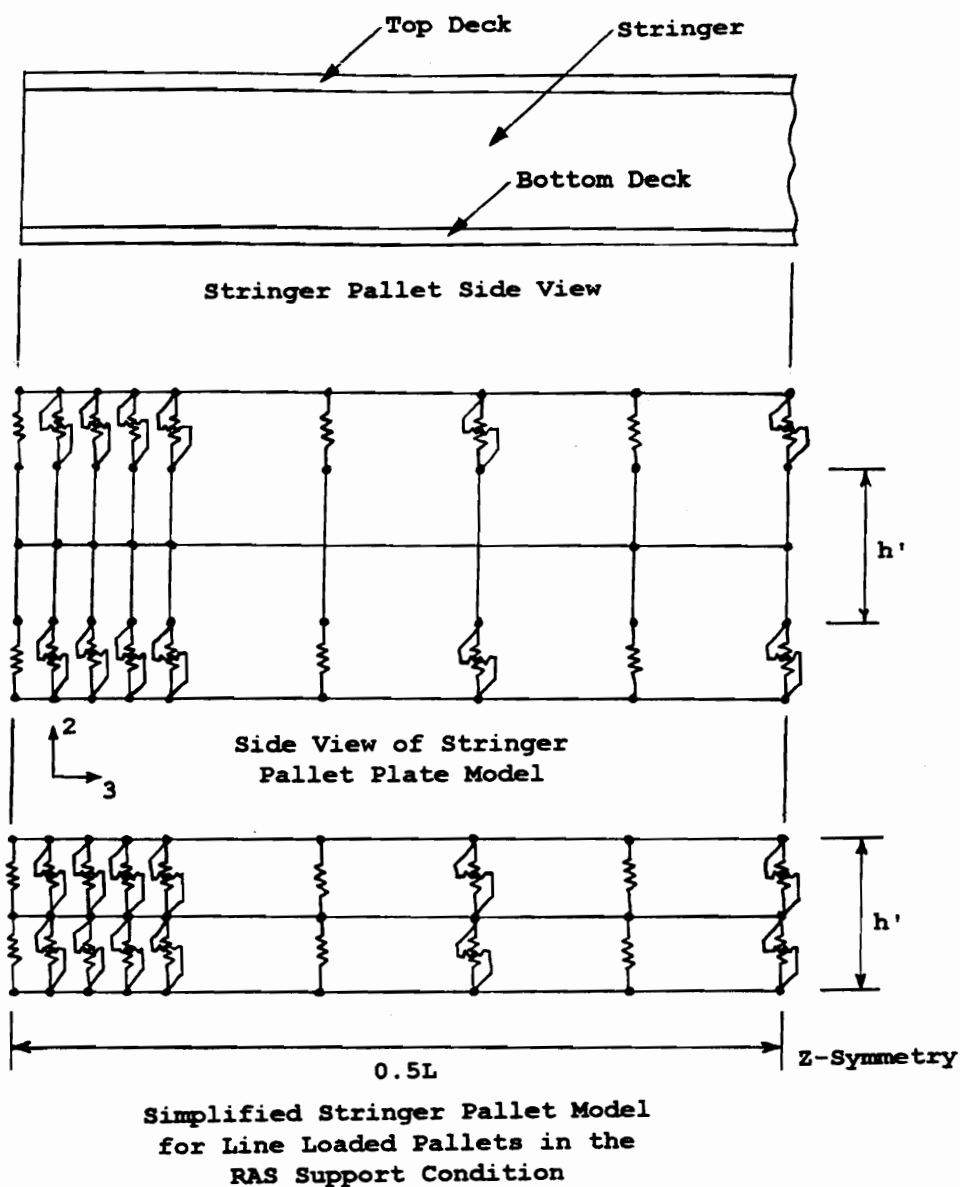
PALLET ID. NUMBER	MAXIMUM	MAXIMUM DEFLECTION (D)		
	S-RD S11 STRESS (psi)	S-RD D (in.)	ABTM D (in.)	PERCENT ERROR (%)
32 inch Test Span:				
S4PP(JC) -2	1096	-0.300	-0.306	-2.0
S400(JC) -1	435	-0.170	-0.167	1.8
36 inch Test Span:				
S4PP(JC) -2	1213	-0.203	-0.217	-6.5
S400(JC) -1	460	-0.229	-0.223	2.7

- Notes: 1. S-RD - Simplified RAD model for stringer
pallets
2. ABTM - Deflections experimentally measued
using air-bag test machine
3. Loads were as follows (P = Total Load):
S4PP Pallets: UDL = 1.000 psi (1920 lbs)
S400 Pallets: UDL = 0.250 psi (480 lbs)

load was oriented perpendicular to the stringers and was rigid. Because a rigid line load was assumed, transverse normal stresses oriented in the direction of the line load were minimal and should not govern pallet failure. Deflection variations in the transverse direction were also minimized.

Figure 4.33 shows a cross-sectional view of a stringer pallet supported in the RAS support condition, along with a cross-section of the corresponding plate model. If the width of the stringers are summed and the pallet is assumed to have a cross-section as shown, a two-dimensional model can be used to predict pallet behavior. An average modulus of elasticity value (normally longitudinal E) for the stringers is used as input to the model. Deck properties should reflect the characteristics of the panel or deckboards being modeled.

To maintain consistency between the RAS line load model and the RAS uniform load model, similar node and element configurations were used to model the spacing between the top and bottom decks. Because of computer memory limitations, primarily with the full and partial uniform load model for the RAS support condition, stringer assemblages shared nodes with the top and bottom decks in the simplified model shown in Figure 4.33. This is a fundamental difference between the plate and simplified



Where: L = Pallet Length
 h' = Stringer Height + 0.5(Top Deck Thickness)
+ 0.5(Bottom Deck Thickness)

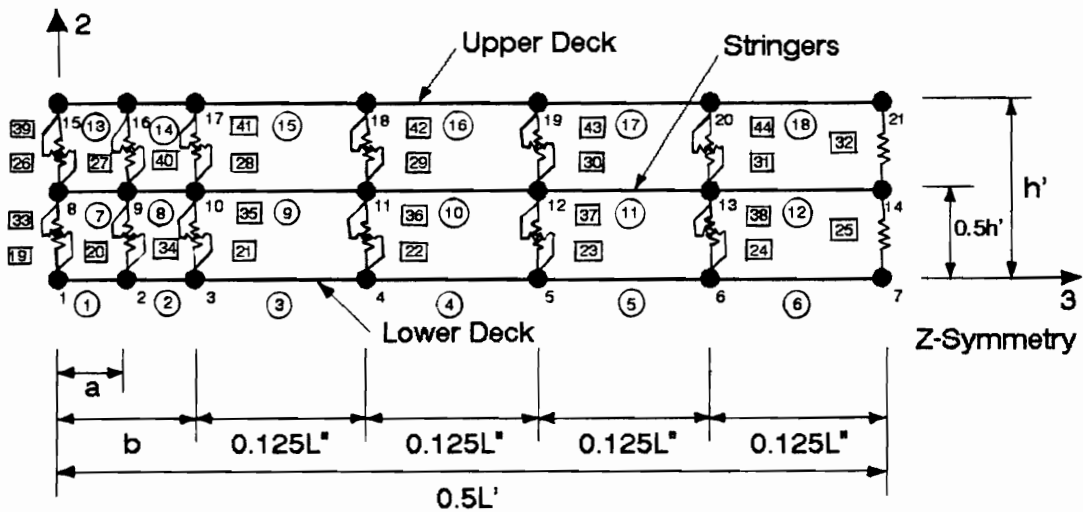
•• - Beam Element Attaching Two Nodes
- - - Contact Element
- - - Lateral Stiffness Element

Figure 4.33. Proposed Line Load Model for Predicting the Behavior of Stringer Pallets in the RAS Support Condition.

models. The effects of this simplifying assumption are discussed further in Section 4.4.3.2.

The simplified model proposed for use in PDS-PANEL is shown in Figure 4.34. Maximum normal stress (S11) and deflection predicted for a test case used to evaluate the performance of this model are presented in Table 4.18, along with comparisons to plate model predictions. Additional information regarding this test case can be found in Volume II, Section 17 of Mackes (1998). Comparisons revealed that significant differences exist between the plate and simplified model results. The simplified model prediction for maximum S11 stress was 20.2 percent greater than that of the plate model and the maximum deflection prediction was 30.7 percent greater.

Although the stress profile and deflection patterns predicted by the simplified model, shown in Figure 4.35, appeared as expected, a sensitivity study revealed that the simplified model behaves differently than the plate model. A summary of results for this study are presented in Table 4.19. These results show that the plate model predicted a significant impact on both stresses and deflections with changes in stringer stiffness, while the simplified model predicted an even greater effect on deflections, but almost no affect on stresses. The plate model was also extremely sensitive to deck spacing and lateral stiffness, while the



$h' = \text{Stringer height} + 0.5 \text{ thickness of bottom and top decks}$

Stringer Pallet without Lead Edge Boards:

- $a = 0.5b$
- $b = \text{Distance from outer pallet edge to support}$
- $L' = \text{Pallet length}$
- $L'' = \text{Length of pallet spanning support}$

Stringer Pallet with Lead Edge Boards:

- If supports are located under lead edge board,
- $b = \text{Distance from outer pallet edge to support}$
- $L' = L - 2(W_{LE} - b)$

Where: $L = \text{Pallet length}$
 $LE = \text{Width of lead edge board}$

$$L'' = L' - 2b$$

- Notes:
1. Elements 1, 2, 13, and 14 are dummied.
 2. Uniform load application:
 - a. Uniform load applied to elements 15, 16, 17, and 18.
 - b. Concentrated load applied to Node 15 based on W_{LE} .

If supports are located under bottom panel,

- $a = 0.5W_{LE}$
- $b = \text{Distance from neutral axis of lead edge board to support}$
- $L' = L - 2a$
- $L'' = L' - 2b$

- Notes:
1. Elements 1 and 13 are dummied.
 2. Uniform load application:
 - a. Uniform load applied to elements 14, 15, 16, 17, and 18.
 - b. Concentrated load applied to Node 15 based on W_{LE} .

Figure 4.34. Simplified Model for Line Loaded Pallets in the RAS Support Condition.

Table 4.18. Comparison of Simplified and Plate Model Solutions for a Line Loaded Stringer Pallet in the RAS Support Condition.

PARAMETER	FINITE ELEMENT SOLUTION SIMPLIFIED MODEL S-RS-LL	FINITE ELEMENT SOLUTION Plate Model P-RS-LL	PERCENT DIFFERENCE (%)
Test Case #1:			
S11 Stress (maximum, psi)	4674.0	3888.0	20.2
Deflection (maximum, in.)	-0.2388	-0.1827	30.7

- Notes:
1. Solutions were generated using Test Pallet SPP3-1 properties.
 2. Absolute maximum stress (S11) magnitude is reported.
 3. Line Load = 96 lbs/in. applied at mid-span (Total Load = 3840 pounds).

Table 4.19. Sensitivity of the Simplified and Plate Models to Changes in Stringer, Deck, and Nail Joint Properties for a Line Loaded Stringer Pallet in the RAS Support Condition.

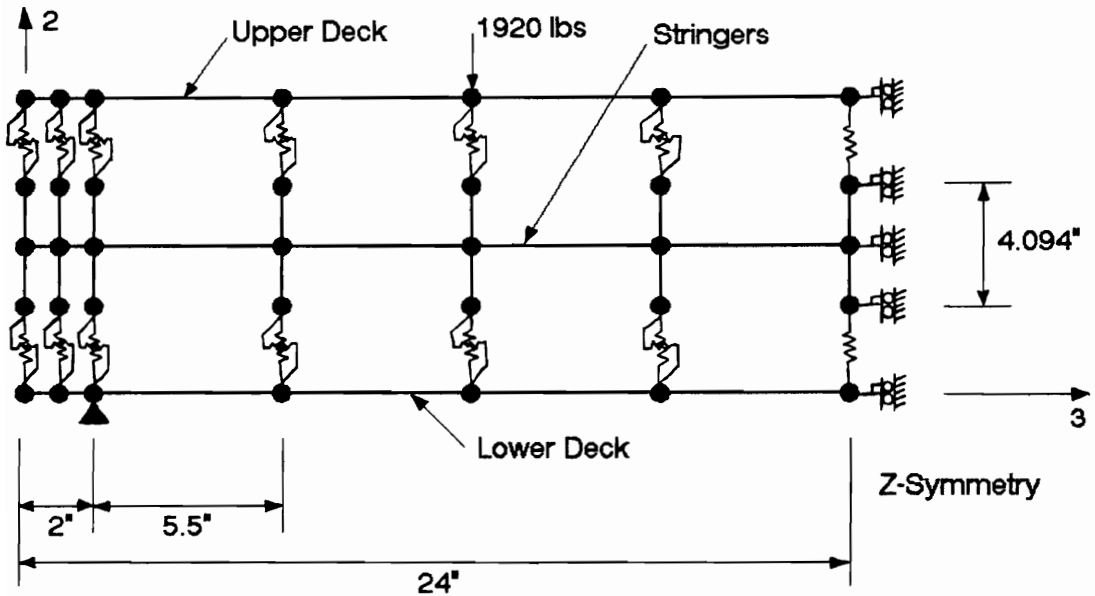
MODEL	0.5 X ACTUAL PROPERTY VALUE				2.0 X ACTUAL PROPERTY VALUE			
	MAXIMUM S11 (psi)	CHANGE (%)	MAXIMUM D2 (in)	CHANGE (%)	MAXIMUM S11 (psi)	CHANGE (%)	MAXIMUM D2 (in)	CHANGE (%)
Stringer Stiffness (E1):								
P-RS-LL	3366.0	-13.4	-0.2952	61.6	4255.0	9.4	-0.1045	-42.8
S-RS-LL	4592.0	-1.8	-0.4690	96.4	4716.0	0.9	-0.1205	-49.5
Deck Spacing (Stringer height plus one-half top and bottom deck thickness):								
P-RS-LL	4444.0	14.3	-0.2205	20.7	2838.0	-27.0	-0.1128	-38.3
S-RS-LL	4674.0	0.0	-0.2388	0.0	4674.0	0.0	-0.2388	0.0
Deck Stiffness (E for panel axis oriented in 3-Direction along stringers):								
P-RS-LL	4003.0	3.0	-0.1890	3.4	3773.0	-3.0	-0.1771	-3.1
S-RS-LL	4716.0	0.9	-0.2410	0.9	4592.0	-1.8	-0.2346	-1.8
Deck Thickness:								
P-RS-LL	4062.0	4.5	-0.1910	4.5	3402.0	-12.5	-0.1630	-10.8
S-RS-LL	4748.0	1.6	-0.2426	1.6	4154.0	-11.1	-0.2123	-11.1
Withdrawal/Head Embedment Stiffness Properties:								
P-RS-LL	3886.0	-0.1	-0.1828	0.1	3892.0	0.1	-0.1824	-0.2
S-RS-LL	4674.0	0.0	-0.2388	0.0	4674.0	0.0	-0.2388	0.0
Lateral Stiffness Properties (3-Direction along stringers):								
P-RS-LL	4203.0	8.1	-0.2035	11.4	3505.0	-9.9	-0.1579	-13.6
S-RS-LL	4674.0	0.0	-0.2388	0.0	4674.0	0.0	-0.2388	0.0

- Notes: 1. Property data is for Test Pallet SPP3-1 (See Volume II, Section 18 of Mackes (1998) for initial property values).
2. Stringer Pallet SPP3-1 evaluated by applying a line load with a magnitude of 96 lbs/inch (3840 lbs) at mid-span.
3. Maximum Predicted Normal S11 Stress:
Model P-RS-LL: S11= 3888 psi (edge stringer at mid-span)
Model S-RS-LL: S11= 4674 psi (stringer at mid-span)
- Maximum Predicted Lower Deck Deflection (D2):
Model P-RS-LL: D2 = -0.1827 inches (mid-span)
Model S-RS-LL: D2 = -0.2388 inches (mid-span)
4. Absolute maximum normal stress (S11) magnitudes are reported.

simplified model was not. Both models were somewhat sensitive to deck thickness and stiffness, although the plate model was again more sensitive. Neither model was sensitive to the withdrawal/head embedment stiffness of the nail joints.

Based on test observations and what is currently known about pallet behavior, the plate model is thought to better predict pallet behavior. Factors such as lateral stiffness of nail joints and deck spacing, which the simplified model is not sensitive to, have significant impact on pallet behavior. To incorporate these factors into the simplified model, two additional rows of nodes can be added as shown in Figure 4.36. Comparisons of results for this enhanced simplified model and the plate model, given in Table 4.20, reveal that agreement between the enhanced simplified model and plate model is quite good, with differences of less than 1 percent between maximum stress (S11) predictions and less than 5 percent for maximum deflection predictions. More importantly, sensitivity study results presented in Table 4.21 indicate that the enhanced simplified model and plate model behave similarly.

Although the enhanced model better simulates the behavior of a pallet, effectively modeling factors such as lateral stiffness and deck spacing, it requires considerably more computer memory. Therefore, even though the simplified



- ▲ - Restrained in the 2-direction only
- ⦿ - Restrained in the 3-direction and the Fourth Rotational Degree of Freedom
- - Beam Element Attaching Two Nodes
- ⋯ - Contact Element
- ⌋ - Lateral Stiffness Element

Figure 4.36. Enhanced Simplified Model for Simulating the Behavior of Line Loaded Stringer Pallet SPP3-1 in the RAS Support Condition.

Table 4.20. Comparison of Enhanced Simplified and Plate Model Solutions for a Line Loaded Stringer Pallet in the RAS Support Condition.

PARAMETER	FINITE ELEMENT SOLUTION SIMPLIFIED MODEL ES-RS-LL	FINITE ELEMENT SOLUTION Plate Model P-RS-LL	PERCENT DIFFERENCE (%)
Test Case #1:			
S11 Stress (maximum, psi)	3915.0	3888.0	0.7
Deflection (maximum, in.)	-0.1905	-0.1827	4.3

- Notes:
1. Solutions were generated using Test Pallet SPP3-1 properties.
 2. Absolute maximum stress (S11) magnitude is reported.
 3. Line Load = 96 lbs/in. applied at mid-span (Total Load = 3840 pounds).

Table 4.21. Sensitivity of the Enhanced Simplified and Plate Models to Changes in Stringer, Deck, and Nail Joint Properties for a Line Loaded Stringer Pallet in the RAS Support Condition.

MODEL	0.5 X ACTUAL PROPERTY VALUE				2.0 X ACTUAL PROPERTY VALUE			
	MAXIMUM S11 (psi)	CHANGE (%)	MAXIMUM D2 (in)	CHANGE (%)	MAXIMUM S11 (psi)	CHANGE (%)	MAXIMUM D2 (in)	CHANGE (%)
Stringer Stiffness (E1):								
P-RS-LL	3366.0	-13.4	-0.2952	61.6	4255.0	9.4	-0.1045	-42.8
ES-RS-LL	3371.0	-13.9	-0.3138	64.7	4286.0	9.5	-0.1068	-43.9
Deck Spacing (Stringer height plus one-half top and bottom deck thickness):								
P-RS-LL	4444.0	14.3	-0.2205	20.7	2838.0	-27.0	-0.1128	-38.3
ES-RS-LL	4448.0	13.6	-0.2244	17.8	2835.0	-27.6	-0.1225	-35.7
Deck Stiffness (E for panel axis oriented in 3-Direction along stringers):								
P-RS-LL	4003.0	3.0	-0.1890	3.4	3773.0	-3.0	-0.1771	-3.1
ES-RS-LL	4001.0	2.2	-0.1954	2.6	3827.0	-2.2	-0.1858	-2.5
Deck Thickness:								
P-RS-LL	4062.0	4.5	-0.1910	4.5	3402.0	-12.5	-0.1630	-10.8
ES-RS-LL	4024.0	2.8	-0.1965	3.1	3517.0	-10.2	-0.1715	-10.0
Withdrawal/Head Embedment Stiffness Properties:								
P-RS-LL	3886.0	-0.1	-0.1828	0.1	3892.0	0.1	-0.1824	-0.2
ES-RS-LL	3915.0	0.0	-0.1905	0.0	3915.0	0.0	-0.1905	0.0
Lateral Stiffness Properties (3-Direction along stringers):								
P-RS-LL	4203.0	8.1	-0.2035	11.4	3505.0	-9.9	-0.1579	-13.6
ES-RS-LL	4230.0	8.0	-0.2105	10.5	3497.0	-10.7	-0.1640	-13.9

Notes: 1. Property data is for Test Pallet SPP3-1 (See Volume II, Section 18 of Mackes (1998) for initial property values).

2. Stringer Pallet SPP3-1 evaluated by applying a line load with a magnitude of 96 lbs/inch (3840 lbs) at mid-span.

3. Maximum Predicted Normal S11 Stress:

Model P-RS-LL: S11= 3888 psi (edge stringer at mid-span)

Model ES-RS-LL: S11= 3915 psi (stringer at mid-span)

Maximum Predicted Lower Deck Deflection (D2):

Model P-RS-LL: D2 = -0.1827 inches (mid-span)

Model ES-RS-LL: D2 = -0.1905 inches (mid-span)

4. Absolute maximum normal stress (S11) magnitudes are reported.

model shown in Figure 4.34 behaves differently from the plate model, it conservatively predicts pallet behavior (both in terms of maximum stress and deflection) and because of computer memory limitations, it was utilized. However, with ever increasing PC computer memory capacity, it should become feasible in the future to incorporate the enhanced simplified model into the PDS-PANEL program.

4.4.3.2 Full and Partial Uniform Load Model

The simplified RAS model developed to predict the behavior of stringer pallets is shown in Figure 4.37. The node and element numbering scheme for this model is given in Volume II, Section 18 of Mackes (1998). This model uses quarter-symmetry. Panel decks are modeled using grids, with 7 grid members oriented in the 1-direction and 7 in the 3-direction. The first grid member oriented in the 1-direction is used to model lead edge boards. This grid member is dummied if no lead edge board is present.

Stringer pallets with lumber bottom decks are modeled by positioning grid members, normally those in the 1-direction, to correspond with the location of deckboards. Lower deck grid members which do not correspond with a deckboard are dummied. This model can be used to predict the behavior of stringer pallets with a lumber bottom deck having up to 13 deckboards, including lead edge boards.

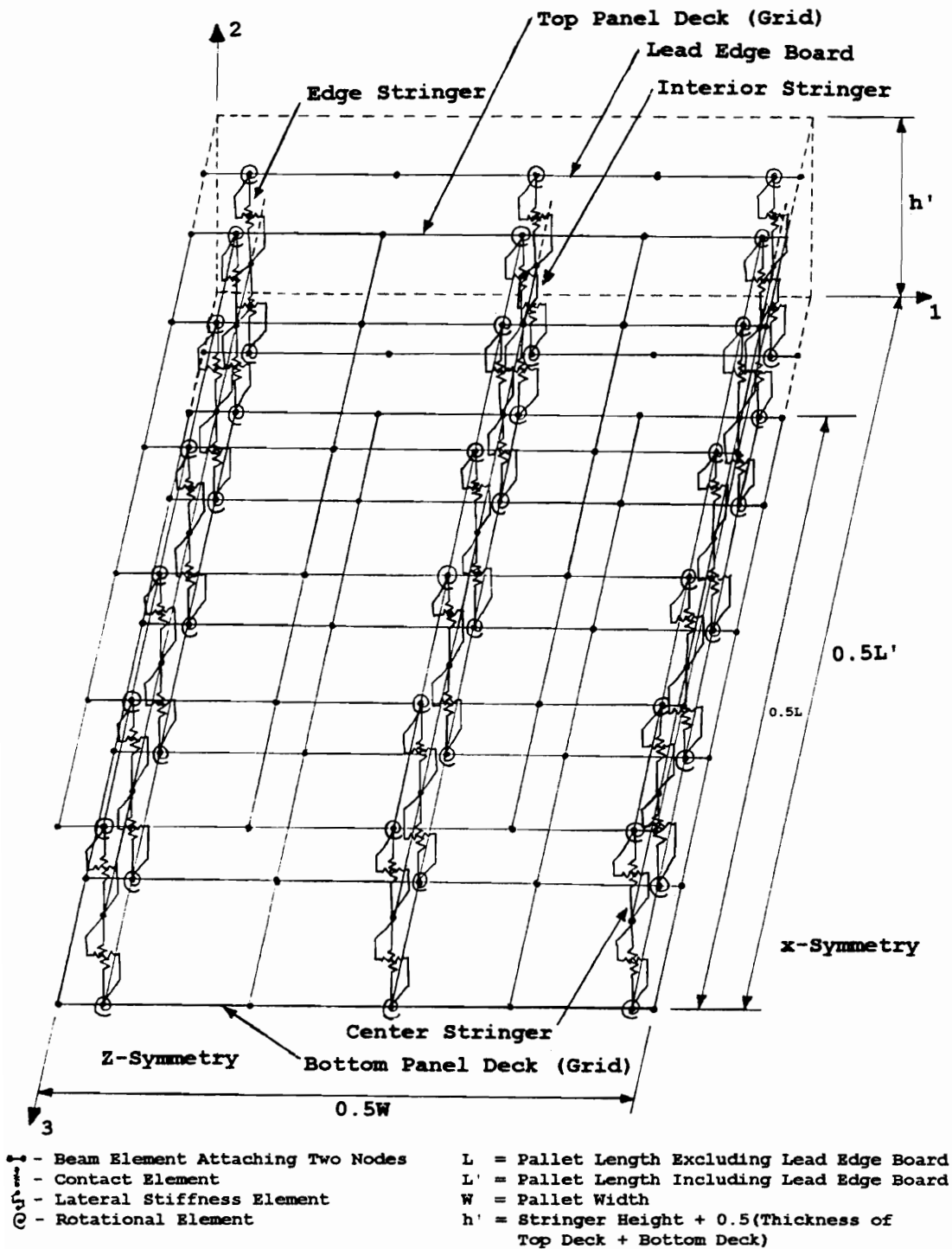


Figure 4.37. Simplified Grid Model used to Predict the Behavior of Stringer Pallets in the RAS Support Condition.

Deck grid members are connected to assemblages of beam elements that simulate stringer behavior. For 3-stringer pallets, the interior or second stringer element assemblage is dummied, while the edge and center stringer assemblages are active. The center stringer element assemblage is dummied for 4-stringer pallets, with the edge and second stringer element assemblages being active. All stringer element assemblages are active when modeling 5-stringer pallets.

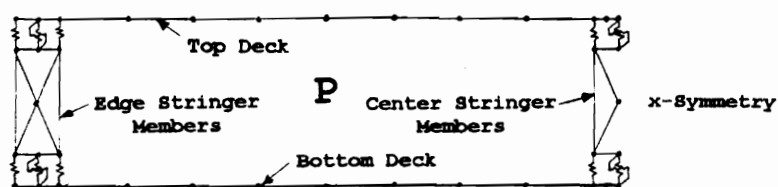
The stringer assemblages share nodes with the decks. As shown with the RAS line load model, this has adverse effects on model performance. It *flattens* out the model, negating the spacing effect of the stringers and the impact of lateral stability imposed on the structure by nail joints. The result is substantially increased deflections and stresses. The primary advantage of this node sharing, is a significant reduction in degrees of freedom and subsequently, a decrease in model complexity. Because this simplification generally leads to conservative predictions and became necessary to meet PC memory requirements, it was implemented.

Withdrawal/head embedment stiffness of nail joints was represented in the model using rotational springs. Lateral stiffness was simulated in both the 1- and 3-directions using axial springs. Although lateral springs have minimal

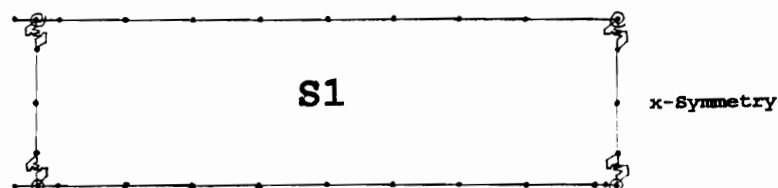
effect in this simplified model, they were maintained in the model because they still have some impact on model performance. Joint stiffnesses, both rotational and lateral, were assigned by summing the stiffness of nails attaching the deck to the stringer and assigning a constant to the springs based on tributary area. Stiffness values for stringer test cases are also given in Volume II, Section 18 of Mackes (1998).

Contact zones between the decks and stringers are modeled using axial springs oriented in the 2-direction. Stiffness assigned to contact springs was again based on tributary area. Positioning of springs in the simplified RAS model was evaluated. The details of this evaluation are presented by Mackes (1998, Volume II, Section 19). Potential locations for attachment of stringers to decks are shown in Figure 4.38. A summary of comparisons between the plate and simplified RAS models implementing these various options is presented in Table 4.22. Although option S3 performed better for the test cases considered, it is thought that option S2 is more general in application and this option simplifies assembly conceptually between the top deck, stringers, and bottom deck. Therefore, option S2 was used.

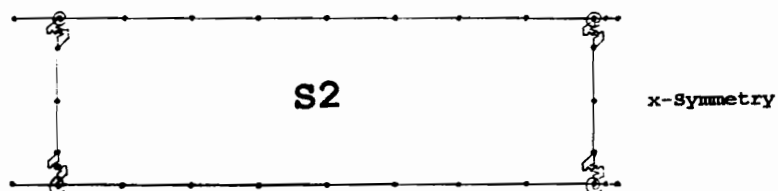
As part of the simplification process, the RAS grid model was evaluated to determine which degrees of freedom



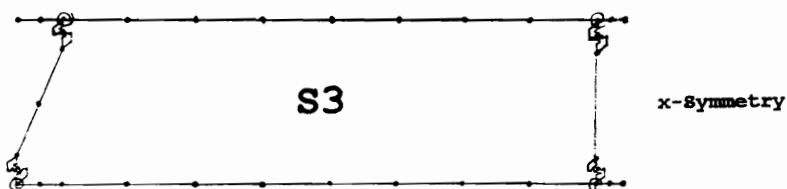
Cross-Section of Three-Stringer Pallet
Plate Model in the RAS Support Condition



Cross-Section of Simplified Three-Stringer
RAS Model with Stringer Members located
at the Neutral Axis of Stringers



Cross-Section of Simplified Three-Stringer
RAS Model with Stringer Members located
at the Inner Edge of Stringers



Cross-Section of Simplified Three-Stringer RAS
Model with Stringer Members located to Emulate
Path of Load Transfer in Analytical Model

- - Beam Element Attaching Two Nodes
- ⋮ - Contact Element
- ⌒ - Lateral Element
- @ - Rotational Element

Figure 4.38. Potential Locations for
Attachment of Stringer Elements to Deck
Elements in the RAS Grid Model.

Table 4.22. Comparison of Load Distribution predicted by the Plate Model and Various Configurations of the Simplified Model in the RAS Support Condition.

MODEL	LOAD DISTRIBUTION			
	EDGE STRINGERS (%)	PERCENT DIFFERENCE (%)	CENTER STRINGER (%)	PERCENT DIFFERENCE (%)
P-RS	52.3	***	47.7	***
S-RS-1	54.1	3.4	45.9	-3.8
S-RS-2	51.8	-1.0	48.2	1.0
S-RS-3	52.1	-0.4	47.9	0.4

- Notes:
1. Refer to Figure 4.38 or Volume II, Section 19 of Mackes (1998) for model configurations.
 2. SPP3-1 pallet data was used.
 3. SPP3-1 was a three-stringer 48 x 40 inch pallet with 19/32 inch plywood decks top and bottom.
 4. Uniformly distributed load of 1.0 psi was applied.

could be held fixed without affecting model performance. This analysis was done systematically and is presented in Volume II, Section 20 of Mackes (1998). A summary of degrees of freedom which can be effectively removed from the model is presented in Table 4.23.

Comparisons of results obtained for the simplified RAS model and plate model are presented in Table 4.24. An example of an ABAQUS input file and ABAQUS output files for test cases considered are given in Volume II, Section 21 of Mackes (1998). Generally, maximum deflections predicted by the simplified RAS model are considerably greater, up to 22.6 percent, than those predicted by the plate model. Maximum S11 normal stresses predicted by the simplified RAS model, with one exception, are also greater, up to 33.3 percent. As stated previously, both maximum stresses and deflections tend to be significantly greater for the simplified model because the stringer and deck assemblages share nodes.

Although the deflection patterns and stress profiles for the components of test pallet SPP3-1, shown in Figures 4.39 through 4.42 appear more or less as expected, significant differences between patterns and profiles predicted by the simplified and plate models can exist. This is primarily because they do not behave similarly with regards to load transfer from the top deck to the stringers.

Table 4.23. Summary of the Degrees of Freedom which can be Restrained in the RAS Grid Model for Stringer Pallets without significantly Impacting Stress and Deflection Predictions.

NODE (S)	DEGREE (S) OF FREEDOM RESTRAINED
Bottom Deck:	
All Nodes (1 - 49)	1, 3, & 5
43 - 49	4
7, 14, 21, 28, 35, 42, & 49	6
Stringers:	
All Nodes (50 - 70)	1, 3, & 5
56, 63, & 70	4
64 - 70	6
Top Deck:	
All Nodes (71 - 119)	1, 3, & 5
113 - 119	4
77, 84, 91, 98, 105, 112, & 119	6

Note: Refer to Figure 4.38 or Volume II, Section 19 of Mackes (1998) for model configurations.

Table 4.24. Comparison of selected Simplified
RAS Grid Model (S-RS) Results to Plate
Model (P-RS) Predictions.

PALLET ID. NUMBER	LCTN	S-RS S11 (psi)	P-RS S11 (psi)	DIF (%)	S-RS D (in.)	P-RS D (in.)	DIF (%)
42 inch Test Span:							
SPP3-3	CS	1568	1279	22.6	-0.068	-0.051	33.3
44 inch Test Span:							
SPP3-1	CS	1443	1179	22.4	-0.093	-0.074	25.7
SPP3-2	CS	1389	1169	18.8	-0.092	-0.075	22.7
MEAN		1416	1174	20.6	-0.093	-0.075	24.2
S003-1	CS	1544	1351	14.3	-0.096	-0.083	15.7
S003-2	CS	1551	1347	15.1	-0.093	-0.080	16.3
S003-3	CS	1531	1317	16.2	-0.109	-0.093	17.2
MEAN		1542	1338	15.2	-0.099	-0.085	16.4
S400-1	IS	959	796	20.5	-0.060	-0.066	-9.1
S400-2	IS	836	729	14.7	-0.098	-0.086	14.0
S400-3	IS	816	713	14.4	-0.095	-0.084	13.1
MEAN		870	746	16.7	-0.084	-0.079	7.2

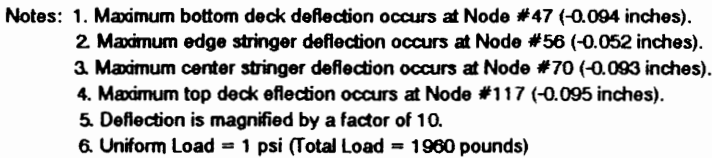
Notes: 1. LCTN - Location of comparison:

CS - Center Stringer at mid-span

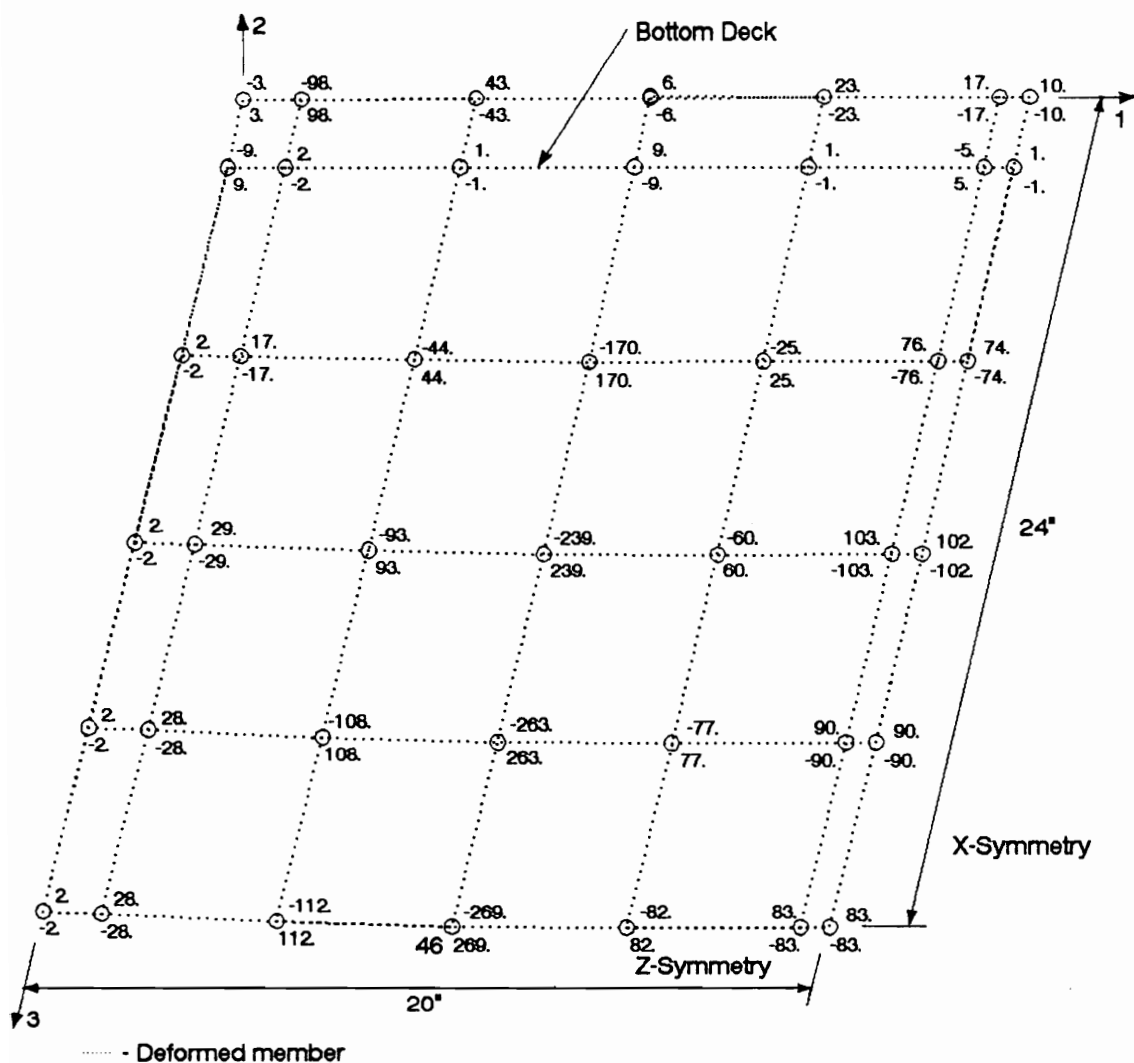
IS - Interior Stringer at mid-span

2. DIF - Difference between predicted and
experimental deflections.

3. For SPP3, S003, and S400 pallets in the
RAS support condition, the full uniformly
distributed load was 1.0 psi (1920 lbs).

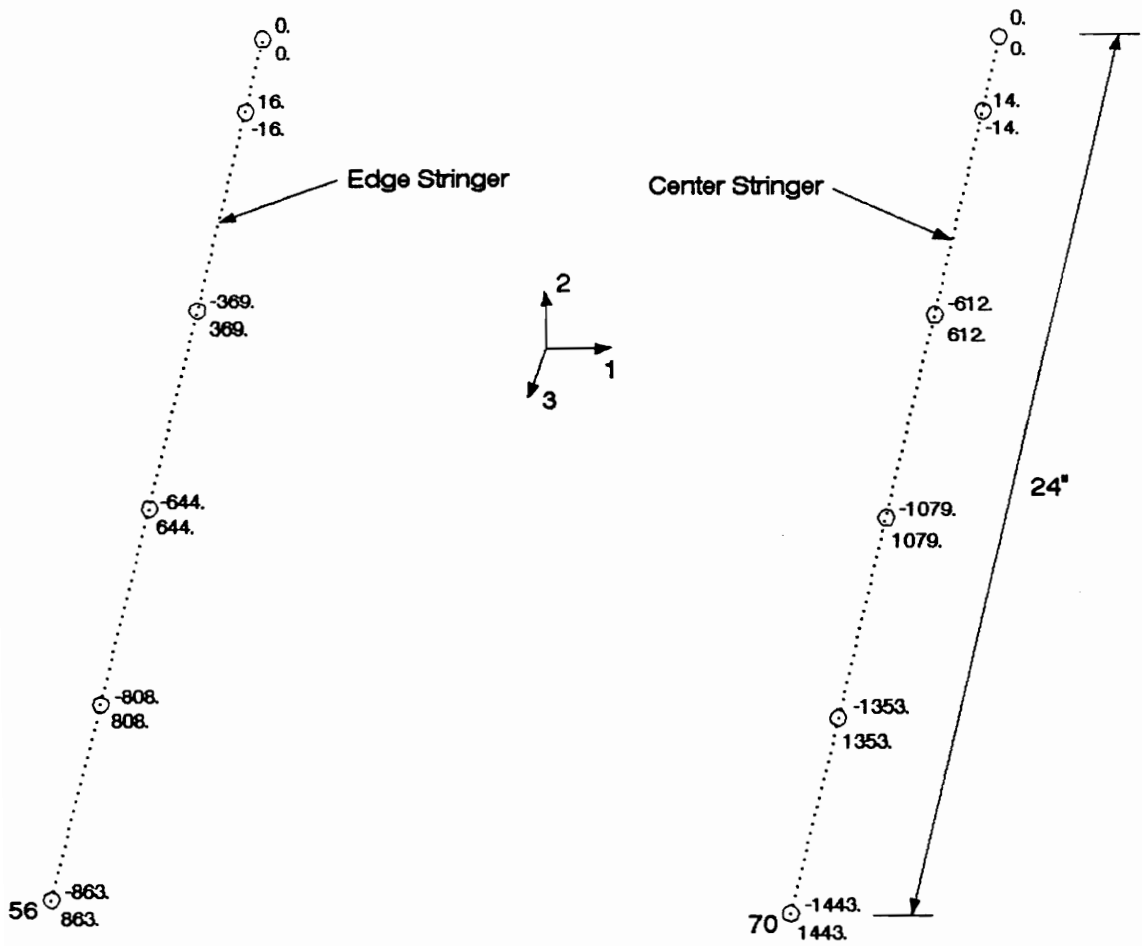


- 291 -



- Notes: 1. Maximum bottom deck S11 stress occurs at Node #46 (+/- 269. psi).
 2. Uniform Load = 1.0 psi (Total Load = 1920 pounds)
 3. Units of stress are psi.

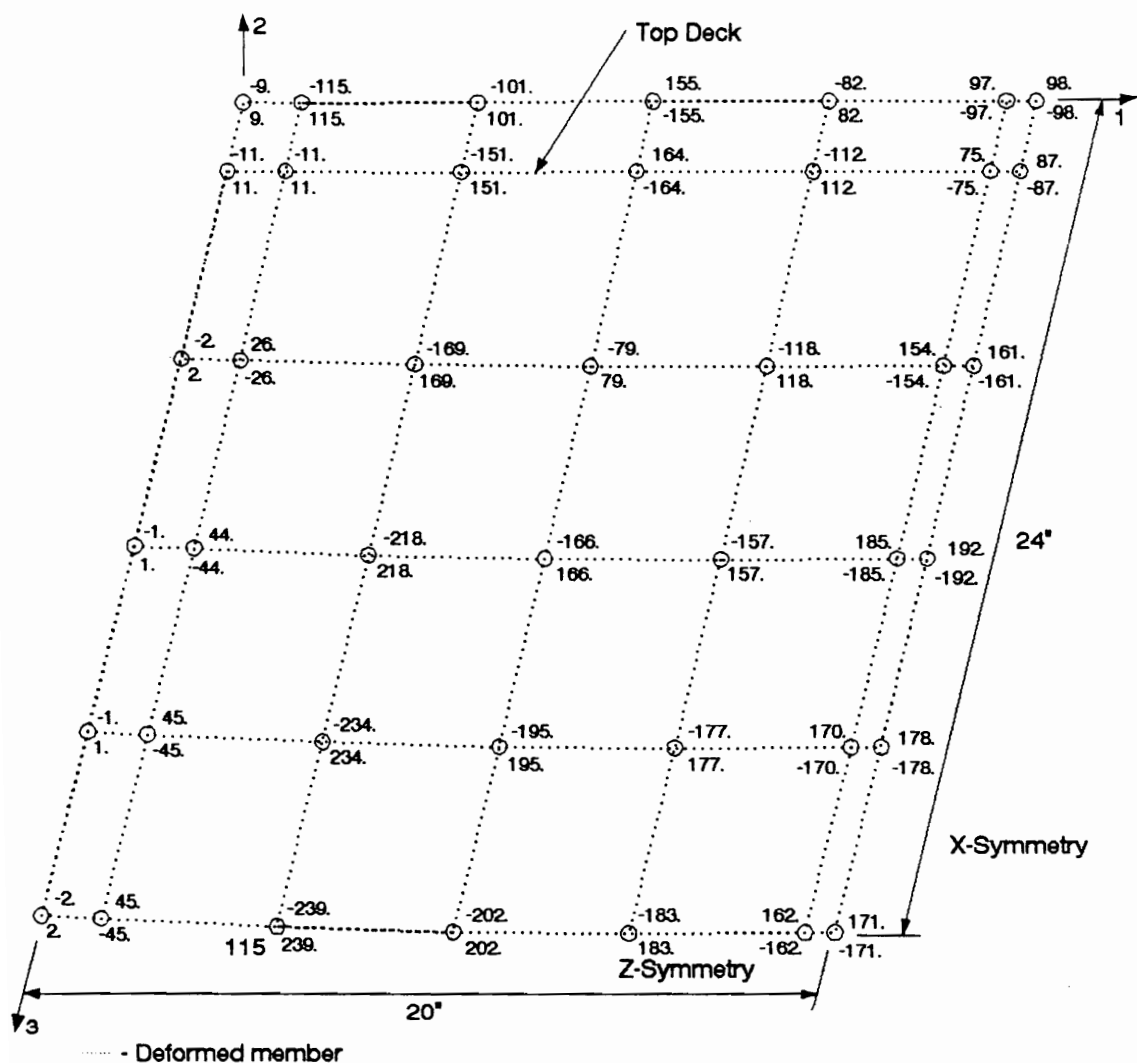
Figure 4.40. S11 Stress Profile predicted for the Bottom Deck of Test Pallet SPP3-1 by the Simplified RAS Grid Model.



..... - Deformed member

- Notes:
1. Maximum edge stringer S11 stress occurs at Node #56 (+/- 863. psi).
 2. Maximum center stringer S11 stress occurs at Node #70 (+/- 1443. psi).
 3. Uniform Load = 1.0 psi (Total Load = 1960 pounds)
 4. Units of stress are psi.

Figure 4.41. S11 Stress Profile predicted for the Stringers of Test Pallet SPP3-1 by the Simplified RAS Grid Model.



- Notes: 1. Maximum top deck S11 stress occurs at Node #115 (+/- 239. psi).
 2. Uniform Load = 1.0 psi (Total Load = 1920 pounds)
 3. Units of stress are psi.

Figure 4.42. S11 Stress Profile predicted for the Top Deck of Test Pallet SPP3-1 by the Simplified RAS Grid Model.

The impact of the decks, primarily related to composite action is lost in the simplified model. This has a definite affect on load transfer.

Similar to the simplified RAS line load model, the simplified RAS model for uniformly loaded stringer pallets can be enhanced by adding two additional rows of elements to each stringer assemblage as shown in Figure 4.43. The node and element numbering scheme for the enhanced simplified model is given in Volume II, Section 22 of Mackes (1998). A comparison of results between the enhanced simplified and plate models is presented in Table 4.25. The agreement between the models is quite good, with differences of 1.1 percent or less between maximum stress (S11) predictions and 3 percent or less for maximum deflection predictions. The models behave similarly.

As with line load models, the enhanced RAS model for uniformly loaded model stringer pallets better predicts actual pallet behavior, effectively modeling factors such as lateral stiffness, deck spacing, and composite action of the decks and stringers interacting. However, it also requires considerably more computer memory. Because of computer memory limitations the enhanced simplified model shown previously in Figure 4.43 is not utilized. Nonetheless, it is strongly recommended that the enhanced model be

Table 4.25. Comparison of selected Enhanced Simplified RAS Grid Model (S-RS) Results to Plate Model (P-RS) Predictions.

PALLET ID. NUMBER	LCTN	S-RS S11 (psi)	P-RS S11 (psi)	DIF (%)	S-RS D (in.)	P-RS D (in.)	DIF (%)
42 inch Test Span:							
SPP3-3	CS	1300	1279	1.6	-0.052	-0.051	2.0
44 inch Test Span:							
SPP3-1	CS	1187	1179	0.7	-0.076	-0.074	2.7
SPP3-2	CS	1157	1169	-1.0	-0.076	-0.075	1.3
MEAN		1172	1174	-0.2	-0.076	-0.075	2.0
SOO3-1	CS	1354	1351	0.2	-0.085	-0.083	2.4
SOO3-2	CS	1353	1347	0.4	-0.082	-0.080	2.5
S003-3	CS	1309	1317	-0.6	-0.093	-0.093	0.0
MEAN		1339	1338	0.0	-0.087	-0.085	1.6
S400-1	IS	787	796	-1.1	-0.064	-0.066	-3.0
S400-2	IS	721	729	-1.1	-0.084	-0.086	-2.3
S400-3	IS	706	713	-1.0	-0.082	-0.084	-2.4
MEAN		738	746	-1.1	-0.077	-0.079	-2.5

Notes: 1. LCTN - Location of comparison:

CS - Center Stringer at mid-span

IS - Interior Stringer at mid-span

2. DIF - Difference between predicted and experimental deflections.

3. For SPP3, SOO3, and S400 pallets in the RAS support condition, the full uniformly distributed load was 1.0 psi (1920 lbs).

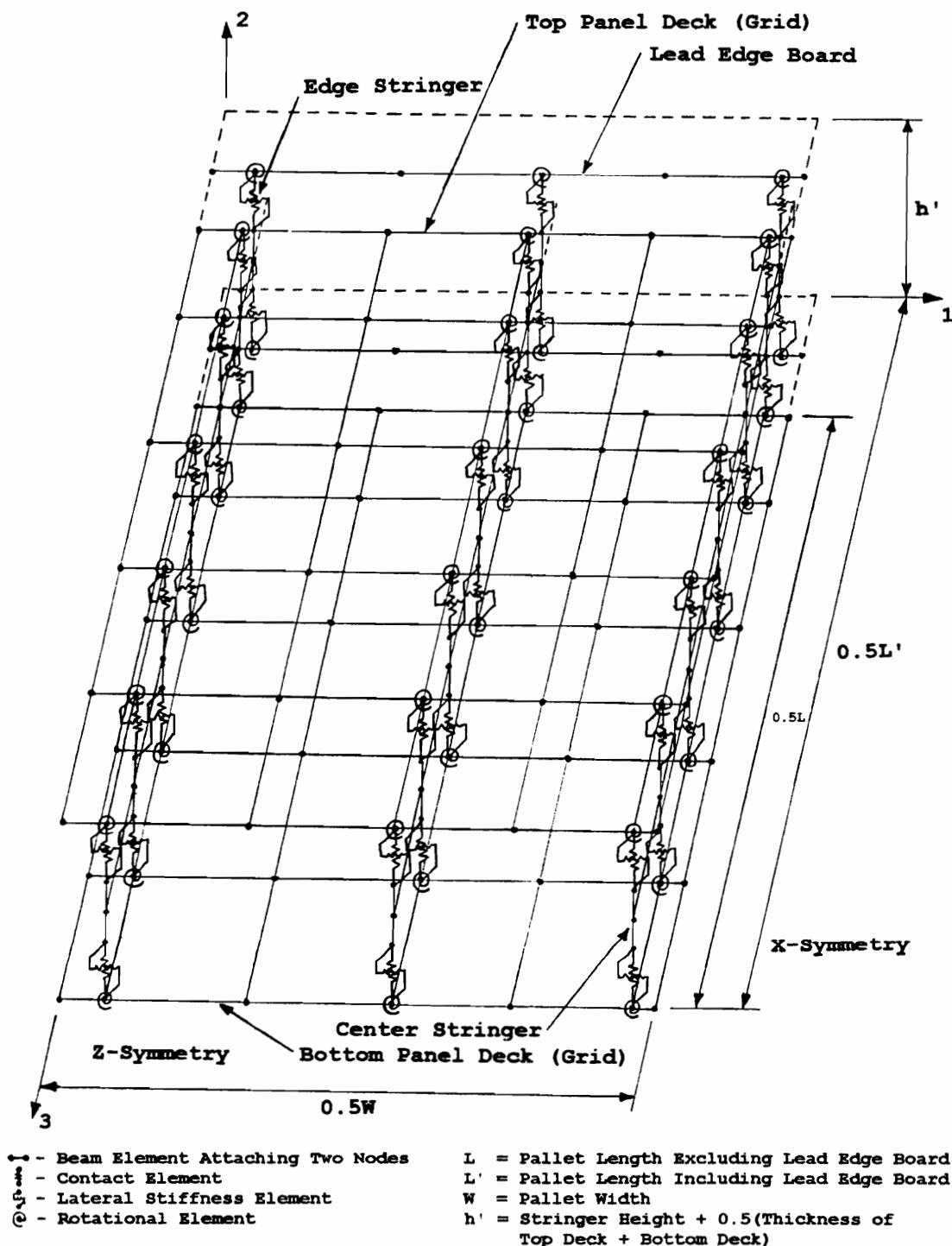


Figure 4.43. Proposed Grid Model for Predicting the Behavior of Stringer Pallets in the RAS Support Condition.

incorporated into PDS-Panel when it becomes feasible to do so in the future.

5.0 Modeling Block Pallets

As with Stringer pallets, block pallets were modeled in this research using ABAQUS (Hibbitt, Karlsson, and Sorenson, Inc., 1996). Three-dimensional finite element plate models were developed to predict the behavior of block pallets under load. To validate model performance, predicted deflections were compared to experimental values for block pallets obtained using an air-bag testing machine. Sensitivity studies conducted with the plate models are presented. These studies provided a basis for the development of simplified PC-compatible models with reduced degrees of freedom. Simplified PC-compatible models for important block pallet configurations and support conditions are fully discussed in this chapter.

5.1 Development of Plate Models for Block Pallets

To evaluate block pallet behavior, three-dimensional finite element models were assembled using ABAQUS. The behavior of pallet components and joints can be predicted using the modeling techniques outlined in Chapter 3. Similar to stringer pallet models, the assembly process used to construct block pallet models was systematic. The bottom deck was assembled first, followed by the spacers (blocks), and then the top deck. Nail joints and contact elements were then added.

Four principal types of plate models for block pallets were built and refined. These were:

1. Full four-way entry, reversible nine block pallet with panel decks top and bottom.
2. Full four-way entry, nine block pallet with panel deck top and panel deck bottom with wheel openings.
3. Full four-way entry, nine block pallet with panel deck top and a unidirectional-base lumber bottom deck.
4. Full four-way entry, nine block pallet with panel deck top and a perimeter-base lumber bottom deck.

The pallet model for pallets with a unidirectional-base lumber bottom deck was designed to accommodate top deck hand-holds which were present in the unidirectional-base pallets physically tested for comparative purposes.

5.1.1 Block Pallets with Panel Decks Top and Bottom

The plate model used to predict the behavior of block pallets with panel decks top and bottom was constructed similarly to plate models for stringer pallets. Shell elements were used to simulate panels. Assemblages of beam elements were used to simulate blocks and strip-type decking. Zero-length spring elements were used to simulate nail joints and block/deck contact zones.

The finite element mesh used to simulate the panels of block pallets, shown in Figure 5.1, was finer than that required for decks of stringer pallets. Additional mesh

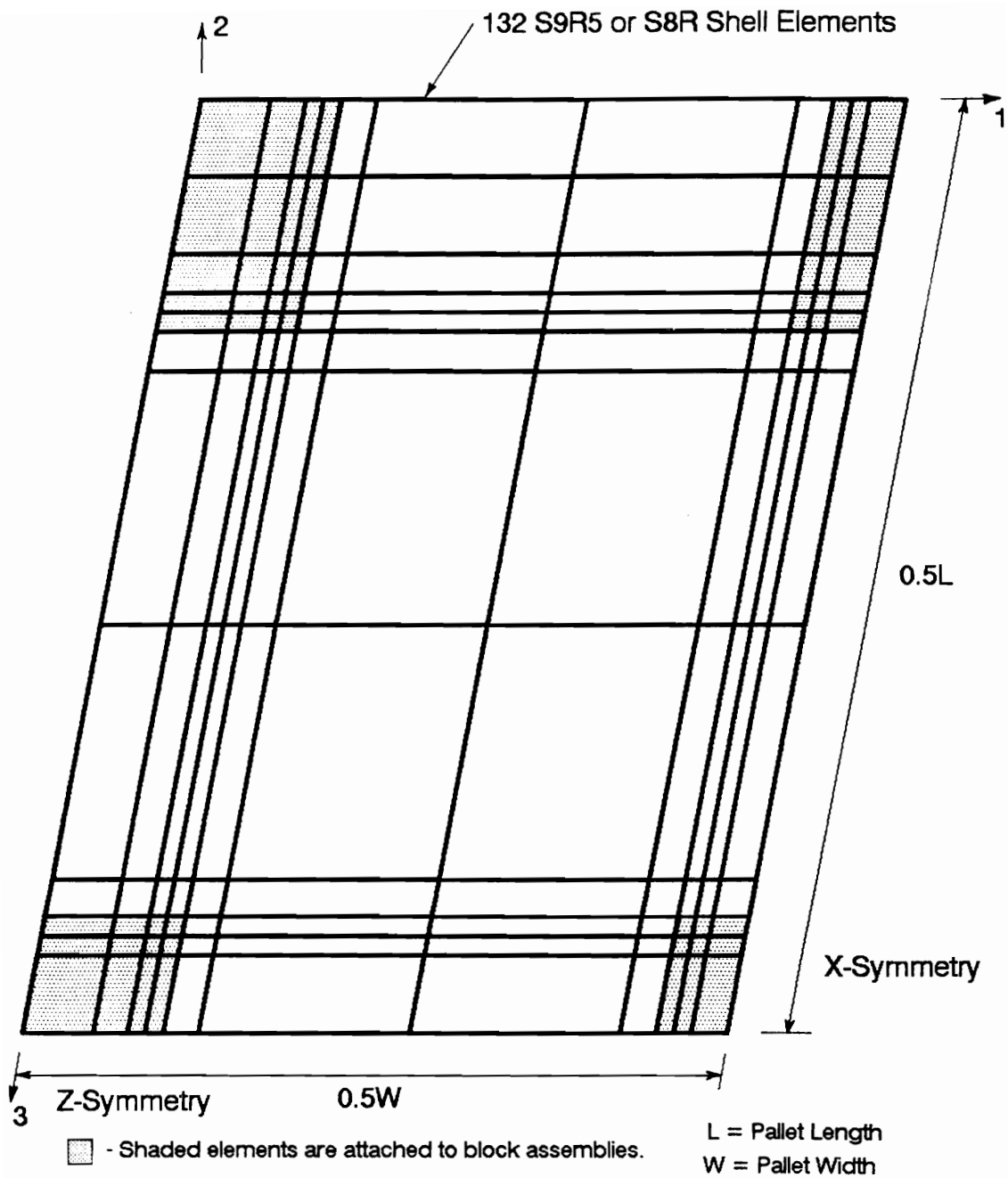


Figure 5.1. Finite Element Mesh Configuration used to Simulate the Panel Decks of Block Pallets.

fineness was required to adequately model block/deck contact. The finite element mesh used to model blocks was shown previously in Figure 3.18 (Type I).

Figure 5.2 shows how the plate model appeared when all members are assembled together. The model displayed is a nine-block reversible pallet. Diagrams identifying node and element locations for this model are presented by Mackes (1998, Volume III, Section 1), along with an example of the ABAQUS input program. By changing coordinates appropriately, this model was used to model block pallets of practically any length or width. Pallets with 4, 5, 6, or 9 blocks were modeled by activating blocks as shown in Figure 5.3. Inactive blocks and associated contact and joint elements were dummed-out by assigning them near zero properties. Changing the geometric and material properties of component elements was also easily achieved.

Contact elements were assigned stiffness based on tributary area and the perpendicular-to-grain modulus of elasticity of the block as discussed in Section 3.5.3.2. An iterative approach was used to determine which contact springs were active. Initially all springs were assumed to be active, with the deck fully in contact with the blocks. Additionally, all nail joints were assumed to be inactive with regards to withdrawal/head embedment. Lateral stiffness of nail joints was maintained throughout. Initial

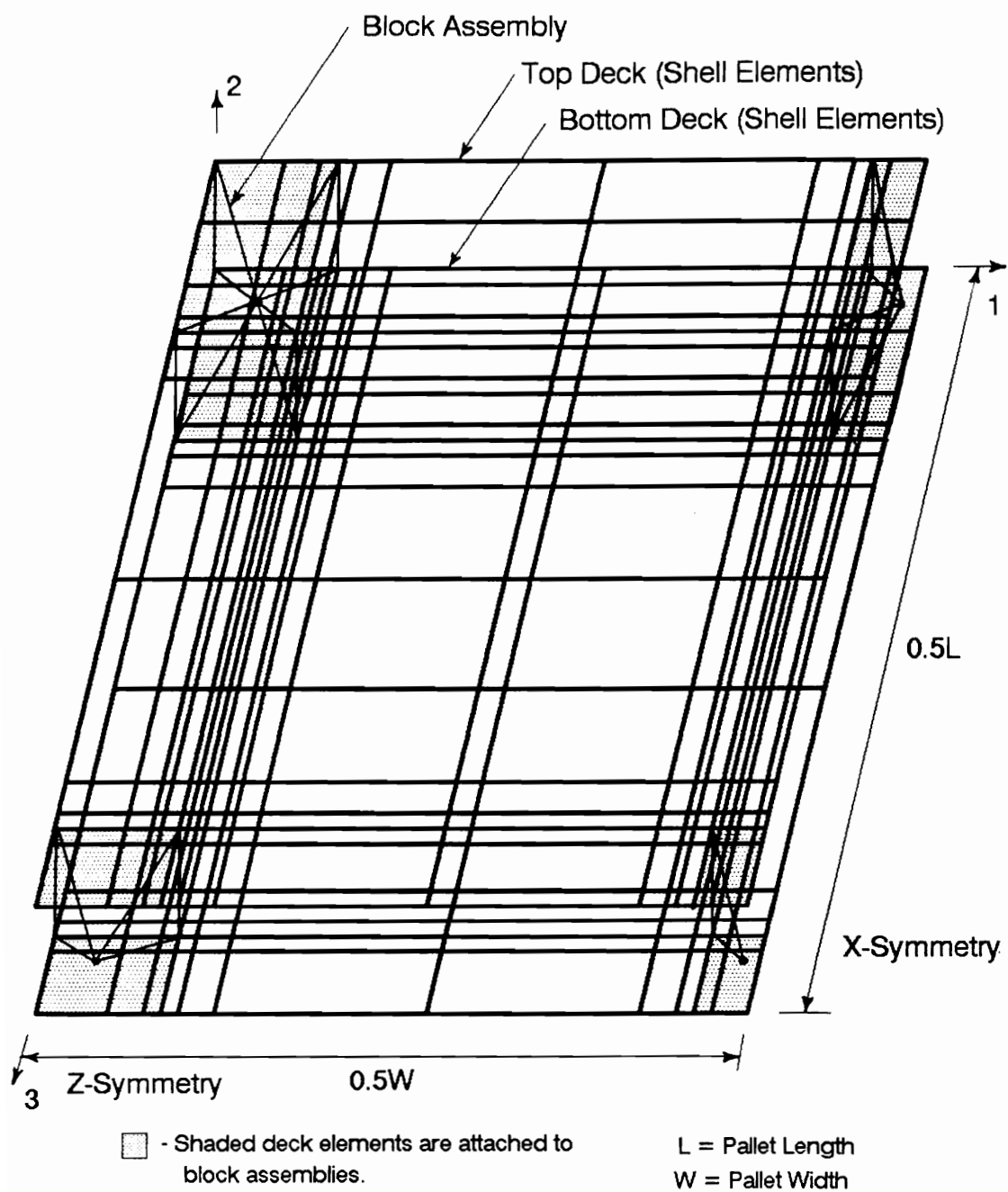


Figure 5.2. Finite Element Mesh Configuration for Block Pallets with Panel Decks Top and Bottom.

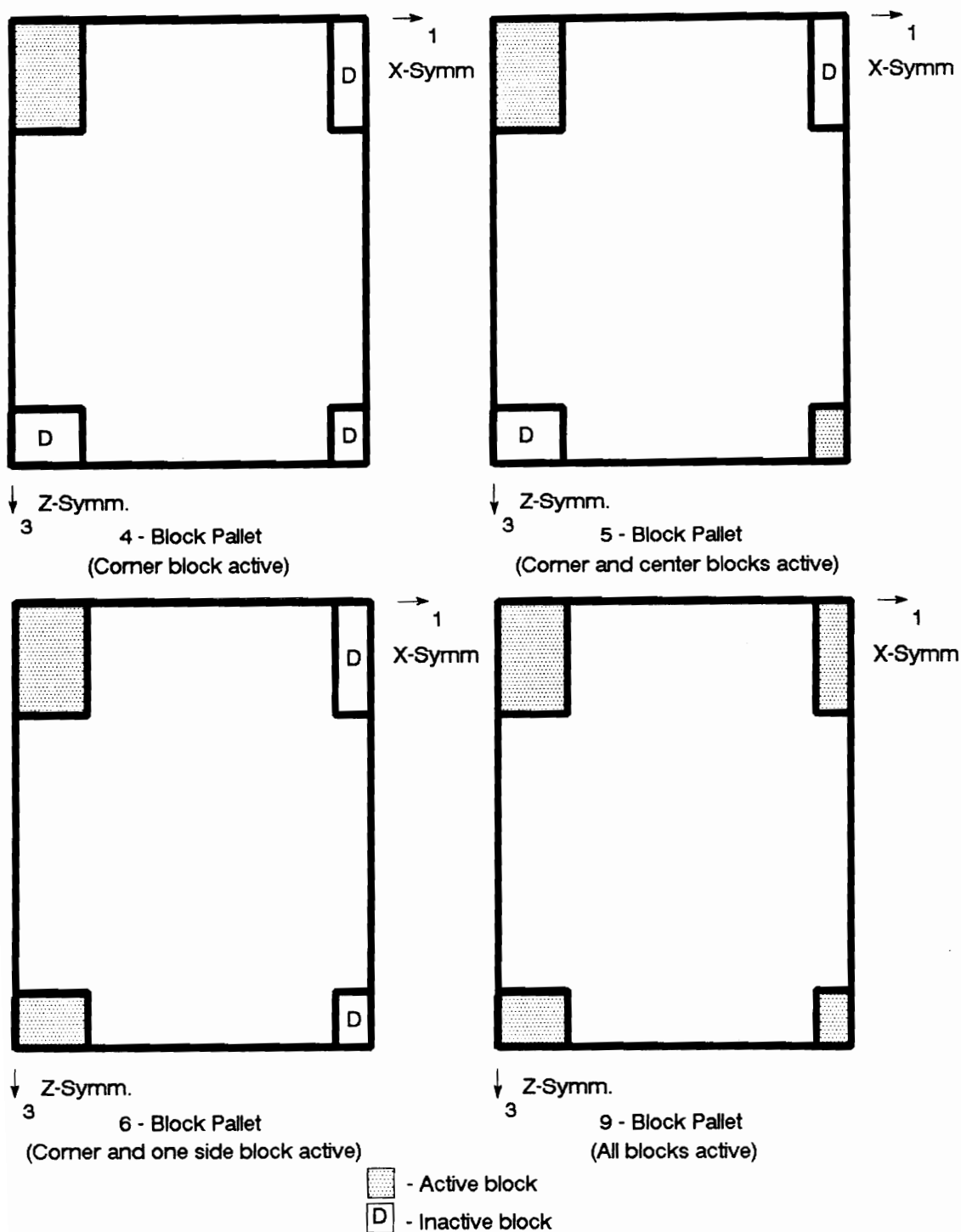


Figure 5.3. Block Activation Scheme for Modeling 4-, 5-, 6-, and 9-Block Pallets.

solutions were then generated using ABAQUS. Contact elements which displaced in tension were either dummied or assigned withdrawal/head embedment stiffness if the element occurred at a nail joint location. Springs which displaced in compression were maintained as contact elements. Subsequent solutions were generated iteratively with additional elements in tension dummied or assigned nail joint properties until no active contact elements were in tension and no inactive contact elements were in compression. Achieving this state of equilibrium generally required five to six iterations. Based on this approach, profiles of deck/block contact were established. Examples of contact profiles are shown in ensuing sections.

5.1.2 Block Pallet with Panel Deck Top and Panel Deck Bottom with Wheel Openings

For block pallets having a panel bottom deck with cut-outs functioning as wheel openings, the model developed to predict the behavior of block pallets with panel decks top and bottom was used. No significant modifications to the mesh developed in Section 5.1.1 were required. An example of a finite element mesh used to simulate the bottom deck of block pallets with wheel openings is shown in Figure 5.4. To model wheel openings, the mesh simulating the bottom deck was configured so the cut-out was contained within shell

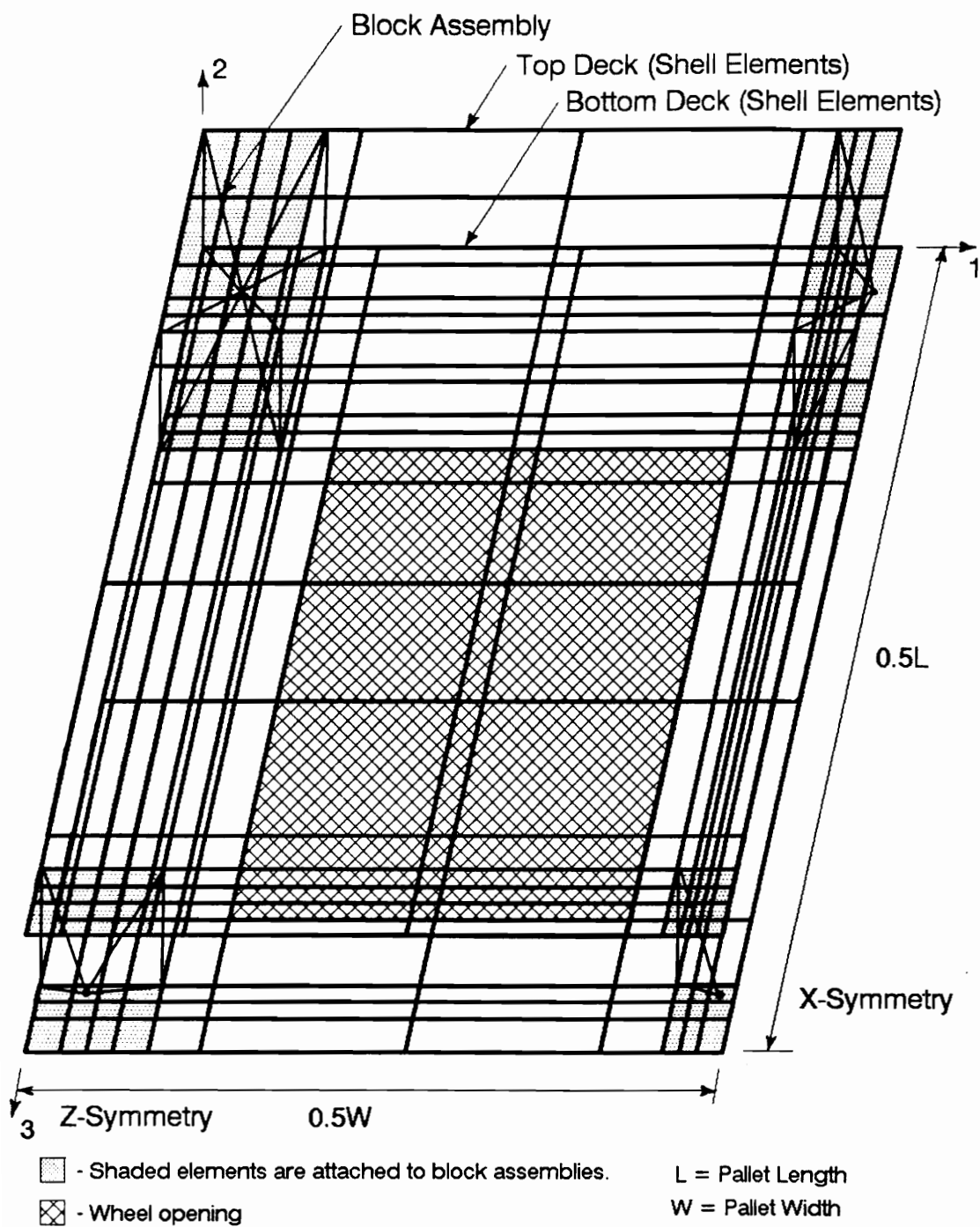


Figure 5.4. Finite Element Mesh Configuration for Block Pallets with Bottom Deck Wheel Openings.

elements as shown. These elements were then assigned near zero stiffness.

5.1.3 Block Pallets with Panel Deck Tops and Strip-type Bottom Decks

Plate models were developed for two pallet types having panel deck tops and strip-type decking on the bottom. These two pallet types were unidirectional-base pallets and perimeter-base pallets. Initially, an attempt was made to build one model capable of predicting behavior for both pallet types; however, it was more convenient and efficient to model them separately. This is because of the complex butted joints found in perimeter-base pallets.

5.1.3.1 Unidirectional-Base Pallets

To predict the behavior of unidirectional-base block pallets, the existing plate model for block pallets with panel decks top and bottom was modified. The configuration of the finite element mesh simulating the top panel deck was unchanged from previous block models. The bottom surface of the beam assemblages simulating blocks were modified to accommodate strip-type decking as shown in Figure 3.18 (Type III). Strip-type bottom decks were modeled using beam elements. Attachment between the blocks and strip-type decking was accomplished using zero-length spring elements which were used to simulate nail joints and contact zones.

The iterative approach described in Section 5.1.1 was used to determine whether nail joints and contact elements were active. The plate model for unidirectional-base block pallets is shown in Figure 5.5. The location of nodes and elements for test cases considered are given in Volume III, Section 2 of Mackes (1998).

5.1.3.2 Perimeter-Base Block Pallets

The existing unidirectional-base plate model was modified to predict the behavior of perimeter-base block pallets. The bottom surface of beam assemblages simulating blocks were modified to accommodate strip-type decking along the pallet length (3-direction), in addition to the width (1-direction). This mesh modification is shown in Figure 3.18 (Type II). This modification is designed to provide the capability of modeling butted joints normally found in perimeter-base pallets. When butted joints are present, the *short sections* high-lighted in Figure 3.18 are given near zero stiffness.

The plate model developed to predict the behavior of perimeter-base pallets is shown in Figure 5.6. Strip-type decking oriented in both directions was modeled using beam elements. The blocks and strip-type decking were again attached using zero-length springs which simulate nail joints and contact zones. The iterative approach described

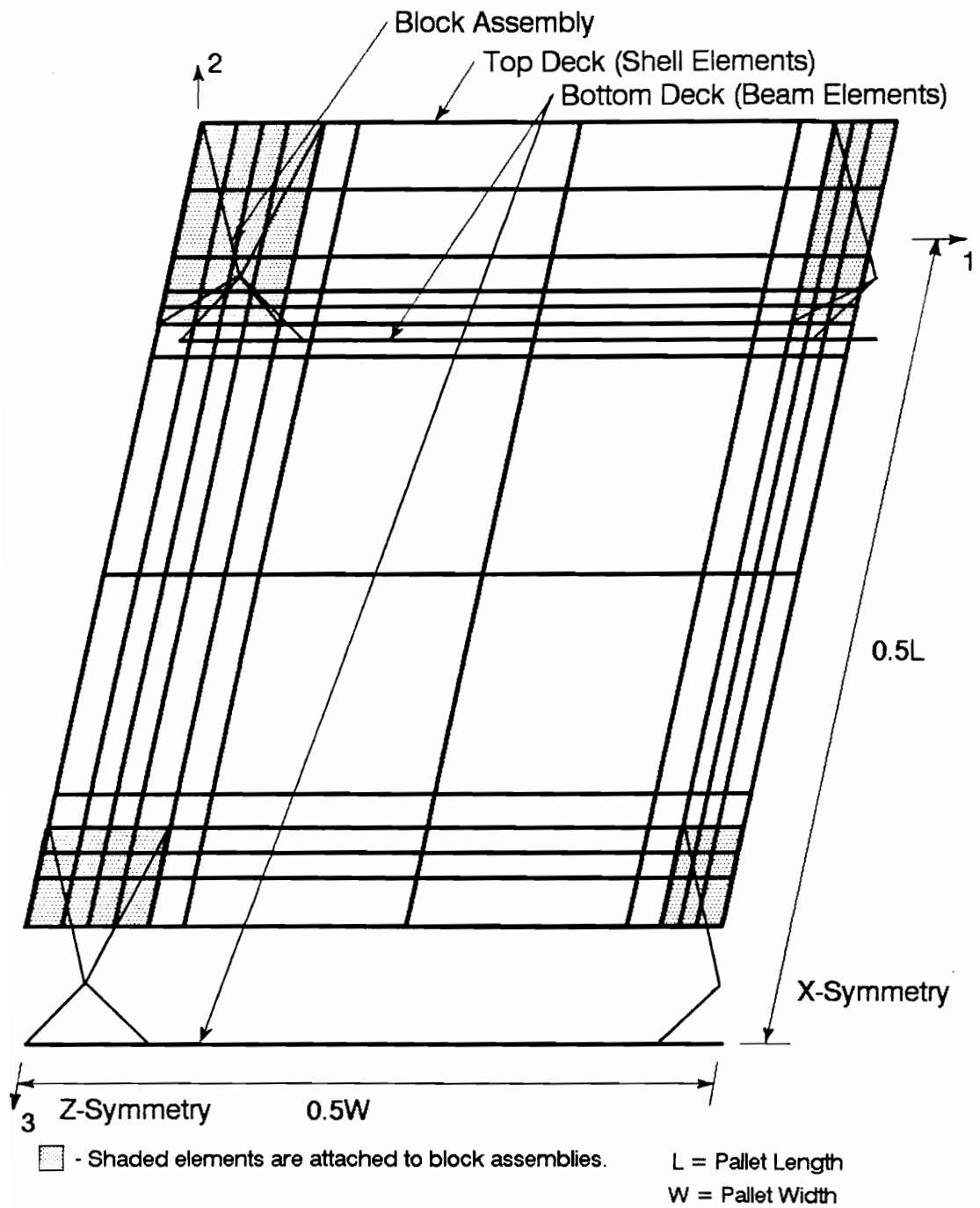


Figure 5.5. Finite Element Mesh Configuration for Block Pallets with Panel Top Deck and Unidirectional Lumber Bottom Deck.

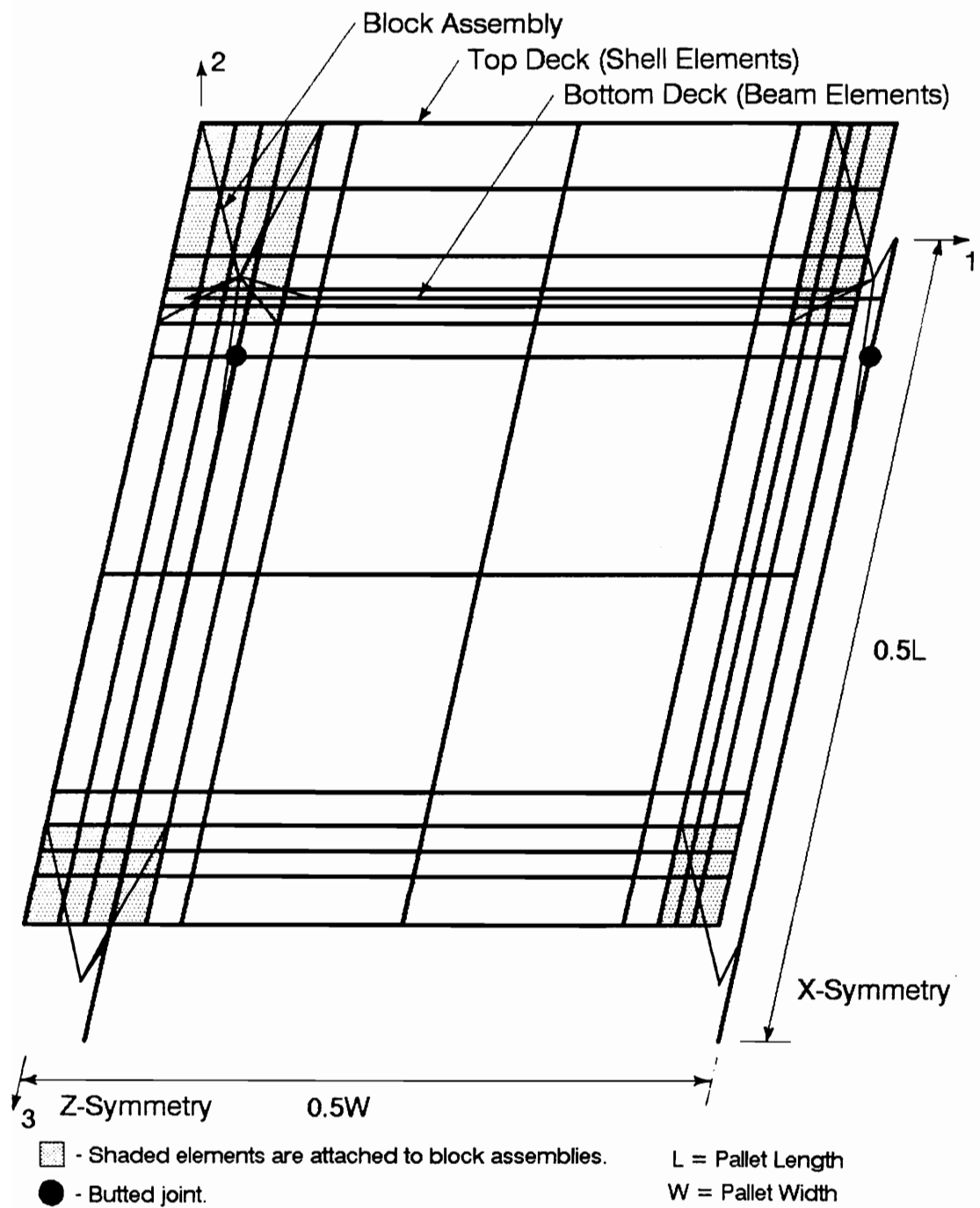


Figure 5.6. Finite Element Mesh Configuration for Block Pallets with Panel Top Deck and Perimeter-Base of Lumber.

in Section 5.1.1 was used to determine whether nail joints and contact elements were active. Node and element locations for the perimeter-base block pallets evaluated are presented by Mackes (1998, Volume III, Section 3).

5.2 Validation of Block Pallet Plate Models

As with plate models developed for stringer pallets, it was necessary to validate the block pallet plate models. Predicted pallet deflections determined using plate models were compared to experimental values obtained utilizing the air-bag test machine at VPI & SU. Block pallets were tested nondestructively in the stack, RAD, and RAS support conditions. Except for modulus of elasticity values of panel decks, geometric and material properties required as input to the models were determined prior to full-pallet testing. Modulus of elasticity values for panel decks were determined after full-pallet testing because panels were cut into 2 inch strips to determine them.

In this section, procedures and techniques used to determine the properties of block pallet components are described. The assembly process used to prepare block pallets and the configurations of components comprising the block pallets are reviewed. Details of block pallet testing are summarized. Data analysis and results, including

comparisons of predicted to experimental deflections, are presented and discussed.

5.2.1 Determining Pallet Member Properties

Plate models used to predict block pallet behavior required important material and geometric properties of components as input. For panel decks, this included panel thickness, moduli of elasticity (both E_s and E_w , strong and weak panel axes), Poisson's ratio (1-2 plane), and moduli of rigidity (G_{12} , G_{13} , and G_{23}). Cross-sectional properties (width and height) and modulus of elasticity along the length were required for strip-type decking. Properties were also determined for nail joints and contact elements.

Geometric properties of block pallet components were measured using hand-held calipers accurate to 0.001 inches. Modulus of elasticity values were determined experimentally. Poisson's ratio was determined using either Equation 2.2 or 2.3. Modulus of rigidity values were taken from literature (Bodig and Jayne, 1982). Nail joint and contact elements were assigned stiffness properties (spring constants) using the methodologies discussed in section 3.5.

Test procedures used to determine material properties for block pallet components were similar to those used for stringer pallet components. Test procedures are discussed for panel decks in Section 4.2.1.1 and Section 4.2.1.3 for

strip-type decking. As with stringer pallet panels, for block pallets tested in the stack support condition, panel properties were determined experimentally in both directions using 2 inch strips cut from the panels. For pallets tested in the rack conditions, all material was cut into either 40 inch strips for pallets tested in the RAW condition or 48 inch strips for the RAL condition. The modulus of elasticity value for the direction not tested was estimated based on full-panel testing. A summary of property data for block pallet components is given by Mackes (1998, Volume III, Section 4).

5.2.2 Preparation of Pallets

Block pallet components were clearly identified and marked prior to pallet assembly. As pallets were assembled the location of each component was recorded. The location of components used to assemble each block pallet tested can be found in Volume III, Section 5 of Mackes (1998).

All pallets built and tested in this research had nine-block configurations. Pallet components were assembled into four basic configurations, as follows:

1. Nine-block reversible pallet with plywood panel deck top and bottom (BPP)
2. Nine-block pallet with a plywood panel deck top and a bottom plywood panel deck with wheel openings (BPPC)

3. Nine-block pallet with a plywood panel deck top and a unidirectional-base plywood strip bottom deck (BPU)
4. Nine-block pallet with an OSB panel deck top and a perimeter-base lumber bottom deck (BOLP)

Drawings of these pallet configurations are presented in Figure 5.7. The size of all the block pallets built were 40 by 48 inches, with the strong axis of the panel oriented along the 48 inch length.

Panels used for BPP and BPPC pallet types were cut from 4 by 8 foot sheets of either 19/32 inch plywood with a span rating of 40/20, or 23/32 inch plywood with a span rating of 48/24. The plywood used to fabricate BPU pallets had a thickness of 15/32 inch, with a span rating of 32/16. All plywood selected for use was constructed with 5-ply of southern yellow pine veneers.

Panels used in BOLP pallets were either 7/16 inch OSB with a span rating of 24/16, or 23/32 inch OSB with a span rating of 48/24. The OSB used in block pallets was comprised of hardwood flakes, identified as cottonwood or aspen. The 6 inch wide strips used to fabricate BPU pallets were cut from 15/32 inch plywood panels. The lumber comprising the bottom deck of BOLP pallets was cut from nominal 1 x 4 boards of spruce-pine-fir.

As with stringer pallets, pallet assembly was accomplished using pallet nails hand driven into members using hammers. Nails selected for use in assembling BPP

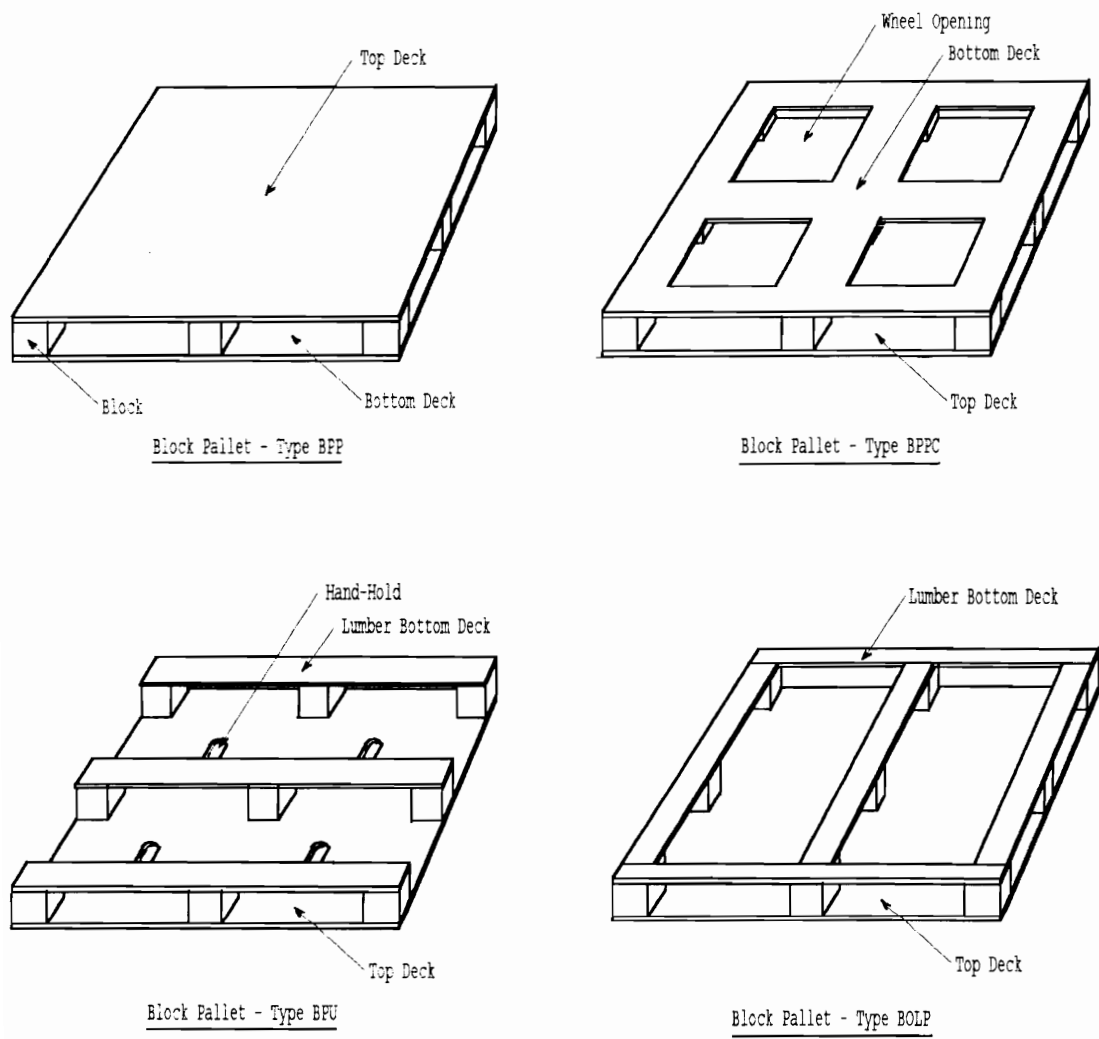


Figure 5.7. Block Pallet Configurations Evaluated.

pallets with 19/32 inch plywood decks, BPU pallets, and BOLP pallets with 7/16 inch decks were 2 inch long Philstone nails. BPP and BOLP pallets with 23/32 inch plywood decks were assembled with 2.25 inch long Greenwood nails. Properties for these nail types are given in Volume I, Section 9 of Mackes (1998). The nailing patterns used to assemble block pallets are shown in Figure 5.8.

5.2.3 Block Pallet Testing

Procedures used to test block pallets were similar to those used for stringer pallets. The air-bag test machine was used to measure the deflection of block pallets under load. Three replications of each block pallet type were tested in the stack and rack (RAW and RAL) support conditions. Block pallets were stressed at relatively low loads in the elastic range to avoid damage. Each block pallet was loaded three times, the first two times to work the pallet joints and the third time to obtain deflection readings. The rate of loading was 0.10 inch per minute which is equivalent to 18 liters of air per minute entering the air-bag. Block pallet testing is discussed further for principal support conditions in subsequent sections.

5.2.3.1 Stack Support Condition

Nine-block pallets were tested in the stack condition using the air-bag test machine. The test machine was fitted

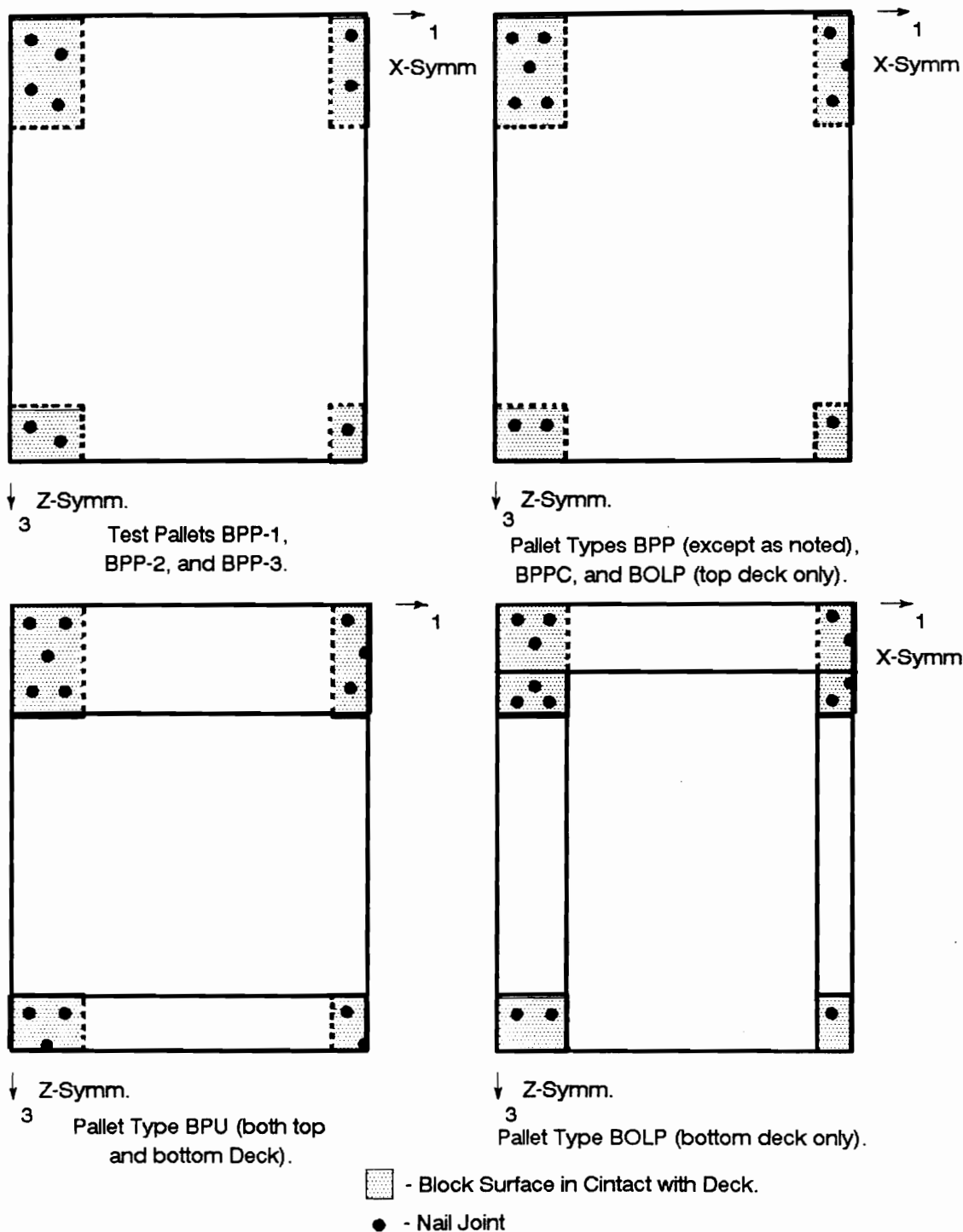


Figure 5.8. Nailing Patterns used to Assemble Block Pallets.

with three steel I-beams which supported the pallet under each block as shown in Figure 5.9. This Figure shows a uniform load test in progress. Panel decks were uniformly loaded by direct contact with the surface of the air-bag. Except for BPU type pallets, a maximum uniform load of 2.604 psi (5000 pounds) was applied to panel decks. A maximum uniformly distributed load of 1.0 psi (1920 pounds) was applied to BPU type pallets.

Holes were drilled in the bottom deck of reversible block pallets (type BPP) to allow clear access for LVDT attachment to the top deck. Only the top decks of reversible pallets were tested. This modification was not necessary for non-reversible pallet types (BPPC, BOLP, and BPU). Deflections were measured at the mid-spans between the blocks as shown in Figure 5.9. Because only two LVDT's were available for measuring pallet deflections, deflection data were collected for one side of the pallet first, followed by the other side. As done during stringer pallet testing, the third (center) LVDT was attached to the test setup (I-beam) at the pallet center to monitor deformation of the support structure, including I-beam bending. Pallet deflections are adjusted for this factor as discussed in Section 5.2.4.

The bottom deck of non-reversible block pallets was tested in the stack support condition using line loads. As

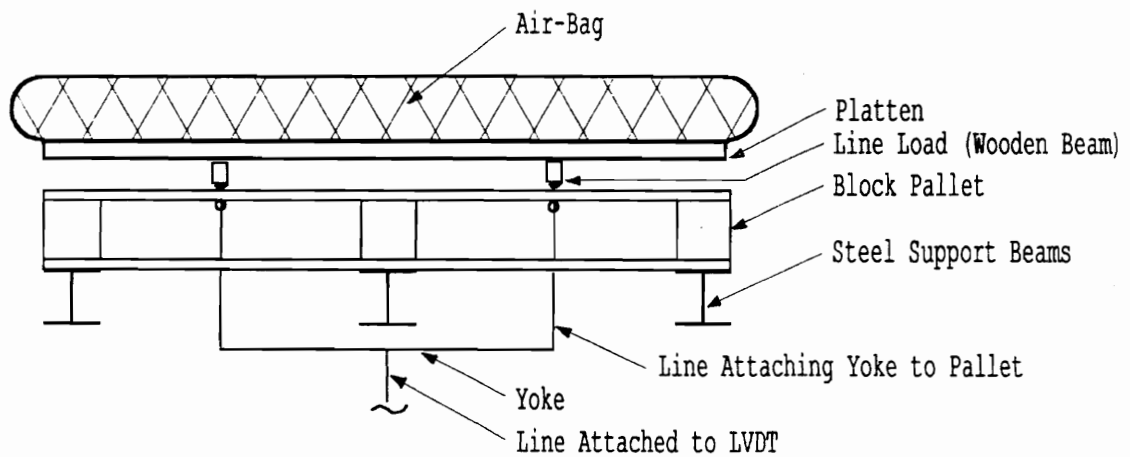


Figure 5.9. Diagram of Block Pallet in the Air-Bag Test Machine with I-Beams positioned to Simulate the Stack Support Condition.

with stringer pallets, load was applied to the bottom deck of the block pallets using a platen with two attached wood members acting as line loads. The platen was inserted between the air-bag and the pallet in the test machine.

Line loads were applied at the mid-spans between the blocks. For pallet types BPPC and BOLP, maximum line loads of 50 pounds per inch were used. When oriented along the 48 inch length of the pallet this was a maximum applied load of 4800 pounds and a maximum of 4000 pounds when oriented across the 40 inch width. For BPU type block pallets, the targeted load was 1600 pounds, two line loads of 20 pounds per inch applied across the width of the pallet. A summary of loads applied to block pallets tested in the stack support condition is presented in Table 5.1.

Deflection measurements were also recorded at the mid-spans between the blocks at each edge. Because only one LVDT was available along each edge, a yoke was used to obtain an average value for both sides at once. Several deckboards did fail during testing. Failures were usually associated with defects such as knots.

5.2.3.2 Rack (RAW and RAL) Support Conditions

Block pallets tested using the air-bag test machine in the rack conditions were either simply supported along the 48 inch sides (RAW) or along the 40 inch sides (RAL), and

Table 5.1. Loads Applied to Block Pallets.

PALLET TYPE (NUMBER)	LOAD TYPE	TOTAL APPLIED LOAD (lbs)
Stack Support Condition (Top Deck):		
BPP (1 - 3)	UDL (2.604 psi)	5000
BPP (16 - 18)	UDL (2.604 psi)	5000
BPPC (7 - 9)	UDL (2.604 psi)	5000
BPU (7 - 9)	UDL (1.0 psi)	1920
BOLP (7 - 9)	UDL (2.604 psi)	5000
BOLP (16 - 18)	UDL (2.604 psi)	5000
Stack Support Condition (Bottom Deck):		
Line Loads Applied along the Width of Pallet:		
BPP (1 - 3)	LL-W (50.0 lbs/in)	4000
BPP (16 - 18)	LL-W (50.0 lbs/in)	4000
BPPC (7 - 9)	LL-W (50.0 lbs/in)	4000
BPU (7 - 9)	LL-W (20.0 lbs/in)	1600
BOLP (7 - 9)	LL-W (50.0 lbs/in)	4000
BOLP (16 - 18)	LL-W (50.0 lbs/in)	4000
Line Loads Applied along the Length of Pallet:		
BPP (1 - 3)	LL-L (50.0 lbs/in)	4800
BPP (16 - 18)	LL-L (50.0 lbs/in)	4800
BPPC (7 - 9)	LL-L (50.0 lbs/in)	4800
BOLP (7 - 9)	LL-L (50.0 lbs/in)	4800
BOLP (16 - 18)	LL-L (50.0 lbs/in)	4800
Racked-Along-Width (RAW) along the Width of Pallet:		
BPP (1 - 3)	UDL (1.0 psi)	1920
BPP (13 - 15)	UDL (1.0 psi)	1920
BPPC (4 - 6)	UDL (1.0 psi)	1920
BPU (4 - 6)	UDL (0.25 psi)	480
BOLP (4 - 6)	UDL (0.5 psi)	960
BOLP (13 - 15)	UDL (0.25 psi)	480
Racked-Across Length (RAL) Support Condition:		
BPP (1 - 3)	UDL (1.0 psi)	1920
BPP (10 - 12)	UDL (1.0 psi)	1920
BPPC (1 - 3)	UDL (1.0 psi)	1920
BPU (1 - 3)	UDL (0.1 psi)	192
BOLP (1 - 3)	UDL (0.5 psi)	960
BOLP (10 - 12)	UDL (0.25 psi)	480

- Notes: 1. UDL = Uniformly Distributed Applied to Entire Surface of Top Deck (Panel)
2. LL-W = Two 40 inch Line Loads
3. LL-L = Two 48 inch Line Loads

free along the other two sides. Figure 5.10 shows rack testing of a block pallet in progress. The test span for all block pallet types tested was either 36 inches in the RAW support Condition or 44 inches in the RAL. The pallets did overhang the supports by 2 inches on each side.

A uniformly distributed load was applied to the top deck of the pallets. The uniform loads applied to the various block pallet types are also given in Table 5.1. The maximum loads given in this table are target values and the actual loads (maximums) applied to the pallets did deviate considerably based on individual pallet performance. As with stringer pallets, deflection values were measured at the mid-span along each free edge and at the pallet center for both the RAW and RAL support conditions.

During testing, gaps did appear to form in the joints of all block pallets tested, although formation was often difficult to observe. Because of the differing pallet designs, the mechanisms of gap formation in block pallets appeared more complex. Figure 5.11 schematically shows gap formation for a BPP type pallet in the rack support conditions. The pattern of gap formation is similar to that observed during stringer pallet testing in the RAD support condition. Gap formation during testing for a perimeter-base pallet in the RAL support condition is illustrated schematically in Figure 5.12. Gap formation is more complex

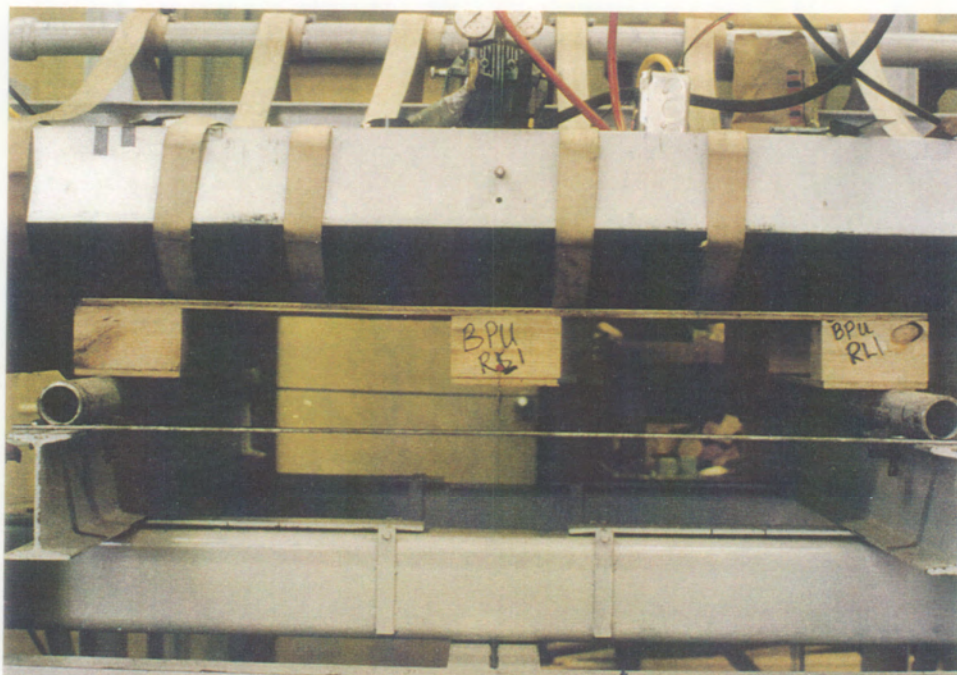


Figure 5.10. Block Pallet being Tested in Flexure (RAL Support Condition) using the Air-Bag Test Machine at VPI & SU.

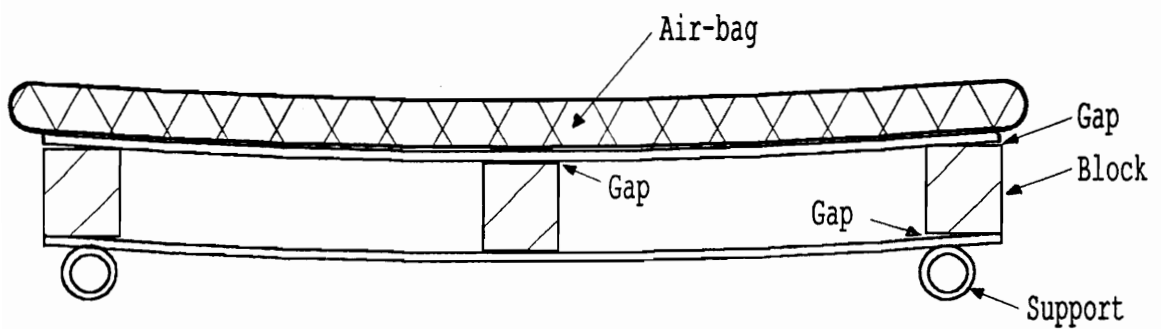


Figure 5.11. Schematic of Observed Gap Formation for BPP Type Block Pallets during Testing in the Rack Support Conditions.

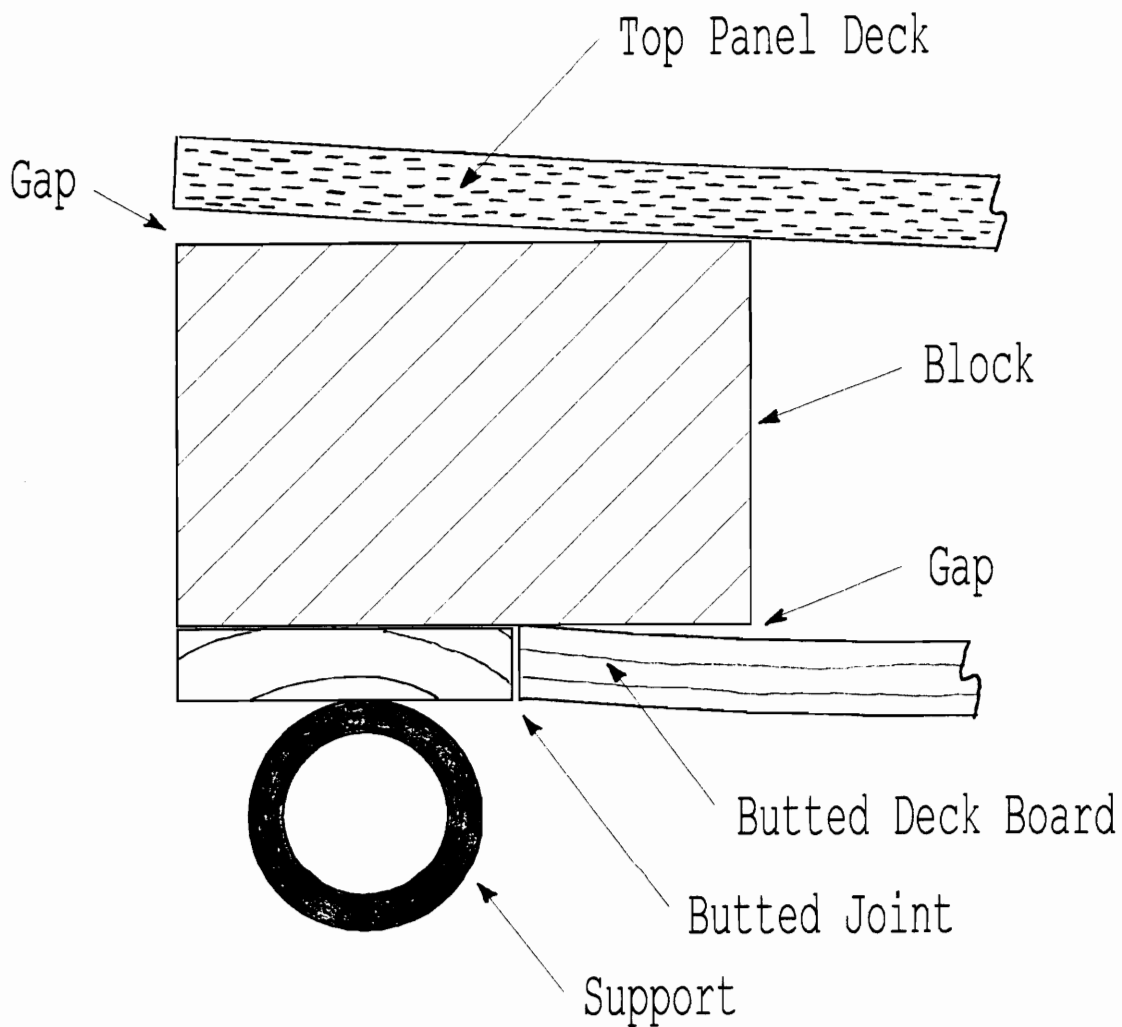


Figure 5.12. Schematic of Observed Gap Formation at the Butted Joint of Perimeter-Base Block Pallets Tested in the Rack Support Conditions.

because of the butted joint. Nonetheless, for all block pallet designs, the blocks function primarily as spacers transferring load from the top deck to the bottom deck.

5.2.4 Data Analysis and Results

Load versus deflection data were recorded by a data acquisition computer as block pallets were loaded in the air-bag test machine. As with stringer pallet data, the data were adjusted for support settlement based on recommendations presented by Mackes et al. (1996). Further discussion of data adjustments is given in Volume II, Section 8 of Mackes (1998).

Typical plots of load versus deflection are similar to those for stringer pallets shown in Figure 4.17. As expected, these plots are linear except at low load levels. Non-linearity's at low load levels were again attributed to pallet joint settlement, support settlement not considered in the data adjustment, and warped pallets. These non-linear data were discarded. The slope of the linear region of load versus deflection plots was calculated using a linear regression analysis. Deflection of the block pallet was then calculated at selected load levels based on the slope for comparison to the plate models. Results of comparisons for the stack, RAW, and RAL support conditions

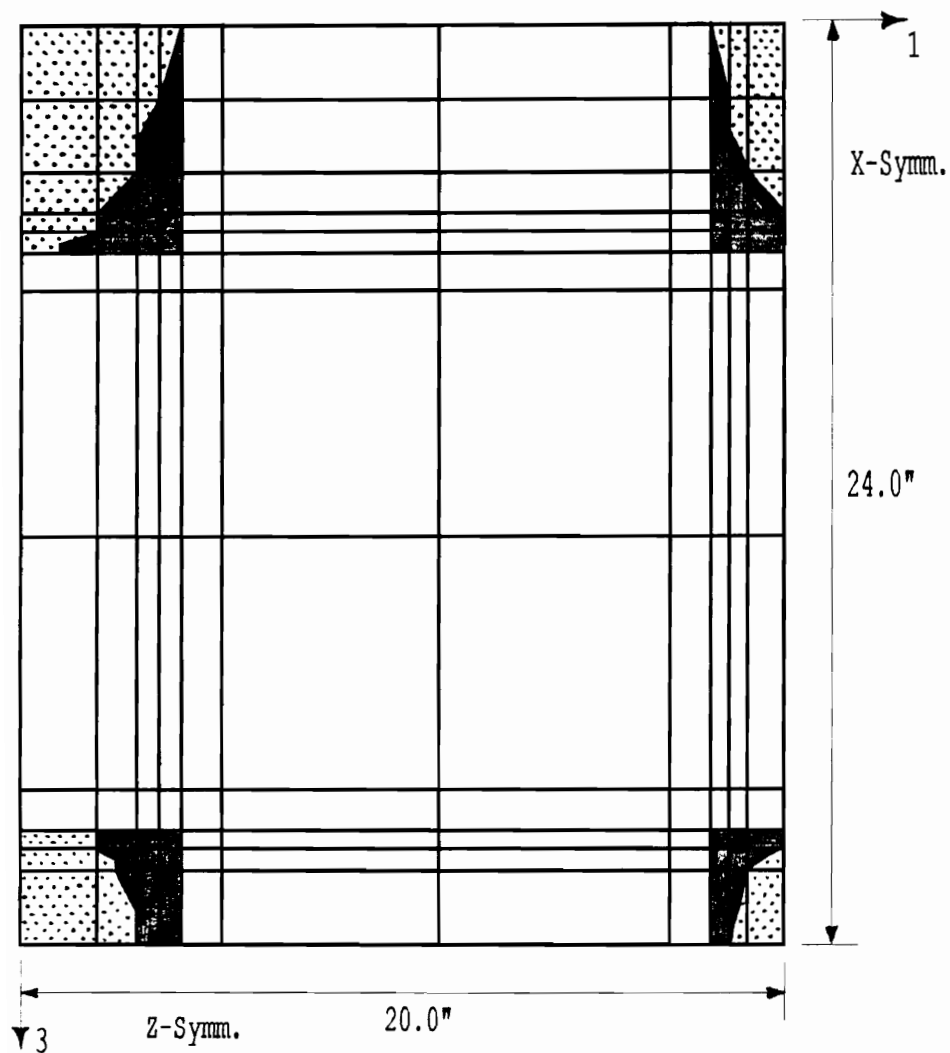
are presented in subsequent sections, along with results for a model assembled to validate solution convergence.

5.2.4.1 Stack Support Condition

Results generated using the plate models were compared to experimental results and observations. Because similar configurations of beam elements were used to model strip-type decking in both the plate and simplified models, predictions generated for these members using the simplified stack model for strip-type decking were compared directly to experimental results. Simplified model predictions for decks with wheel openings were also compared directly to experimental results.

For block pallets tested in the stack support condition, predicted block/top deck contact profiles were generated using plate models, implementing the iterative approach described in Section 5.1.1. The block/top deck contact profile for test pallet BPP-1 is shown in Figure 5.13. Although gap formation during physical block pallet testing was difficult to observe in the stack support condition, the predicted profile appears consistent with observations. Factors which influenced contact area are discussed further in Section 5.3.1.

The deflection profile predicted by the plate model used to predict behavior for the top deck of test pallet



- ▤ - Block Surface beneath Top Deck not in Contact with It
- - Area of Block in Contact with Top Deck (Block/Top Deck Contact Zone)

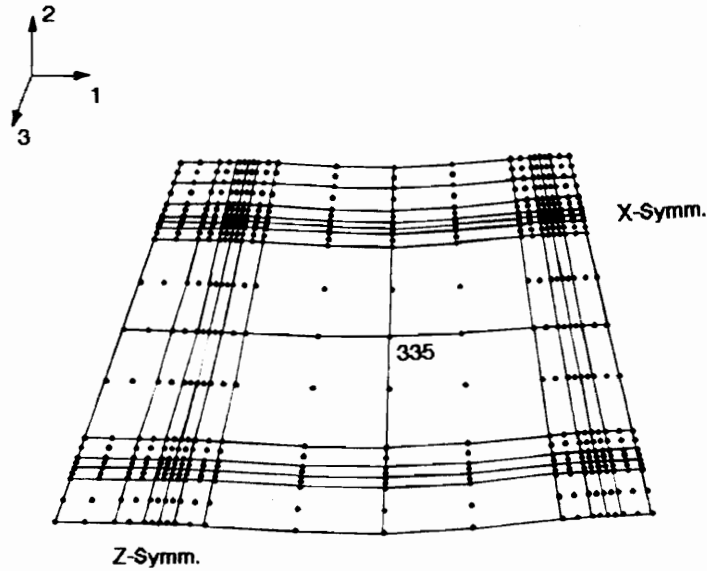
Figure 5.13. Block/Top Deck Contact Profile for Test Pallet BPP-1 Loaded in the Stack Support Condition.

BPP-1 evaluated in the stack support condition is shown in Figure 5.14. As indicated in Figure 5.14, maximum deflection occurred near the center of the section spanning between blocks. This is consistent with experimental observations. At a uniform load of 1.0 psi, the maximum predicted deflection for test pallet BPP-1 is 0.064 inches which agrees closely with the mean of experimentally measured deflections for test pallet BPP-1, 0.060 inches. The difference is 6.7 percent.

A summary of deflection comparisons for all block pallets tested in the stack support condition is presented in Table 5.2. Agreement between predicted and experimental deflections for all the block pallets is good, with differences of less than 9.7 percent.

An S33 Stress profile for test pallet BPP-1 is shown in Figure 5.15. Maximum normal stresses in the deck occurred in the vicinity of the interface with the block corners. Although this phenomenon was not experimentally verified, it seems reasonable that these regions would be areas of high stress. Maximum stresses for all block pallets evaluated in the stack support condition are presented in Table 5.3.

The version of the plate model used to evaluate test pallets BPP-1, BPP-2, and BPP-3 was modified to provide transfer (rolling) shear values for comparison to simplified



- Notes: 1. Deformed state under a uniformly distributed load of -1.0 psi.
2. Maximum deflection (-0.064 inches) occurs at Node 335.
3. Deflections magnified by a factor of 10.

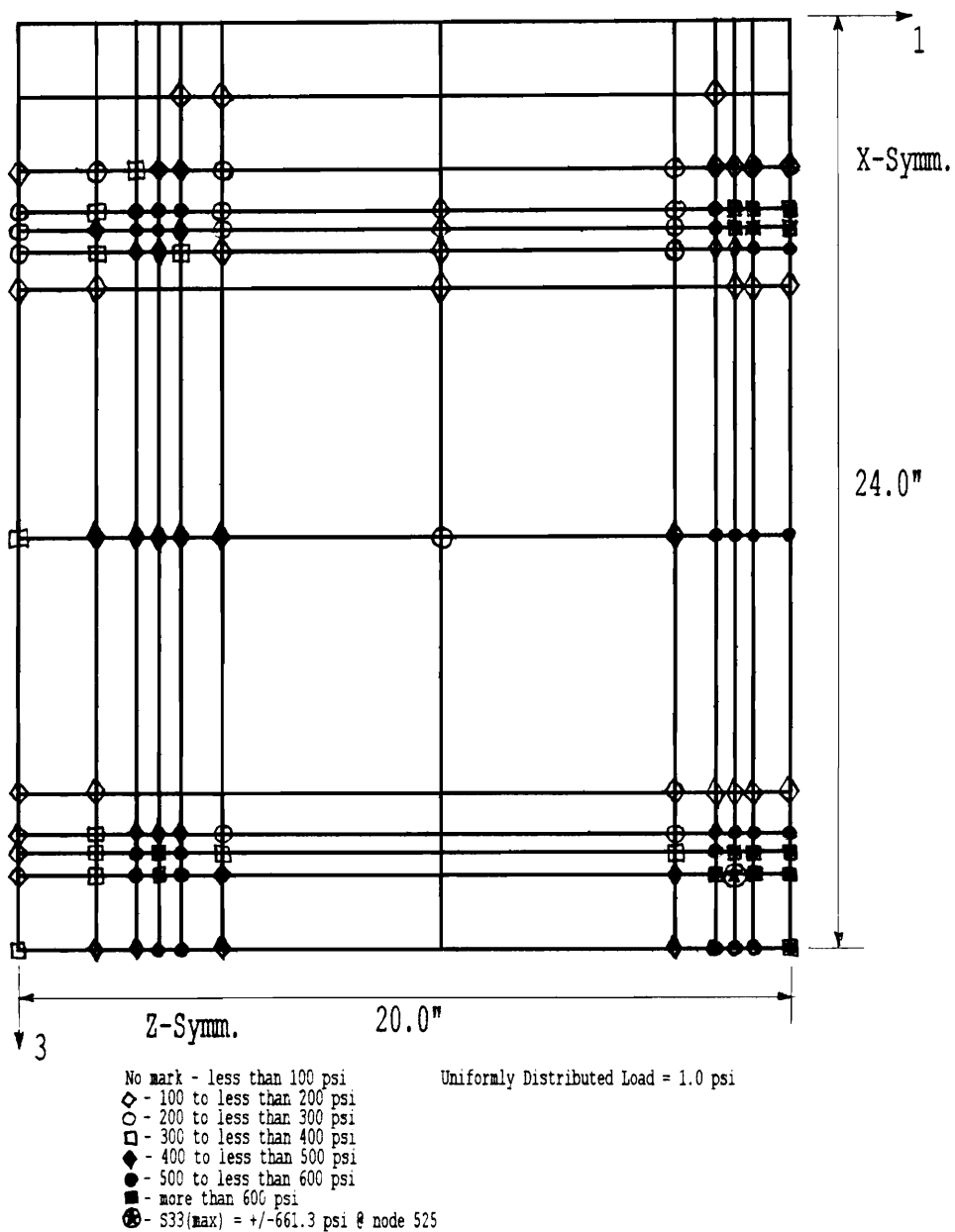
Figure 5.14. Predicted Deflection Profile for the Top Deck of Pallet BPP-1 evaluated in the Stack Support Condition using the Block Pallet Plate Model.

Table 5.2. Comparison of Predicted to Experimental (ABTM) Deflections for the Top Panel Decks of Block Pallets evaluated in the Stack Support Condition.

PALLET ID. NUMBER	PREDICTED DEFLECTION (in.)	ABTM DEFLECTION (in.)	PERCENT DIFFERENCE (%)
BPP-1	-0.064	-0.060	6.7
BPP-2	-0.050	-0.053	-5.7
BPP-3	-0.052	-0.051	2.0
MEAN	-0.055	-0.055	1.2
BPPC-7	-0.059	-0.059	0.0
BPPC-8	-0.061	-0.061	0.0
BPPC-9	-0.073	-0.067	9.0
MEAN	-0.064	-0.062	3.2
BPP-16	-0.068	-0.062	9.7
BPP-17	-0.056	-0.055	1.8
BPP-18	-0.054	-0.056	-3.6
MEAN	-0.059	-0.058	2.9
BOLP-7	-0.061	-0.058	5.2
BOLP-8	-0.056	-0.052	7.7
BOLP-9	-0.058	-0.058	0.8
MEAN	-0.058	-0.056	4.2
BOLP-16	-0.196	-0.189	3.7
BOLP-17	-0.213	-0.207	2.9
BOLP-18	-0.231	-0.215	7.4
MEAN	-0.213	-0.204	4.7
BPU-7	-0.196	-0.197	-0.5
BPU-8	-0.214	-0.219	-2.3
BPU-9	-0.196	-0.204	-3.9
MEAN	-0.202	-0.207	-2.3

Notes: 1. Reported deflections are the mean of four values measured (predicted) at the center of quarter panel sections spanning between the blocks.

2. Applied load equals 1 psi.



S33 Stress Profile

Figure 5.15. Stress Profile for the Top Deck of Test Pallet BPP-1 loaded in the Stack Support Condition.

Table 5.3. Maximum Stresses Predicted for the
Top Panel Deck of Block Pallets evaluated
in the Stack Support Condition.

PALLET ID. NUMBER	MAXIMUM STRESS		
	S11 (+/- psi)	S33 (+/- psi)	S13 (+/- psi)
BPP-1	427.7	661.3	151.9
BPP-2	454.9	697.2	130.0
BPP-3	468.5	723.3	133.2
MEAN	450.4	693.9	138.4
BPPC-7	422.8	848.1	121.0
BPPC-8	418.4	766.7	129.2
BPPC-9	401.0	703.7	147.4
MEAN	414.1	772.8	132.5
BPP-16	373.9	737.1	133.1
BPP-17	416.9	882.5	111.6
BPP-18	478.8	706.3	128.3
MEAN	423.2	775.3	124.3
BOLP-7	470.7	777.6	130.6
BOLP-8	498.1	711.7	128.1
BOLP-9	486.0	770.0	127.8
MEAN	484.9	753.1	128.8
BOLP-16	847.0	1472.0	370.5
BOLP-17	935.8	1520.0	397.9
BOLP-18	953.7	1468.0	421.3
MEAN	912.2	1486.7	396.6
BPU-7	792.6	1204.0	360.6
BPU-8	783.0	1142.0	381.3
BPU-9	849.0	1393.0	360.5
MEAN	808.2	1246.3	367.5

Notes: 1. S11 - Normal stress in the global 1-direction.
S33 - Normal stress in the global 3-direction.
S13 - Shear stress in the global 1-3 plane.

2. Stress values are averaged at the nodes.

3. Uniformly distributed load equals 1.0 psi.

model results. This was accomplished by replacing S9R5 plate elements with S8R elements. Additional changes to the model were minimal, limited to reapportioning the stiffness of affected contact elements and nail joint locations. Maximum stress and deflection values for these three test cases are shown in Table 5.4, along with values for test pallets BPU-7, BPU-8, and BPU-9, which were initially modeled using S8R elements.

5.2.4.2 Rack (RAW and RAL) Support Conditions

Because of plate model complexity and the similarity in pallet behavior between the RAW and RAL support conditions, only selected block pallets were evaluated. In the RAW support condition, test pallets BPP-4, BPP-5, and BPP-6, BPPC-4, BPPC-5, and BPPC-6, and BPU-4, BPU-5, and BPU-6 were evaluated. In the RAL support condition, test pallets BOLP-1, BOLP-2, and BOLP-3 were evaluated.

As for block pallets tested in the stack support condition, predicted block/deck contact profiles were generated for block pallets evaluated in the rack support conditions by implementing the iterative approach described in Section 5.1.1. The block/deck contact profiles for test pallet BPP-1 evaluated in the RAW support condition are shown in Figure 5.16. Predicted profiles were consistent with observations.

Table 5.4. Maximum Stresses, including Transverse (Rolling) Shear Stresses, Predicted for the Top Panel Decks of Block Pallets evaluated in the Stack Support Condition.

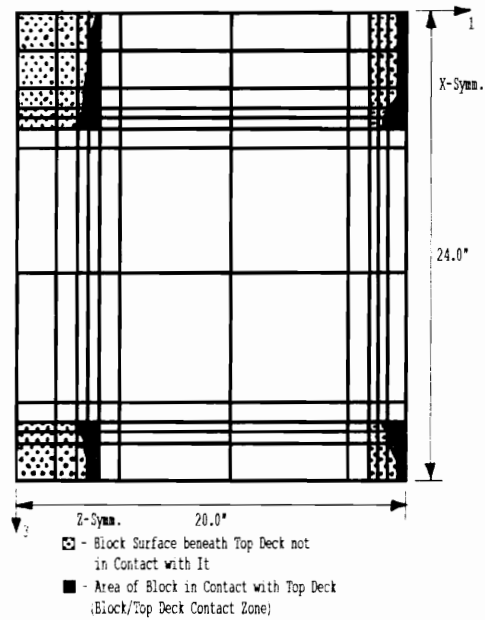
PALLET ID. NUMBER	MAXIMUM STRESS				
	S11 (+/- psi)	S33 (+/- psi)	S13 (+/- psi)	TSHR12 (psi)	TSHR32 (psi)
BPP-1	421.7	680.7	143.2	-52.7	-67.6
BPP-2	449.3	720.2	120.9	-47.1	-63.7
BPP-3	462.3	745.3	125.7	-48.0	-65.0
MEAN	444.4	715.4	129.9	-49.3	-65.4
BPU-7	792.6	1204.0	360.6	-92.9	-152.7
BPU-8	783.0	1142.0	381.3	-94.4	-153.3
BPU-9	849.0	1393.0	360.5	-93.6	-164.1
MEAN	808.2	1246.3	367.5	-93.6	-156.7

- Notes:
1. S11 - Normal stress in the global 1-direction.
S33 - Normal stress in the global 3-direction.
S13 - Shear stress in the global 1-3 plane.
TSHR12 - Tranverse (rolling) shear in the global 1-2 plane.
TSHR32 - Tranverse (rolling) shear in the global 3-2 plane.
 2. Stress values are averaged at the nodes.
 3. Uniformly distributed load equals 1.0 psi.

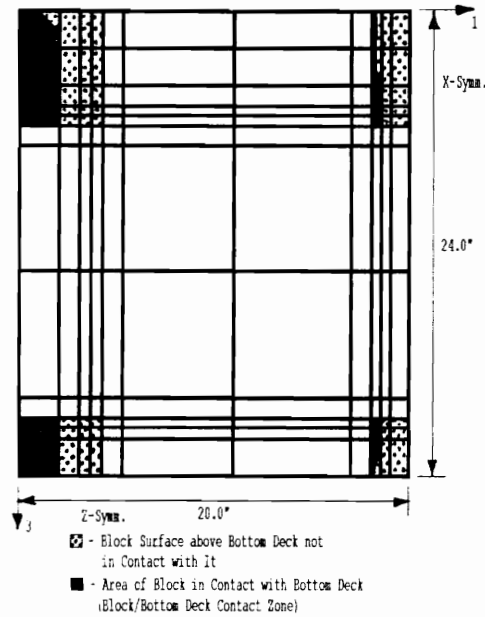
The deformed state predicted by the plate model used to predict behavior for test pallet BPP-1 evaluated in the RAW support condition is shown in Figure 5.17. Maximum deflection of the upper deck occurred at mid-span between blocks. Maximum deflection of the lower deck occurred at the pallet center which was consistent with experimental observations. At a uniform load of -0.5 psi, the maximum predicted deflection for test pallet BPP-1 was -0.257 inches. This agreed closely with the experimentally measured deflection of -0.261 inches, a difference of 1.6 percent.

A summary of deflection comparisons for the block pallets evaluated in the rack support conditions is presented in Table 5.5. Mean differences between predicted and experimental deflections for all the block pallet types evaluated are not greater than 10.5 percent.

A profile of S11 stress for the top deck of test pallet BPP-1 is shown in Figure 5.18. The model predicted that the highest regions of stress occur in the top deck (lower surface) where it interfaces with the edge blocks located over the rack support. Lower maximum stresses were predicted for the bottom deck. A summary of maximum stress predictions for all block pallets evaluated in the rack support conditions is given in Table 5.6.

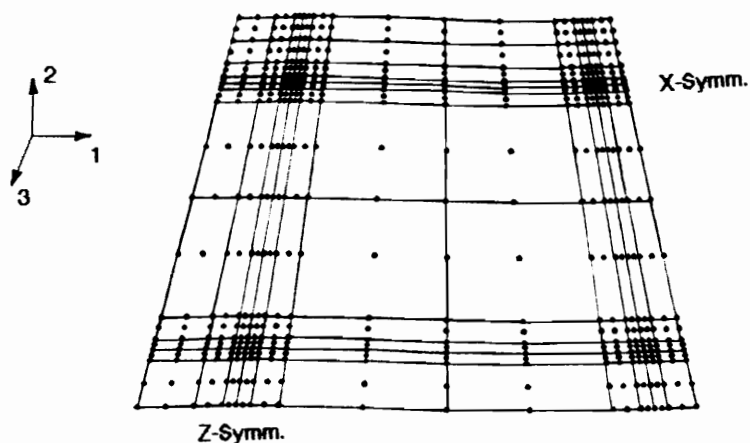


Block/Top Deck Contact Profile

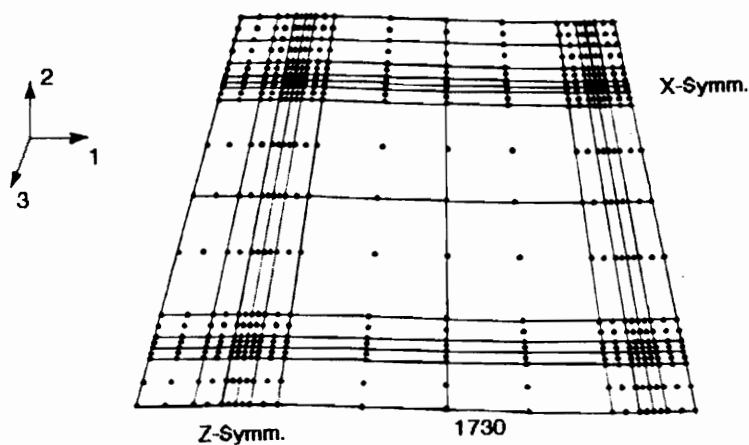


Block/Bottom Deck Contact Profile

Figure 5.16. Block/Deck Contact Profiles for Test Pallet BPP-1 Loaded in the RAW Support Condition.



Top Deck (Deformed State)



Bottom Deck (Deformed State)

- Notes: 1. Deformed state under a uniformly distributed load of -0.5 psi.
2. Maximum bottom deck deflection (-0.257 inches) occurs at Node 1730.
3. Deflections magnified by a factor of 4.

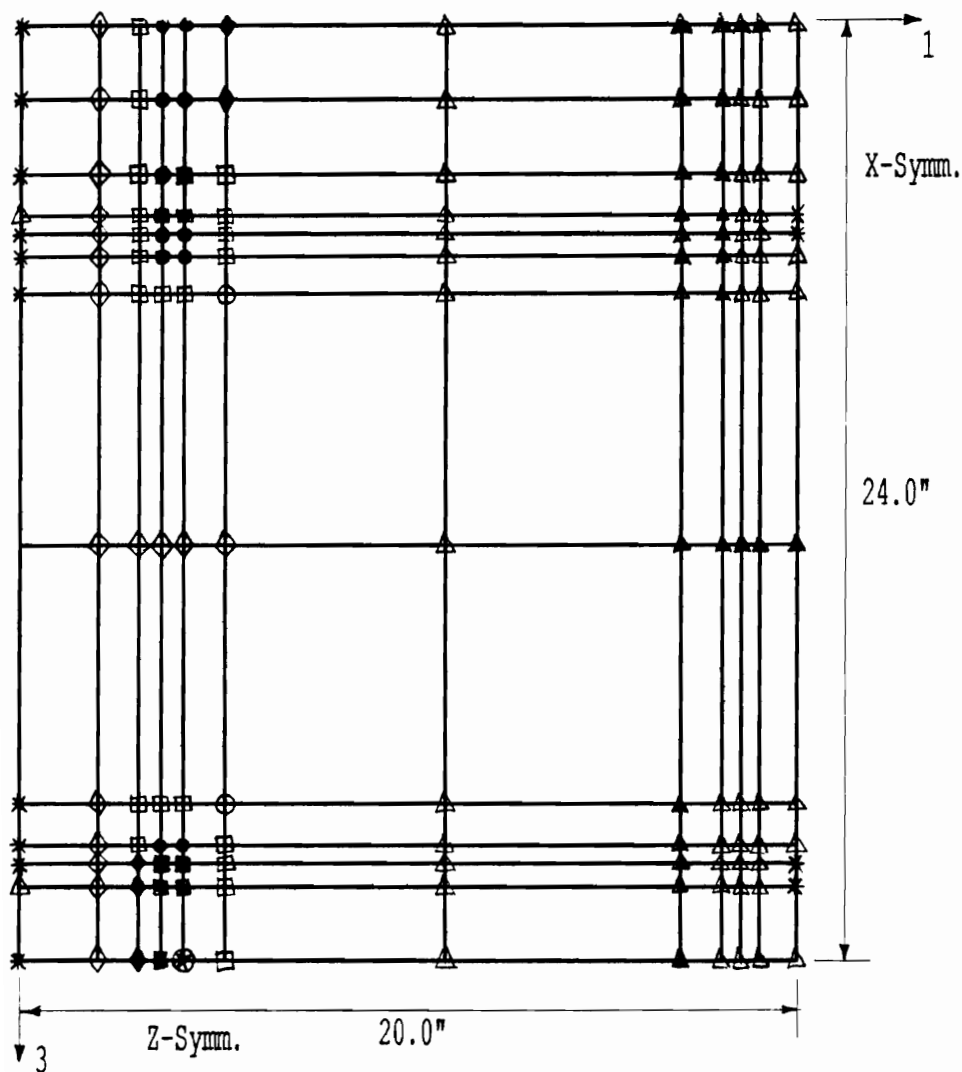
Figure 5.17. Predicted Deflection Profiles for the Decks of Pallet BPP-1 evaluated in the Racked-Across-Width Support Condition using the Block Pallet Plate Model.

**Table 5.5. Comparison of Predicted to Experimental
(ABTM) Deflections for the Bottom Decks of Block
Pallets evaluated in the Rack Support Conditions.**

PALLET ID. NUMBER	EDGE AT MID-SPAN			PALLET CENTER		
	BPPM D (in.)	ABTM D (in.)	DIF (%)	BPPM D (in.)	ABTM D (in.)	DIF (%)
Racked-Across-Width Support Condition:						
BPP-1	-0.250	-0.261	-4.2	-0.257	-0.261	-1.5
BPP-2	-0.197	-0.213	-7.5	-0.203	-0.223	-9.0
BPP-3	-0.206	-0.217	-5.1	-0.212	-0.223	-4.9
MEAN	-0.218	-0.230	-5.5	-0.224	-0.236	-5.0
BPPC-4	-0.268	-0.269	-0.4	-0.281	-0.279	0.7
BPPC-5	-0.233	-0.213	9.4	-0.247	-0.221	11.8
BPPC-6	-0.248	-0.234	6.0	-0.261	-0.247	5.7
MEAN	-0.250	-0.239	4.6	-0.263	-0.249	5.6
BPU-4	-0.140	-0.140	0.0	-0.165	-0.170	-2.9
BPU-5	-0.124	-0.114	8.8	-0.150	-0.153	-2.0
BPU-6	-0.123	-0.128	-3.9	-0.152	-0.157	-3.2
MEAN	-0.129	-0.127	1.3	-0.156	-0.160	-2.7
Racked-Across-Length Support Condition:						
BOLP-1	-0.143	-0.156	-8.3	-0.197	-0.179	10.1
BOLP-2	-0.152	-0.170	-10.6	-0.210	-0.182	15.4
BOLP-3	-0.146	-0.162	-9.9	-0.201	-0.190	5.8
MEAN	-0.147	-0.163	-9.6	-0.203	-0.184	10.5

Notes: 1. BPPM - Block Pallet Plate Model Predictions
 ABTM - Experimentally Measured Deflection
 DIF - Difference between BPPM and SBM
 predictions.

2. Predictions reported are for pallets under the
 following uniformly distributed loads:
 Type BPP, BPPC, and BOLP Pallets - 0.125 psi
 Type BPU - 0.5 psi



- | | |
|--------------------------------|-----------------------------------|
| ■ - more than -600 psi | ◇ - -100 to less than -200 psi |
| ● - -500 to less than -600 psi | No mark - 0 to less than -100 psi |
| ◆ - -400 to less than -500 psi | * - 0 to less than 100 psi |
| □ - -300 to less than -400 psi | △ - 100 to less than 200 psi |
| ○ - -200 to less than -300 psi | ▲ - more than 200 psi |

⊕ - $S_{11}(\max) = -663.3$ psi @ node 561

Uniformly Distributed Load = 0.5 psi

S_{11} Stress Profile (Lower Surface)

Figure 5.18. Stress Profile for the Top Deck of Test Pallet BPP-1 loaded in the Rack Support Condition.

Table 5.6. Maximum Stress Predictions for Block Pallets evaluated in the Rack Support Conditions using Block Pallet Plate Models.

PALLET ID. NUMBER	TOP DECK			BOTTOM DECK		
	S11 (psi)	S33 (psi)	S13 (psi)	S11 (psi)	S33 (psi)	S13 (psi)
Racked-Across-Width Support Condition:						
BPP-1	663.3	582.8	256.4	473.6	419.2	222.9
BPP-2	666.0	586.1	220.9	478.5	452.3	205.5
BPP-3	694.3	615.9	227.9	498.5	476.7	211.6
MEAN	674.5	594.9	235.1	483.5	449.4	213.3
BPPC-4	525.7	548.3	232.5	435.0	332.9	332.1
BPPC-5	539.2	522.6	213.5	455.5	260.9	314.3
BPPC-6	520.6	580.5	218.1	484.7	343.5	331.5
MEAN	528.5	550.5	221.4	458.4	312.4	326.0
BPU-4	291.2	196.6	177.7	510.6	***	***
BPU-5	267.2	176.2	169.2	544.8	***	***
BPU-6	305.0	229.9	159.3	457.8	***	***
MEAN	287.8	200.9	168.7	504.4	***	***
Racked-Across-Length Support Condition:						
BOLP-1	576.7	1675.0	329.7	***	1961.0	***
BOLP-2	601.7	1660.0	345.7	***	1740.0	***
BOLP-3	603.6	1771.0	334.1	***	1520.0	***
MEAN	594.0	1702.0	336.5	***	1740.3	***

- Notes: 1. Predictions reported are for pallets under the following uniformly distributed loads:
Type BPP, BPPC, and BOLP Pallets - 0.5 psi
Type BPU - 0.125 psi
2. Reported stress predictions (magnitudes) are absolute.

5.3 Block Pallet Sensitivity Studies

Block pallet sensitivity studies for the stack and rack (RAW and RAL) support conditions are presented in this section. Similar to stringer pallet sensitivity studies, block pallet studies were used to systematically determine which geometric and material properties significantly influence block pallet behavior. The approach used was also the same. The property value of interest was reduced by a factor of 0.5 and increased by a factor of 2.0, with all other properties remaining unchanged. Response of the whole structure was then compared, calculating the percentage of change in both maximum normal stress (S11 or S33) and deflection (D2). Block pallet sensitivity studies formed a rational basis for reducing the degrees of freedom required to predict block pallet behavior in simplified PC-based pallet models.

5.3.1 Stack Condition

Sensitivity Studies were conducted using block pallet plate models. Test case BPP-1 data were used for this evaluation. As with stringer pallet models, bottom deck properties were not significant (important) if the top deck was being evaluated (loaded) and vice versa. Therefore, focus was on the deck being loaded.

Results for geometric and material properties evaluated are presented in Table 5.7. Panel thickness and the moduli

**Table 5.7. Sensitivity of the Block Pallet Plate Model
to Changes in Geometric and Material Properties
in the Stack Support Condition.**

PROPERTY ALTERED	0.5 X ACTUAL PROPERTY VALUE				2.0 X ACTUAL PROPERTY VALUE			
	MAXIMUM S33 (psi)	CHANGE (%)	MAXIMUM D2 (in)	CHANGE (%)	MAXIMUM S33 (psi)	CHANGE (%)	MAXIMUM D2 (in)	CHANGE (%)
Top Deck Properties (loaded surface):								
T	3013.0	355.6	-0.3913	511.4	203.7	-69.2	-0.0128	-80.0
E1	750.1	13.4	-0.0991	54.8	643.9	-2.6	-0.0444	-30.6
E3	589.3	-10.9	-0.0787	23.0	883.5	33.6	-0.0556	-13.1
V12	625.0	-5.5	-0.0646	0.9	735.4	11.2	-0.0620	-3.1
G	723.7	9.4	-0.0647	1.1	591.5	-10.6	-0.0634	-0.9

Notes: 1. Property Data are for Test Pallet BPP1.

Top Deck Properties (loaded surface):

Panel Thickness (T) = 0.0571 inches

E1 = 0.339 E+6 psi; E3 = 1.469 E+6 psi

V12 = 0.048; G12 = G13 = G23 = 0.325 E+6 psi

2. For a uniformly distributed load of 1 psi,

Maximum Predicted Stress (S33) = +/-661.3 psi

Maximum Predicted Deflection (D2) = -0.0640 in.

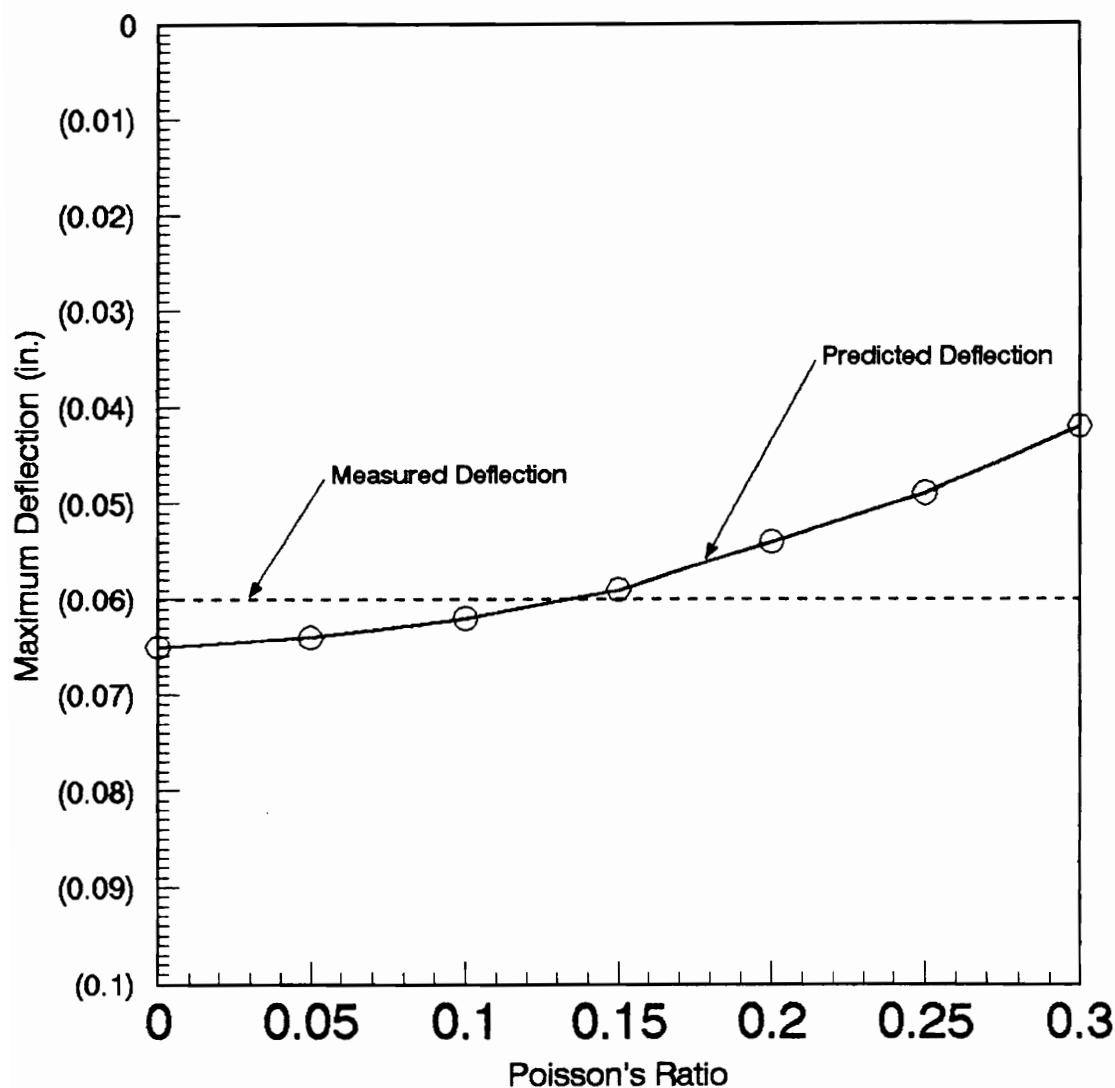
3. Absolute maximum stress (S11) magnitudes are reported.

of elasticity in both principal axes of the panel were important. Unlike the stringer pallet models where Poisson's ratio and moduli of rigidity have little impact on model predictions, these factors had a significant, but still relatively small effect on block model solutions. These effects are further illustrated for Poisson's ratio by Figures 5.19 and 5.20.

Joint properties were evaluated and results are shown in Table 5.8. While withdrawal/head embedment stiffness was significant, lateral stiffness was not. Therefore lateral stiffness can be removed from simplified models used to predict block pallet behavior in the stack support condition. As with stringer pallet models, the stiffness assigned to contact elements significantly affected deflection, but did not have a significant effect on stresses.

5.3.2 Rack (RAW and RAL) Support Conditions

As for pallets supported in the stack support condition, sensitivity studies were conducted for the rack support conditions using block pallet plate models. Test case BPP-1 data were again used in this evaluation. Geometric, material, and joint properties were evaluated. Because test pallet BPP-1 behaves similarly in both RAW and RAL support conditions, only the RAW analysis is presented.



Uniformly Distributed Load = 1 psi

Figure 5.19. The Effect of Poisson's Ratio on the Maximum Predicted Top Deck Deflection of Test Pallet BPP1 Uniformly Loaded in the Stack Support Condition.

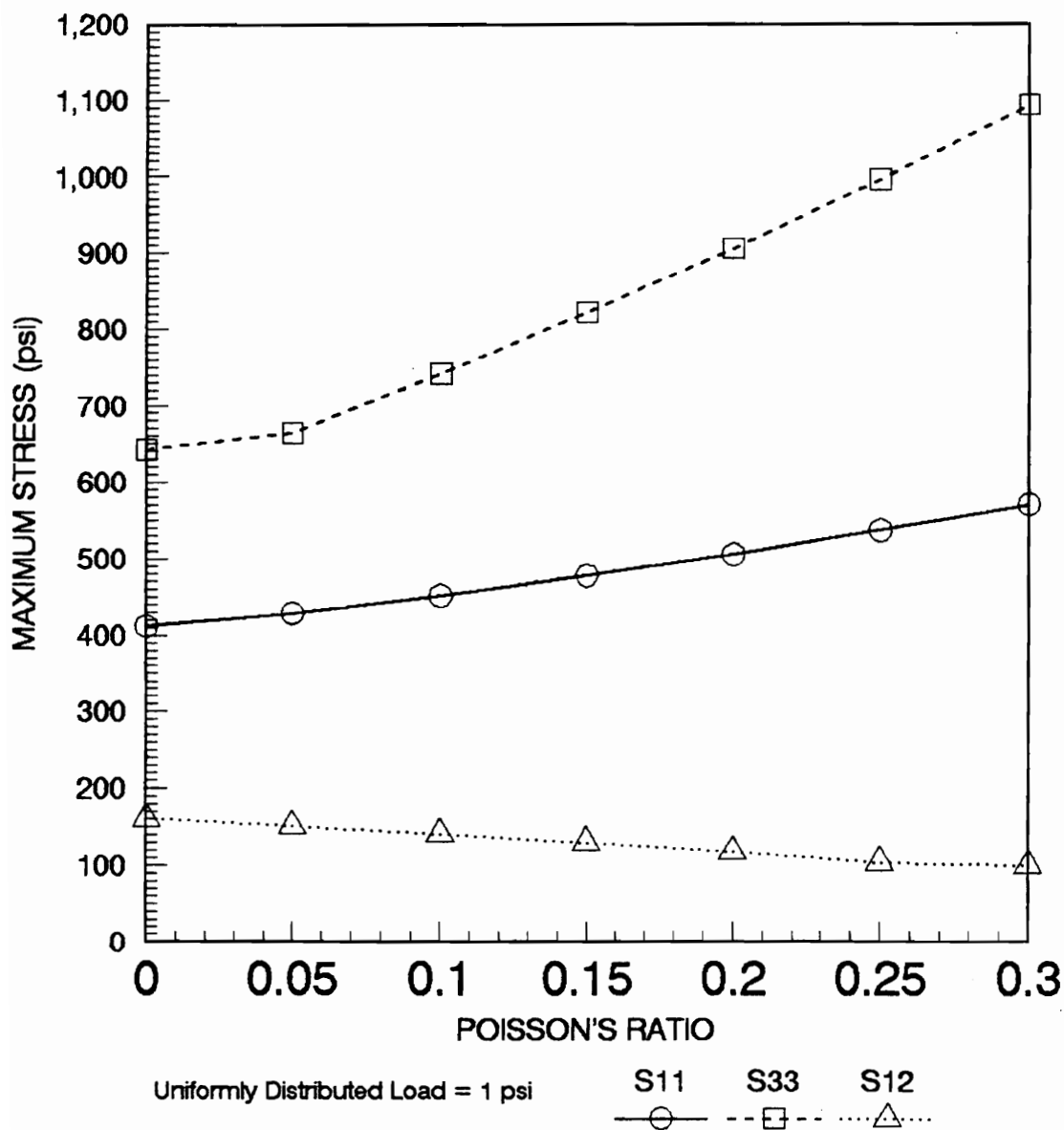


Figure 5.20. The Effect of Poisson's Ratio on the Maximum Predicted Top Deck Stresses of Test Pallet BPP1 Uniformly Loaded in the Stack Support Condition.

**Table 5.8. Sensitivity of the Block Pallet Plate Model
to Changes in Block/Deck Contact and Nail Joint
Properties in the Stack Support Condition.**

PROPERTY ALTERED	0.5 X ACTUAL PROPERTY VALUE				2.0 X ACTUAL PROPERTY VALUE			
	MAXIMUM S33 (psi)	CHANGE (%)	MAXIMUM D2 (in)	CHANGE (%)	MAXIMUM S33 (psi)	CHANGE (%)	MAXIMUM D2 (in)	CHANGE (%)
Block/Top Deck Contact Siffness Properties:								
K(CS)	710.4	7.4	-0.0709	10.8	670.9	1.5	-0.0586	-8.4
Withdrawal/Head Embedment Siffness Properties:								
K(W/HE)	667.1	0.9	-0.0650	1.6	656.6	-0.7	-0.0633	-1.1
Lateral Stiffness Properties:								
K(LS1)	661.3	0.0	-0.0640	0.0	661.3	0.0	-0.0640	0.0
K(LS3)	661.3	0.0	-0.0640	0.0	661.3	0.0	-0.0640	0.0

- Notes: 1. Property data are for Test Pallet BPP1.
2. For a uniformly distributed load of 1 psi,
Maximum Predicted Stress (S33) = +/-661.3 psi
Maximum Predicted Deflection (D2) = -0.0640 inches
3. Absolute maximum stress (S11) magnitudes are reported.

A summary of results for the geometric and material properties evaluated are presented in Table 5.9. Panel thickness and the modulus of elasticity in both principal axes of the panel were important. The effect of Poisson's ratio (ν_{12}) and moduli of rigidity on block pallet behavior were more significant than for stringers pallets, but still small. Because blocks act as spacers and stiffen the system through composite action, results reveal that changing the spacing between decks had a significant effect on block pallet behavior. Therefore, in the rack support conditions, accurately modeling the distance between the neutral axes of the top and bottom decks was important.

Results for model sensitivity to changing joint properties are presented in Table 5.10. Lateral stiffness in the direction spanning the rack supports was important. In the example given, test pallet BPP-1 racked-across-width, this was the 1-direction. Lateral stiffness perpendicular to this direction had no effect. Withdrawal/head embedment and the stiffness assigned to contact elements were also not as significant.

5.4 Development of PC Compatible Block Pallet Models

PC compatible block pallet models were more complex than stringer pallet models requiring the use of extended PC memory. While still compatible with current PDS versions

**Table 5.9. Sensitivity of the Block Pallet Plate Model
to Changes in Geometric and Material Properties
in the Rack (RAW) Support Condition.**

PROPERTY ALTERED	0.5 X ACTUAL PROPERTY VALUE				2.0 X ACTUAL PROPERTY VALUE			
	MAXIMUM NS (psi)	CHANGE (%)	MAXIMUM D2 (in)	CHANGE (%)	MAXIMUM NS (psi)	CHANGE (%)	MAXIMUM D2 (in)	CHANGE (%)
Top Deck Properties (loaded surface):								
T	*1957.0	235.8	-0.4305	67.6	181.6	-72.6	-0.0948	-63.1
E1	784.6	18.3	-0.3188	24.1	786.9	18.6	-0.1960	-23.7
E3	667.7	0.7	-0.2595	1.1	*829.7	42.4	-0.2532	-1.4
V12	656.6	-1.0	-0.2579	0.4	*692.1	18.8	-0.2532	-1.4
G	712.1	7.4	-0.2613	1.8	616.3	-7.1	-0.2525	-1.7
Bottom Deck Properties (no load applied directly to surface):								
T	982.2	48.1	-0.4143	61.3	*409.3	-29.8	-0.0877	-65.8
E1	784.6	18.3	-0.3188	24.1	**625.1	32.0	-0.1949	-24.1
E3	668.2	0.7	-0.2596	1.1	656.9	-1.0	-0.2532	-1.4
V12	665.2	0.3	-0.2577	0.4	657.0	-0.9	-0.2537	-1.2
G	670.1	1.0	-0.2607	1.5	656.6	-1.0	-0.2530	-1.5
Deck Spacing:								
DS	613.0	-7.6	-0.3396	32.2	685.7	3.4	-0.2322	-9.6

Notes: 1. Property data are for Test Pallet BPP1.

See Table 5.7 for property values assigned to members.

Both top and bottom decks were taken from the same panel and have the same properties.

2. Maximum Predicted Normal Stresses (NS):

Top Deck: S11 = -663.3 psi; S33 = +582.8 psi

Bottom Deck: S11 = +473.6 psi; S33 = +419.2 psi

Maximum Predicted Deflection (D2):

Bottom Deck: D2 = -0.2568 inches

3. Absolute maximum normal stress (NS) values are reported.

4. Maximum NS occurred in the same location as the initial test case except as indicated (see below):

"*" - Indicates that S33 was maximum and occurred in the top deck.

"***" - Indicates that S11 was maximum and occurred in the bottom deck.

**Table 5.10. Sensitivity of the Block Pallet Plate Model
to Changes in Block/Deck Contact and Nail Joint
Properties in the Rack (RAW) Support Condition.**

PROPERTY ALTERED	0.5 X ACTUAL PROPERTY VALUE				2.0 X ACTUAL PROPERTY VALUE			
	MAXIMUM S11 (psi)	CHANGE (%)	MAXIMUM D2 (in)	CHANGE (%)	MAXIMUM S11 (psi)	CHANGE (%)	MAXIMUM D2 (in)	CHANGE (%)
Block/Top Deck Contact Siffness Properties:								
K(CS)	652.1	-1.7	-0.2669	3.9	677.1	2.1	-0.2489	-3.1
Withdrawal/Head Embedment Siffness Properties:								
K(W/HE)	650.5	-1.9	-0.2658	3.5	667.1	0.6	-0.2502	-2.6
Lateral Stiffness Properties:								
K(LS1)	624.4	-5.9	-0.2823	9.9	685.9	3.4	-0.2432	-5.3
K(LS3)	663.9	0.1	-0.2570	0.1	662.8	-0.1	-0.2566	-0.1

Notes: 1. Property data are for Test Pallet BPP1.

2. Maximum Predicted Normal Stresses (NS):

Top Deck: S11 = -663.3 psi; S33 = +582.8 psi

Bottom Deck: S11 = +473.6 psi; S33 = +419.2 psi

Maximum Predicted Deflection (D2):

Bottom Deck: D2 = -0.2568 inches

3. Absolute maximum normal stress (NS) values are reported.

4. Maximum S11 stress values reported in the table are for the top deck.

and capable of running on a 286 or more Powerful PC, these models were developed to provide solutions in less than 2 minutes on more advanced 486 microcomputers with high speed processors (50 mhz or greater). Solution times on less powerful machines will be longer.

PC compatible models were simplified from corresponding plate models for block pallets. The process used to develop simplified models with reduced degrees of freedom is presented in this section. Separate models were developed for the stack and rack (RAW and RAL) support conditions. Additional efficiency was gained by using separate models based on pallet configuration. This was true for both stack and rack support conditions. Methodologies developed for modeling cut-outs, including top deck hand-holds and bottom deck wheel openings are also presented.

5.4.1 Stack Support Condition

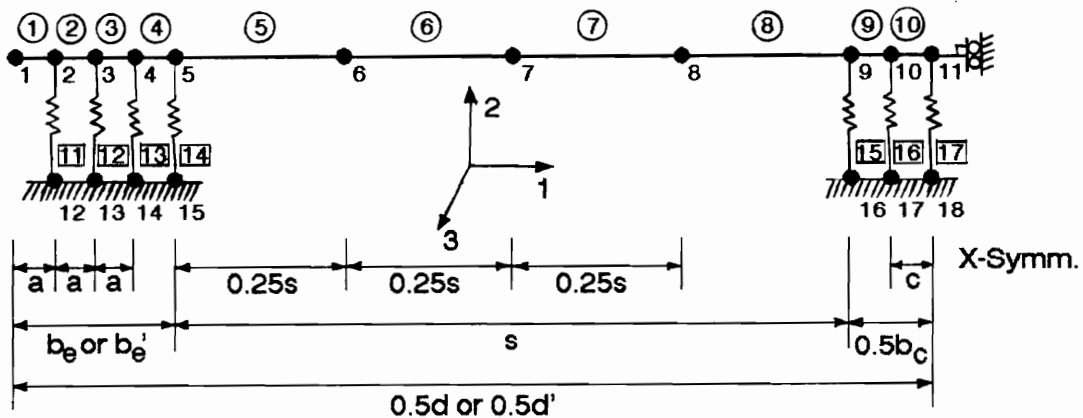
In this research, two separate models were used to predict block pallet behavior in the stack support condition. A two-dimensional model was used to simulate lumber bottom decks and a three-dimensional grid model to simulate panel decks. The grid model was used to model full uniformly, partial uniformly, and line loaded block pallets in the stack support condition. Stack models for block pallets are discussed further in subsequent sections.

5.4.1.1 Bottom Strip-Type Deck Model

The PC model developed to predict the behavior of strip-type bottom decks was two-dimensional. Strip-type decking included lumber deckboards and strips of plywood or OSB. The final version of this two-dimensional stack model is shown in Figure 5.21. The model used x-symmetry. The block and lower deck response was incorporated into contact elements; therefore, only the bottom deck was used. Beam elements were used to model the bottom deck and zero-length springs to model nail joints and contact zones. Lateral stiffness of nail joints was not considered.

Node and element locations for the test cases evaluated are presented by Mackes (1998, Volume III, Section 6), along with an example of an ABAQUS input file. Geometric inputs to the model included thickness and width. The primary material input was modulus of elasticity (E) along the length of the strip (deckboard). For uniformly distributed loads, strips were modeled individually with loads assigned based on tributary area. For rigid line loads, the width of strips were summed and the members were modeled in aggregate. An average thickness and modulus of elasticity value were used for the aggregate.

Withdrawal/head embedment stiffness of the nail joints was considered in this model using axial springs. For solid lumber blocks, spring stiffness (k_w/h_e) was determined using



Where: b_e = Edge Block Width or Length
 b_e' = Edge Block Width or Length in Contact with
 Butted-Deckboard (Perimeter-Base Pallets)
 b_c = Center Block Width or Length
 a = $0.25b_e$ or $0.25b_e'$
 c = $0.5b_c$
 s = Span Between Blocks
 d = Deckboard Length
 d' = Butted-Deckboard Length (Perimeter-Base Pallets)

/// - Restrained in the 1- and 2-Directions, and the Sixth Rotational Degree of Freedom

—|— - Restrained in the 1-Direction and the Sixth Rotational Degree of Freedom

—•— - Beam Element Connecting Two Nodes (1 - 10)

—•— - Contact Element and Potential Nail Joints (11 - 17)

Notes: 1. Elements 1 through 10 are bottom deck beam elements.
 2. Elements 14 and 15 are contact elements.
 3. Elements 11, 12, 13, 16, and 17 are potential nail joint locations (withdrawal/head embedment stiffness).

Figure 5.21. Simplified Model for the Bottom Decks of Perimeter- and Unidirectional-Base Block Pallets in the Stack Support Condition.

the methodology outlined in Section 3.5.1. A spring constant of 12,000 pounds per inch was used for composite blocks of plywood or OSB.

Only 9-block pallets were physically evaluated (tested) in this research for comparison to the model. However, this model can be used to evaluate 4, 5, and 6 block pallets by using dummy (near zero stiffness) contact and nail joint elements appropriately. All block contact elements were active when modeling 9-block pallets.

To validate the simplified model, deflections and maximum stresses obtained using this model were compared to experimental deflections. These comparisons are presented in Table 5.11. Agreement between the simplified PC model and the three dimensional plate models is good with differences of 11.0 percent or less. An example of stress and deflection profiles generated by the model for test case BOLP7 (along the width) is shown in Figure 5.22. These profiles indicate that the model was performing as expected.

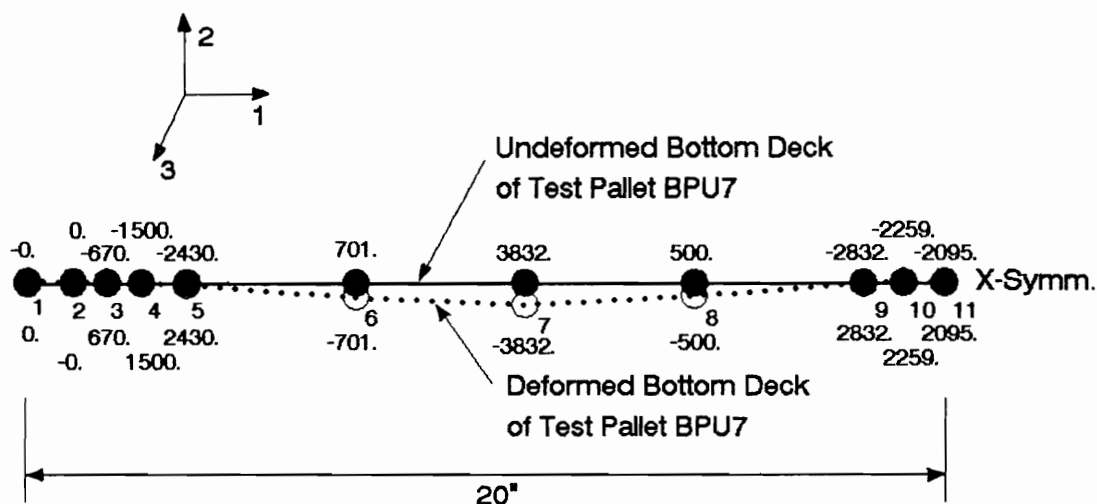
5.4.1.2 Panel Deck Model

A three-dimensional grid model was used to simulate the panel decks of block pallets supported in the stack condition. The grid model developed is shown in Figure 5.23. An example of the ABAQUS input file for this model is given in Volume III, Section 7 of Mackes (1998). It had 19

Table 5.11. Maximum Stress and Deflection Predictions generated using the Simplified Model for the Bottom Deck of Perimeter-Base Block Pallets in the Stack Support Condition.

PALLET ID.	FEM S1 (max) (psi)	FEM D2 (max) (psi)	EXP D2 (max) (in.)	PERCENT DIFFERENCE
LENGTH ORIENTATION (LINE LOAD APPLIED ALONG THE WIDTH)				
BOLP-7	2758	-0.116	-0.129	-10.1
BOLP-8	2799	-0.112	-0.113	-0.9
BOLP-9	2753	-0.104	-0.104	0.0
MEAN	2770	-0.111	-0.115	-4.0
BOLP-16	2805	-0.092	-0.083	10.8
BOLP-17	2867	-0.104	-0.099	5.1
BOLP-18	2735	-0.126	-0.132	-4.5
MEAN	2802	-0.107	-0.105	2.5
WIDTH ORIENTATION (LINE LOAD APPLIED ALONG THE LENGTH)				
BOLP-7	3776	-0.144	-0.144	0.0
BOLP-8	3887	-0.120	-0.132	-9.1
BOLP-9	3813	-0.120	-0.115	4.3
MEAN	3825	-0.128	-0.130	-1.8
BOLP-16	3704	-0.141	-0.127	11.0
BOLP-17	3716	-0.122	-0.127	-3.9
BOLP-18	3798	-0.124	-0.126	-1.6
MEAN	3739	-0.129	-0.127	1.8

- Notes:
1. FEM S1(max) is the maximum predicted (finite element model) stress in the 1-direction
 2. FEM D2(MAX) is the maximum predicted (finite element model) deflection in the 2-direction
 3. EXP D2(MAX) = Maximum experimental (air-bag test machine) deflection in the 2-direction
 4. Two rigid line loads applied at the mid-span between blocks (Applied load = 1920 pounds)



- Notes:
1. Stress magnitudes are maximum values averaged at each node.
 2. Units of stress magnitude are psi.
 3. Maximum stress occurs at Node 7 and has a magnitude of ± 3832 psi.
 4. Maximum deflection occurs at Node 7 and is -0.266 inches.
 5. Line-load of 20 pounds per inch (960 pounds) applied at node 7.

- - Nodes
 ---- - Beam Elements in deformed state

Figure 5.22. Stress (S11) and Deflection Profiles predicted for the Bottom Deck of Test Pallet BPU7 in the Stack Support Condition.

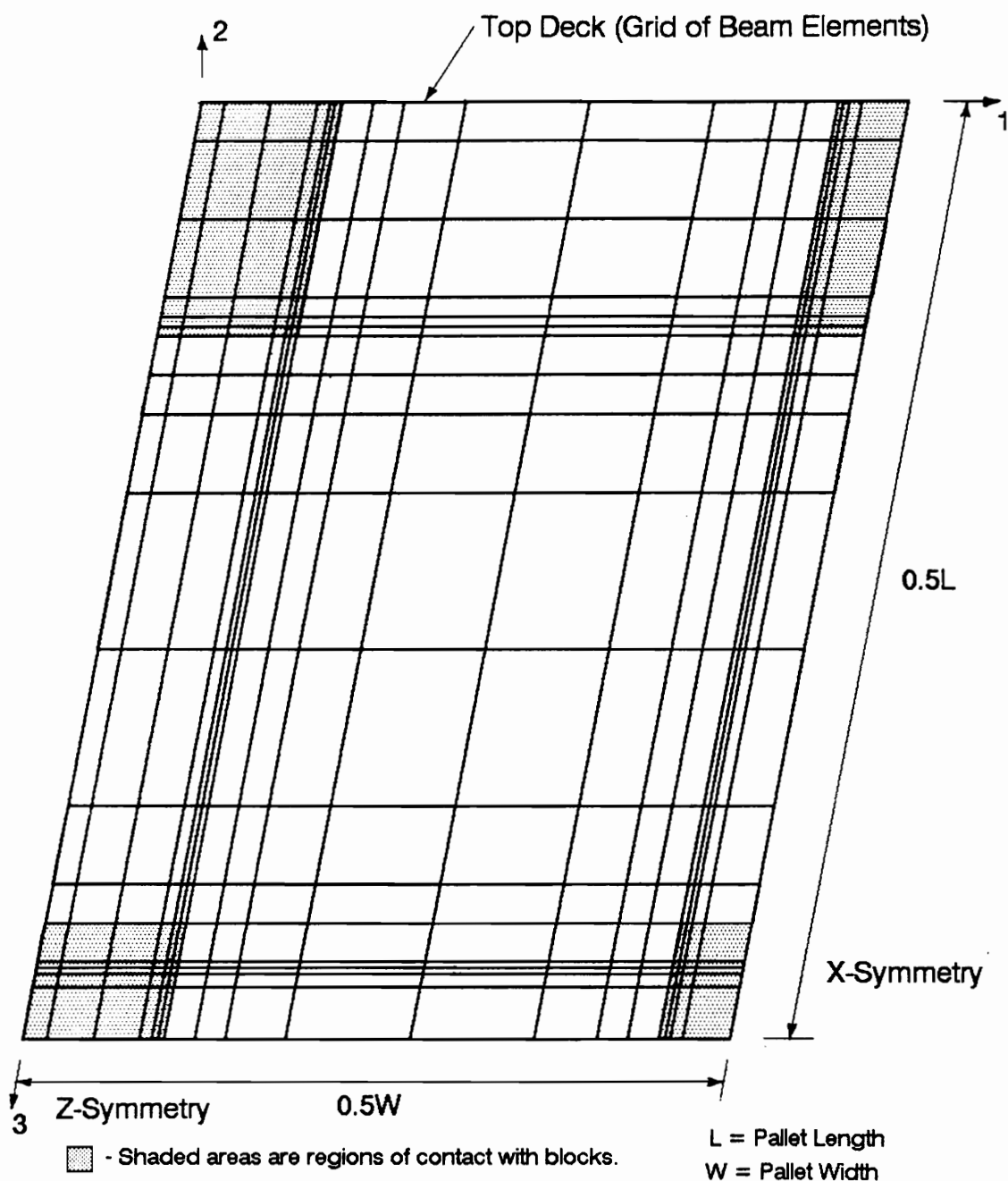


Figure 5.23. Finite Element Mesh Configuration of Simplified Model for Panel Decks of Block Pallets loaded in the Stack Support Condition.

members oriented in the global 1-direction and 19 members oriented in the global 3-direction. The grid members were comprised of beam elements. Grid member locations are defined in Figure 5.24. They were assigned a width based on tributary area.

Contact elements were represented using zero-length springs oriented in the global 2-direction. They were assigned stiffness based on tributary area and the modulus of elasticity of the block in compression, as discussed in Section 3.5.3.2. The pattern of block/deck contact used in the simplified stack model for block pallets is shown in Figure 5.25. This pattern was selected subjectively based on review of numerous contact profiles predicted for block pallets having a wide range of properties thought to influence contact stiffness. These properties included deck thickness, deck stiffness, span between blocks, and block stiffness in compression.

Nail joints were also represented using zero-length springs. Springs simulating withdrawal/head embedment were oriented in the global 2-direction. Spring stiffness was assigned as discussed in Section 3.5.1. Potential nail joint locations were also shown in Figure 5.25. Guidelines regarding nail joint activation for various nailing patterns are given in Volume III, Section 8 of Mackes (1998). Up to nine nails could be used to fasten the deck to a block.

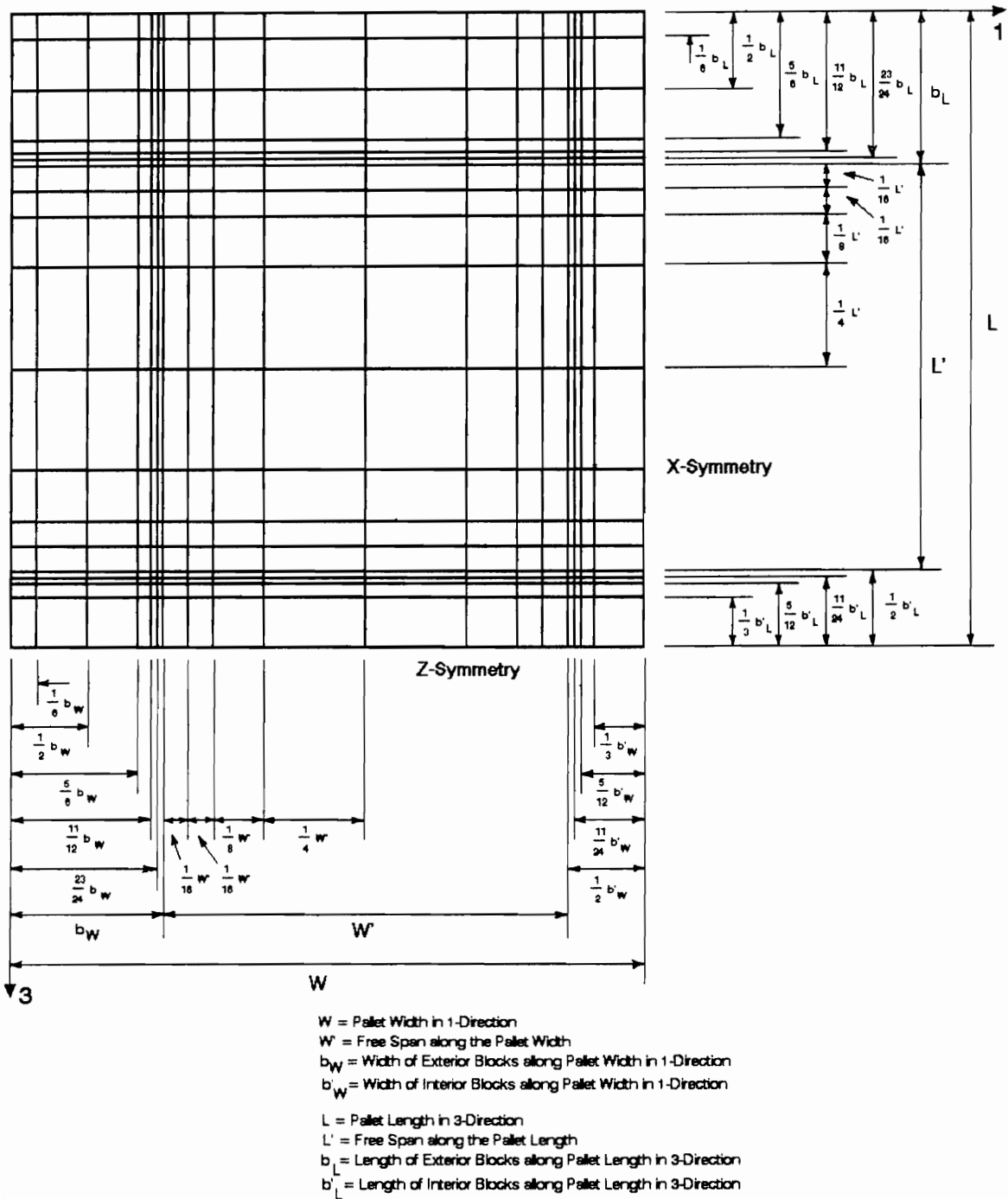
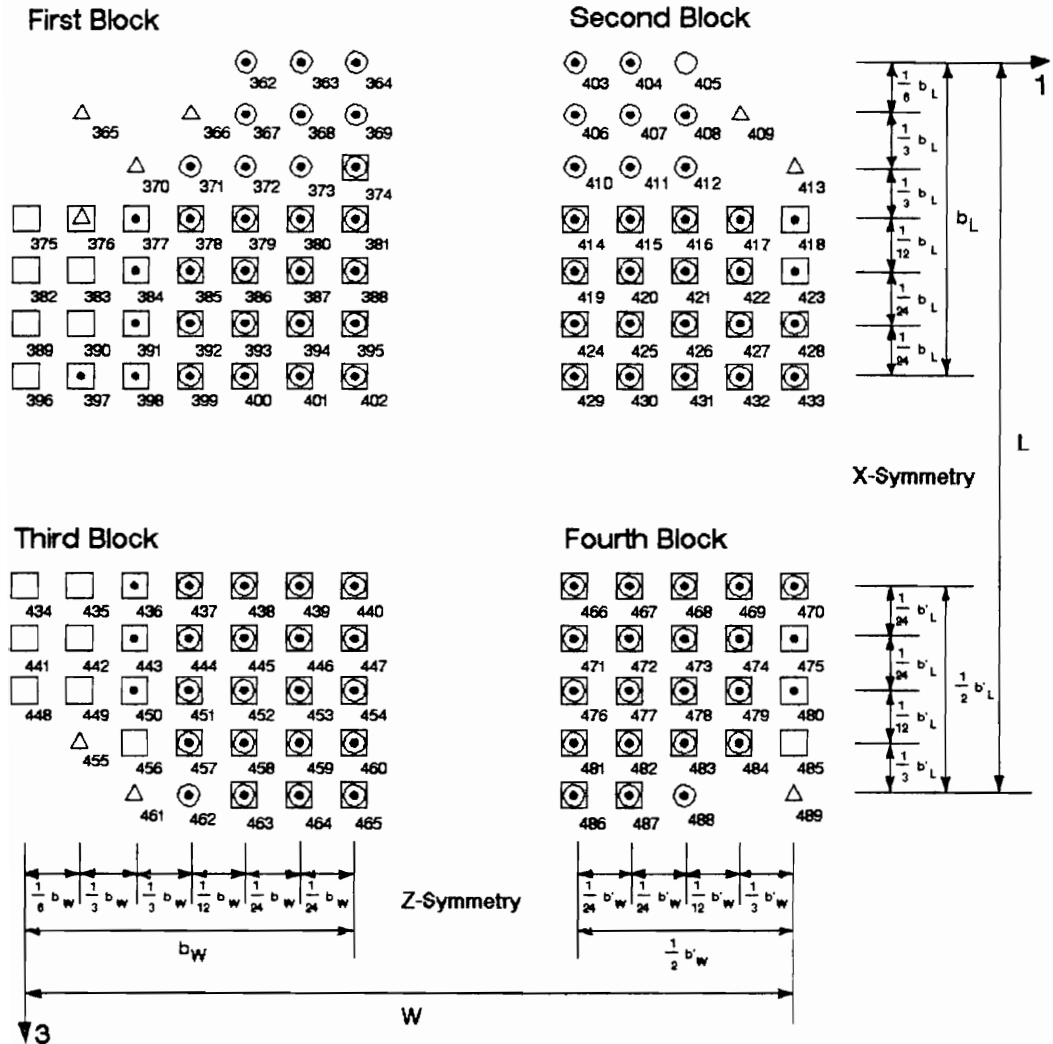


Figure 5.24. Grid Member Locations used in the Simplified Stack Model for Block Pallets.



W = Pallet Width in 1-Direction

b_W = Width of Exterior Blocks along Pallet Width in 1-Direction

b'_W = Width of Interior Blocks along Pallet Width in 1-Direction

L = Pallet Length in 3-Direction

b_L = Length of Exterior Blocks along Pallet Length in 3-Direction

b'_L = Length of Interior Blocks along Pallet Length in 3-Direction

- - Uniform Load Contact Element
- - Line Load Contact Element (1-Direction)
- - Line Load Contact Element (3-Direction)
- △ - Potential Nail Joint

Figure 5.25. Block/Deck Contact Pattern used in the Simplified Stack Model for Block Pallets.

Because lateral stiffness was not a factor in theory, lateral springs in the global 1- and 3-directions are omitted from the model.

Prediction comparisons between the simplified and plate model are presented in Table 5.12. The agreement between maximum predicted deflections was good with mean differences of less than 4.1 percent. However, agreement between normal stress predictions were not as good with mean differences ranging up to 26.8 percent.

There are two primary reasons why these differences occurred, the Poisson's effect and using an assumed pattern to assign top deck/block contact stiffness. The plate model considers Poisson's effect, which is not considered in theory by simplified grid models. For example, the effect of not considering Poisson's ratio is given for test case BPP-16 in Table 5.13. Assigning a value of approximately zero to Poisson's ratio in the plate model decreased the maximum normal stress prediction in the 3-direction by 6.1 percent for this test case. Using an assumed top deck/block contact pattern as opposed to an actual pattern determined using an iterative approach potentially had an even greater impact on stress predictions. For test pallet BPP-16, using the assumed contact pattern decreased the maximum stress predicted in the 3-direction by 12.1 percent. As shown in Table 5.13, adjusting for these factors reduced differences

**Table 5.12. Comparison of Predicted Deflections for
the Top Panel Decks of Block Pallets evaluated
in the Stack Support Condition.**

PALLET ID. NUMBER	SBPM S11 (psi)	BPPM S11 (psi)	DIF (%)	SBPM S33 (psi)	BPPM S33 (psi)	DIF (%)	SBPM D (in.)	BPPM D (in.)	DIF (%)
BPP-1	455.1	421.7	7.9	642.8	680.7	-5.6	-0.066	-0.064	3.1
BPP-2	456.7	449.3	1.6	639.9	720.2	-11.1	-0.051	-0.050	2.0
BPP-3	473.2	462.3	2.4	663.5	745.3	-11.0	-0.054	-0.052	3.8
MEAN	461.7	444.4	3.9	648.7	715.4	-9.3	-0.057	-0.055	3.0
BPPC-7	374.0	422.8	-11.5	620.9	848.1	-26.8	-0.058	-0.059	-1.7
BPPC-8	376.8	418.4	-9.9	588.7	766.7	-23.2	-0.060	-0.061	-1.6
BPPC-9	386.8	401.0	-3.5	587.0	703.7	-16.6	-0.072	-0.073	-1.4
MEAN	379.2	414.1	-8.4	598.9	772.8	-22.5	-0.063	-0.064	-1.6
BPP-16	353.5	373.9	-5.5	583.3	737.1	-20.9	-0.067	-0.068	-1.5
BPP-17	361.0	416.9	-13.4	622.0	882.5	-29.5	-0.054	-0.056	-3.6
BPP-18	409.5	478.8	-14.5	547.9	706.3	-22.4	-0.053	-0.054	-1.9
MEAN	374.7	423.2	-11.5	584.4	775.3	-24.6	-0.058	-0.059	-2.2
BOLP-7	394.4	470.7	-16.2	567.7	777.6	-27.0	-0.062	-0.061	1.6
BOLP-8	406.4	498.1	-18.4	528.2	711.7	-25.8	-0.057	-0.056	1.8
BOLP-9	399.1	486.0	-17.9	557.6	770.0	-27.6	-0.059	-0.058	1.7
MEAN	400.0	484.9	-17.5	551.2	753.1	-26.8	-0.059	-0.058	1.7
BOLP-16	857.3	847.0	1.2	1307.0	1472.0	-11.2	-0.200	-0.196	2.0
BOLP-17	932.8	935.8	-0.3	1375.0	1520.0	-9.5	-0.219	-0.213	2.8
BOLP-18	962.7	953.7	0.9	1377.0	1468.0	-6.2	-0.238	-0.231	3.0
MEAN	917.6	912.2	0.6	1353.0	1486.7	-9.0	-0.219	-0.213	2.7
BPU-7	773.1	792.6	-2.5	954.5	1204.0	-20.7	-0.204	-0.196	4.1
BPU-8	767.4	783.0	-2.0	950.1	1142.0	-16.8	-0.225	-0.214	5.1
BPU-9	818.4	849.0	-3.6	1032.0	1393.0	-25.9	-0.202	-0.196	3.1
MEAN	786.3	808.2	-2.7	978.9	1246.3	-21.5	-0.210	-0.202	4.1

Notes: 1. BPPM - Plate Model Deflection
SBPM - Simplified Model Deflection

2. Applied load equals 1.0 psi (total load = 1920 pounds).

3. Absolute maximum stress magnitudes are reported.

Table 5.13. Prediction Comparisons for Various Versions of Plate and Simplified Block Models simulating Test Pallet BPP-16 Behavior in the Stack Support Condition.

PROPERTY	11x12 MESH OF S9R PLATE ELEMENTS (V13=0.000)	11x12 MESH OF S9R PLATE ELEMENTS (V13=0.045)	DIF (%)	19X19 GRID OF B33 BEAM ELEMENTS (actual)	19X19 GRID OF B33 BEAM ELEMENTS (assumed)	DIF (%)	19X19 GRID OF B33 BEAM ELEMENTS (actual)	11x12 MESH OF S9R PLATE ELEMENTS (V13=0.000)	DIF (%)
S11 (+/-psi)	359.3	373.9	-3.9	361.7	353.5	2.3	361.7	359.3	0.7
S33 (+/-psi)	692.5	737.1	-6.1	653.7	583.3	12.1	653.7	692.5	-5.6
D2 (in)	-0.0673	-0.0680	-1.0	-0.0667	-0.0670	-0.4	-0.0667	-0.0673	-0.9

Notes: 1. Properties defined as follows::

- S11 - Normal stress 1-direction
- S33 - Normal stress 3-direction
- D2 - Deflection 2-direction
- V13 - Poisson's ratio (1-3 plane)

2. 19x19 grid model terminology as follows:

- Actual - Contact elements assigned stiffness based on iterative approach.
- Assumed - Contact elements assigned stiffness based on the pattern shown in Figure 5.25.

between the simplified and plate models to less than 5.6 percent.

McLeod (1996) translated the finite element grid model illustrated in Figures 5.23 through 5.25 into a matrix structural analysis model for inclusion into PDS-PANEL. Table 5.14 reveals that there is excellent agreement between stress and deflection predictions generated using the PDS-PANEL grid model and various plate models used to predict the behavior of test pallet BPP-16. Reported differences are less than 10.2 percent.

The deflection pattern predicted by the simplified block model for test pallet BPP-1 is shown in Figure 5.26. It appears similar to that predicted by the plate model. The same is true for the S11 stress profile of test pallet BPP-1 shown in Figure 5.27. These profiles, along with generally good results obtained using the PDS-PANEL grid model, suggest that the simplified stack model for block pallets with panel decks can adequately predict pallet behavior.

5.4.2 Rack (RAW and RAL) Support Conditions

Simplified models developed to predict block pallet behavior in the rack condition are generally more complex than stack models, requiring more degrees of freedom. Because of this complexity, solution time became a critical

Table 5.14. Comparison of Maximum Stress and Deflection Predictions for Test Pallet BPP-16 in the Stack Support Condition.

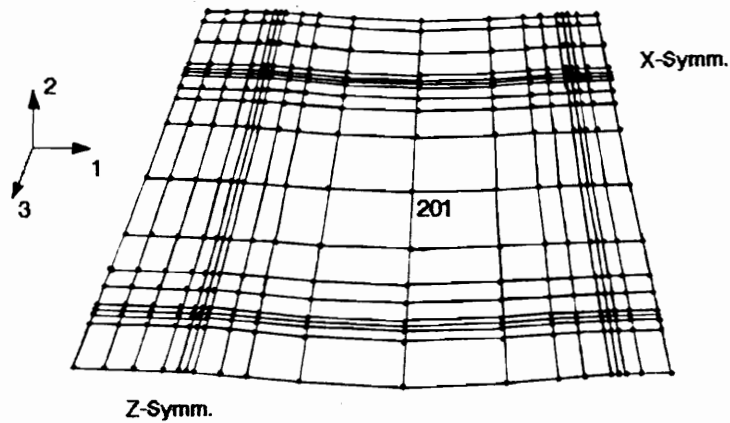
PROPERTY	PDS PANEL GRID MODEL	BPPM (S9R5)	DIF (%)	PDS PANEL GRID MODEL	BPPM (S8R)	DIF (%)
S11 (psi)	363.7	373.9	-2.7	363.7	359.3	1.2
S33 (psi)	742.4	737.1	0.7	742.4	692.5	7.2
TSHR12 (psi)	***	***	***	48.1	48.4	-0.6
TSHR32 (psi)	***	***	***	67.9	61.6	10.2
D2 (in)	-0.0671	-0.0680	-1.3	-0.0671	-0.0673	-0.3

Notes: 1. BPPM (S9R5) - Block Pallet Plate Model with
11 x 12 mesh of S9R5 Elements

BPPM (S8R) - Block Pallet Plate Model with
11 x 12 mesh of S8R Elements

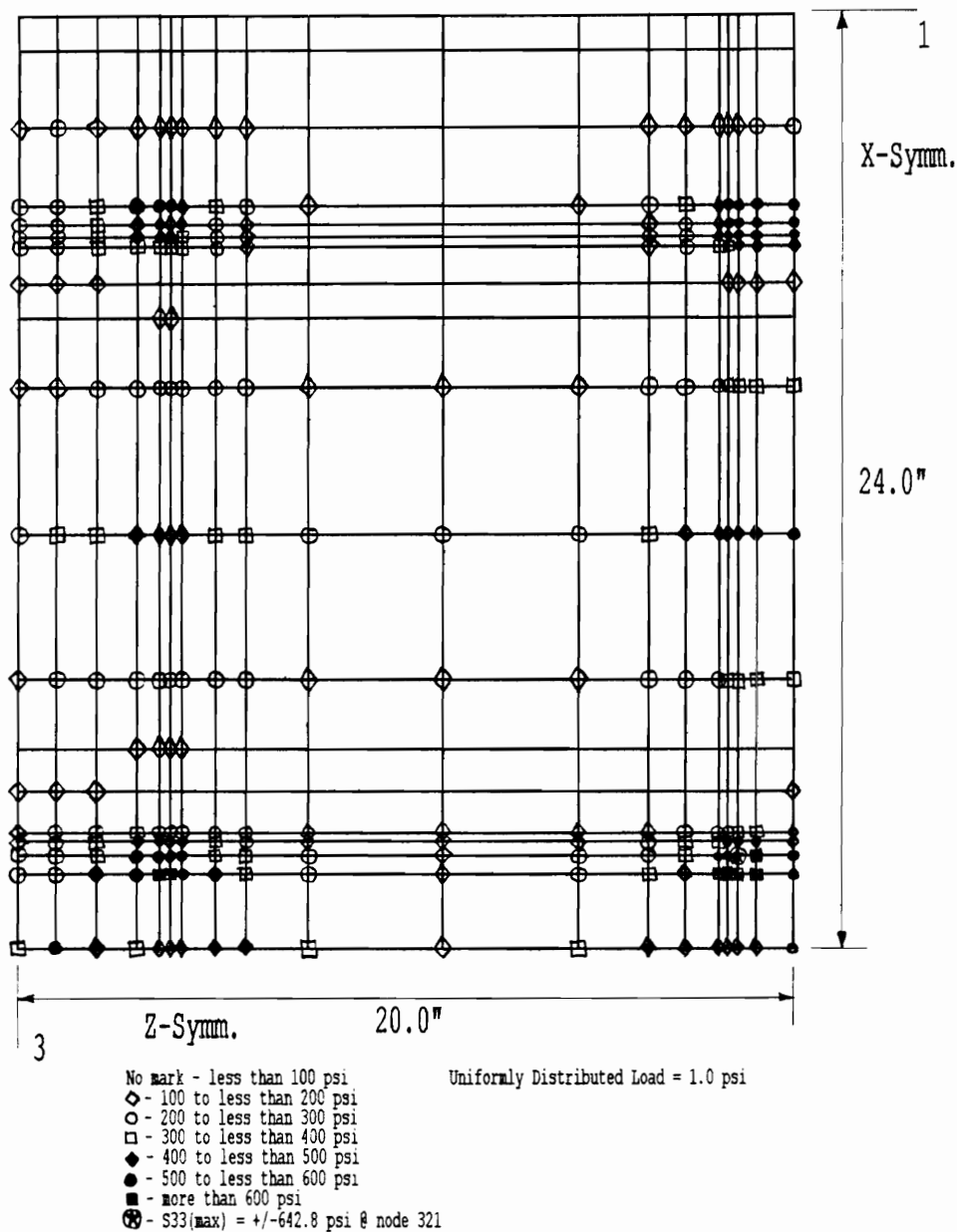
2. Absolute maximum stress magnitudes are reported.

3. Properties defined as follows:
S11 - Normal stress 1-direction
S33 - Normal stress 3-direction
TSHR12 - Shear stress 1-2 plane
TSHR32 - Shear stress 3-2 plane
D2 - Deflection 2-direction



- Notes: 1. Deformed state under a uniformly distributed load of -1.0 psi.
2. Maximum deflection (-0.066 inches) occurs at Node 201.
3. Deflections magnified by a factor of 10.

Figure 5.26. Predicted Deflection Profile for the Top Deck of Pallet BPP-1 evaluated in the Stack Support Condition using the Simplified Block Pallet Model.



S33 Stress Profile

Figure 5.27. Stress Profile for the Top Deck of Test Pallet BPP-1 loaded in the Stack Support Condition.

issue. Rack models were developed to predict the behavior of block pallets supported in both the RAW and RAL condition. The model for unidirectional-base block pallets was developed first because this is the least complex configuration. This model was then modified for perimeter-base block pallets, and extended to simulate block pallets with panel decks top and bottom. Methodologies used to model cut-outs such as hand-holds and bottom deck wheel openings are also discussed.

5.4.2.1 Unidirectional-Base Model

The simplified model for unidirectional-base block pallets was three-dimensional. An example of this model is shown in Figure 5.28. The model used quarter-symmetry. Definition of node and element locations are given in Volume III, Section 9 of Mackes (1998), along with an example of the ABAQUS input file.

Both top and bottom decks were comprised of beam elements. The top panel deck was a grid. As with the simplified stack model, the grid selected had 19 members oriented in the global 1-direction and 19 members oriented in the global 3-direction. Members were assigned a width based on tributary area. The lower deck was configured to simulate strip-type decking. Members were assigned width based on actual strip width.

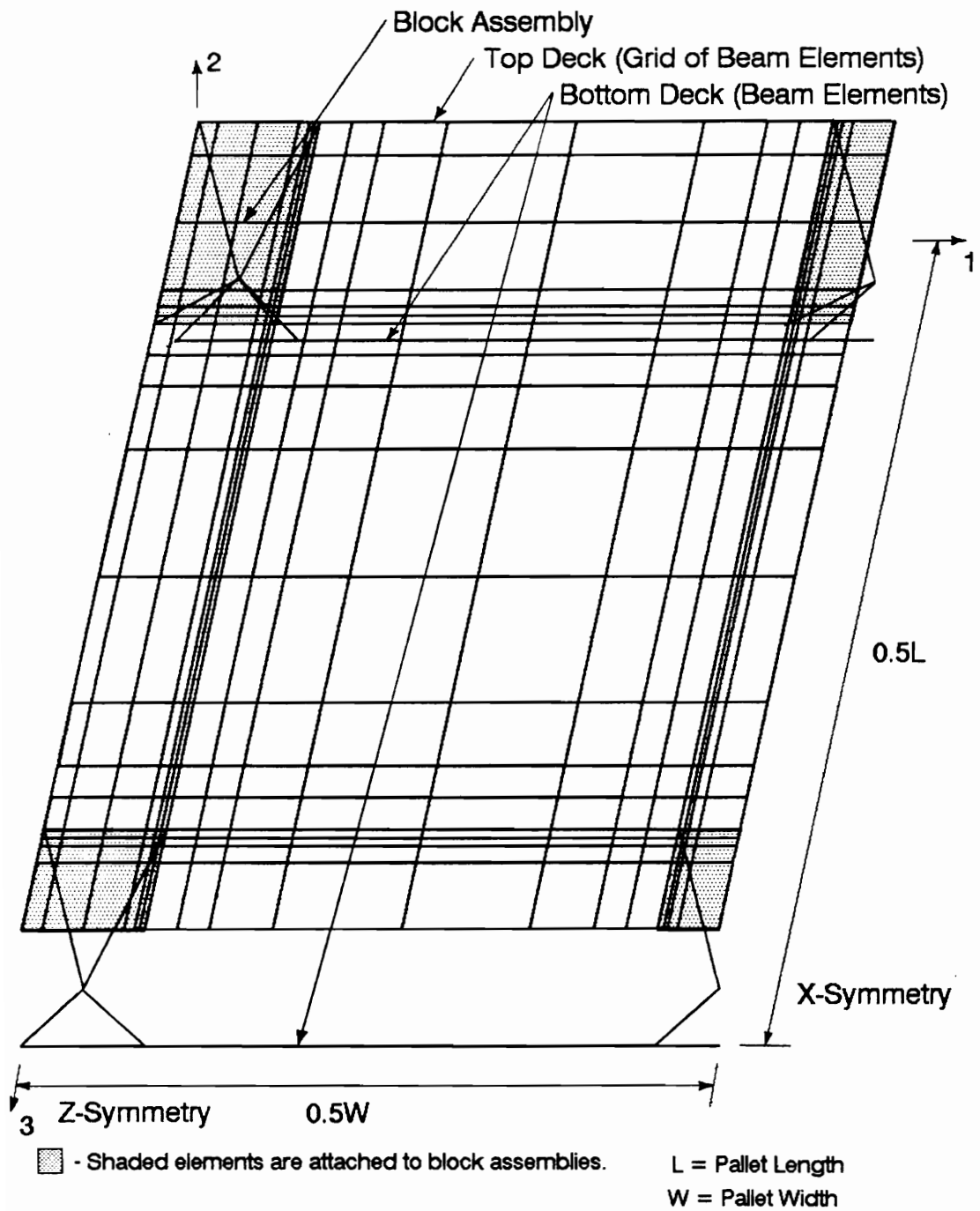


Figure 5.28. Finite Element Mesh Configuration of Simplified Model for Unidirectional-Base Block Pallets in the Rack Support Condition.

Blocks were also represented using beam elements as discussed previously in Section 3.4. The top and bottom surfaces of the block were configured to match the finite element mesh simulating the deck they correspond to. Beam members were assigned an arbitrarily high stiffness and behaved as a rigid body, with block deformation behavior incorporated into contact elements.

Similar to previous models, contact elements were represented using zero-length springs oriented in the global 2-direction and were assigned stiffness as summarized by Mackes (1998, Volume III, Section 10). The pattern of block/top deck contact used in the simplified rack models for unidirectional-base block pallets are shown in Figures 5.29 and 5.30. These patterns were selected subjectively based on the review of contact profiles. The methodology used to simulate block/bottom deck contact was based on that used for stringer pallets in the RAD support condition. Because maximum stress and deflection values predicted by the model were not sensitive to contact stiffness, these contact elements are assigned conservative values provided in Volume III , Section 10 of Mackes (1998). The location of contact nodes between edge blocks and the lower deck were determined as discussed in Section 3.5.3.2.

Zero-length springs were also used to simulate nail joints. Withdrawal/head embedment springs were oriented in

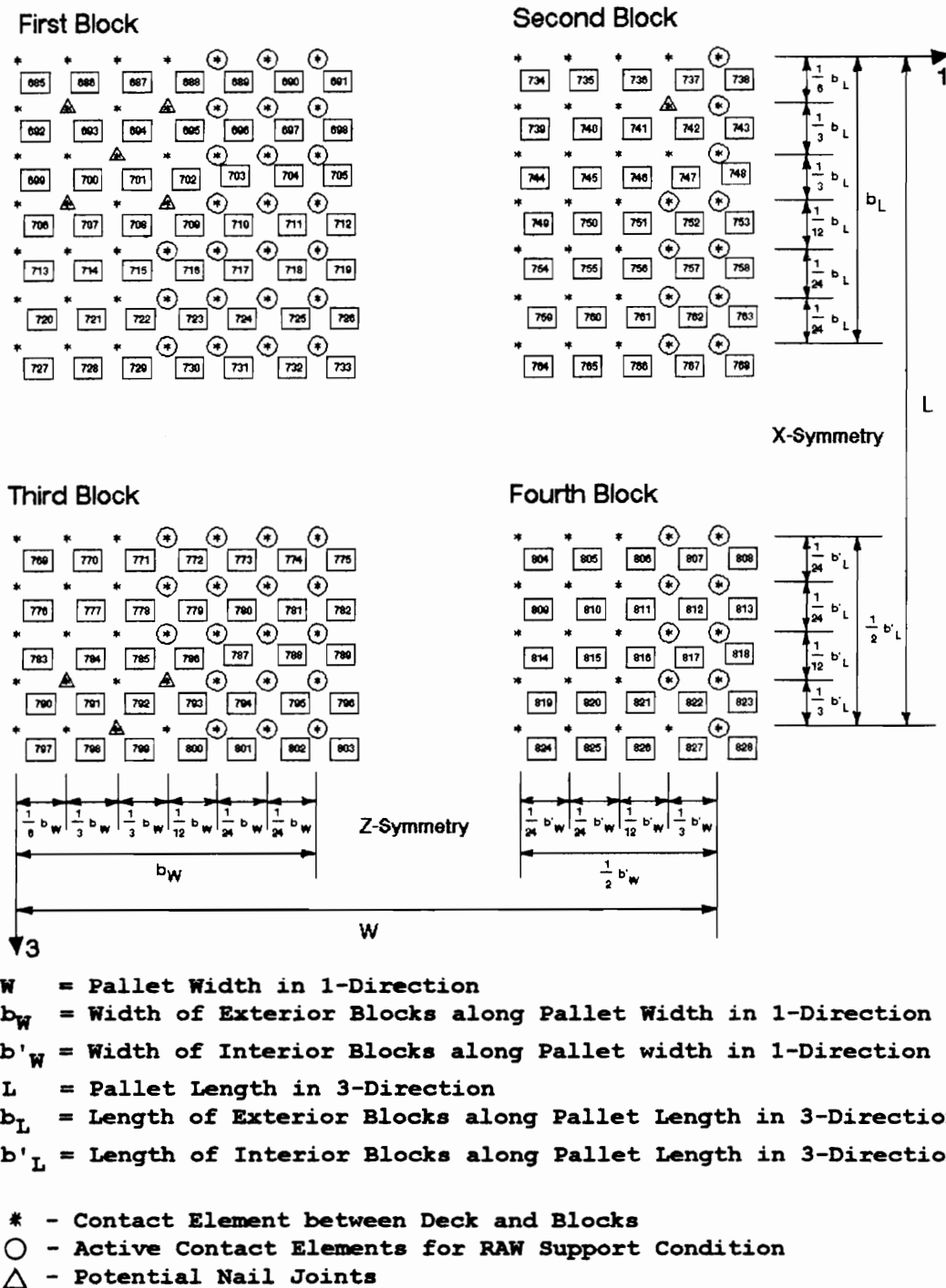


Figure 5.29. Block/Upper Deck Contact Pattern used in the Simplified Model for Block Pallets supported Racked Across the Bottom Deckboards (Strips).

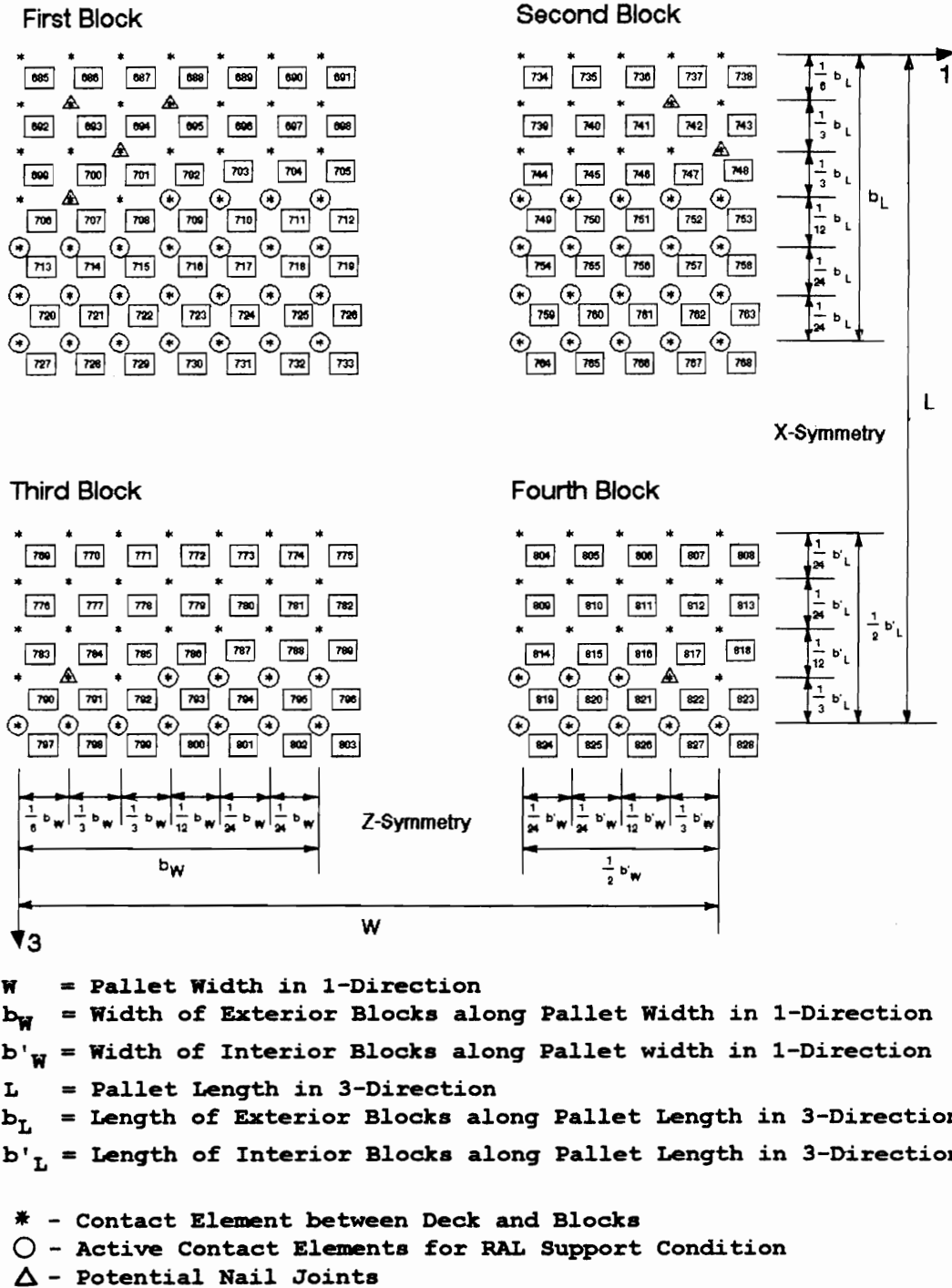


Figure 5.30. Block/Upper Deck Contact Pattern used in the Simplified Model for Block Pallets supported Racked Along the Bottom Deckboards (Strips).

the global 2-direction. Spring stiffness was assigned as discussed in Section 3.5.1. Potential nail joint locations for both top and bottom decks are also shown in Figures 5.29 and 5.30. Guidelines regarding nail location for various nailing patterns are given in Volume III, Section 11 of Mackes (1998). Up to nine nails could be used to fasten the deck to a block. Lateral stiffness was represented by zero-length springs oriented in the global 1- and 3-directions. Generally, if a nail was present at a potential location, lateral stiffness was applied, even if the nail joint was not active with respect to withdrawal/head embedment stiffness. The lateral stiffness assigned was based on current PDS prediction methodologies as defined for various nailing patterns by Mackes (1998, Volume III, Section 11).

The simplified model for unidirectional-base block pallets supported in the rack condition was evaluated to determine which degrees of freedom could be removed without affecting model performance. Results from this systematic analysis are presented by Mackes (1998, Volume III, Section 12). A summary of degrees of freedom which can be effectively removed from the model is presented in Table 5.15.

To evaluate model performance, plate and simplified model predictions for BPU type pallets were compared. A summary of prediction comparisons are presented in Table

Table 5.15. Summary of the Degrees of Freedom which can be restrained in the Simplified Model for Unidirectional-Base Block Pallets in the Rack Support Conditions without significantly impacting Stress and Deflection Predictions.

NODE (S)	DEGREE (S) OF FREEDOM RESTRAINED
Racked-Along-Strip-Type Decking:	
Bottom Deck Nodes	1, 3, 4, 5, & 6
First Block Nodes	1, 5, & 6
Second Block Nodes	1, 5, & 6
Third Block Nodes	1, 3, 4, 5, & 6
Fourth Block Nodes	1, 3, 4, 5, & 6
Top Deck Nodes	1, 3, & 5
Racked-Across-Strip-Type Decking:	
Bottom Deck Nodes	1, 3, 4, & 5
First Block Nodes	5
Second Block Nodes	1, 5, & 6
Third Block Nodes	3, 4, & 5
Fourth Block Nodes	1, 3, 4, 5, & 6
Top Deck Nodes	1, 3, & 5

Note: Refer to Figure 5.28 or Volume III, Section 9 of Mackes (1998) for model configurations.

5.16. Mean differences between maximum normal stress predictions in both the 1-direction (S11) and the 3-direction (S33) were acceptable, at less than 6.1 percent. Agreement between maximum deflection predictions was also good, with mean differences of less than 6.4 percent. The deflection profile for test pallet BPU-4 is shown in Figure 5.31 and appears as expected. For the test cases considered, the rack model for unidirectional-base block pallet performed adequately.

5.4.2.2 Perimeter-Base Model

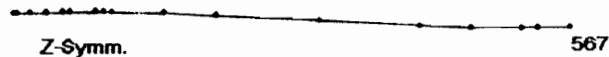
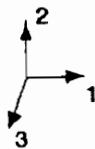
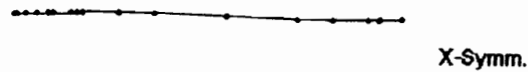
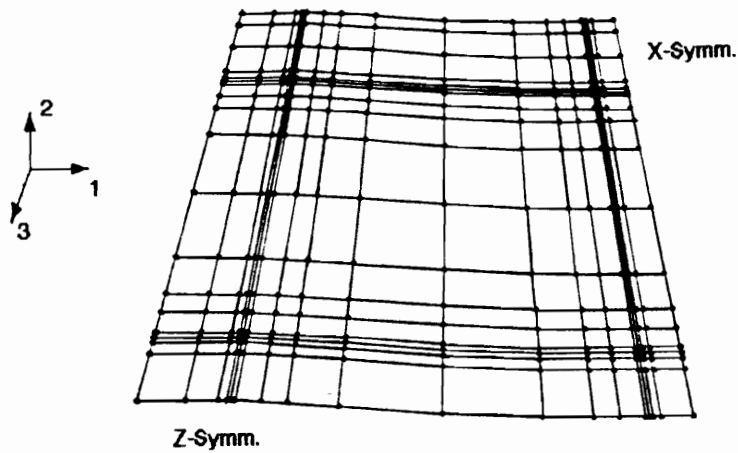
A modified version of the simplified unidirectional-base block model was used to predict the behavior of perimeter-base block pallets in the rack support condition. Modifications were made primarily to the bottom deck and bottom block surfaces, including associated contact and nail joint elements. Additional information regarding modifications is given in Volume III, Section 13 of Mackes (1998).

Because the pallet was always supported along the 3-direction and racked spanning across the supports in the 1-direction in the model, it was necessary for the model to be able to simulate two separate pallet configurations. One for pallets racked across the butted deckboards (normally the RAL direction) and the other for pallets racked along

Table 5.16. Comparison of Model Predictions
for Unidirectional-Base Pallets in the
Racked-Across-Width Support Condition.

PALLET ID. NUMBER	MAXIMUM STRESS			MAXIMUM DEFLECTION		
	SBPM S11 (psi)	BPPM S11 (psi)	DIF (%)	SBPM D (in.)	BPPM D (in.)	DIF (%)
Top Deck Predictions:						
BPU-4	298.8	291.2	2.6	-0.176	-0.168	4.8
BPU-5	284.6	267.2	6.5	-0.166	-0.155	7.1
BPU-6	300.8	305.0	-1.4	-0.158	-0.151	4.6
MEAN	294.7	287.8	2.4	-0.167	-0.158	5.5
Bottom Deck Predictions:						
BPU-4	561.3	510.6	9.9	-0.175	-0.165	6.1
BPU-5	608.9	544.8	11.8	-0.163	-0.150	8.7
BPU-6	435.6	457.8	-4.8	-0.159	-0.152	4.6
MEAN	535.3	504.4	6.1	-0.166	-0.156	6.4

- Notes: 1. BPPM - Plate Model Predictions
SBPM - Simplified Model Predictions
DIF - Difference between BPPM and SBPM
predictions.
2. Predictions reported are for pallets under a
uniformly distributed load of 0.125 psi (240
pounds).
3. Absolute maximum S11 stress magnitudes are
reported.



- Notes: 1. Deformed state under a uniformly distributed load of -0.125 psi.
2. Maximum bottom deck deflection (-0.175 inches) occurs at Node 567.
3. Deflections magnified by a factor of 8.

Figure 5.31. Predicted Deflection Profiles for the Decks of Pallet BPU-4 evaluated in the Racked-Across-Width Support Condition using the Simplified Unidirectional-Base Block Pallet Model.

the butted deckboards (normally the RAW direction). An example of the model configured for pallets racked across the butted deckboards is shown in Figure 5.32.

The bottom deck of this model was subsequently modified further by adding elements to the bottom deck. These elements were added to reduce the bandwidth of stiffness matrices in the PC version of the models. Other than this, adding these additional elements has no significant impact on model predictions.

Comparisons of predictions generated using both the plate and simplified models are given in Table 5.17. Generally, mean differences between maximum stress and deflection predictions were acceptable. Mean differences in maximum stress were less than -13.1 percent and less than -1.6 percent for maximum deflection. This suggests that the model satisfactorily predicted pallet behavior.

5.4.2.3 Panel Deck Top and Bottom Model

For block pallets with full panel decks top and bottom, full grids were proposed to model both decks. This simplified model is shown in Figure 5.33. Results summarized in Table 5.18 for Test Case BPP-1, indicated that agreement between values predicted by the plate model and this simplified model was acceptable. However, solution times for this simplified model exceeded 2 minutes because

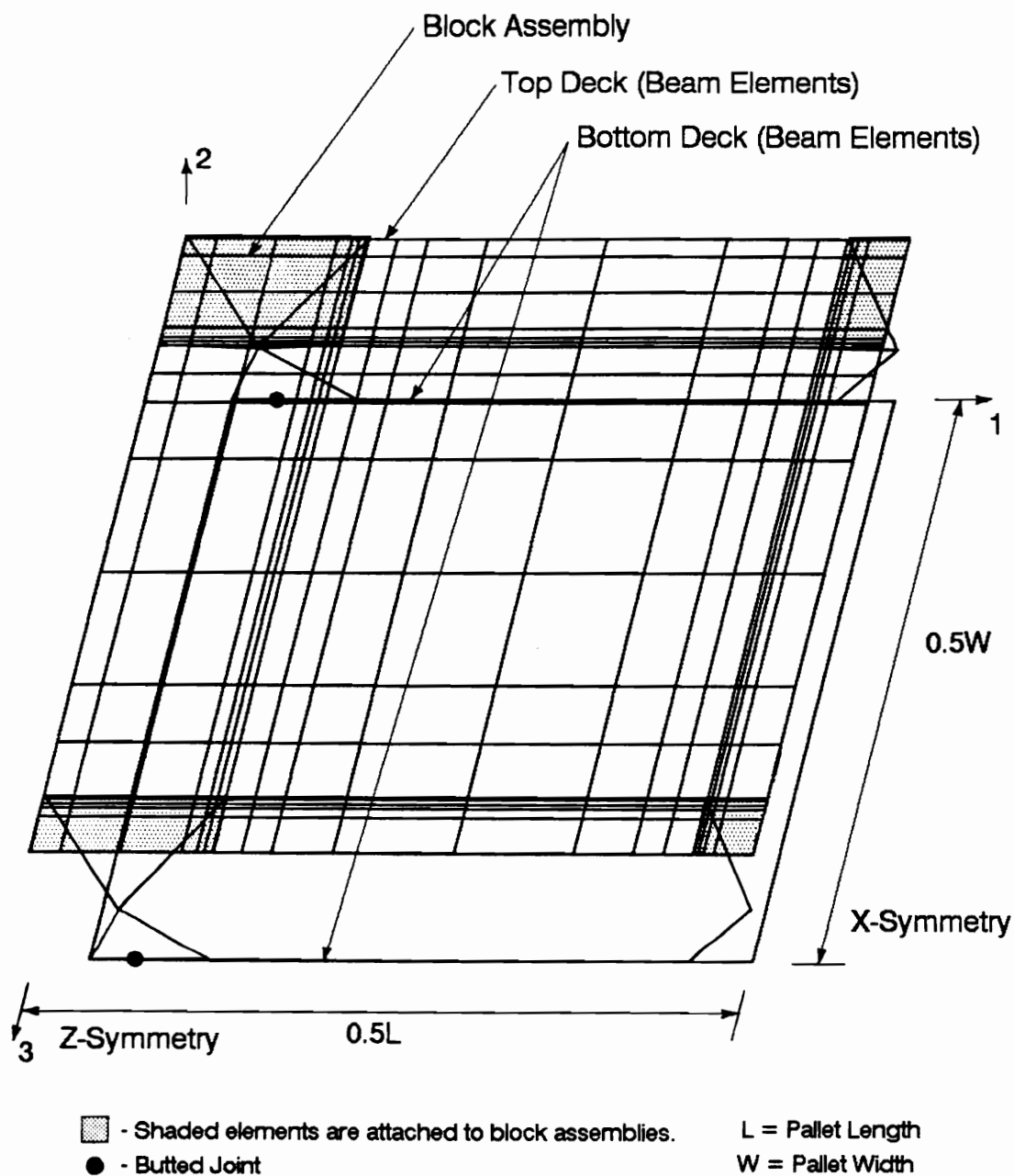


Figure 5.32. Proposed Finite Element Mesh Configuration of Simplified Model for Perimeter-Base Block Pallets Racked Across the Butted Deckboards.

Table 5.17. Comparison of Model Predictions
for Perimeter-Base Block Pallets in the
Racked-Across-Length Support Condition.

PALLET ID. NUMBER	MAXIMUM STRESS			MAXIMUM DEFLECTION		
	SBPM S33 (psi)	BPPM S33 (psi)	DIF (%)	SBPM D (in.)	BPPM D (in.)	DIF (%)
Top Deck Predictions:						
BOLP-1	1446.0	1675.0	-13.7	-0.395	-0.398	-0.8
BOLP-2	1465.0	1660.0	-11.7	-0.421	-0.423	-0.5
BOLP-3	1528.0	1771.0	-13.7	-0.397	-0.403	-1.5
MEAN	1479.7	1702.0	-13.1	-0.404	-0.408	-0.9
Bottom Deck Predictions:						
BOLP-1	1948.0	1961.0	-0.7	-0.388	-0.394	-1.5
BOLP-2	1738.0	1740.0	-0.1	-0.416	-0.420	-1.0
BOLP-3	1495.0	1520.0	-1.6	-0.392	-0.402	-2.5
MEAN	1727.0	1740.3	-0.8	-0.399	-0.405	-1.6

- Notes: 1. BPPM - Plate Model Predictions
SBPM - Simplified Model Predictions
DIF - Difference between BPPM and SBPM
predictions.
2. Predictions reported are for pallets under a
uniformly distributed load of 1.0 psi (1920
pounds).
3. Absolute maximum S11 stress magnitudes are
reported.

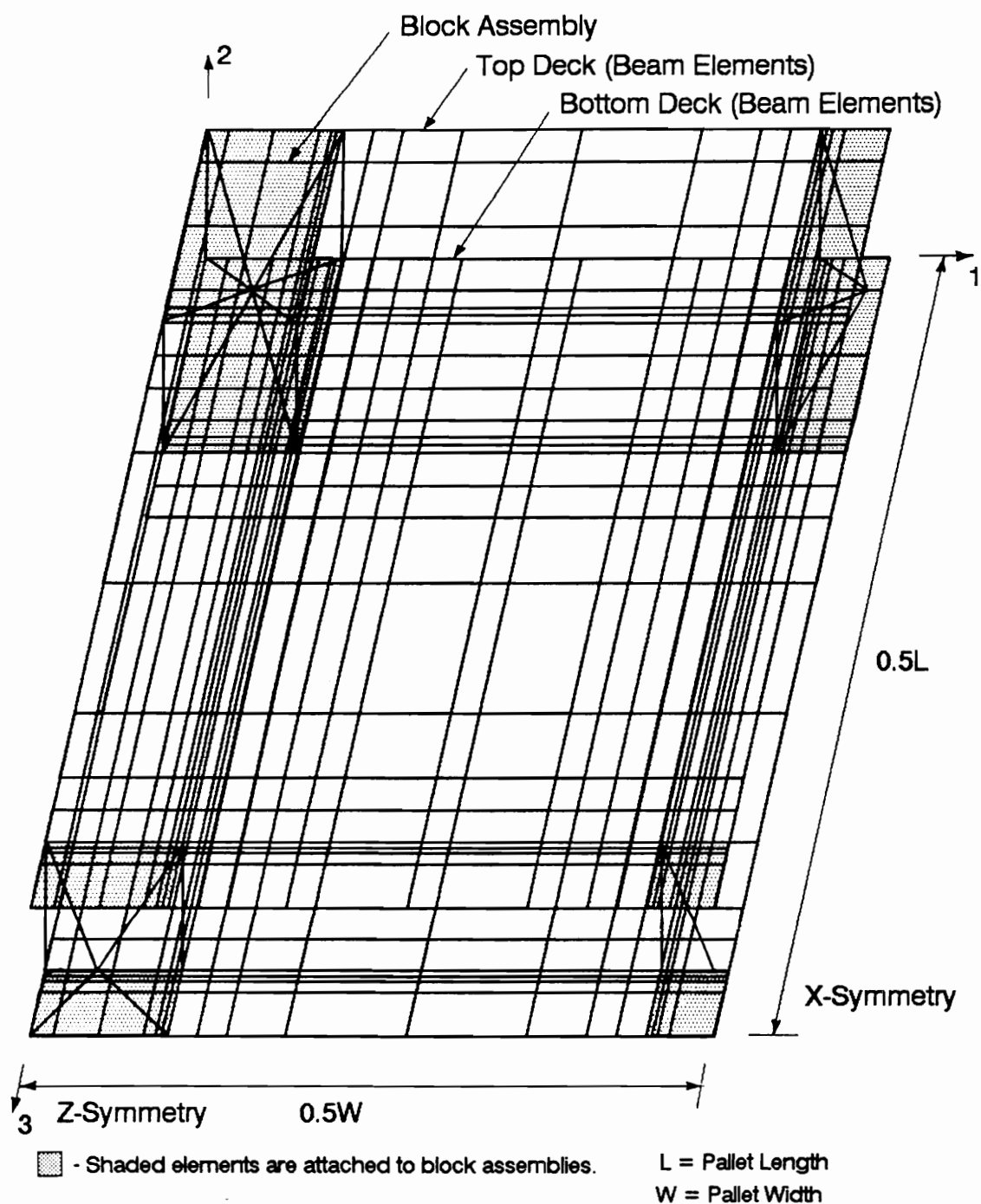


Figure 5.33. Proposed Finite Element Mesh Configuration of Simplified Model for Block Pallets with Panel Decks Top and Bottom loaded in the Rack Support Conditions.

Table 5.18. Comparison of Model Predictions for Block Pallets with Panel Decks Top and Bottom in the Racked-Across-Width Support Condition.

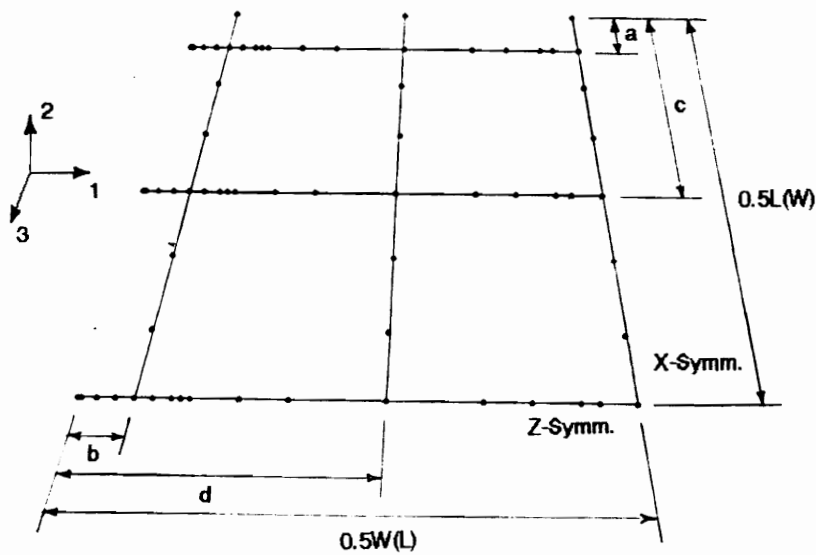
PALLET ID. NUMBER	MAXIMUM STRESS			MAXIMUM DEFLECTION		
	SBPM S11 (psi)	BPPM S11 (psi)	DIF (%)	SBPM D (in.)	BPPM D (in.)	DIF (%)
Top Deck Predictions:						
BPP-1	695.5	663.3	4.9	-0.268	-0.259	3.5
BPP-2	676.9	666.0	1.6	-0.209	-0.205	2.0
BPP-3	703.0	694.3	1.3	-0.218	-0.214	1.9
MEAN	691.8	674.5	2.6	-0.232	-0.226	2.5
Bottom Deck Predictions:						
BPP-1	473.2	473.6	-0.1	-0.264	-0.257	2.7
BPP-2	474.1	478.5	-0.9	-0.206	-0.203	1.5
BPP-3	490.3	498.5	-1.6	-0.215	-0.212	1.4
MEAN	479.2	483.5	-0.9	-0.228	-0.224	1.9

- Notes: 1. BPPM - Plate Model Predictions
SBPM - Predictions for Simplified Block Model with 19 x 19 Grids Simulating both Top and Bottom Decks
DIF - Difference between BPPM and SBPM predictions.
2. Predictions reported are for pallets under a uniformly distributed load of 0.5 psi (960.0 pounds).
3. Absolute maximum S11 stress magnitudes are reported.

using a full grid for the bottom deck substantially increases model complexity and size. Therefore, the model used to simulate perimeter-base block pallets in the rack support conditions was adapted to model pallets with a full panel-deck bottom.

The adapted finite element mesh appeared the same as the perimeter-base model, except for the bottom deck configuration which was modified as shown in Figure 5.34 to better simulate a full panel-deck. Grid members were assigned width based on panel dimensions and tributary area. Grid members oriented across the width of the panel (1-direction) were assigned properties consistent with panel orientation, as were grid members oriented along the length of the panel (3-direction).

A comparison of predictions generated by plate and simplified models is given in Table 5.19. Agreement between maximum stress and deflection predictions was acceptable, with mean differences of less than -9.4 percent. Both stress and deflection profiles, shown respectively for test pallet BPP-1 in Figures 5.35 and 5.36, were very comparable with those generated using the plate model. These results suggest that the proposed model adapted for modeling block pallets with full panel decks was capable of generating acceptable predictions.



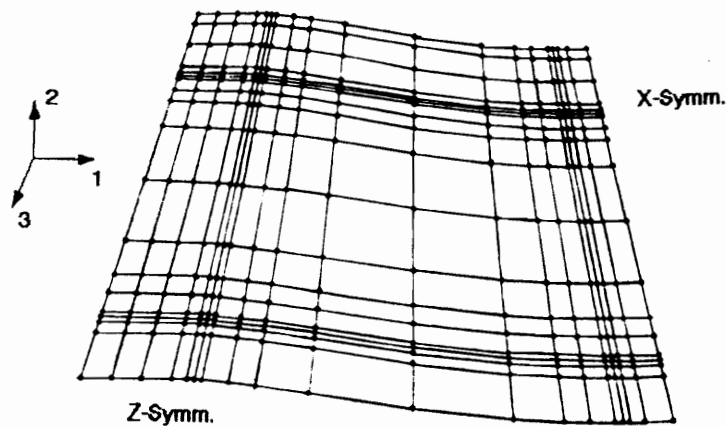
Where: L = Pallet length
W = Pallet width
a = 0.5 x edge block width (length) or distance from pallet edge to support
b = 0.5 x edge block length (width) or distance from pallet edge to support
c = (edge block length(width) + (0.5L(W) - 0.5 x center block length(width)))/2
d = (edge block width(length) + (0.5L(W) - 0.5 x center block width(length)))/2

Figure 5.34. Proposed Bottom Deck Configuration of the Simplified Model for Block Pallets with Panel Decks Top and Bottom supported in a Rack Condition.

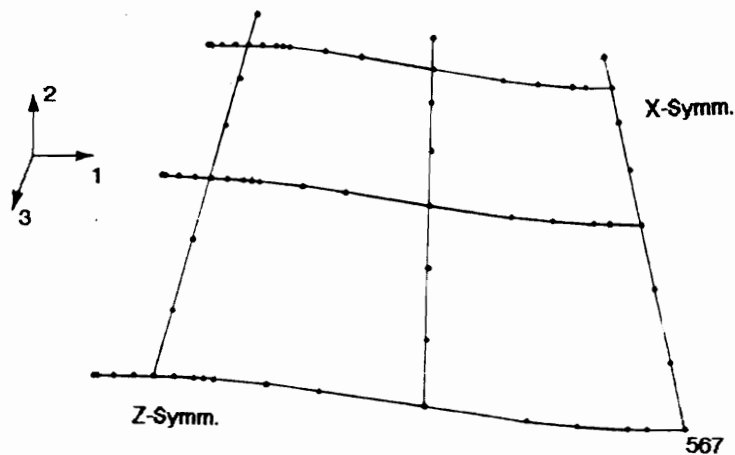
Table 5.19. Comparison of Model Predictions for Block Pallets with Panel Decks Top and Bottom in the Racked-Across-Width Support Condition.

PALLET ID. NUMBER	MAXIMUM STRESS			MAXIMUM DEFLECTION		
	SBPM S11 (psi)	BPPM S11 (psi)	DIF (%)	SBPM D (in.)	BPPM D (in.)	DIF (%)
Top Deck Predictions:						
BPP-1	660.3	663.3	-0.5	-0.258	-0.259	-0.4
BPP-2	642.3	666.0	-3.6	-0.201	-0.205	-2.0
BPP-3	667.3	694.3	-3.9	-0.210	-0.214	-1.9
MEAN	656.6	674.5	-2.7	-0.223	-0.226	-1.3
Bottom Deck Predictions:						
BPP-1	430.5	473.6	-9.1	-0.254	-0.257	-1.2
BPP-2	434.7	478.5	-9.2	-0.198	-0.203	-2.5
BPP-3	449.6	498.5	-9.8	-0.207	-0.212	-2.4
MEAN	438.3	483.5	-9.4	-0.220	-0.224	-1.9

- Notes: 1. BPPM - Plate Model Predictions
SBPM - Predictions for Simplified Block Model with a 19 x 19 Grid Simulating the Top Deck and a 3 x 3 Grid the Bottom Deck
DIF - Difference between BPPM and SBPM predictions.
2. Predictions reported are for pallets under a uniformly distributed load of 0.5 psi (960.0 pounds).
3. Absolute maximum S11 stress magnitudes are reported.



Top Deck (Deformed State)



Bottom Deck (Deformed State)

- Notes: 1. Deformed state under a uniformly distributed load of -0.5 psi.
2. Maximum bottom deck deflection (-0.254 inches) occurs at Node 567.
3. Deflections magnified by a factor of 10.

Figure 5.35. Predicted Deflection Profiles for the Decks of Pallet BPP-1 evaluated in the Racked-Across-Width Support Condition using the Simplified Block Pallet Model.

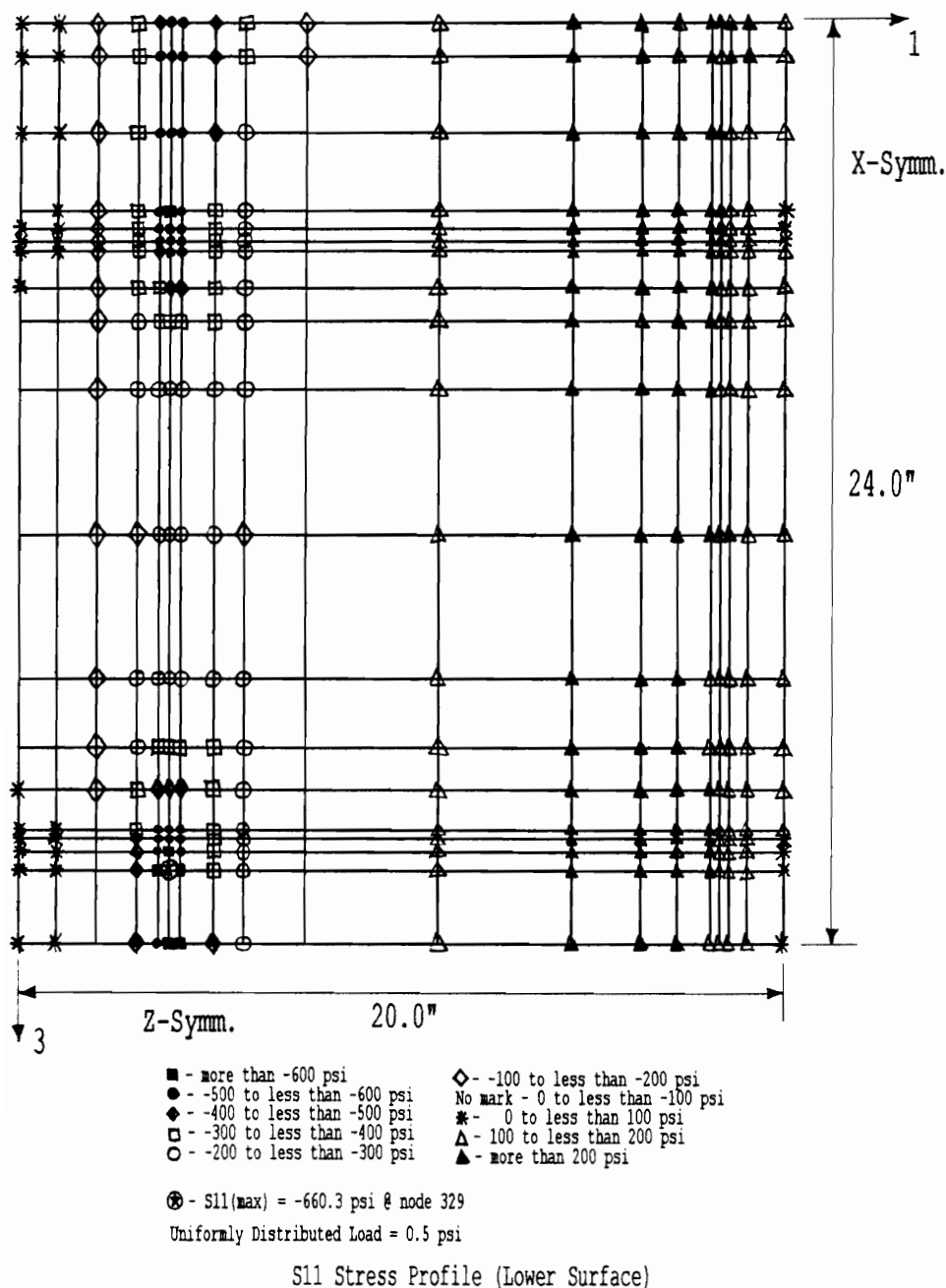


Figure 5.36. Stress Profile predicted by the Simplified Block Model for the Top Deck of Test Pallet BPP-1 loaded in the RAW Support Condition..

5.4.3 Models for Block Pallets with Cut-Outs

For plate models used to predict block pallet behavior, cut-outs such as hand-holds or bottom deck wheel openings were contained within shell (plate) elements which were given near zero stiffness properties. The methodology used to model cut-outs in simplified block pallet (grid) models was similar to that used for the simplified grid model simulating stringer pallets in the RAS support condition. The geometric dimensions of grid members in the vicinity of the cut-out were modified. This methodology is discussed for hand-holds and bottom deck wheel openings in subsequent sections.

As with stringer pallet models, the approaches used to model cut-outs incorporated into block pallets were based on the assumption that stress concentrations caused by the cut-outs do not govern failure. While probably valid for hand-holds, this assumption may not be valid for bottom deck wheel openings, particularly for OSB which is considerably more brittle than plywood.

5.4.3.1 Hand-Holds

Hand-holds were incorporated into the finite element mesh (grid) which simulated the top deck of block pallets by adjusting the width of elements in the vicinity of the cut-out. Potential hand-hold locations in the top deck were previously specified in Figure 3.42. Hand-holds are not

allowed in other locations. Determination as to whether or not an element falls in a hand-hold region was based on the geometric properties of the cut-out and the tributary area of grid members in the vicinity. The entire length of elements which fall in the hand-hold region(s) were adjusted, even though only a portion of the element may actually fall in the region. The mesh modifications required to incorporate hand-holds at specified locations in the top deck are outlined by Mackes (1998, Volume III, Section 14).

Model performance was evaluated to insure that behavior was as expected when hand-holds were incorporated into the simplified mesh. This was accomplished using the data for BPU test cases, which contain top deck hand-holds. Deflection and stress predictions were generated using the plate and simplified block models developed to simulate pallets both with and without hand-holds in the stack and racked-across-width support conditions. Predicted values are presented in Table 5.20. Comparisons revealed that incorporating a top deck hand-hold into the simplified (grid) model increased maximum deflection by up to 15.4 percent and maximum stress by up to 6.4 percent. These differences were comparable to plate model results and were generally as expected. Incorporating hand-holds into the pallet has less impact on the racked-across-width support

Table 5.20. The Effect of Top Deck Hand-Holds
on Simplified Block Model Predictions.

PALLET ID. NUMBER	MAXIMUM STRESS			MAXIMUM DEFLECTION		
	W/HH S11 (psi)	WO/HH S11 (psi)	DIF (%)	W/HH D (in.)	WO/HH D (in.)	DIF (%)
Racked-Across-Width Support Condition (Top Deck):						
BPU4	298.8	292.0	2.3	-0.176	-0.172	2.3
BPU5	284.6	278.3	2.3	-0.166	-0.162	2.5
BPU6	300.8	292.9	2.7	-0.158	-0.153	3.3
MEAN	294.7	287.7	2.4	-0.167	-0.162	2.7
Racked-Across-Width Support Condition (Bottom Deck):						
BPU4	561.3	547.4	2.5	-0.175	-0.170	2.9
BPU5	608.9	594.1	2.5	-0.163	-0.159	2.5
BPU6	435.6	423.5	2.9	-0.159	-0.154	3.2
MEAN	535.3	521.7	2.6	-0.166	-0.161	2.9
Stack Support Condition:						
BPU7	773.1	726.6	6.4	-0.204	-0.177	15.3
BPU8	767.4	723.4	6.1	-0.225	-0.195	15.4
BPU9	818.4	767.9	6.6	-0.202	-0.175	15.4
MEAN	786.3	739.3	6.4	-0.210	-0.182	15.4

- Notes: 1. W/HH - Top Deck with Hand-Holds
WO/HH - Top Deck without Hand-Holds
DIF - Difference between predictions
2. Uniformly distributed loads are as follows:
Rack Condition - 0.125 psi (240 pounds total)
Stack Condition - 1.0 psi (1920 pounds total)
3. Stress predictions (magnitudes) are absolute.

condition, increasing maximum stress by up to 2.9 percent and maximum deflection up to 3.3 percent.

The methodology used to incorporate hand-holds into the bottom deck was similar. Potential hand-hold locations in the bottom deck were essentially the same as those for the top deck. As for top deck hand-holds, the finite element mesh simulating the bottom deck was modified in the region of the hand-hold(s). These modifications are also outlined in Volume III, Section 14 of Mackes (1998).

5.4.3.2 Bottom Deck Wheel Openings

As with stringer pallets, the simplified block pallet models were designed to accommodate one wheel opening per quarter section of the pallet. Because quarter symmetry was used, incorporating a wheel opening into the model effectively did so for each quarter section. The wheel openings could be of any practical size and location within the quarter section of the pallet. The methodologies used to model wheel openings differed, based on the support condition. Methodologies are discussed for both the stack and rack support conditions in subsequent sections

5.4.3.2.1 Stack Support Condition

In the stack support condition, panels with wheel openings were modeled using a simplified model developed from that used to simulate strip-type bottom decks which is

discussed in Section 5.4.1.1. The model developed is shown in Figure 5.37. Node and element locations for this model are presented by Mackes (1998, Volume III, Section 15), along with an example of an ABAQUS input file.

Comparisons between the simplified model predictions and experimentally measured results for the BPPC test pallets, which have bottom deck wheel openings, are presented in Table 5.21. Deflection comparisons were acceptable for both the RAW and RAL support conditions, with mean differences of less than -5.2 percent. Both stress and deflection profiles shown for test pallet BPU-7 in Figure 5.38 are as expected.

5.4.3.2.2 Rack (RAW and RAL) Support Conditions

The methodology used to model block pallets with wheel openings in the rack support condition was similar to that used for perimeter-base pallets and pallets with a full panel-deck bottom. The finite element mesh appeared similar to the simplified perimeter-base model shown in Figure 5.32. Bottom deck wheel openings were incorporated into the model by appropriately adjusting the width of the grid members based on the dimensions of the cut-out. Grid members were assigned panel properties consistent with cut-out dimensions and orientation.

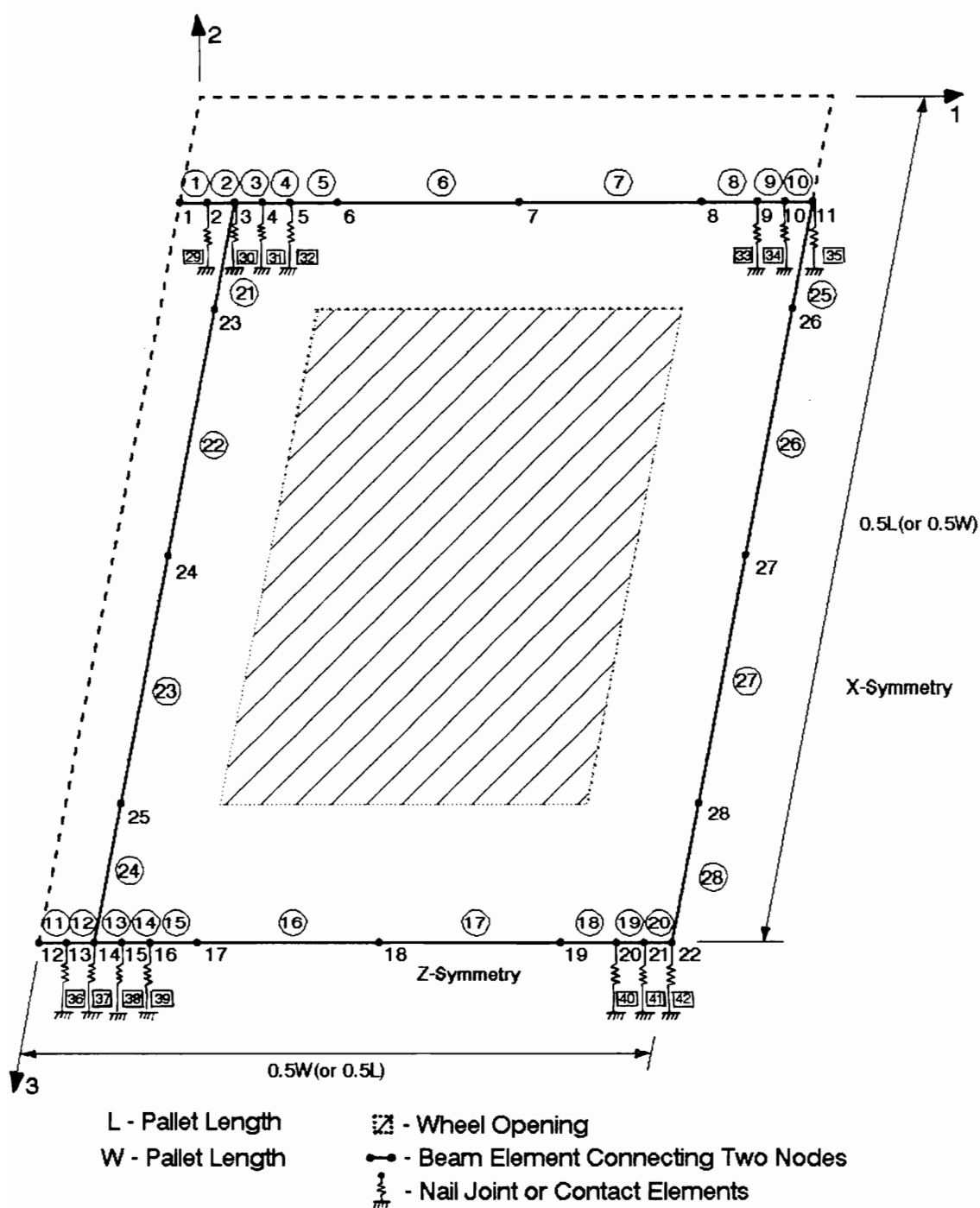
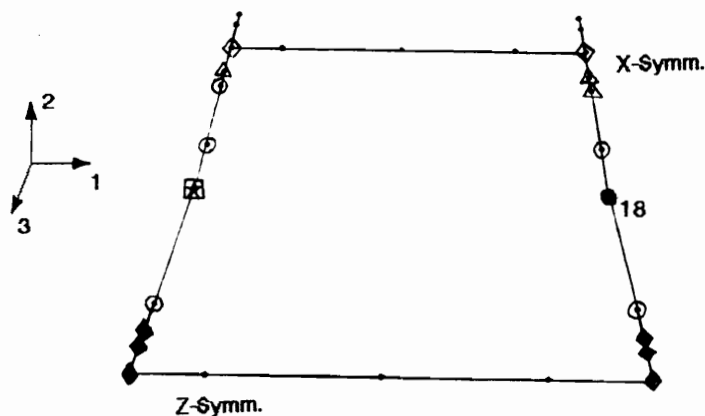


Figure 5.37. Configuration of Simplified Model for the Bottom Decks of Block Pallets with Wheel Openings in the Stack Support Condition.

Table 5.21. Stress and Deflection Values predicted using the Simplified Model Simulating the Bottom Deck Behavior of Block Pallets with Wheel Openings in the Stack Support Condition.

PALLET ID.	FEM S1(max) (+/- psi)	FEM D2 (avg) (in.)	EXP D2 (avg) (in.)	PERCENT DIFFERENCE
LENGTH ORIENTATION (LINE-LOAD APPLIED ALONG THE WIDTH)				
BPPC-7	1673	-0.083	-0.087	-4.6
BPPC-8	1669	-0.095	-0.100	-5.0
BPPC-9	1715	-0.078	-0.083	-6.0
MEAN	1686	-0.085	-0.090	-5.2
WIDTH ORIENTATION (LINE-LOAD APPLIED ALONG THE LENGTH)				
BPPC-7	1207	-0.172	-0.167	3.0
BPPC-8	1236	-0.151	-0.151	0.0
BPPC-9	1232	-0.167	-0.166	0.6
MEAN	1225	-0.163	-0.161	1.2

- Notes:
1. FEM S1(max) is the maximum predicted (finite element model) stress in the 1-direction
 2. FEM D2(avg) is average deflection predicted in the 2-direction along the pallet at mid-span between blocks by the simplified finite element model.
 3. FEM D2(avg) is average measured deflection in the 2-direction along the pallet at mid-span between blocks obtained using the air-bag test machine.
 4. Two rigid line loads applied at the mid-span between blocks (Applied load = 1920 pounds)



Bottom Deck (Deformed State)

Notes: 1. Stress levels are as follows:

- No mark - 0 to less than 200 psi
- ◇ - 200 to less than 400 psi
- △ - 400 to less than 600 psi
- - 600 to less than 400 psi
- - 800 to less than 600 psi
- ◆ - 1000 to less than 400 psi
- ▲ - 1200 to less than 600 psi
- - 1400 to less than 400 psi
- - more than 1600 psi
- ⊠ - S33(max) = +/-1673 psi @ node 7

2. Deformed state under two rigid line loads applied at mid-span between blocks (Total applied load = 1920 pounds).

2. Maximum bottom deck deflection (-0.083 inches) occurs at Node 18.

3. Deflections magnified by a factor of 10.

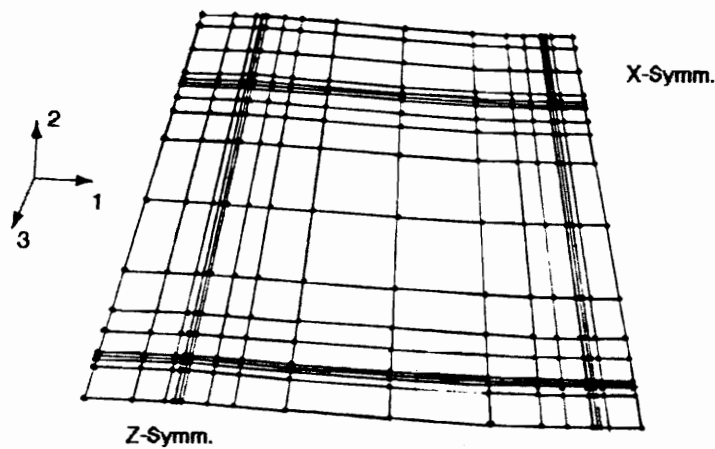
Figure 5.38. Predicted Deflection and Stress Profiles for the Bottom Deck of Pallet BPPC-7 evaluated in the Stack Support Condition using the Simplified Block Pallet Model.

Predictions generated by plate and simplified models developed to simulate test pallets containing bottom deck wheel openings are presented and compared in Table 5.22. Agreement between maximum values for stress and deflections are acceptable, with mean differences of less than 10 percent for maximum S11 stress and less than 6.1 percent for maximum deflection. As with previous results, the predicted deflection profile, shown in Figure 5.39, appears as expected. Based on these results, the model predicted behavior satisfactorily.

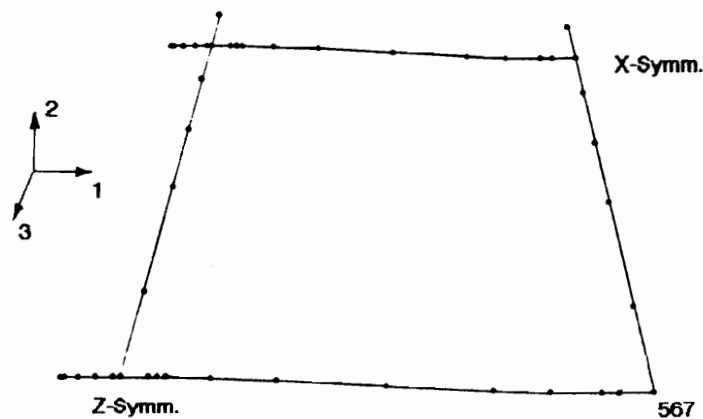
Table 5.22. Comparison of Model Predictions for Block Pallets with Bottom Deck Wheel Openings in the Racked-Across-Width Support Condition.

PALLET ID. NUMBER	MAXIMUM STRESS			MAXIMUM DEFLECTION		
	SBPM S11 (psi)	BPPM S11 (psi)	DIF (%)	SBPM D (in.)	BPPM D (in.)	DIF (%)
Top Deck Predictions:						
BPPC-4	505.5	525.7	-3.8	-0.298	-0.283	5.3
BPPC-5	508.0	539.2	-5.8	-0.259	-0.249	4.0
BPPC-6	489.0	520.6	-6.1	-0.276	-0.263	4.9
MEAN	500.8	528.5	-5.2	-0.278	-0.265	4.8
Bottom Deck Predictions:						
BPPC-4	393.5	435.0	-9.5	-0.300	-0.281	6.8
BPPC-5	408.5	455.5	-10.3	-0.260	-0.247	5.3
BPPC-6	435.2	484.7	-10.2	-0.277	-0.261	6.1
MEAN	412.4	458.4	-10.0	-0.279	-0.263	6.1

- Notes: 1. BPPM - Plate Model Predictions
SBPM - Simplified Model Predictions
DIF - Difference between BPPM and SBPM predictions.
2. Predictions reported are for pallets under a uniformly distributed load of 1.0 psi (1920 pounds).
3. Absolute maximum S11 stress magnitudes are reported.



Top Deck (Deformed State)



Bottom Deck (Deformed State)

- Notes: 1. Deformed state under a uniformly distributed load of -0.5 psi.
2. Maximum bottom deck deflection (-0.300 inches) occurs at Node 567.
3. Deflections magnified by a factor of 4.

Figure 5.39. Predicted Deflection Profiles for the Decks of Pallet BPPC-4 evaluated in the Racked-Across-Width Support Condition using the Simplified Block Pallet Model.

6.0 Summary and Conclusions

With the increased utilization of pallets constructed using structural panel decks, there is a need for a standardized reliability-based design system to assist in the design and manufacture of panel-deck pallets. Development of a reliability-based methodology, PDS-PANEL, provides a rational basis for designing efficient and safe pallets. The models developed in this research are the prototypes of models used to predict the behavior of panel-deck pallets designed using PDS-PANEL.

The primary objective of this research was to develop PC compatible models which have solutions times of less than 2 minutes on existing PC computers and could be incorporated into the existing PDS-PANEL program framework. PC model predictions should not differ from predictions derived with considerably more sophisticated plate models by more than 15 percent. Models were developed for both stringer and block type pallets in three principal support conditions, the stack, RAD (RAW), and RAS (RAL) conditions. Stringer and block models developed for use in PDS-PANEL can be used to estimate the static bending behavior of pallets constructed with at least one panel deck.

The research plan used to accomplish PC model development is outlined previously in Figure 1.4. Finite element models were developed for both stringer and block

pallets using plate elements to simulate deck behavior. Plate models were validated by comparing predicted deflections to experimentally measured deflections. Differences were considerably less than the allowable 15 percent for both stringer and block models. Sensitivity studies conducted with these models provided a rational basis for model simplification.

The PC stringer models can be used to model pallets with at least one panel deck of plywood or OSB, normally considered to be the top deck. The lower deck can either be a panel or strip-type decking of lumber or composite (plywood or OSB) strips. Pallets with two, three, four, or five Stringers, notched or unnotched, can be analyzed. Models were developed which can be used to evaluate pallets under partial-uniform, full-uniform, one-line, two-line, and three-line loads. These models also can be used to predict the behavior of pallets with features such as lead edge board reinforcement and cut-outs.

For stringer pallets, different PC models were used to predict panel-deck pallet behavior for each support condition. Only the deck (either top or bottom) being evaluated was used to model behavior in the stack support condition. For full uniform loads and line loads, a two-dimensional model was used, with beam elements simulating deck behavior. A grid model was used for partial uniform

loads. A two-dimensional model was used to model pallets in the RAD support condition. In the RAS support condition, a two-dimensional model was used to predict the behavior of line loaded stringer pallets and a three-dimensional grid model was used to predict behavior of uniformly loaded stringer pallets.

Generally, except for the RAS models, the PC stringer models developed predict stringer pallet behavior adequately and differences between plate and simplified model predictions were less than 15 percent. The RAS model predictions did differ conservatively from plate model predictions by more than 15 percent. Simplifying assumptions resulted in fundamental behavior differences between the plate and simplified models. This was true for both the RAS line load model and grid model for uniformly loaded pallets where deck spacing effects and lateral stiffness of nail joints were not considered effectively.

Block models were also developed to model pallets with at least one panel deck of plywood or OSB, normally considered to be the top deck. As with stringer pallets, the lower deck can either be a panel or strip type decking of lumber or composite (plywood or OSB) strips. PC models can be used to analyze block pallets constructed with four, five, six, or nine blocks. As for stringer pallets, block pallets under partial-uniform, full-uniform, one-line, two-

line, and three-line loads can be evaluated. These models can also be used to predict the behavior of pallets with features such as cut-outs.

Different PC models were used to predict panel-deck pallet behavior for stack and rack support conditions. Because pallets supported in the RAW and RAL conditions behaved similarly, the same model was used to predict pallet behavior for these two support conditions. However, it was necessary to develop separate models to analyze block pallets with various base configurations, including block pallets with a unidirectional-base of strip-type decking, a perimeter-base of strip-type decking, and panel bottom decks, with or without bottom deck wheel openings.

As with stringer pallets, only the deck (either top or bottom) being evaluated was considered in the stack support condition. A 19 by 19 grid of beam elements was used to simulate panel deck behavior as opposed to plate elements. The model utilized an assumed pattern of contact between the deck and blocks which differs from the iterative approach used to determine contact patterns in the plate model evaluations. These simplifying assumptions resulted in significant differences between plate and PC model stress predictions. For several test cases errors exceeded 15 percent, with mean differences as great as 26.8 percent.

Deflection differences were not as great, with mean differences of 4.1 percent or less.

In the RAW and RAL support conditions, grids were again used to model panel decks. A 19 by 19 grid of beam elements was used to model the top deck and a much coarser grid (either a 2 by 2 or 3 by 3) to model panel bottom decks. For unidirectional- and perimeter-base pallets, assemblages of beam elements were used to predict the behavior of lumber or composite (plywood or OSB) strips. An assumed pattern of contact between the decks and blocks was again used. The agreement between the plate and simplified model predictions was acceptable for all the different configurations considered and differences between both stress and deflection predictions were less than 15 percent. Based on this evidence, it was concluded that the PC models adequately predict pallet behavior for block pallets in the RAW and RAL support conditions.

PC models developed in this research were proposed for inclusion in PDS-PANEL. The models were translated into matrix structural analysis programs compatible with the existing PDS framework (McLeod, 1996). Predictions generated by the matrix structural analysis programs utilized in PDS-PANEL were compared to results presented in this dissertation. Generally, differences between the stress and deflection predictions were small. These matrix

structural analysis programs, based on models developed in this research, form the basis for predicting the behavior of panel-deck pallets in PDS-PANEL, a reliability-based design program for pallets with panel decks.

6.1 Recommendations for Further Research

Although both the stringer and block models developed for use on PC computers in this research can be used to adequately predict the behavior of panel-deck pallets, as the memory capacity and processing capabilities of PC computers increase these models can be upgraded. Potential improvements to the models are discussed subsequently.

With regards to notched stringers, it should be possible to model these members directly using modified sections and the conjugate beam theory. Further research is required, building on work by Gerhardt (1985) and Zalph (1989), to develop a method for predicting the effect of stress concentrations which occur at the notch corners, incorporating this methodology into the prediction program. Any methodology developed must consider the various notch configurations, including the impact of differing radii commonly used at notch corners to reduce stress.

Further study is also required to determine if the stress concentrations at the corners of cut-outs govern failure. While these stress concentrations are not thought

to be governing with hand-holds, their impact with respect to panels with wheel-openings is uncertain. This is particularly true for OSB panels where failures are generally more brittle and catastrophic.

When PC memory capacities and processing capabilities increase sufficiently, the RAS model for stringer pallets should be modified, incorporating deck spacing and lateral stability back into the model. This is accomplished by using different nodes for stringer and deck assemblages, rather than sharing nodes as currently done. Stringer and deck nodes are then connected using zero-length springs. Although considerably more complex, this element configuration predicts pallet behavior more accurately.

Although the modeling techniques used to model block pallets are quite sophisticated, two simplifying assumptions in particular decrease the precision of PC models. These are using a grid of beam elements as opposed to plate elements to model panel decks and an assumed pattern of contact between the decks and spacers. It should become feasible at some point to replace the grids of beam elements currently used in PC models with plate elements. Although it would require considerable effort to incorporate plate elements into the existing PDS framework, ultimately doing so would reduce model complexity (at least in terms of element numbers) and improve model performance. Further

study would be required to develop a more sophisticated method for better estimating contact between the decks and spacers.

All the recommendations for further research involve improving model performance through increased model sophistication and complexity. With advances in PC memory and processing capacities, these advances should become feasible. Existing models are developed such that these upgrades can be added in the future.

Literature Cited

- (1) American Plywood Association. 1991. Design Capacities of APA Performance Rated Structural-Use Panels. APA Technical Note N375A. Tacoma, Washington.
- (2) American Plywood Association. 1986. APA Industrial Use Guide - Pallets. Tacoma, Washington.
- (3) American Society for Testing and Materials. 1994. Standard Methods of Testing Small Clear Specimens. ASTM D 143-83. ASTM, Philadelphia, PA.
- (4) American Society for Testing and Materials. 1994. Standard Methods of Static Tests of Timbers in Structural Sizes. ASTM D 198-84. ASTM, Philadelphia, PA.
- (5) American Society for Testing and Materials. 1994. Standard Practice for Establishing Structural Grades and Related Allowable Properties for Visually Graded Lumber. ASTM D 245-93. ASTM, Philadelphia, PA.
- (6) American Society for Testing and Materials. 1994. Standard Test Methods for Pallets and Related Structures Employed in Materials Handling and Shipping. ASTM D 1185-94 (Reapproved 1994). ASTM, Philadelphia, PA.
- (7) American Society for Testing and Materials. 1994. Standard Test Methods for Establishing Clear Wood Strength Values. ASTM D 2555-88. ASTM, Philadelphia, PA.
- (8) American Society for Testing and Materials. 1994. Standard Methods of Testing Structural Panels in Flexure. ASTM D 3043-87. ASTM, Philadelphia, PA.
- (9) American Society of Mechanical Engineers. 1989. Pallet Definitions and Terminology. ASME MH1.1.2-1989. ASME, New York, NY.
- (10) American Society of Mechanical Engineers. 1997. Pallet Sizes. ASME MH1.2.2-1997. ASME, New York, NY.

- (11) American Society of Mechanical Engineers. 1989. Procedures for Testing Pallets. ASME MH1.4.1M-1989. ASME, New York, N. Y.
- (12) Bastendorf, K. M., and A. Polensek. 1984. Strength and Stiffness of Red Alder and Big Leaf Maple Pallet Materials. *Forest Products Journal*. 34(7/8): 51-56.
- (13) Bathe, K. J. 1982. *Finite Element Procedures in Engineering Analysis*. Prentice-Hall, Inc., Englewood Cliffs, NJ.
- (14) Bodig, J., and B. A. Jayne. 1982. *Mechanics of Wood and Wood Composites*. Van Nostrand Reinhold. 712 pp.
- (15) Bulleit, W. M. 1985. Elastic Analysis of Surface Reinforced Particleboard. *Forest Products Journal*. 35(5):61-68.
- (16) Cook, R. D. 1981. *Concepts and Applications of Finite Element Analysis*, Second Edition. John Wiley & Sons.
- (17) Colclough, R. G. 1987. The Development and Verification of Analysis Models for Block-Type Wooden Pallets. M. S. Thesis. VPI & SU, Blacksburg, VA.
- (18) Collie, S. T. 1984. Laboratory Verification of Pallet Design Procedures. M. S. Thesis. VPI & SU, Blacksburg, VA.
- (19) Criswell, M. E. 1979. Concepts for Design Methodology for Wood Transmission Structures. EPRI Meeting Notes, June 1979, Colorado State University, Fort Collins, CO.
- (20) Elias, E. G. 1986. Plywood Pallet - In Rack Performance. R&D 85-27. APA, Tacoma, Washington.
- (21) Fagen, C. B. 1982. Load-Support Conditions and Computerized Test Apparatus for Wood Pallets. M. S. Thesis. VPI & SU, Blacksburg, VA.
- (22) Freas, A. D. 1964. Bending Strength and Stiffness of Plywood. U. S. Forest Service Research Note, FPL-059. Madison, WI.

- (23) Gerhardt, T. D. 1985. Strength and Stiffness Analysis of Notched, Green Oak Stringers. USDA Forest Service Research Paper, FPL 452. Madison, WI.
- (24) Goehring, C. B., and W. B. Wallin. 1981. A Survey of loads, Loading Conditions, and Handling Environment Conditions for Wooden Pallets. Northeastern Forest Experiment Station, Forestry Sciences Laboratory, Princeton, West Virginia.
- (25) Hibbitt, Karlsson, & Sorensen, Inc. 1989. ABAQUS - User's Manual, Version 4.8.
- (26) Holzer, S. M. 1985. *Computer Analysis of Structures: Matrix Structural Analysis - Structured Programming*. Elsevier Science Publishing Co., Inc., NY.
- (27) Hrennikoff, A. 1941. Solutions of Problems of Elasticity by the Framework Method. *Journal of Applied Mechanics*. ASME. New York, NY. Vol. 63, December, 1941, p. A-169.
- (28) International Organization for Standardization. 1988. General-purpose flat pallets for through transit of goods - Test Methods. ISO 8611.
- (29) International Organization for Standardization. 1989. General-purpose flat pallets for through transit of goods - Performance Standards. ISO TR 10233.
- (30) Iyer, R. G. 1989. A Novel Grid Analogy for Transversely Loaded Orthotropic Plates. M. S. Thesis. VPI & SU, Blacksburg, VA.
- (31) Kurtenacker, R. S. 1974. Wood-base Panel Products for Pallet Decks. USDA Forest Service Research Paper, FPL 273. Madison, WI.
- (32) Kyokong, B. 1979. The Development of a Model of the Mechanical Behavior of Wooden Pallets. Ph. D. Dissertation. VPI & SU, Blacksburg, VA.

- (33) Lauer, I. E., and M. S. White. 1992. Laboratory Evaluation of the Performance of the Perimeter Base, Plywood Deck, Block Style Pallet. W. H. Sardo Jr. Pallet and Container Laboratory Report. Dept. of Forest Products, VPI & SU, Blacksburg, VA.
- (34) Leichti, R. J. 1986. Assessing the Reliability of Wood Composite I-Beams. Ph. D. Dissertation. Auburn University, Auburn, Alabama.
- (35) Lekhnitskii, S. G., S. W. Tsai, and T. Cheron. 1968. *Anisotropic Plates*. Gordon and Breach Science Publishers, NY.
- (36) Livesley, R. K. 1975. *Matrix Methods of Structural Analysis*, 2nd ed. Pergamon Press, Oxford.
- (37) Loferski, J. R. 1985. A Reliability Based Design Procedure for Wood Pallets. Ph. D. Dissertation. Dept. of Forest Products, VPI & SU, Blacksburg, VA.
- (38) Loferski, J. R., and T. E. McLain. 1987. Development of a Reliability-Based Design Procedure for Wood Pallets, *Forest Products Journal*. 37(7/8): 7-14.
- (39) Lyons, B. E. 1970. Plywood Pallets. Research Report 107. APA, Tacoma, Washington.
- (40) Mackes, K. H. 1998. Predicting the Static Bending Behavior of Pallets with Panel Decks - Laboratory Report (Volume I). W. H. Sardo Jr. Pallet and Container Research Lab. Bulletin No. 24 - Volume I. Dept. of Forest Products, VPI & SU, Blacksburg, VA.
- (41) Mackes, K. H. 1998. Predicting the Static Bending Behavior of Pallets with Panel Decks - Laboratory Report (Volume II). W. H. Sardo Jr. Pallet and Container Research Lab. Bulletin No. 24 - Volume II. Dept. of Forest Products, VPI & SU, Blacksburg, VA.
- (42) Mackes, K. H. 1998. Predicting the Static Bending Behavior of Pallets with Panel Decks - Laboratory Report (Volume III). W. H. Sardo Jr. Pallet and Container Research Lab. Bulletin No. 24 - Volume III. Dept. of Forest Products, VPI & SU, Blacksburg, VA.

- (43) Mackes, K. H., J. R. Loferski, and M. S. White. A Pneumatic Pressure Bag Testing Machine for Applying a Uniform Load to Panels and Pallets. *Journal of Testing and Evaluation*. JTEVA, Vol. 23, No. 4, July 1995, pp. 295-299.
- (44) McGuire, W., and R. H. Gallagher. 1979. *Matrix Structural Analysis*. Wiley, New York.
- (45) McLain, T. E., W. B. Wallin, M. S. White, and J. A. McLeod. 1990. Pallet Design Short Course Manual. Dept. of Forest Products, VPI & SU, Blacksburg, VA.
- (46) McLain, T. E. 1976. Curvilinear Load Slip Relations in Laterally Loaded Nail Joints, "Recent Research with Mechanical Fasteners in Wood." Proceeding No. p-76-16. Forest Products Research Society, Madison, Wisconsin (July).
- (47) McLeod, J. A. 1996. PDS-PANEL. Personal Correspondence. Dept. of Forest Products, VPI & SU, Blacksburg, VA.
- (48) McNatt, J. D., R. W. Wellwood, and L. Bach. 1990. Relationships between small-specimen and large panel bending tests on structural wood-based panels. *Forest Products Journal*. 40(9):10-16.
- (49) National Wooden Pallet & Container Association. 1988. PDS-BLOCK - Source Code. NWPCA, Arlington, VA.
- (50) National Wooden Pallet & Container Association. 1984. PDS-STRINGER - Source Code. NWPCA, Arlington, VA.
- (51) National Wooden Pallet & Container Association and American Plywood Association. 1980. Specifications for Softwood Plywood Pallets, pp. 61-72. Arlington, VA.
- (52) Reddy, V. S., R. J. Bush, M. S. Bumgardner, J. L. Chamberlain, and P. A. Araman. 1997. Wood Use in the U. S. Pallet and Container Industry: 1995. Center for Forest Products Marketing and Management, Dept. of Wood Sci. and Forest Prod., VPI & SU, Blacksburg, VA.

- (53) Samarasinghe, S. 1987. Predicting Rotation Modulus for Block Pallet Joints. M. S. Thesis. VPI & SU, Blacksburg, VA.
- (54) Superfesky, M. J., H. M., Montry, and T. J. Ramaker. 1977. Floor and Roof Sheathing Subjected to Static Loads. *Wood Science*, 10(2):31-41.
- (55) USDA. 1987. Wood Handbook-Wood as an Engineering Material. U. S. Depart. of Agriculture, Washington, DC.
- (56) Wallin, W. B., and E. G. Stern. 1974. Design of Pallet Joints from Different Species. Northeastern Forest Experiment Station, Forestry Sciences Laboratory, Princeton, West Virginia.
- (57) Wallin, W. B., E. G. Stern, and J. J. Strobel. 1975. Pallet-Exchange Program Research Findings Indicate Need for Pallet Standards. Wood Research and Wood Construction Laboratory Bulletin No. 134. VPI & SU, Blacksburg, VA.
- (58) Wallin, W. B., E. G. Stern, and J. A. Johnson. 1976. Determination of Flexural of Stringer-Type Pallets and Skids. Wood Research and Wood Construction Laboratory Bulletin No. 156. VPI & SU, Blacksburg, VA.
- (59) White, M. S. 1993. Comparative Performance of 48x40-inch 9-Post Oriented Strand Board Double-Deck Non-Reversible Pallets. W. H. Sardo Jr. Pallet and Container Laboratory Report, Dept. of Forest Products, VPI & SU, Blacksburg, VA.
- (60) Wilkinson, T. L. 1971. Theoretical Lateral Resistance of Wood Nailed Joints, *Journal of the Structural Division, ASCE*. 97(5): pp. 1381-1398.
- (61) Yettram, A. L., and H. M. Husain. 1965. Grid-Framework Method for Plates in Flexure. *Journal of the Mechanics Division. Proceedings of the ASCE*. No. EM 3. June, 1965.
- (62) Zalph, B. L. 1989. Predicting the Strength of Notched Wood Beams. Ph. D. Dissertation. Dept. of Forest Products, VPI & SU, Blacksburg, VA.

VITA

Kurt Mackes was born in Morristown, New Jersey on April 26, 1958. He grew up in Denver, Colorado where he graduated from Northglenn Highschool in May 1976. Kurt earned his Bachelor of Science degree in Wood Science and Technology from Colorado State University. He continued on in the graduate program at Colorado State university and in August 1985 completed his Master of Science Degree in Forest and Wood Science. Kurt completed his degree while employed by BQP Industries located in Denver, Colorado. In May 1985, Kurt founded Western Die and Form, a small die-cutting company.

In November 1990, Kurt entered the graduate program at Virginia Polytechnic Institute and State University as a research assistant in the Department of Forest Products and Wood Science at the William H. Sardo National Pallet Laboratory. Kurt now resides with his family in Fort Collins, Colorado and anticipates completing all requirements for his Ph.D. in Forest Products by Winter 1998. Since relocating to Colorado, Kurt founded KH Consulting and does consulting work related to forest products. Kurt is a member of the *Forest Products Society*, the *Society of Wood Science and Technology*, and the *American Society for Testing and Materials*.